50272-101

REPORT DOCUMENTATION PAGE

1. REPORT NO. NSF/CEE-83013

2.

3. Recipient's Accession No. PB84 118272

4. Title and Subtitle
Dynamic Analysis of Multiply Tuned and Arbitrarily Supported Secondary Systems

5. Report Date July 1983

6.

7. Author(s)
Takeru Igusa and Armen Der Kiureghian

8. Performing Organization Rept. No. UCB/EERC-83/07

9. Performing Organization Name and Address
Earthquake Engineering Research Center
University of California, Berkeley
47th Street & Hoffman Blvd.
Richmond, Calif. 94804

10. Project/Task/Work Unit No.

11. Contract(C) or Grant(G) No.
(C)
(G) CEE-8105790

12. Sponsoring Organization Name and Address
National Science Foundation
1800 G Street, N.W.
Washington, D.C. 20550

13. Type of Report & Period Covered

14.

15. Supplementary Notes

16. Abstract (Limit: 200 words)

The objective of this study is to include all of the important and complicated dynamic characteristics in a dynamic analysis of linear, multi-degree-of-freedom (MDOF) secondary subsystems with multiple support points attached to linear MODF primary subsystems. These characteristics include: interaction between the two subsystems; cross-correlations between motions of the support points and modal responses for stochastic input; resonance or tuning phenomena when a set of frequencies of one system is tuned with one or more frequencies of the other system; and non-classical damping effects when the damping ratio of the two subsystems are different. The basic approach of the analysis is to consider the combined primary and secondary subsystems as a single dynamic assemblage. Such an approach implicitly includes the effects of interaction, multiple support motions, resonance, and non-classical damping, but was avoided in the past due to the size and complexity of the resulting eigenvalue problem and the fact that such systems are non-classically damped. The main results of the analysis are applied to several representative example systems and compared with results obtained from numerical analysis.

17. Document Analysis a. Descriptors

b. Identifiers/Open-Ended Terms

c. COSATI Field/Group

18. Availability Statement: Release Unlimited

19. Security Class (This Report)

20. Security Class (This Page)

21. No. of Pages 240

22. Price

REPORT NO.
UCB/EERC-83/07
JULY 1983

EARTHQUAKE ENGINEERING RESEARCH CENTER

DYNAMIC ANALYSIS OF MULTIPLY TUNED AND ARBITRARILY SUPPORTED SECONDARY SYSTEMS

by

TAKERU IGUSA
ARMEN DER KIUREGHIAN

Report to the National Science Foundation
and the Electric Power Research Insitute

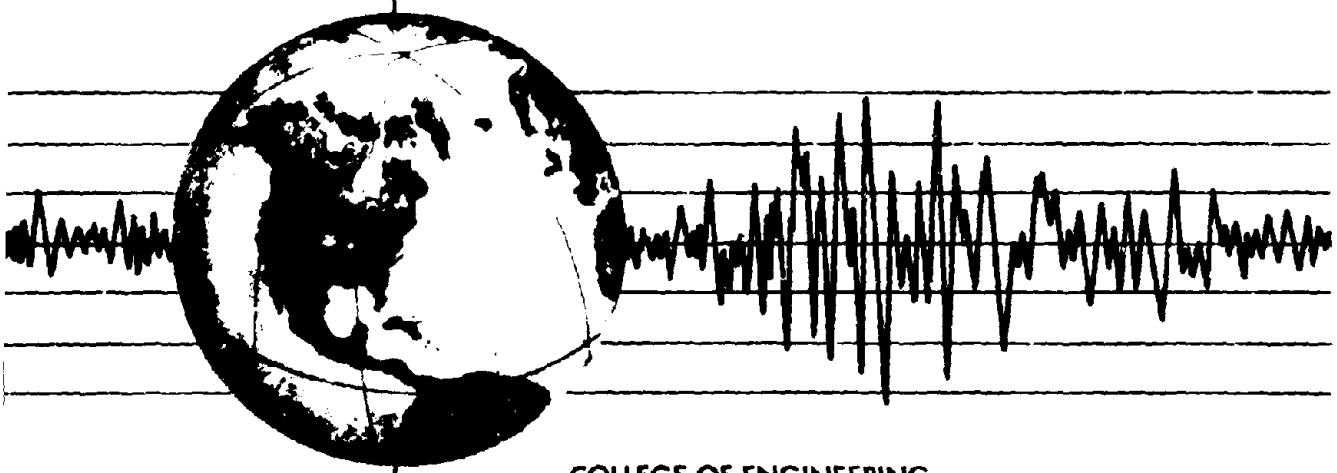

COLLEGE OF ENGINEERING

UNIVERSITY OF CALIFORNIA · Berkeley, California

DYNAMIC ANALYSIS OF MULTIPLY TUNED AND ARBITRARILY SUPPORTED SECONDARY SYSTEMS

By

Takeru Igusa

Assistant Research Engineer

University of California, Berkeley

Armen Der Kiureghian

Associate Professor of Civil Engineering

University of California, Berkeley

A report on research sponsored by

the National Science Foundation

and the Electric Power Research Institute

Report No. UCB/EERC-83/07

Earthquake Engineering Research Center

College of Engineering

University of California, Berkeley

July 1983

DYNAMIC ANALYSIS OF MULTIPLY TUNED AND ARBITRARILY SUPPORTED SECONDARY SYSTEMS

ABSTRACT

The subject of this study is the dynamic analysis of linear, multi-degree-of-freedom (MDOF) secondary subsystems with multiple support points attached to linear MDOF primary subsystems. It is known that such systems possess a number of important and complicated dynamic characteristics. These characteristics include: interaction between the two subsystems; cross-correlations between motions of the support points and modal responses for stochastic input; resonance or tuning phenomena when a set of frequencies of one system is tuned with one or more frequencies of the other system; and non-classical damping effects when the damping ratio of the two subsystems are different. In past research, one or more of these dynamic characteristics have not been given full or adequate attention; the objective of this study is to include all of these characteristics in a dynamic analysis of the complete system.

The basic approach of the analysis is to consider the combined primary and secondary subsystems as a single dynamic assemblage. Such an approach implicitly includes the effects of interaction, multiple support motions, resonance, and non-classical damping, but was avoided in the past due to the size and complexity of the resulting eigenvalue problem and the fact that such systems are non-classically damped. These problems are resolved in this study in the following manner: (1) A modal decomposition method is developed for non-classically damped systems with closed-form expressions for combining modal responses. Derivations are included for stationary stochastic input specified by the power spectral density or response spectra and indications are given for considering non-stationary input. (2) Perturbation methods are systematically applied to the analysis of the complex-valued eigenvalue problem to reduce the analysis into a physically meaningful and mathematically manageable form. Expressions are

subsequently derived for the modal properties, which are in closed form for all but multiply tuned modes

The analysis of the systems follows a logical development, beginning with the simplest 2-DOF system and progressing to the most general MDOF system. For completeness, frequency response function analysis is presented and compared with modal decomposition results. Also, as one extension of the theory, the results are simplified to the important case of non-interacting subsystems where the secondary subsystem masses are sufficiently small in comparison with the primary subsystem masses. Finally, the main results of the analysis are applied to several representative example systems and compared with results obtained from numerical analysis. Favorable agreement is found for all cases.

ACKNOWLEDGMENTS

The authors would like to express special thanks to Professor Jerome L. Sackman for his providing the initial impetus for our interest in this problem and for many resourceful and enlightening discussions that we have had with him during the course of this study.

This research work was sponsored by the National Science Foundation under Grant No. CEE-8105790 and the Electric Power Research Institute under Grant No. RP964-8. This sponsorship is gratefully acknowledged.

TABLE OF CONTENTS

LIST OF TABLES

LIST OF FIGURES

CHAPTER 1

INTRODUCTION

1.1 General Remarks

Complex structural systems composed of light secondary components or subsystems attached to heavier primary subsystems are frequently encountered in civil engineering. Piping systems, electrical equipment, laboratory instruments, antennas, computer hardware, and safety devices are a few examples of the attachments which may be found in multi-story buildings and industrial plants and facilities. In many cases the secondary subsystems perform vital tasks or are valuable in themselves and the response of these systems to base excitations have long been of engineering interest.

In the following, the properties of such systems are described, and a detailed literature survey of the studies on these systems is presented, concentrating on the methodology used and the difficulties encountered in the analysis. Then a method to overcome these difficulties is introduced and a plan of analysis, which constitutes the main body of this study, is outlined.

1.2 Description of the Problem

1.2.1 Characteristics of a General Primary-Secondary System

Primary-Secondary (PS) systems have a variety of different forms and characteristics, and in this thesis, those systems that possess certain well-defined, standard properties are studied. These properties are as follows:

1. The primary and secondary subsystems are viscously and classically damped, linear-elastic systems.
2. The mass of the secondary subsystem is considerably smaller than that of the primary subsystem (mathematical criteria are given in Chapter 3).

3. The system does not include the interaction effects of a foundation, cascaded tertiary or higher level subsystems, or other separate secondary subsystems that may be attached to the primary subsystem. It is assumed that any such effects, if significant, are accounted for by properly modifying the input excitation (in the case of interacting foundation) or the properties of the primary subsystem (in the case of other secondary subsystems).

4. All attachment points of the PS system to the base are subjected to the same input excitation.

PS systems that have the above properties are quite general and have a number of important dynamic characteristics which have been topics of intense study in the past. The main dynamic characteristics are:

1. Multi-degree-of-freedom (MDOF) subsystems: Both primary and secondary subsystems are in general MDOF systems. Either subsystem can be composed of more than one independent subsystem.

2. General attachment configuration: The secondary subsystem may be attached to the primary subsystem in an arbitrary number of locations and may also be attached to the base of the combined system. The secondary subsystem may be attached to more than one primary subsystem.

3. General resonance (tuning) characteristics: Any number of the frequencies of one subsystem may be arbitrarily close to or coincident with the frequencies of the other subsystem. This condition is known as tuning. When a group of closely spaced frequencies of any subsystem is tuned with one or more frequencies of the other subsystem, the frequencies are said to be in multiple tuning.

4. Dynamic interaction: For arbitrary PS systems, the primary and secondary subsystems interact with each other, particularly if the secondary subsystem modal masses are non-negligible and the frequencies of the two subsystems are tuned.

5. Stochastic correlation: For stochastic input, the effects of correlation cannot be neglected,

and for PS systems, this effect is an important, integral part of their dynamic behavior. For tuned systems, the cross-correlations between modal responses is significant and must be accurately determined in any dynamic analysis. Also, motions at various support points of the secondary subsystem are, in general, correlated.

6. Non-classical damping: This effect occurs in systems which have different damping ratios in the primary and secondary subsystems and is particularly significant at tuning.

1.2.2 Common Restrictions and Approximations

In principle, the theoretically exact response of a general secondary subsystem which includes the above effects can be obtained using standard methods of analysis on the combined PS system. However, this procedure presents a number of difficulties. The number of degrees of freedom (DOF) of the combined system is usually prohibitively large and the differences in the magnitudes of the stiffness, damping, and mass terms between the primary and secondary subsystems pose serious numerical problems [48]. Also, the analysis and design of the secondary subsystem is usually performed well after the design and analysis of the primary subsystem is completed and several secondary subsystem may be attached to a single primary subsystem. Consequently, alternative methods of analysis for this problem are required.

In general, researchers have used several well-defined approximations and restrictions on the physical and dynamic properties of PS systems to reduce the analysis to a simpler and more manageable form. In these restrictions and approximations, one or more of the six dynamic characteristics of PS systems listed above are not given full or accurate consideration, or are neglected altogether. For instance, some studies neglect interaction, some consider secondary systems with only a single DOF, and others assume that none of the modes are tuned. Many times, a combination of restrictions are used.

In order to present an organized review of the literature, four categories are considered. Studies which make the non-interaction approximation are reviewed first, followed by those works which include the interaction effect. Then, works which consider multiply supported sys-

tems are discussed. Finally, in Section 1.4, several recent studies which provide the background to the theory and methods of analysis in this thesis are examined.

1.3 Literature Survey

1.3.1 Non-Interaction Studies

A commonly used method of analysis which neglects interaction is the floor response spectrum method. In this method, the motions of the support points of the secondary subsystem are calculated by time history analyses of the primary subsystem. The response spectra of the support motions are known as floor spectra which are used as input to the secondary subsystem. Realizing that this method is lengthy and inefficient, several authors have developed more direct methods of finding floor spectra using the modal properties of the primary subsystem and the ground response spectrum. Biggs and Roesset [6] developed an empirical rule for finding the floor spectra using the modal properties of the primary subsystem, which was later modified by Kapur and Shao [25] using more mathematically based premises. An alternate approach based on Fourier transforms was developed by Scanlan and Sachs [38]. Singh [40], Chakravarti and Vanmarke [9], Singh [41], and Vanmarke [46] incorporated ideas from random vibration theory.

All of these methods have been shown to give reasonable accuracy for single-degree-of-freedom (SDOF) secondary subsystems with relatively small masses and frequencies that are not tuned to a frequency of the primary subsystem. However, when the two subsystems are tuned to each other, the methods consistently fail. One problem is that the effect of interaction becomes important and as pointed out by Crandall and Mark [11], Singh [41], and Kapur and Shao [25], significant error is introduced in the analysis of such secondary subsystems if this effect is neglected. The other problem is inherent in the analysis. Many formulations that were derived in the above works yield infinite results at tuning. Singh [42] and Peters, et. al. [35] provide rough approximations for perfectly tuned systems, but these results continue to ignore interaction and are inaccurate for nearly tuned systems, where the tuned frequencies are not

exactly coincident. Since tuning is considered important and, frequently, critical in the analysis of secondary systems [2], it is clear that the above non-interaction studies are not adequate for a proper analysis of such systems.

1.3.2 Studies Considering Interaction

A number of analytical methods have been developed to account for the dynamic interaction between the primary and secondary subsystem. In these methods, the combined equations of motion must be analyzed without decoupling to account for this effect. Crandall and Mark [11] used the exact equations for a combined 2-DOF system to compute the root-mean-square response to stationary excitation. In other studies, approximations are made to reduce and simplify the analysis of the combined system. Penzien and Chopra [34] reduce a system composed of an N-DOF primary subsystem and a single DOF (SDOF) secondary subsystem to a series of N 2-DOF subsystems; however, the analysis is in terms of 2-DOF response spectra, which are not generally available, and the responses are combined with the square-root-of-sum-of-squares (SRSS) rule which is inaccurate at tuning.

Newmark [33] used a notion of effective mass ratio to obtain approximate mode shapes and frequencies and combined modal responses with the conservative absolute sum rule. This method was improved by Nakhata et. al. [31]. These two modal approaches have sound theoretical bases, however a certain level of accuracy is required both in the formulations for the modal properties and the combination of modal response quantities to obtain good approximations for the system response [48]. This accuracy was not attained until later works, as detailed in Section 1.4.

1.3.3 Multiple Support Excitations

As stated earlier, a common assumption in the analysis of PS systems is that the secondary subsystem has only one DOF or is attached to the primary subsystem at a single point. This assumption is satisfactory for simple systems or for obtaining floor spectra. However, for more general secondary subsystems, the important effect of multiple support excitations must

be analyzed.

In the earliest research efforts the effect of interaction was not included in the analysis so that simplified decoupled equations of motion could be used. A straightforward method for analyzing decoupled multiply-supported secondary subsystems is the time history approach. The base time history is used to find the resulting motions of the support points and these motions are subsequently input into the equations of motion for the secondary subsystem [27]. This method is both inefficient and cumbersome and researchers have investigated alternate methods based on response spectra and random vibration techniques.

Amin, et. al. [4], Shaw [39], and Vashi [47] formulated the response analysis of the secondary subsystem in terms of the motions of the individual support points using heuristic procedures for combining these motions. Vashi provides three methods for combining responses: one based on the absolute sum method for support motions which are in phase, another based on the SRSS rule for motions which are independent, and the third based on a combination of the two methods for motions which are neither in phase nor independent. No precise procedure is given to determine the classification of the support motions; therefore the analysis becomes subjective in nature.

In the industry, it is considered standard to decompose the response of the secondary subsystem into "inertial" or "dynamic" effects and effects due to "relative seismic support displacements" or "pseudo-static motion" [2]. However, this artificial formulation complicates the analysis, particularly in the consideration of correlation between the numerous decomposed response quantities.

Recently, Lee [26] introduced a method based on frequency response analysis to include the correlation between support motions and modal responses. However, the frequency response formulations are not readily useful in the analysis of secondary subsystems. Der Kiureghian, et. al. [18, 19] used a modal approach to develop a practical response spectrum method of analysis. The basis of their method is the theory of perturbations, which is explained in terms of secondary subsystems in the next section.

1.4 The Perturbation Approach

1.4.1 Overview

The perturbation method and its associated theory of asymptotic expansions are long established tools of mathematics [20]. During the past quarter century, applications of these methods have been made in fluid dynamics and related branches of hydraulic engineering [32], which have resulted in considerable developments in these fields. These methods have also been used in various branches of mechanical and structural engineering, however systematic applications of these methods to PS systems has not been carried out until very recently.

1.4.2 Past Applications in PS Systems

Perturbation methods are useful in solving differential equations which contain small parameters. Such equations occur in the analysis of PS systems, the small parameters are the mass, stiffness, and damping terms of the secondary subsystem. Sackman and Kelly [37] were among the first to recognize this and they were able to cast a new form to the equations describing the PS system using perturbation methods. With this new formulation, they were able to accurately analyze tuned 2-DOF systems which, in previous works, were treated in a rough, approximate manner, and obtain closed form expressions for the frequencies. These results were subsequently used in an analysis of more general PS systems with a single DOF secondary subsystem using Laplace transforms.

Other research work in this area has used the modal approach to the analysis of PS systems [36, 48, 18, 19]. Basically, the modal approach is as follows: Perturbation techniques are used to obtain approximations for the mode shapes and frequencies of the combined system. From these modal properties, the modal responses are found which are subsequently combined using a modal combination rule. This approach is standard in the analysis of most linear structural systems [10], however for PS systems special problems are encountered. For systems with even slight differences of the damping ratios in the primary and secondary subsystems, the mode shapes are complex-valued. Also, for tuned subsystems, some of the frequencies of the

combined system are very closely-spaced and the corresponding mode shapes are large and nearly opposite in sign. Consequently, the modal responses must be combined in a precise and theoretically sound manner. In the following, a survey of several recent studies based on perturbation applications to modal analysis of PS systems is presented and the difficulties encountered are discussed.

Ruzicka and Robinson [36] obtained expressions for the modal properties of fairly general PS systems, however, the important non-classical damping characteristic was given only an approximate consideration. Also, the response analysis was in terms of the Fourier transform of the ground motion, which is generally not available. Villaverde and Newmark [48] concentrated their efforts on systems with only one or two attachment points, which restricted their analysis. Also, the non-classical damping effect was not given precise treatment in their work. Der Kiureghian, et. al. [18,19] studied systems restricted to single DOF secondary subsystems and classical damping and obtained relatively good results for the modal properties of these systems and derived the response to ground motions specified by their response spectra. Der Kiureghian, et. al. [17] extended this method to account for multiple support excitations by defining cross-floor spectra which are in terms of the cross-correlations between two SDOF oscillators attached to the same primary subsystem. However, this latter approach in its present formulation does not account for interaction. Also, none of the above mentioned studies considered the important case of multiple tuning.

From the above works, it is clear that the perturbation approach is a powerful tool in analyzing PS systems. However, its use has been limited and its capabilities have only partially been utilized. The important effects of non-classical damping, multiple tuning, and interaction are yet to be given accurate consideration.

1.4.3 Plan of Analysis

In the present thesis, the methods of perturbation analysis are applied to general PS systems in a logical, systematic manner. The emphasis is on completeness and the limitations imposed on the previous works discussed above are lifted. Thus, all of the important

characteristics listed in Section 1.2.1 are included in the analysis. The equations of motion are set up for interacting, multi-degree-of-freedom subsystems with general attachment configuration and the modal properties are obtained from a complex eigenvalue formulation which explicitly accounts for non-classical damping and general tuning characteristics of the combined system. Finally, methods of random vibrations are used in combining modal responses to include the effects of correlation between modal responses and between the motions of the attachment points. This analysis procedure appears to be straightforward, however, several important rules must be closely and carefully followed in the plan of analysis to insure accuracy and completeness in the results.

All of the analysis revolves around the complete equations of motion of the combined PS system. The separation of the coordinates into dynamic and static parts are not necessary since all of the coordinates of the primary and secondary subsystems are considered together as *dynamic* responses to the base motion. Also, the behavior at the support points need not be explicitly analyzed; this complex effect is included implicitly in the analysis since the PS system is considered as a single dynamic assemblage. Thus, by treating the PS system as a whole, the analysis becomes, in many ways, simpler and more direct. This approach was avoided until recently partly because the applicability of perturbation methods in such an analysis was not exploited. However, this application of perturbation methods is by no means trivial, and the studies discussed above in Section 1.4.2 did not fully and accurately apply these methods to the analysis of general PS systems.

The thesis is organized to follow a logical plan of analysis beginning with the simplest PS system where both primary and secondary subsystems have only a single DOF, and progressing to the most general case where both subsystems have multiple DOF. The reason for this is clear: the most general systems are also the most complex and many of the important dynamic characteristics of these systems which must be included in the analysis is obscured by the complexity of the problem. Thus, the simplest PS system is examined first, where most of the results of the analysis is formulated in simple closed form expressions. The important dynamic

characteristics are readily seen and are thoroughly studied before more general systems are studied. In the analysis of more general systems, these same dynamic properties are recognized from the a priori knowledge gained from the analysis of the simpler systems. In this way, the properties listed in Section 1.2.1 are identified in the most general PS systems, studied in detail, and the results of the analysis presented using theoretically derived formulations.

The secondary subsystem is constantly interpreted as a perturbation of the primary subsystem in order to make full use of the perturbation methods of analysis. To achieve this level of analysis, precise and clear definitions are used for the relationships between the terms used in the perturbation approach. Also, the criteria for the application of the perturbation methods are explicitly marked out and strictly adhered to. This helps in maintaining consistency in all of the resulting expressions of the analysis.

Finally, no approximations are used except those that are allowed in the mathematical framework of the theory of perturbation methods. Thus, within this framework, the analysis is exact. Consequently, all of the dynamic properties, such as general tuning characteristics, multiple attachment configuration, non-classical damping, interaction, and all correlations, which were not all adequately accounted for in previous works, are included in the analysis in a mathematically precise manner. This final premise avoids some of the inaccuracies and inherent deficiencies found in earlier works and provides results that are comprehensive and theoretically sound within the scope of the analysis.

1.5 Scope and Limitations

In Section 1.2.1, the scope of the type of PS systems that are being considered was described in detail. In this section, the scope of the type of input and the corresponding response quantities is discussed.

In the analysis of PS systems presented in this study, two alternate formulations describing the dynamic properties of these systems are presented. One is in terms of the frequency response function of the response of the secondary subsystem and the other is a modal descrip-

tion based on the mode shapes and frequencies of the combined system. These formulations have applications in a variety of methods of dynamic analysis. Attention here is focused on the response of PS systems to stationary stochastic input and response to seismic input described by the ground response spectrum.

A method for obtaining the power spectral density (PSD) is provided and expressions for the first few moments of the PSD are derived. Most practical response quantities can be found from these moments, including the mean square of the response and its time derivative, and for Gaussian excitation, the response mean frequency, distribution of the peak response over a specified duration and its mean and variance, and the distribution of the peaks of the response. These results form the basis for the response spectrum method for seismic analysis of PS systems.

Once the characteristics of the combined systems are determined, the response of PS systems can be found for more general inputs such as non-stationary inputs and procedures for these extensions are indicated in the text, however, a detailed analysis for such inputs is beyond the intended scope of this report.

1.6 Approach of Analysis

From the discussion in Section 1.4.2, it is clear that a modal combination rule which correctly accounts for correlation between modes with closely spaced frequencies and is general enough to analyze non-classically damped systems is necessary in the modal analysis of PS systems. Consequently, in the first step of this study, a modal combination rule for stationary response satisfying these properties is developed. The method is a generalization of that for classically damped systems developed by Der Kiureghian [15, 16], which was found to be suitable for classically damped PS systems [19]. The remainder of the study follows the ideas outlined in Section 1.4.3. A synopsis of the approach of the analysis follows:

Chapter 2. Modal Decomposition Method for Stochastic Response of Non-Classically Damped Systems

Based on the complex mode shapes and frequencies of non-classically damped systems, general formulae for the response PSD and its moments are derived. The expressions are in terms of the cross-spectral moments between the modes of the system. Comparisons are made with results for classically damped systems and closed form solutions for the moments are obtained for white-noise input. These results are used to formulate a response spectrum method for seismic analysis of general systems with nonclassical damping.

Chapter 3. Analysis of the Basic 2-DOF PS System

The basic 2-DOF system is the simplest PS system and consists of a SDOF secondary subsystem attached to a SDOF primary subsystem. The frequency response approach is used to derive accurate closed form expressions for the PSD and its first three moments. After a careful derivation and investigation of the mode shapes and frequencies, both tuned and detuned systems are analyzed using the modal decomposition approach and a criterion for tuning is mathematically derived. A similar analysis for very light equipment is carried out and a mathematical criterion for decoupling between the primary and secondary subsystems is derived.

Chapter 4. Analysis of SDOF Equipment Attached to MDOF Structures (MDOF/SDOF PS System)

The methods developed for the analysis of the 2-DOF system are generalized for MDOF/SDOF systems. There are more complex problems to be handled such as multiple support excitations and multiple tuning, however the framework established through the perturbation approach effectively solves these problems, as mentioned earlier.

Chapter 5. Analysis of MDOF Secondary Subsystems Attached to SDOF Primary Subsystems (SDOF/MDOF PS System)

The results for MDOF/SDOF systems are found to be closely related to those for SDOF/MDOF systems. This relation is explored and utilized to derive expressions for

the response of SDOF/MDOF systems based on the results of Chapter 4.

Chapter 6. Analysis of MDOF Secondary Subsystems Attached to MDOF Primary Subsystems (MDOF/MDOF PS System)

All of the results derived in the previous chapters form the theoretical background for analyzing this most general and complex class of PS systems. By adhering to the rules laid out in Section 1.4.3, the analysis encompasses all of the dynamic characteristics described above. Multiple support configurations, general tuning, non-classical damping, and interaction are implicitly included in the equations of motion and the corresponding eigenvalue problem, and all correlation effects are explicitly accounted for in the combination of modal responses.

Numerical examples are presented for each of the above types of PS systems to illustrate the accuracy of the proposed methods.

CHAPTER 2

MODAL DECOMPOSITION METHOD FOR STOCHASTIC RESPONSE OF NON-CLASSICALLY DAMPED SYSTEMS

2.1 Introduction

In dynamic analysis of linear systems, such as structures subjected to seismic excitations, it is common to assume that the system is classically damped. Under this assumption, the equations of motion can be transformed into a set of independent modal equations using the real-valued eigenvectors and eigenvalues of the undamped system [10]. However, in most real systems the modal equations are coupled by the damping matrix [49]; these systems are defined to be non-classically damped. In practice, non-classically damped systems can be approximated by a classically damped system, and the results are usually of sufficient accuracy. One common approximation is to neglect coupling damping terms in the modal equations. There are important situations, however, where the effect of non-classical damping is essential and must be included in the analysis [49]. As indicated in the introduction, this effect is found in PS systems and numerical examples are presented in this chapter.

A classical method for analyzing non-classically damped systems is to use modal decomposition employing the complex-valued eigenvectors and eigenvalues [21]. This method has been used in certain applications of deterministic dynamic analysis such as in soil-dynamics where the effect of non-classical damping is significant. Investigators have also studied response to random input. Caughey [8] and Masri [30] considered non-stationary input and responses and Debchandhury and Gasparini [14] used a state space approach to the problem. Many of the results of the analysis of PS systems in the succeeding chapters can be used in the above mentioned methods for finding the response to deterministic or non-stationary random input, however the final results are relatively complex and are not obtainable in closed form.

Singh [43] applied the modal decomposition approach to the analysis of the response of non-classically damped systems and was able to derive a response spectrum method for such systems. However, his formulations are in terms of a set of four simultaneous equations which are difficult to interpret physically and are unsuitable for analytical purposes where closed form solutions are sought. In this chapter, a modal decomposition approach is used to develop an alternate response spectrum method that is more simple and direct than Singh's method in that the response quantities are given in closed form expressions directly in terms of the modal properties of the system. This formulation is particularly well-suited for the analysis of general PS systems which is carried out in the succeeding chapters. Another advantage of this method is that a full probabilistic description of the response is given rather than only the mean of the peak response as given in Singh's work.

The emphasis in this study is on a second-moment characterization of the stationary response, $v(t)$, of non-classically damped systems under random excitation which is given by the one-sided power spectral density function, $G_{vv}(\omega)$. It is well known [15,44] that most response quantities of engineering interest can be expressed in terms of the first few spectral moments

$$\lambda_m = \int_0^\infty \omega^m G_{vv}\, d\omega\,, \quad m = 0,1,2,\cdots\,. \tag{1}$$

For example, λ_0 and λ_2 are the mean squares of the response and its time-rate respectively [28]. If the excitation is Gaussian, as is assumed for most engineering applications, the power spectral density provides a complete characterization of the response process. Many additional response quantities in that case are given in terms of the spectral moments λ_m. For example, $\bar{\omega}=\sqrt{\lambda_2/\lambda_0}$ denotes the mean frequency of the response process [28] and $\delta=\sqrt{1-\lambda_1^2/(\lambda_0\lambda_2)}$, known as the shape factor, is a measure of the narrow-bandedness of the response power spectral density shape [44]. (δ ranges between 0 and 1 and decreases with increasing narrow-bandedness.) The three moments λ_0, λ_1, and λ_2 also describe several properties of the envelope process associated with the response [29]. Using the envelope process, expressions have been derived for the distribution of the peak response over a specified duration [45] and

its mean and variance [13, 15] in terms of these three moments. These expressions are used in deriving the response spectrum method for non-classically damped systems. For fatigue study applications, the moments λ_0, λ_2, and λ_4 may be used to find the distribution of the peaks of the response [7].

Expressions for the spectral moments of the response of a multi-degree-of-freedom system subjected to stationary input have been derived [15] for the case of classical damping using a modal decomposition approach. In this chapter, these results are generalized to systems with non-classical damping. First, the basic equations of motion and their modal coordinates are laid out using standard methods of analysis. These equations are integrated and solved in terms of Duhamel integrals and their derivatives. From this formulation, the auto-correlation function of the response process is obtained which is used to derive the power spectral density function and its moments in terms of the modal properties of the original system. Attention is focused on the important case of white-noise input, for which exact closed form expressions and simple first-order approximations are derived. These expressions are subsequently used to formulate a response spectrum method using the theory of stationary random vibrations [22]. Throughout the analysis, results for non-classical damping are compared with previous results for classical damping.

Example studies for simple systems have shown that the effect of non-classical damping can be highly significant in two types of systems: soil-structure systems, where the difference of damping ratios is very large; and nearly tuned equipment-structure systems, where the mass ratio is small and the damping ratios are unequal. It is found that in each case as the difference of the damping ratios of the two subsystems increases or the mass ratio decreases, the classically damped approximation to the response becomes less accurate. Numerical examples for several typical systems are presented which indicate significant errors associated with neglecting the effect of non-classical damping.

The results of this chapter form the foundation of the modal analysis of PS systems in the remainder of this study. The various formulations derived here which are in terms of the com-

plex eigenvalue analysis of the system are particularly well-suited to the analysis of general multiply-supported, multiply-tuned secondary systems.

2.2 Response to Base Input in Time Domain

First, the equations of motion are laid out and, for the sake of review, the solution is derived for classically damped systems. Let **M**, **C**, and **K** be the mass, damping, and stiffness matrices of an n-degree-of-freedom, viscously damped linear system. For a base acceleration $\ddot{x}_g(t)$, the equation for the system relative displacement response $\mathbf{x}(t)$ is

$$\mathbf{M}\ddot{\mathbf{x}} + \mathbf{C}\dot{\mathbf{x}} + \mathbf{K}\mathbf{x} = -\mathbf{M}\mathbf{r}\ddot{x}_g(t) \tag{2}$$

where $\mathbf{r}$ is the influence vector that couples the ground motion to the degrees of freedom of the structure. The mode shapes, $\boldsymbol{\phi}_i$, and natural frequencies, ω_i, $i=1,2,\cdots,n$, associated with the undamped system are found from the following $n \times n$ eigenvalue problem

$$\mathbf{K}\boldsymbol{\phi}_i = \omega_i^2 \mathbf{M}\boldsymbol{\phi}_i \tag{3}$$

If the damping matrix $\mathbf{C}$ is orthogonal with respect to the undamped mode shapes $\boldsymbol{\phi}_i$, the system is said to be classically damped, and the equations of motion can be decoupled into n modal equations. This is accomplished by using the transformation $\mathbf{x}=\boldsymbol{\Phi}\mathbf{u}$ in Eq.2, where $\boldsymbol{\Phi}=[\boldsymbol{\phi}_1\boldsymbol{\phi}_2\cdots\boldsymbol{\phi}_n]$, and in turn premultiplying that equation by $\boldsymbol{\phi}_i^T$. The ith decoupled modal equation is of the form

$$\ddot{u}_i + 2\xi_i\omega_i\dot{u}_i + \omega_i^2 u_i = -\Gamma_i\ddot{x}_g(t) \tag{4}$$

in which $\Gamma_i=(\boldsymbol{\phi}_i^T\mathbf{M}\mathbf{r})/M_i$ is the modal participation factor and $\xi_i=\boldsymbol{\phi}_i^T\mathbf{C}\boldsymbol{\phi}_i/2\omega_i M_i$ is the estimated damping ratio for mode i, where $M_i=\boldsymbol{\phi}_i^T\mathbf{M}\boldsymbol{\phi}_i$ is the modal mass. The homogeneous solution of Eq.4 is of the form $\exp(s_i t)$ where

$$s_i = -\xi_i\omega_i \pm i\omega_{Di}, \qquad \omega_{Di} = \omega_i\sqrt{1-\xi_i^2} \tag{5}$$

and the solution for an input $\ddot{x}_g(t)$ is given by

$$u_i(t) = -\frac{\Gamma_i}{\omega_{Di}}\int_0^t \ddot{x}_g(\tau)\exp[-\xi_i\omega_i(t-\tau)]\sin\omega_{Di}(t-\tau)\,d\tau = -\Gamma_i h_i(t) \tag{6}$$

where $h_i(t)$ is the well-known Duhamel integral

$$h_i(t) = \frac{1}{\omega_{Di}}\int_0^t \ddot{x}_g(\tau)\exp[-\xi_i\omega_i(t-\tau)]\sin\omega_{Di}(t-\tau)\,d\tau \tag{7}$$

In general, the response quantity of interest is a linear combination of the components of the displacement vector $\mathbf{x}$,

$$r = \mathbf{q}^T\mathbf{x} = \sum_{i}^{n}\mathbf{q}^T\boldsymbol{\phi}_i u_i = \sum_{i}^{n}\mathbf{q}^T\boldsymbol{\phi}_i \Gamma_i h_i(t) = \sum_{i}^{n}\psi_i h_i(t) \tag{8}$$

where $\mathbf{q}$ is an n-vector of constants and $\psi_i \equiv \mathbf{q}^T\boldsymbol{\phi}_i\Gamma_i$ is known as the effective modal participation factor.

For the general case of non-classical damping, the above modal equations cannot be used and the classical mathematical approach [21] to solve Eq.2 is to reformulate it into a first-order $2n$-dimensional equation

$$\mathbf{A}\dot{\mathbf{y}} + \mathbf{B}\mathbf{y} = \mathbf{F}\ddot{x}_g(t) \tag{9}$$

where,

$$\mathbf{A} = \begin{bmatrix} 0 & \mathbf{M} \\ \mathbf{M} & \mathbf{C} \end{bmatrix},\ \mathbf{B} = \begin{bmatrix} -\mathbf{M} & 0 \\ 0 & \mathbf{K} \end{bmatrix},\ \mathbf{F} = \begin{Bmatrix} 0 \\ -\mathbf{M}\mathbf{r} \end{Bmatrix},\ \text{and}\ \ \mathbf{y} = \begin{Bmatrix} \dot{\mathbf{x}} \\ \mathbf{x} \end{Bmatrix} \tag{10}$$

The associated eigenvalue equation is

$$\mathbf{B}\hat{\boldsymbol{\phi}}_i = -s_i\mathbf{A}\hat{\boldsymbol{\phi}}_i \tag{11}$$

Due to the symmetry of the matrices $\mathbf{A}$ and $\mathbf{B}$, the solutions $\{\hat{\boldsymbol{\phi}}_i, s_i\}$ occur in conjugate pairs. From the definition of $\mathbf{y}$ it is clear that $\hat{\boldsymbol{\phi}}_i$ is of the form

$$\hat{\boldsymbol{\phi}}_i = \begin{Bmatrix} s_i\boldsymbol{\phi}_i \\ \boldsymbol{\phi}_i \end{Bmatrix} \tag{12}$$

Also, for the sake of comparison with the case of classical damping, the following notation, which was also used by Singh [43], is introduced:

$$s_i = -\xi_i\omega_i \pm i\omega_{D_i} \tag{13}$$

where ω_i, ω_{D_i}, and ξ_i are determined by

$$\omega_i = |s_i|,\ \ \xi_i = -\mathrm{Re}(s_i)/|s_i|,\ \text{and}\ \ \omega_{D_i} = \omega_i\sqrt{1-\xi_i^2} \tag{14}$$

In summary, for non-classically damped systems, the eigenvalue problem is complex and of order $2n$ and is given by Eq.11. The resulting mode shapes and frequencies $\{\boldsymbol{\phi}_i, s_i\}$ occur in conjugate pairs and can be expressed as in Eqs.12 and 13. For non-classical damping, $\boldsymbol{\phi}_i$ are complex vectors, in the special case of classical damping, $\boldsymbol{\phi}_i$ are real.

At this point, a physical interpretation of the meaning of complex mode shapes and frequencies is in order. The terms ω and ξ are the natural frequencies and damping ratios of the system with the same meaning as for classically damped systems. The complex values for the coordinates of a mode shape lead to different phase angles of the free vibration harmonic motions of the various degrees of freedom of the system [21]. This concept is illustrated in Fig.2.1 which shows a 2-DOF system with a mode shape given by $\phi_1 = [\ 1\ \ r\ ]^T$ and period T_1 at different time intervals during free vibration. It can be observed that the motion of each degree of freedom is out-of-phase with the other.

For a classically damped system, Eq.2 was reduced to n decoupled modal equations by transforming to modal coordinates. Likewise, for non-classically damped systems, Eq.9 can be reduced to $2n$ decoupled modal equations which occur in conjugate pairs by using the modal coordinates $\mathbf{z}$ obtained from the transformation $\mathbf{y}=\hat{\mathbf{\Phi}}\mathbf{z}$ where $\hat{\mathbf{\Phi}}=[\hat{\boldsymbol{\phi}}_1\hat{\boldsymbol{\phi}}_2\cdots\hat{\boldsymbol{\phi}}_{2n}]$. The ith modal equation is

$$A_i \dot{z}_i + B_i z_i = \hat{\boldsymbol{\phi}}_i^T \mathbf{F} \ddot{x}_g(t) \tag{15}$$

or alternatively

$$\dot{z}_i - s_i z_i = r_i \ddot{x}_g(t) \tag{16}$$

where

$$A_i = \hat{\boldsymbol{\phi}}_i^T \mathbf{A} \hat{\boldsymbol{\phi}}_i \tag{17a}$$

$$B_i = \hat{\boldsymbol{\phi}}_i^T \mathbf{B} \hat{\boldsymbol{\phi}}_i = -s_i A_i \tag{17b}$$

$$r_i = \hat{\boldsymbol{\phi}}_i^T \mathbf{F} / A_i = -\boldsymbol{\phi}_i^T \mathbf{M}\mathbf{r} / A_i \tag{17c}$$

The solution of the first-order equation Eq.16, is the integral

$$z_i = r_i \int_0^t \ddot{x}_g(\tau) \exp[s_i(t-\tau)]\, d\tau \tag{18}$$

which is analogous to Eq.6 for classically damped systems. Combining modal response quantities as before, one obtains

$$v = \mathbf{q}^T \mathbf{x} = \sum_{i=1}^{2n} \mathbf{q}^T \boldsymbol{\phi}_i z_i = \sum_{i=1}^{2n} b_i \int_0^t \ddot{x}_g(\tau) \exp[s_i(t-\tau)]\, d\tau \tag{19}$$

where

$$b_r = \mathbf{q}^T \boldsymbol{\phi}_r \tag{20}$$

Since b_r and s_r occur in conjugate pairs, $y(t)$ is always real.

In general, b_r is complex, however, if the system is classically damped, b_r is pure imaginary. In fact, for such systems

$$A_r = -\frac{1}{s_r} B_r = -\frac{1}{s_r}[\boldsymbol{\phi}_r^T \mathbf{K} \boldsymbol{\phi}_r - s_r^2 \boldsymbol{\phi}_r^T \mathbf{M} \boldsymbol{\phi}_r] = \left[\frac{\omega_r^2 - s_r^2}{-s_r}\right] M_r \tag{21}$$

where $M_r = \boldsymbol{\phi}_r^T \mathbf{M} \boldsymbol{\phi}_r$ is the conventional modal mass. Using Eq.13 for s_r and substituting the above result in the expression for b_r yields

$$b_r = \frac{(\mathbf{q}^T \boldsymbol{\phi}_r)(\boldsymbol{\phi}_r^T \mathbf{M} \mathbf{r})}{\pm 2 i \omega_{D_r} M_r} = \pm \frac{i \psi_r}{2 \omega_{D_r}} \tag{22}$$

for systems with classical damping

Up to this point, the analysis has been a review, and all of the above equations can be found in standard textbooks such as Hurty and Rubinstein [21]. However, the subsequent treatment of these equation is open to invention. Singh [43] used a straightforward method of analysis which led to a set of four simultaneous equations in the derivation of the power spectral density function of response to stationary random input. Here, these equations are expressed in terms of the Duhamel integral, which is helpful in deriving simpler and more direct expressions for the PSD and its moments.

Using the fact that b_r and s_r occur in conjugate pairs, and letting $b_{r'} = \bar{b}_r$ and $s_{r'} = \bar{s}_r$, where the superposed bar denotes the complex conjugate, Eq.19 can be written in the expanded form

$$\begin{aligned} y(t) &= \sum_{r=1}^{n} \left\{ b_r \int_0^t \ddot{x}_g(\tau) \exp[(-\xi_r \omega_r + i\omega_{D_r})(t-\tau)] d\tau \right. \\ &\qquad \left. + \bar{b}_r \int_0^t \ddot{x}_g(\tau) \exp[(-\xi_r \omega_r - i\omega_{D_r})(t-\tau)] d\tau \right\} \\ &= 2 \sum_{r=1}^{n} \left\{ -\mathrm{Im} b_r \int_0^t \ddot{x}_g(\tau) \exp[-\xi_r \omega_r (t-\tau)] \sin \omega_{D_r} (t-\tau) d\tau \right. \\ &\qquad \left. + \mathrm{Re} b_r \int_0^t \ddot{x}_g(\tau) \exp[-\xi_r \omega_r (t-\tau)] \cos \omega_{D_r} (t-\tau) d\tau \right\} \end{aligned} \tag{23}$$

For the special case of classical damping, it was noted that b_r is pure imaginary, therefore only

the first integral term appears in Eq.23, which is in agreement with Eq.8. For the general case of non-classical damping, a second integral expression with a cosine term appears in Eq.23 which is due to the phase differences arising from the complex mode shapes. The first integral can be directly expressed in terms of the Duhamel integral. The appearance of the cosine term in the second integral suggests that this expression can be obtained in terms of the derivative of the Duhamel integral

$$\dot{h}_j(t) = \int_0^t \ddot{x}_g(\tau)\exp[-\xi_j\omega_j(t-\tau)]\cos\omega_{dj}(t-\tau)\,d\tau \qquad \xi_j\omega_j h_j(t) \tag{24}$$

Substituting into Eq.23 yields

$$\begin{aligned} v(t) &= 2\sum_j^n \left\{-\mathrm{Im}b_j[\omega_{dj} h_j(t)] + \mathrm{Re}b_j[\dot{h}_j(t)+\xi_j\omega_j h_j(t)]\right\} \\ &= \sum_j^n [a_j h_j(t) + c_j \dot{h}_j(t)] \end{aligned} \tag{25}$$

where,

$$a_j = -2\mathrm{Re}(b_j\bar{s}_j), \quad c_j = 2\mathrm{Re}(b_j). \tag{26}$$

This formulation is considerably simpler than the earlier expression, Eq.23. It can readily be evaluated in the time domain for deterministic input using several well-known numerical methods for evaluating $h_j(t)$ and $\dot{h}_j(t)$ [5]. It is also in a form suitable for random vibration analysis, as shown in the next section.

Before continuing, several important features of Eq.25 should be pointed out. For classical damping, we recall that $b_j = i\psi_j/2\omega_{dj}$ so that $c_j=0$ and $a_j=\psi_j$, and Eq.25 reduces to Eq.8, as expected. Also, a relationship between c_j can be found by observing that for an impulsive load $\ddot{x}_g(t)=\delta(t)$, where $\delta(t)$ is the Dirac delta function, all displacements must be zero immediately after start at time $t=0^+$. It follows that $v(0^+)=0$ and $h_j(0^+)=0$. Also, $\dot{h}_j(0^+)=1$, as can be seen from Eq.24. Substituting into Eq.25

$$v(0^+) = \sum_{j=1}^n \left\{a_j h_j(0^+) + c_j \dot{h}_j(0^+)\right\} = \sum_{j=1}^n c_j = 0 \tag{27}$$

This fact will be important in subsequent developments in this paper.

2.3 Response to Base Input in Frequency Domain

In this section the autocorrelation function and PSD are derived. The simplicity of the expression for the response, Eq 25, allows for the derivation of closed form results with physical interpretations. This allows for a greater insight in the behavior of non-classically damped systems and is particularly suited for the analysis of PS systems in the next chapters. If the ground motion $\ddot{x}_0(t)$ is a stationary random process, the autocorrelation function of the stationary response $r(t)$ can be obtained as follows:

$$\begin{aligned} R_{rr}(\tau) &= E[r(t)r(t+\tau)] \\ &= \sum_i^n \sum_j^n \Big\{ a_i a_j E[h_i(t)h_j(t+\tau)] + a_i c_j E[h_i(t)\dot{h}_j(t+\tau)] \\ &\quad + a_j c_i E[\dot{h}_i(t)h_j(t+\tau)] + c_i c_j E[\dot{h}_i(t)\dot{h}_j(t+\tau)] \Big\} \end{aligned} \tag{28}$$

It is well known [28] that if $R_{ij}(\tau) \equiv E[h_i(t)h_j(t+\tau)]$ represents the cross-correlation function of $h_i(t)$ and $h_j(t)$, then

$$E[h_i(t)\dot{h}_j(t+\tau)] = R'_{ij}(\tau) \tag{29a}$$

$$E[\dot{h}_i(t)h_j(t+\tau)] = -R'_{ij}(\tau) \tag{29b}$$

$$E[\dot{h}_i(t)\dot{h}_j(t+\tau)] = -R''_{ij}(\tau) \tag{29c}$$

where a prime denotes differentiation with respect to τ. Thus the autocorrelation function simplifies to

$$R_{rr}(\tau) = \sum_i^n \sum_j^n [a_i a_j R_{ij}(\tau) + a_i c_j R'_{ij}(\tau) - a_j c_i R'_{ij}(\tau) - c_i c_j R''_{ij}(\tau)] \tag{30}$$

In order to find the power spectral density function of the response, the Fourier transforms of the above expressions must be derived. The transform $G_{ij}(\omega)$ of the cross-correlation functic $R_{ij}(\tau)$ is the cross spectral density of $h_i(t)$ and $h_j(t)$ and is given by

$$G_{ij}(\omega) = G_0(\omega) H_i(\omega) \bar{H}_j(\omega) \tag{31}$$

where $H_i(\omega)$ is the frequency response function for an oscillator of frequency ω_i and damping ξ_i

$$H_i(\omega) = \frac{1}{\omega_i^2 - \omega^2 + 2i\xi_i\omega_i\omega} \tag{32}$$

and $G_0(\omega)$ is the power spectral density function of the input process $\ddot{x}_0(t)$. From the basic

properties of Fourier transforms, $(i\omega G_{ij}(\omega), R'_{ij}(\tau))$ and $(-\omega^2 G_{ij}(\omega), R''_{ij}(\tau))$ are Fourier transform pairs. Thus, taking the Fourier transform of Eq.30, the power spectral density function for the response $x(t)$ is obtained:

$$G_{xx}(\omega) = \sum_{i=1}^{n}\sum_{j=1}^{n}[C_{ij} + i\omega D_{ij} + \omega^2 E_{ij}]G_{ij}(\omega) \tag{33}$$

where,

$$C_{ij} = a_i a_j, \quad D_{ij} = (a_i c_j - a_j c_i), \text{ and } E_{ij} = c_i c_j \tag{34}$$

This is a generalization of the power spectral density function of a system with classical damping. As was demonstrated earlier, b_i is a pure imaginary number for classically damped systems; therefore, $c_i = c_j = 0$, and $D_{ij} = E_{ij} = 0$. The remaining coefficient C_{ij} is evaluated using Eq.20 and Eq.26. It turns out for this case that Eq.33 reduces to the well known power spectral density function for classically damped systems [10, 15]

$$G_{xx}(\omega) = \sum_{i=1}^{n}\sum_{j=1}^{n}\psi_i \psi_j G_{ij}(\omega) \tag{35}$$

The difference between the above and the more general expression in Eq.33 for non-classically damped systems is the inclusion of extra terms which arise due to the phase effects in the modal responses.

2.4 Spectral Moments of Response

As stated in the Introduction, most statistical measures of the response that are of engineering interest are obtained in terms of the first few spectral moments λ_m, i.e. for m=0,1,2, and 4. Substituting Eq.33 into the integral in Eq.1, the following expression is obtained for the m-th moment

$$\lambda_m = \sum_{i=1}^{n}\sum_{j=1}^{n}\{C_{ij}\mathrm{Re}\lambda_{m,ij} - D_{ij}\mathrm{Im}\lambda_{m+1,ij} + E_{ij}\mathrm{Re}\lambda_{m+2,ij}\} \tag{36}$$

where,

$$\lambda_{m,ij} = \int_0^{\infty}\omega^m G_{ij}(\omega)\,d\omega = \int_{-\infty}^{\infty}\omega^m G_{ih}(\omega) H_j(\omega)\overline{H_j(\omega)}\,d\omega \tag{37}$$

are cross spectral moments associated with $h_i(t)$ and $h_j(t)$.

For the case of classical damping $D_j=E_j=0$ and Eq.36 reduces to

$$\lambda_m = \sum_{j=1}^{n}\sum_{k=1}^{n}\psi_j\psi_k \mathrm{Re}\lambda_{m,jk} \tag{38}$$

which is the same formulation derived by Der Kiureghian [15]. The phase shift in the eigenvectors caused by non-classical damping results in the appearance of higher order moment terms in Eq.36.

The next topic to consider is the important question of convergence of the integral in Eq.37. In previous work, this topic did not receive adequate mathematical clarification, and divergent expressions were left unresolved (e.g., Vanmarke, Ref. 44, pp.437, Eq.44). If the power spectral density function is band limited, i.e. if there is a cutoff frequency ω_0 such that $G_j(\omega)=0$ for all frequencies ω greater than ω_0, then it is clear that the integral for the cross spectral moments in Eq.37 converges for all positive values of m. Thus the moments λ_m, which is a sum of terms involving $\lambda_{m,jk}$, $\lambda_{m,(j+1)k}$, and $\lambda_{m,(j+2)k}$, can be found for any order. However, many theoretical power spectral density functions are not band limited. For large ω, the integrand terms $H_j(\omega)$ and $\overline{H_j(\omega)}$ have the following behavior:

$$\mathrm{Re}\omega^m H_j(\omega)\overline{H_j(\omega)} \to \omega^{m-4} \tag{39a}$$

$$\mathrm{Im}\omega^m H_j(\omega)\overline{H_j(\omega)} \to \omega^{m-3} \tag{39b}$$

Since the entire integrand must be of order smaller than ω^{-1} for large ω to insure convergence, it follows that the integral for $\lambda_{m,jk}$ will converge only if $G_{jk}(\omega)$ is of order smaller than $\omega^{-(m-3)}$ for $\omega\to\infty$. For instance, for white-noise input, where $G_{jk}(\omega)\equiv G_{jk}$ is a constant, $\lambda_{m,jk}$ will converge only for $m<3$. It appears that for this input, the moments λ_m from Eq.36 would only exist for $m=0$. However, for classically damped systems, λ_m is a sum of terms only involving $\lambda_{m,jj}$, so the moment exists for $m=0,1$, and 2. From intuitive considerations, the same moments which exist for classically damped systems should also exist for non-classically damped systems. In other words, if $m=m_0$ is the highest existing order for the cross spectral moments $\lambda_{m,jk}$, then m_0 should also be the highest order for the moment λ_m for both classically damped and non-classically damped structures. This hypothesis will be proven, presently.

Eq.36 can be rewritten in the following form:

$$\lambda_{m} = \sum_{i=1}^{m}\sum_{j=1}^{n}\left\{C_{ij}\mathrm{Re}\lambda_{m-i,j-1} - D_{ij}\mathrm{Im}\lambda_{m-i,j-1}\right\} + \int_{0}^{\infty}\mathrm{Re}\sum_{i=1}^{m}\sum_{j=1}^{n}E_{ij}\omega^{m-i+1}G_{ij}(\omega)\,d\omega \tag{40}$$

If $\lambda_{m,n}$ exists, then $\mathrm{Im}\lambda_{m+1,n-1}$ also exists from the relations Eqs.39a,b. Thus, only the last term in Eq.40 must be tested for convergence.

The problem is that the summation and the infinite integral cannot be interchanged: the form of the expression above converges, yet the alternate formulation with the summation outside the integral diverges. This same problem arises in the previously referenced equation in Vanmarke's study. The problem is solved by rewriting the integrand term $G_{ij}(\omega)$ as a sum of two components, one which vanishes under the summation and the other, defined as a modified power spectral density $G'_{ij}(\omega)$, which converges when the summation and integral is interchanged.

First, $G'_{ij}(\omega)$ is found by subtracting the dominant term from $G_{ij}(\omega)$. Since $H_i(\omega)\overline{H_j(\omega)}$ tends to ω^{-4} for large ω, the dominant term is simply $\omega^{-4}G_{ij}(\omega)$. From partial fraction expansions, it can be shown that the difference,

$$G_{ij}(\omega) - \omega^{-4}G_{ij}(\omega) \to \omega^{-6}G_{ij}(\omega) \qquad \text{for large } \omega \tag{41}$$

The above could be used for the modified power spectral density $G'_{ij}(\omega)$ except that the second term diverges at ω near 0. To correct for this, the following definition is used:

$$G'_{ij}(\omega) = \begin{cases} G_{ij}(\omega) - \omega^{-4}G_{ij}(\omega) & \omega \geq \omega_0 \\ G_{ij}(\omega) & 0 \leq \omega < \omega_0 \end{cases} \tag{42}$$

where ω_0 is any fixed, arbitrary positive frequency. The corresponding modified cross-spectral moment is

$$\lambda'_{m,n} = \int_{0}^{\infty}\omega^{m}G'_{ij}(\omega)\,d\omega \tag{43}$$

which converges because of the relation in Eq.41.

What remains to be shown is that the above expression for $\lambda'_{m+2,n}$ can be substituted into Eq.36 without changing the value for $\lambda_{m,n}$. The last term in Eq.40 can be rewritten

$$\int_{0}^{\infty}\mathrm{Re}\sum_{i=1}^{m}\sum_{j=1}^{n}E_{ij}\omega^{m-i+1}G_{ij}(\omega)\,d\omega$$

$$= \int_{0}^{\omega_0}\mathrm{Re}\sum_{i=1}^{m}\sum_{j=1}^{n}E_{ij}\omega^{m-i+1}G'_{ij}(\omega)\,d\omega + \int_{\omega_0}^{\infty}\mathrm{Re}\sum_{i=1}^{m}\sum_{j=1}^{n}E_{ij}\omega^{m-i+1}[G'_{ij}(\omega)+\omega^{-4}G_{ij}(\omega)]\,d\omega$$

$$= \sum_{j=1}^{n}\sum_{k=1}^{n} E_{jk}\,\mathrm{Re}\lambda'_{jk} + \int_{\omega_0} \mathrm{Re}\omega^{m-2} G_0(\omega) \sum_{j=1}^{n}\sum_{k=1}^{n} E_{jk}\, d\omega \tag{44}$$

Since $\sum_{j=1}^{n}\sum_{k=1}^{n} E_{jk} = \sum_{j=1}^{n} c_j \sum_{k=1}^{n} c_k = 0$ (see Eq.27), the last integral in the above is zero, and it has been shown that the remaining expression is well-defined. Thus, the original hypothesis is proven, and by combining the above with Eq.40, the final expression for the moment λ_m is obtained:

$$\lambda_m = \sum_{j=1}^{n}\sum_{k=1}^{n} \{C_{jk}\,\mathrm{Re}\lambda_{jk}^{m} - D_{jk}\,\mathrm{Im}\lambda_{jk}^{m} + E_{jk}\,\mathrm{Re}\lambda'^{m}_{jk}\} \tag{45}$$

which exists for the same values for m as the corresponding expression for classically damped systems, Eq.38. Note the similarity in form of the expressions in Eqs.45 and 36. In the following, the preceding equation will be used in general with the understanding that the primed moments need be used only when the unprimed moments do not exist.

The above expressions for the spectral moments of response are general. Also, the form of these expressions allow for further analysis and insight into the properties and dynamic response of non-classically damped systems. The evaluation of λ_m has been separated to two independent problems: the calculation of the coefficients C_{jk}, D_{jk}, and E_{jk}, and the determination of the generic cross spectral moments λ_{jk}^{m}. The first problem is one of dynamics and is concerned entirely with the properties of the structural system. Using tools of dynamic analysis, this problem can be routinely solved; for PS systems, procedures are developed for finding analytical and closed form solutions in the remaining chapters of this study. The second problem is one of random vibrations and is concerned with the properties of the input excitation and the frequencies and damping ratios of the system. For any stationary input process with power spectral density function $G_0(\omega)$, the generic integrals in Eqs.37 and 43 can be calculated either by the method of residues, partial fractions, or by numerical integration. Below, closed form solutions are found for these cross-moments for the important case of white noise input. These results form the basis for a response spectrum method for seismic response of non-classically damped systems which is presented at the end of this chapter.

The expression in Eq.25 can also be used for the study of nonstationary input with results that are more general and complicated than those for stationary input. Clearly, the generic cross-correlation function $R_{ij}(t_1,t_2) = E[h_i(t_1)h_j(t_2)]$, and its partial derivatives need to be evaluated. The results of such an approach would be in essence equivalent to the method of Debchandhury et. al. [14]. However, this formulation may yield simpler and more tractable results. This study will be reported in the future.

2.5 Response to White-Noise Input

Attention is drawn to the evaluation of structural response to white-noise input, where $G_0(\omega) \equiv G_0$ is a constant. This special case is important from an analytical viewpoint and is studied in most random vibrations textbooks [28]. The results of the analysis for white noise input are generally simple to interpret and are helpful in the study of more general forms of input. In addition, in this study, the results for the response to white noise input form the basis for the response spectrum method to be presented in Section 2.7.

Using the method of partial fractions and method of residues, closed form solutions for Eqs.37 and 43 have been obtained for all cross-spectral moments required for determining the first three spectral moments λ_0, λ_1, and λ_2 of the response process. It is noted that moments higher than λ_2 for the response to white-noise input do not exist.

The cross spectral moments for response to white-noise input G_0 are

$$\mathrm{Re}\lambda_{0,ij} = \left\{\omega_i\xi_i + \omega_j\xi_j\right\}\frac{2\pi G_0}{K_{ij}} \tag{46a}$$

$$\mathrm{Re}\lambda_{1,ij} = \left\{[(\omega_i^2+\omega_j^2)\xi_i + 2\omega_i\omega_j\xi_j]\frac{1}{\beta_i}\tan^{-1}\frac{\beta_i}{\xi_i} + [(\omega_j^2+\omega_i^2)\xi_j + 2\omega_i\omega_j\xi_i]\frac{1}{\beta_j}\tan^{-1}\frac{\beta_j}{\xi_j} - (\omega_j^2-\omega_i^2)\log\frac{\omega_i}{\omega_j}\right\}\frac{G_0}{K_{ij}} \tag{46b}$$

$$\mathrm{Im}\lambda_{1,ij} = \left\{-\omega_i^2+\omega_j^2\right\}\frac{\pi G_0}{K_{ij}} \tag{46c}$$

$$\mathrm{Re}\lambda_{2,ij} = \left\{\omega_i\xi_i + \omega_j\xi_j\right\}\omega_i\omega_j\frac{2\pi G_0}{K_{ij}} \tag{46d}$$

$$\mathrm{Im}\lambda_{2,ij} = \left\{[-\omega_i^2+\omega_j^2+2\omega_j\xi_j(\omega_i\xi_i+\omega_j\xi_j)]\frac{\omega_i}{\beta_i}\tan^{-1}\frac{\beta_i}{\xi_i}\right.$$

$$+ \{-\omega_i^2+\omega_j^2-2\omega_i\xi_i(\omega_i\xi_i+\omega_j\xi_j)\}\frac{\omega_i}{\beta_i}\tan^{-1}\frac{\beta_i}{\xi_i}$$

$$- 2\omega_i\omega_j(\omega_i\xi_i+\omega_j\xi_j)\log\frac{\omega}{\omega_i}\Bigg\}\frac{G_0}{K_{ij}} \tag{46e}$$

$$\mathrm{Re}\lambda'_{3,ij} = \Bigg\{[3\omega_i^2\xi_i+2\omega_i\omega_j\xi_j-\omega_j^2\xi_i-4\omega_i\xi_i^2(\omega_i\xi_i+\omega_j\xi_j)]\frac{\omega_i^2}{\beta_i}\tan^{-1}\frac{\beta_i}{\xi_i}$$

$$+ [3\omega_j^2\xi_j+2\omega_i\omega_j\xi_i-\omega_i^2\xi_j-4\omega_j\xi_j^2(\omega_i\xi_j+\omega_j\xi_j)]\frac{\omega_j^2}{\beta_j}\tan^{-1}\frac{\beta_j}{\xi_j}$$

$$+ \frac{1}{2}[-\omega_i^4+\omega_j^4+4(\omega_i^2\xi_i^2-\omega_j^2\xi_j^2)]\log\frac{\omega_i}{\omega_j}\Bigg\}\frac{G_0}{K_{ij}} \tag{46f}$$

$$\mathrm{Im}\lambda_{3,ij} = \Bigg\{\omega_i^4-\omega_j^4-4\omega_i\omega_j(\omega_i\xi_i-\omega_j\xi_j)(\omega_i\xi_j+\omega_j\xi_i)\Bigg\}\frac{\pi G_0}{2K_{ij}} \tag{46g}$$

$$\mathrm{Re}\lambda'_{4,ij} = \Bigg\{\omega_i\xi_i[\omega_j^4+2\omega_i^2\omega_j^2-\omega_i^4] + \omega_j\xi_j[-\omega_i^4+2\omega_i^2\omega_j^2+\omega_j^4]$$

$$- 4\omega_i\omega_j(\omega_i\xi_j+\omega_j\xi_i)(\omega_i^2\xi_i^2+\omega_j^2\xi_j^2)\Bigg\}\frac{\pi G_0}{K_{ij}} \tag{46h}$$

where,

$$K_{ij} = (\omega_i^2-\omega_j^2)^2 + 4\omega_i\omega_j(\omega_i\xi_i+\omega_j\xi_j)(\omega_i\xi_j+\omega_j\xi_i) \tag{47a}$$

$$\beta_i = \sqrt{1-\xi_i^2} \tag{47b}$$

For the calculation of $\mathrm{Re}\lambda'_{3,ij}$ and $\mathrm{Re}\lambda'_{4,ij}$, the transition frequency ω_0 used in Eq.42 was set to 1 and 0, respectively. Note that results for these cross-moment terms would be different for other selections of ω_0, but the final result for λ_{ij} would remain unchanged. When the indices i and j are equal, the imaginary parts of the moments become 0 and the real parts reduce to:

$$\lambda_{0,ii} = \frac{\pi G_0}{4\xi_i\omega_i^3} \tag{48a}$$

$$\lambda_{1,ii} = \frac{\pi G_0}{4\xi_i\omega_i^2}\frac{2}{\pi\beta_i}\tan^{-1}\frac{\beta_i}{\xi_i} \tag{48b}$$

$$\lambda_{2,ii} = \frac{\pi G_0}{4\xi_i\omega_i} \tag{48c}$$

$$\lambda'_{3,ii} = \frac{\pi G_0}{4\xi_i}\frac{2(1-2\xi_i^2)}{\pi\beta_i}\tan^{-1}\frac{\beta_i}{\xi_i} \tag{48d}$$

$$\lambda'_{4,ii} = \frac{\pi G_0\omega_i}{4\xi_i}(1-4\xi_i^2) \tag{48e}$$

Good, simple approximations for the above expressions for the cross moments can be made if the damping terms are reasonably small. The error will be of the order ξ_i^2 and ξ_j^2, e.g. if the damping is about 20% the error is only 4%. The approximations are

$$\mathrm{Re}\lambda_{0,ij} = \frac{2\pi G_0}{K_{ij}}\left[\omega_i\xi_i+\omega_j\xi_j\right] \tag{49a}$$

$$\mathrm{Re}\lambda_{1,ij} = \frac{2\pi G_0}{K_{ij}}\left[\frac{1}{4}(\omega_i+\omega_j)^2(\xi_i+\xi_j) - \frac{1}{2\pi}(\omega_i^2-\omega_j^2)\log\frac{\omega_i}{\omega_j}\right] \tag{49b}$$

$$\mathrm{Im}\lambda_{1,ij} = \frac{2\pi G_0}{K_{ij}}\left[\frac{-\omega_i^2+\omega_j^2}{2}\right] \tag{49c}$$

$$\mathrm{Re}\lambda_{2,ij} = \frac{2\pi G_0}{K_{ij}}\left[\omega_i\xi_j+\omega_j\xi_i\right]\omega_i\omega_j \tag{49d}$$

$$\mathrm{Im}\lambda_{2,ij} = \frac{2\pi G_0}{K_{ij}}\left[\frac{1}{4}(-\omega_i^2+\omega_j^2)(\omega_i+\omega_j) - \frac{\omega_i\omega_j}{\pi}(\omega_i\xi_j+\omega_j\xi_i)\log\frac{\omega_i}{\omega_j}\right] \tag{49e}$$

$$\mathrm{Re}\lambda'_{3,ij} = \frac{2\pi G_0}{K_{ij}}\left\{\frac{1}{4}\left[-\omega_i^4\xi_j+2\omega_i^3\omega_j\xi_i+3\omega_i^2\omega_j^2(\xi_i+\xi_j)+2\omega_i\omega_j^3\xi_j-\omega_j^4\xi_i\right] + \frac{1}{4\pi}\left[-\omega_i^4+\omega_j^4\right]\log\frac{\omega_i}{\omega_j}\right\} \tag{49f}$$

$$\mathrm{Im}\lambda_{3,ij} = \frac{2\pi G_0}{K_{ij}}\left[\frac{\omega_j^4-\omega_i^4}{4}\right] \tag{49g}$$

$$\mathrm{Re}\lambda'_{4,ij} = \frac{2\pi G_0}{K_{ij}}\left[\frac{\omega_i\xi_i}{2}(\omega_i^4+2\omega_i^2\omega_j^2-\omega_j^4) + \frac{\omega_j\xi_j}{2}(-\omega_i^4+2\omega_i^2\omega_j^2+\omega_j^4)\right] \tag{49h}$$

$\mathrm{Re}\lambda_{0,ij}$, $\mathrm{Re}\lambda_{1,ij}$, and $\mathrm{Re}\lambda_{2,ij}$ were previously given in the earlier report by Der Kiureghian [15] for systems with classical damping, as they are the only cross moments needed to evaluate λ_0, λ_1, and λ_2 for such systems. The results for $\mathrm{Re}\lambda_{0,ij}$, $\mathrm{Re}\lambda_{1,ij}$, and $\mathrm{Re}\lambda_{2,ij}$ were also previously known [15, 44]. The remaining solutions shown above, which are needed for non-classically damped systems, are new results.

For further insight into the nature of the above terms, the following coefficients are introduced:

$$\rho_{m,ij} = \frac{\mathrm{Re}\lambda_{m,ij}}{\sqrt{\lambda_{m,ii}\lambda_{m,jj}}} \tag{50a}$$

$$\rho'_{m,ij} = \frac{\mathrm{Re}\lambda'_{m,ij}}{\sqrt{\lambda'_{m,ii}\lambda'_{m,jj}}} \tag{50b}$$

$$\eta_{m,ij} = \frac{\mathrm{Im}\lambda_{m,ij}}{\sqrt{\lambda_{m,ii}\lambda_{m,jj}}} \tag{50c}$$

Note that $\rho_{0,ij}$, $\rho_{2,ij}$, and $\rho_{4,ij}$ represent correlation coefficients between the zeroeth, first, and second derivatives of $h_i(t)$ and $h_j(t)$, respectively. The coefficients, $\rho_{0,ij}$, $\rho'_{3,ij}$ and $\eta_{1,ij}$, are plotted for various values of damping and frequency ratios in Fig.2.2. Results for other values

of m are similar and, therefore, are not shown. As expected, $\rho_{r,s}$ and $\rho'_{r,s}$ behave like correlation coefficients, diminishing rapidly as the two frequencies depart, particularly at small damping. Thus, cross modal terms $\mathrm{Re}\lambda_{r,s}$ and $\mathrm{Re}\lambda'_{r,s}$ in Eq.45 are significant only for modes with closely spaced frequencies. The plots indicate that $\eta_{r,s}$ behaves quite differently from $\rho_{r,s}$. For moderately spaced frequencies, it can be seen that while $\rho_{r,s}$ is negligible, the corresponding values for $\eta_{r,s}$ are significant. It appears that the cross modal terms $\mathrm{Im}\lambda_{r,s}$ in Eq.45 may be important with moderately spaced frequencies. However, preliminary example studies have shown that the coefficients D_r in Eq.45 are generally very small.

2.6 Examples

The simplest system having non-classical damping is the 2-degree-of-freedom system in Fig.2.3. This system has been the subject of considerable study in the past. Crandall and Mark [11] and Curtis and Boykin [12] used frequency response function approaches to find the response of this system to white noise input. Their methods, as well as the modal decomposition method developed here are exact, consequently the corresponding results of the analysis of the 2-DOF system agree.

The examples in this Section are chosen to illustrate the effect of non-classical damping. It can be shown that the 2-DOF system is classically damped if and only if the ratio of spring stiffnesses is equal to the ratio of damping coefficients:

$$\frac{k_1}{k_2} = \frac{c_1}{c_2} \tag{51}$$

If the two ratios are not equal, then in the mathematically strict sense, the system is non-classically damped. As stated in the introduction, a common approximate approach in the analysis of non-classically damped structures is to use the free vibration mode shapes and to ignore the off-diagonal terms of the transformed damping matrix to eliminate modal coupling. For certain values of the parameters of the 2-degree-of-freedom system, this approximation appears reasonable. However, an analytical and numerical study of the system revealed two distinct and well-defined sets of parameter values where this classically damped approximation

becomes inaccurate and inappropriate

The first case is the well-known soil-structure system where the damping ratios of the soil (substructure 1) and structure (substructure 2) are significantly different. The second case is the equipment-structure system where the mass ratio $\epsilon=m_2/m_1$ is small, the frequency ratio is close to 1 (tuning), and the difference of the damping ratios satisfies the following inequality:

$$(\xi_1-\xi_2)^2 > \epsilon \tag{52}$$

To illustrate the differences between the approximate classically damped approach and the exact non-classically damped approach, a parameter study was made of the 2-degree-of-freedom soil-structure and equipment-structure systems using the 2 methods of analysis. In the soil structure study, the following fixed parameters were chosen: average damping ratio $\xi_a=(\xi_1+\xi_2)/2=0.20$, mass ratio $\epsilon=m_2/m_1=0.3$, and frequency ratio $\omega_2/\omega_1=1.0$. In the equipment-structure study, the following parameters were chosen: average damping ratio $\xi_a=0.04$, mass ratio $\epsilon=0.001$, and the frequency ratio $\omega_2/\omega_1=1.0$. In both systems, the independent variable was the difference between the damping ratios $\xi_1-\xi_2$. The relative displacement between the two masses was chosen as the response quantity of interest. The first three moments of response to white-noise input were computed using Eq.38 for the classically damped approximation and Eq.45 for the exact results.

From the first three moments, the mean square, λ_0, the mean zero-crossing rate, $\nu=\sqrt{\lambda_2/\lambda_0}/\pi$, and the shape factor, $\delta=\sqrt{1-\lambda_1^2/(\lambda_0\lambda_2)}$, were found and compared. The two approaches yielded very similar values for ν, however, a more significant difference of values were found for δ and λ_m and these variables are plotted for the various 2-degree-of-freedom systems in Figs.2.4 and 2.5. To gain further insight to the three sets of terms in the expression for λ_m in Eq.45, the percentage of the contributions of the terms:

$$\sum_{i=1}^{n}\sum_{j=1}^{n} C_{ij}\mathrm{Re}\lambda_{0,ij}\ ,\quad \sum_{i=1}^{n}\sum_{j=1}^{n} D_{ij}\mathrm{Im}\lambda_{1,ij}\ ,\ \text{and}\ \ \sum_{i=1}^{n}\sum_{j=1}^{n} E_{ij}\mathrm{Re}\lambda_{2,ij} \tag{53}$$

to the total sum, λ_0, is plotted in Fig.2.6.

For both systems, the condition Eq.51 is satisfied when the difference of damping ratios is

zero, therefore the systems are classically damped. Thus, the classically damped approximation yields exact results, as can be seen in Figs.2.4 and 2.5 and the D_{ij} and E_{ij} terms are zero as shown in Fig.2.6. As the difference of damping ratios increases, the character of the system changes from classical damping to non-classical damping. From Figs.2.4 and 2.5 it is apparent that the effect of non-classical damping is not adequately accounted for in the classical damping approximations. This effect is also visible in Fig.2.6, where the E_{ij} terms become prominent for systems with increasing non-classical damping character. This is pronounced in equipment-structure systems with properties satisfying the inequality, Eq.52. This phenomena is discussed more fully in the next chapter.

It should be noted that for all 2-degree-of-freedom systems, the D_{ij} terms in Eq.45 are essentially zero. This phenomenon is a characteristic of the simplicity of the system itself. A more complex 3-degree-of-freedom system was studied and compared with the results of the 2-degree-of-freedom system. Due to the larger number of parameters, the relationships between the parameters and the degree of non-classical damping was less clear. However, from the numerical results it could be generalized that the key parameters were the same as was observed for the 2-degree-of-freedom system, i.e., the difference of damping ratios and the mass ratio. However, unlike the 2-degree-of-freedom system, the D_{ij} terms in Eq.45 were no longer negligible, particularly for soil-structure-type systems.

2.7 Development of the Response Spectrum Method

In this final section, the above results are extended to input specified by its response spectrum. Since the response spectrum is an incomplete description of the input, the method to be developed is necessarily approximate. The proposed method will be most accurate when the input is wide band, has a long stationary duration (several times longer than the fundamental period), and the significant modes of vibration are within the dominant frequencies of vibration.

In order to develop the response spectrum method, Eq.45 is rewritten in the form

$$\lambda_m = \sum_{i=1}^{n}\sum_{j=1}^{n}\left[C_{ij}\rho_{m,ij}w_{m,ij} - D_{ij}\eta_{m,ij}w_{m+1,ij} + E_{ij}\rho_{m+2,ij}w_{m+2,ij}\right]\sqrt{\lambda_{0,ii}\lambda_{0,jj}} \tag{54}$$

where $\rho_{m,ij}$, $\rho'_{m,ij}$, $\eta_{m,ij}$ are defined in Eqs.50a-c, and

$$w_{m,ij} = \frac{\sqrt{\lambda_{m,ii}\lambda_{m,jj}}}{\sqrt{\lambda_{0,ii}\lambda_{0,jj}}} \tag{55}$$

Now we introduce two sets of approximations. The first approximation is to derive expressions for the coefficients $\rho_{m,ij}$, $\eta_{m,ij}$ and $w_{m,ij}$ in terms of the system parameters and independent of the input excitation. Let $\omega_d=(\omega_i+\omega_j)/2$, $\xi_d=(\xi_i+\xi_j)/2$, $\omega_d=\omega_i-\omega_j$, and $\xi_d=\xi_i-\xi_j$. Employing the assumption that the input is a wide-band process, and following the procedure in Ref. 16, it can be shown using results in Eqs.46 for white-noise input, that the following are good approximations

$$\rho_{0,ij} \approx R_{ij}[4\xi_d + \xi_d\omega_d/\omega_d], \quad \rho_{1,ij} \approx R_{ij}[4\xi_d - 2\omega_d^2/(\omega_d^2\pi)] \tag{56a}$$

$$\rho_{2,ij} \approx R_{ij}[4\xi_d - \xi_d\omega_d/\omega_d], \quad \rho'_{3,ij} \approx R_{ij}[4\xi_d + \omega_d^2/(\omega_d^2\pi)] \tag{56b}$$

$$\rho'_{4,ij} \approx \rho_{0,ij} \tag{56c}$$

where $R_{ij} = \omega_0^2\sqrt{\xi_i\xi_j}/[\omega_d^2 + 4\omega_0^2\xi_d^2]$, and

$$\eta_{m,ij} = 2R_{ij}\frac{\omega_d}{\omega_d}, \quad w_{m,ij} = \begin{cases} (\omega_i\omega_j)^{m/2} & \text{for } m \text{ even} \\ (\omega_i\omega_j)^{m/2}\left[\left(1-\frac{2\xi_i}{\pi}\right)\left(1-\frac{2\xi_j}{\pi}\right)\right]^{1/2} & \text{for } m \text{ odd} \end{cases} \tag{57}$$

The second approximation applied to Eq.54 is to estimate the modal spectral moments $\lambda_{0,ii}$ in terms of the input response spectrum. Let $\bar{S}_\tau(\omega,\xi)$ be the mean response spectrum representing the mean value of the maximum absolute response of an oscillator over the duration τ of its the input excitation, where ω and ξ are the oscillator frequency and damping values, respectively. Then, for $\omega=\omega_i$ and $\xi=\xi_i$, the mean response spectrum ordinate can be given in terms of the spectral moment $\lambda_{0,ii}$ [16]

$$\bar{S}_{i\tau} = \bar{S}_\tau(\omega_i,\xi_i) = p_i\sqrt{\lambda_{0,ii}} \tag{58}$$

where p_i is a peak factor associated with mode i which can be derived in terms of system parameters as described below. Substituting the above into Eq.54 yields, for $m=0,1,2$,

$$\lambda_m = \sum_{i=1}^{n}\sum_{j=1}^{n}\left[C_{ij}\rho_{m,ij}w_{m,ij} - D_{ij}\eta_{m,ij}w_{m+1,ij} + E_{ij}\rho_{m+2,ij}w_{m+2,ij}\right]\frac{1}{p_ip_j}\bar{S}_{i\tau}\bar{S}_{j\tau} \tag{59}$$

The above equation provides a modal superposition rule for the spectral moments of response directly in terms of the response spectrum ordinates. These moments can be used to derive various important expressions of the response. In particular, the root-mean-square, and the mean and standard deviation of the peak response over duration τ are given, respectively, by $\sqrt{\lambda_0}$, $p\sqrt{\lambda_0}$, and $q\sqrt{\lambda_0}$, where p and q are peak factors given by [15]

$$p = \sqrt{2\ln\nu_e\tau} + \frac{0.5772}{\sqrt{2\ln\nu_e\tau}} \quad \text{and} \quad q = \frac{1.2}{\sqrt{2\ln\nu_e\tau}} - \frac{5.4}{13+(2\ln\nu_e\tau)^{3/2}} \tag{60}$$

in which

$$\nu_e\tau = \begin{cases} \max(2.1,\ 2\delta\nu\tau), & 0<\delta\leqslant 0.1 \\ (1.638^{0.45}-0.38)\nu\tau, & 0.1<\delta\leqslant 0.69 \\ \nu\tau, & 0.69<\delta\leqslant 1 \end{cases} \tag{61}$$

and $\nu = \sqrt{\lambda_2/\lambda_0}/\pi$ and $\delta = \sqrt{1-\lambda_1^2/\lambda_0\lambda_2}$. Eqs. 60 and 61 are also used in deriving the modal peak factors p_i, in which case $\nu = \omega_i/\pi$ and $\delta = 2\sqrt{\xi_i/\pi}$ [16]. Furthermore, having the three spectral moments one may derive the probability distribution of the peak response as given by Ref.45.

In practical applications, the mean of the peak response is of most interest. If the ratios of peak factors p/p_i are approximated by unity [16], a simplified expression for the mean peak response $\bar{R}_\tau$ is

$$\bar{R}_\tau = \left[\sum_{i=1}^{n}\sum_{j=1}^{n}\left(C_{ij}\rho_{0,ij} - D_{ij}\eta_{1,ij}w_{1,ij} + E_{ij}\rho_{2,ij}w_{2,ij}\right)\bar{S}_{i\tau}\bar{S}_{j\tau}\right]^{1/2} \tag{62}$$

This expression is a generalization of the CQC method introduced in Refs.16 and 50 for classically damped systems.

As an example application of the response spectrum method, a simple system composed of a foundation, structure, and light equipment, described in Fig.2.7 and Table 1, is studied. The modes of each fixed base subsystem have different damping ratios, as shown in Table 2, and as a result, the combined assemblage is characterized by non-classical damping.

Twenty simulated motions and their mean response spectrum were used for input in the analysis. The mean and standard deviation of the peak response of the equipment displacement

relative to the foundation were obtained by using the modal combination rule of the proposed response spectrum method and the results compared with solutions obtained by the modal decomposition rule using a classical damping assumption (i.e., off-diagonal terms in the modal damping matrix were ignored) and exact solutions obtained from the numerical integration of the ground time histories. The results of the comparison, shown in Table 3, show that the response spectrum method is in close agreement with the simulation results and that the effect of non-classical damping can not be ignored in the analysis.

2.8 Summary and Conclusions

The response of multi-degree-of-freedom non-classically damped linear systems to stationary input excitation is examined and a modal decomposition method is developed employing the complex eigenvalues and eigenvectors of the system. A general formula for the spectral moments is derived and compared with the results for the special case of classical damping. The evaluation of these expressions involves two relatively independent problems. One is a dynamics problem in finding a set of coefficients in terms of the free vibration modal properties of the system under study. The other is a random vibrations problem in finding the cross-spectral moments in terms of the input process. Procedures for finding the coefficients for PS systems are derived in the next chapters. For other systems, standard eigenvalue methods can be applied. The cross-spectral moments can be computed by the method of residues, partial fractions, or by direct integration for general input processes.

Closed form solutions for the cross-moments have been derived for the important case of white-noise input. These results were subsequently used to develop a response spectrum method of analysis for non-classically damped systems. This method is based on a set of approximations that were successfully used in previous works for classically damped systems [16, 50] and includes peak factors in the formulation, which are known to be of importance in the study of PS systems [18].

Example studies for simple systems have shown that non-classical damping occurs primarily in two types of systems: soil-structure-type systems, where the difference of damping

ratios is large; and equipment-structure-type systems, where the mass ratio is small and the damping ratios are unequal. It is found that as the difference of the damping ratios increases or the mass ratio decreases, the classically damped approximation to the response becomes less accurate.

In general, for structures with classical damping or slight non-classical damping characteristics, the free vibration mode shapes and the decoupled modal equations, Eq.4, provide a suitable approximation to the true structural behavior. For such systems, the moments of the power spectral density function of response, Eq.38, have a relatively simple form. However, for structures which have predominantly non-classical damping characteristics, such as the soil-structure and equipment-structure systems, the damping matrix produces significant coupling of the free vibration mode shapes and the classically damped approximation is no longer justifiable. This is shown numerically by the examples and mathematically by the more complex expressions for the moments of response, Eq.45.

Table 2.1. Physical Properties of Example System

Subsystem	Frequency (rad/s)	Damping Ratio
Equipment	12.00	0.0100
Structure	4.58	0.0191
	12.00	0.0500
Foundation	11.70	0.3000

Table 2.2. Modal Properties of Fixed Base Subsystems

DOF	Mass (kg)	Interstory Stiffness (kN/m)	Interstory Damping (kN/(m/s))
1	0.1	14.4	0.024
2	200.0	11000.	91.6
3	200.0	11000.	91.6
4	600.0	82100.	4210.0

Table 3. Analysis Results: Equipment Response

Response, m	Exact	Approx.	Classical
$\bar{R}_r$	0.106	0.113	0.046
$\sigma_{\dot{R}_r}$	0.020	0.020	0.011

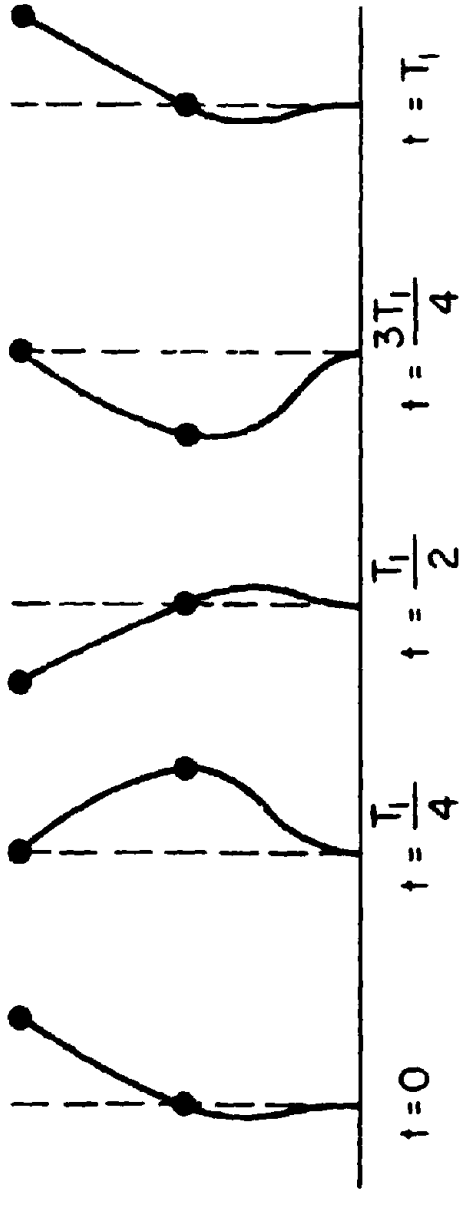

Fig.2.1. One Cycle of an Example Complex-Valued Mode Shape

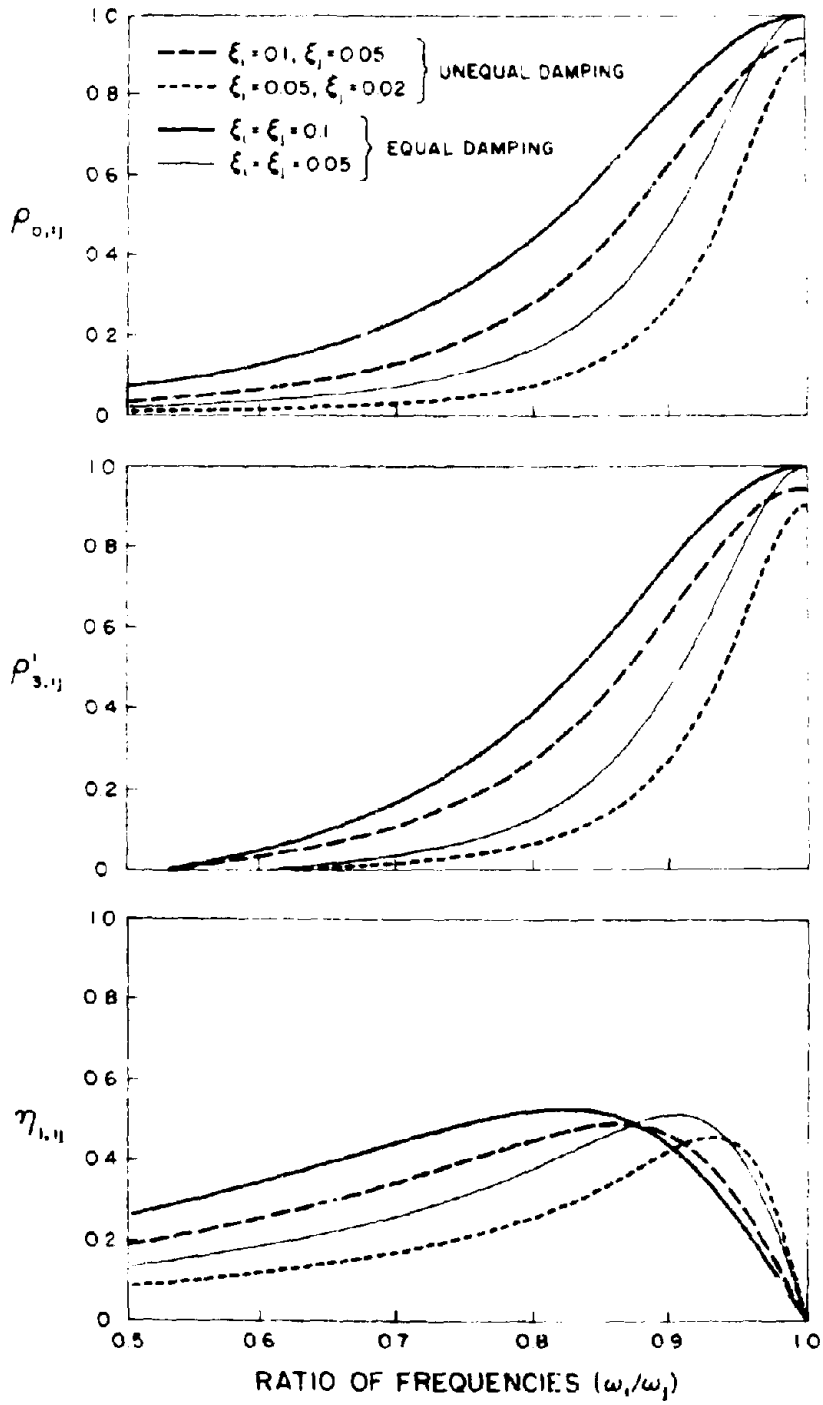

Fig.2.2. Coefficients $\rho_{0,ij}$, $\rho'_{3,ij}$, and $\eta_{1,ij}$ for Response to White-Noise Input

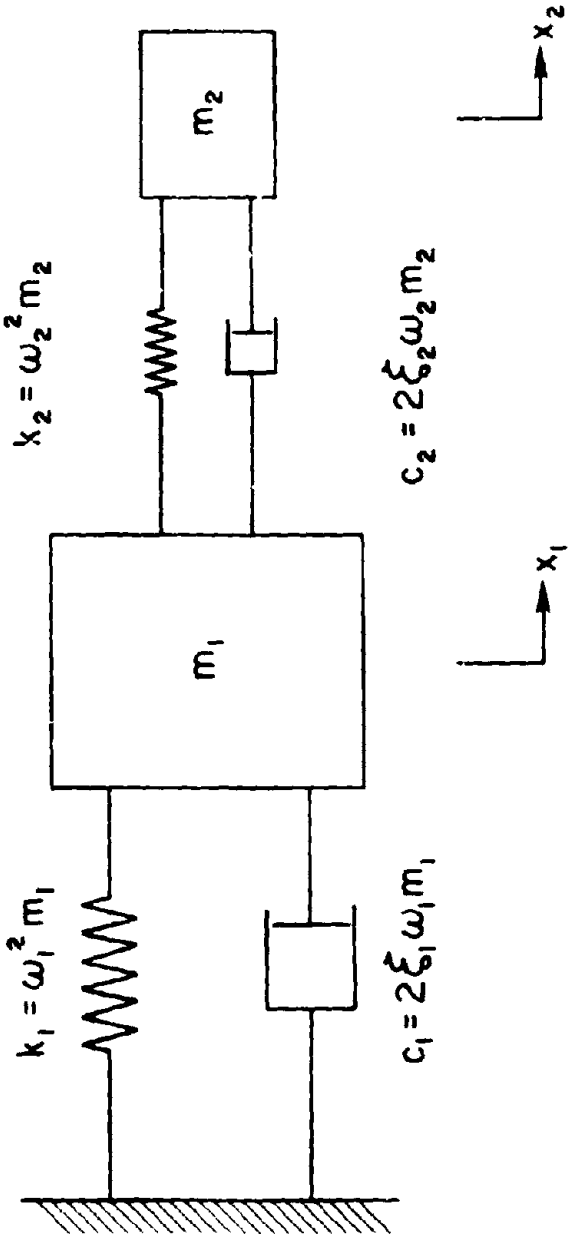

Fig.2.3. Two Degree-of-Freedom Example System

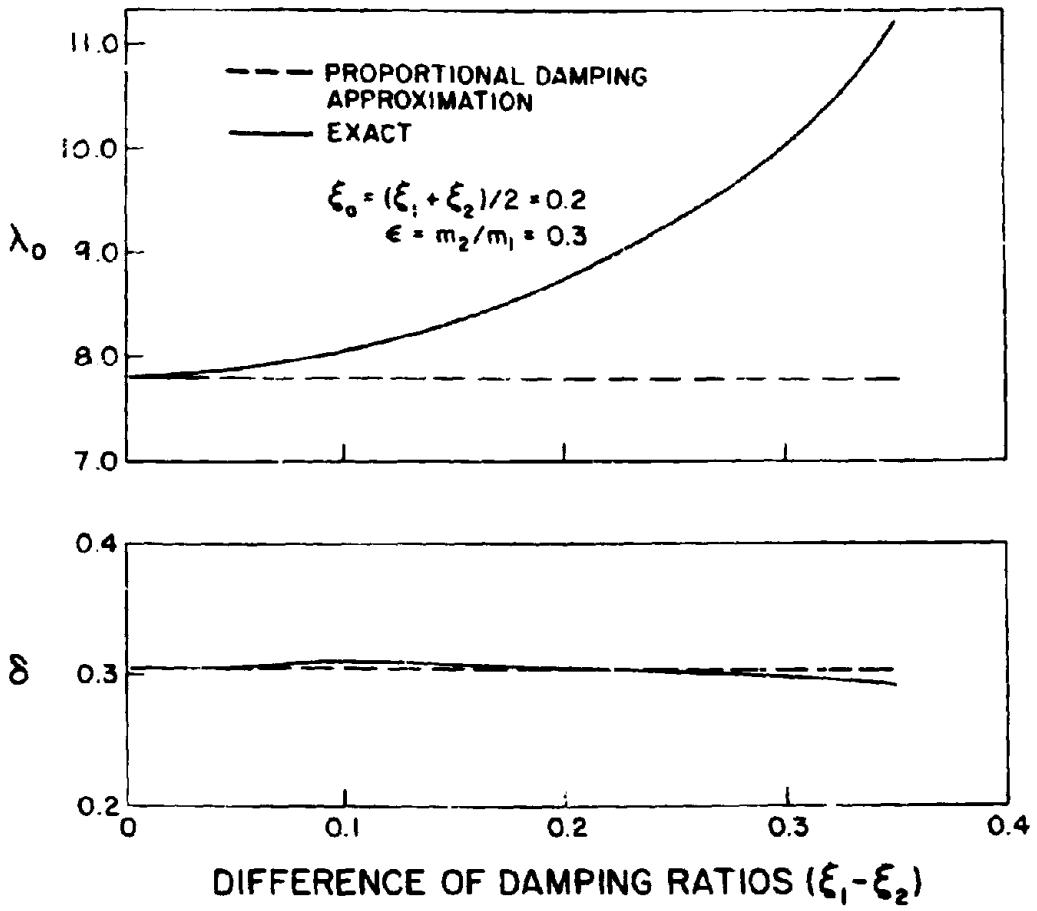

Fig.2.4. Response Parameters δ and λ_0 for Soil-Structure Study

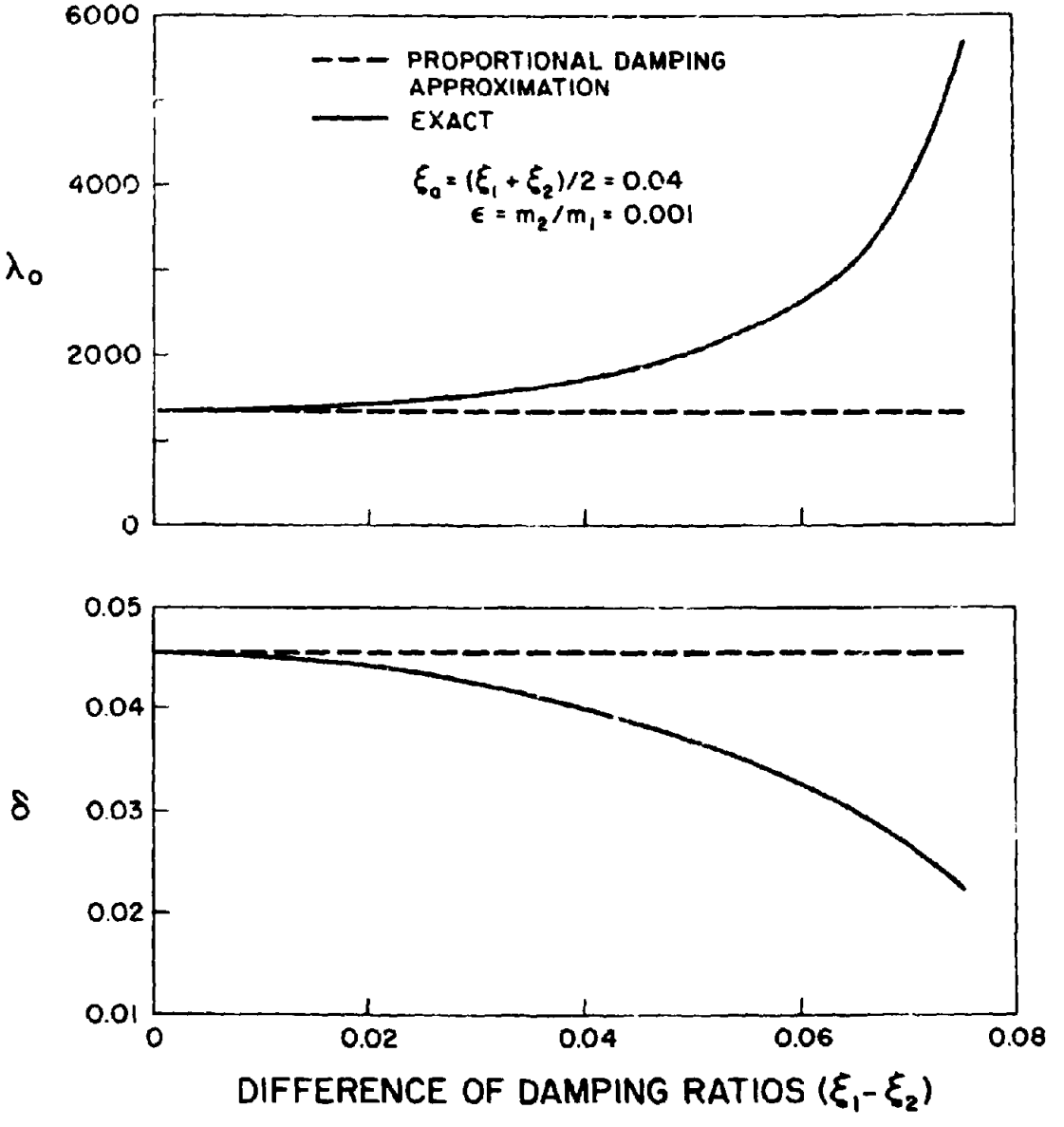

Fig.2.5. Response Parameters δ and λ_0 for Equipment-Structure Study

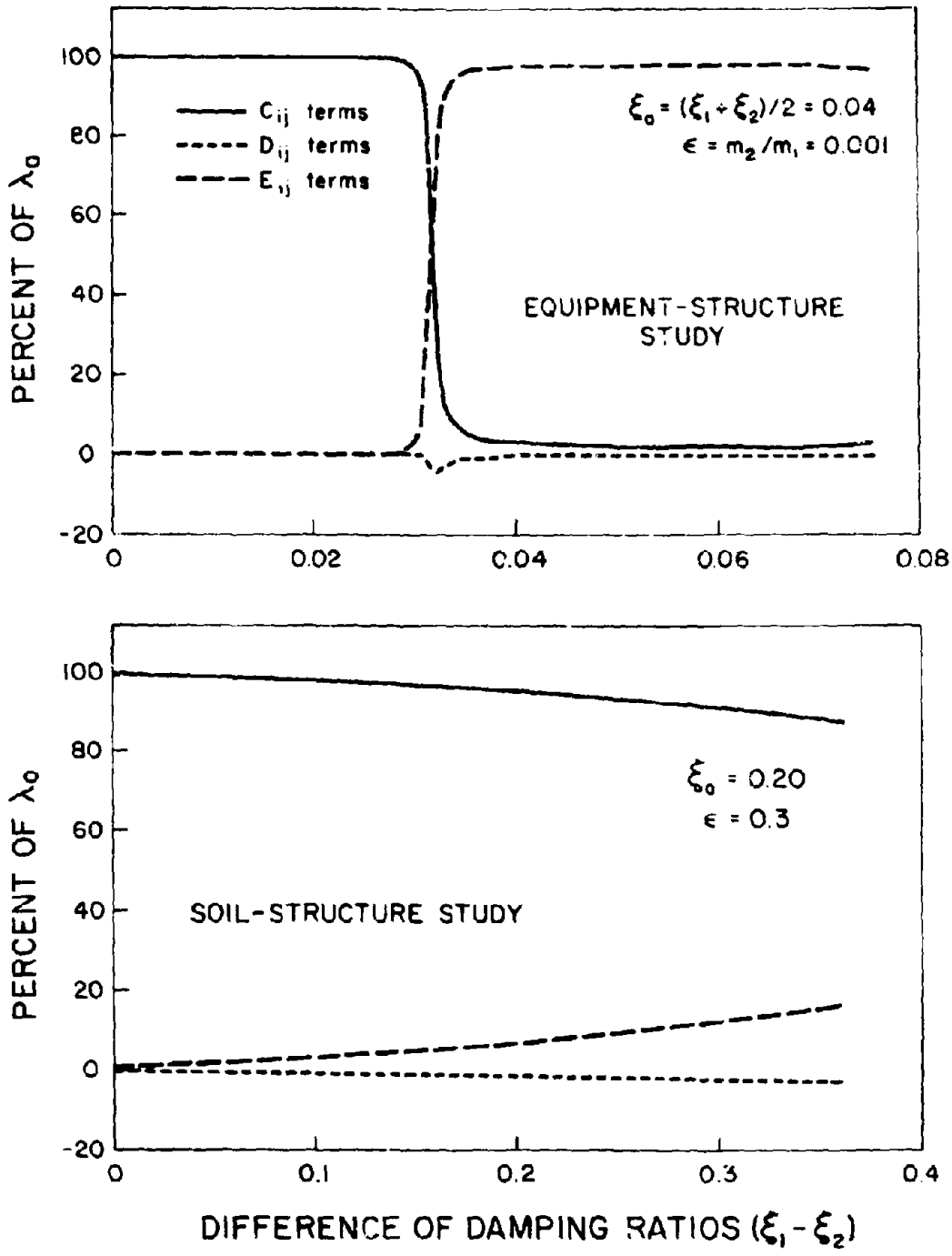

Fig.2.6. Contribution of Terms to λ_0 in Example Studies

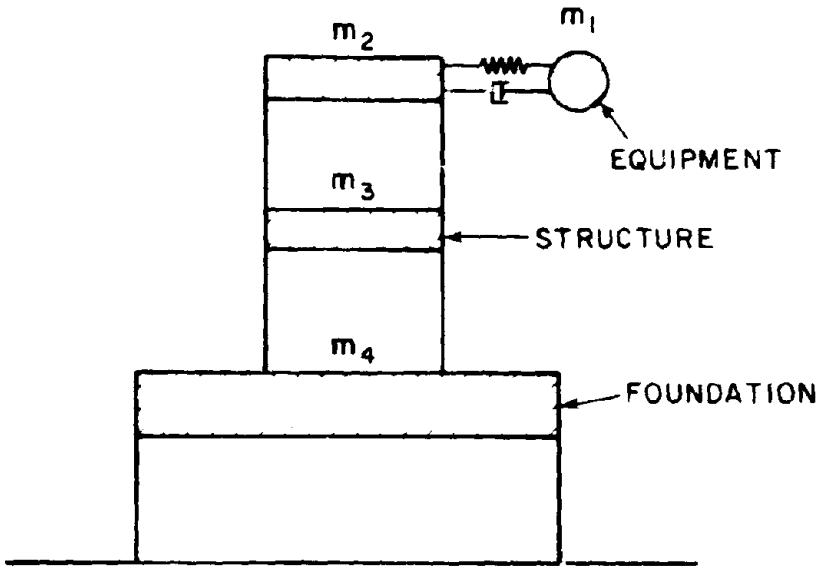

Fig.2.7. Example System for Response Spectrum Study

CHAPTER 3

ANALYSIS OF THE BASIC TWO-DEGREE-OF-FREEDOM EQUIPMENT-STRUCTURE SYSTEM

3.1 Introduction

The study of PS systems is best introduced with the simplest and most fundamental 2-DOF assemblage shown in Fig.3.1. This system is commonly referred to as an equipment-structure (ES) system with the structure and equipment corresponding to the primary and secondary subsystems, respectively. A thorough study of this system is important for several reasons: the analysis of more general and complex MDOF systems is based on the results of the study of the 2-DOF system; the 2-DOF system contains the essential properties that characterize more general PS systems; and the simplicity of this system enables one to identify these properties easily. Also, simple closed form formulae are derived for the 2-DOF system which illustrate clearly and concisely the important relationships between the parameters of the system. The concepts and techniques developed in detail in this chapter will prepare the reader for the study of more complex MDOF PS systems in the following chapters.

As stated in the Introduction, numerous studies have been made on equipment-structure systems. In this chapter, two different approaches will be developed. The first approach is based on the frequency response function of the system. Using perturbation methods based on the light equipment assumption it is possible to reduce the expressions derived by Crandall and Mark for the mean-square response of general 2-DOF systems [11] to rather simple formulae. Closed form expressions for other useful response quantities can be derived as well. The second approach utilizes the modal decomposition method developed in the preceding chapter. The results are a generalization of the previous study by Der Kiureghian, et. al. [18,19]; the primary difference is that the important effect of non-classical damping, which occurs even as slight differences of damping ratios, is fully accounted for. The two approaches developed in

this study yield different formulations for the same response quantities, however it is shown that the two formulations are equivalent.

3.2 Definitions

3.2.1 Parameters

The analysis of the 2-DOF equipment-structure system in Fig.3.1 will be in terms of the parameters of the individual fixed base SDOF structure and equipment oscillators. The physical properties of the two sub-systems are: masses, m_i; damping ratios, ξ_i; and natural frequencies, ω_i; where $i=1$ refers to the structure and $i=2$ refers to the equipment. The displacements x are relative to the ground. Using these properties, the following non-dimensional parameters are defined:

$$\xi_a = \frac{\xi_1+\xi_2}{2} = \text{average damping} \tag{1a}$$

$$\xi_d = \xi_1-\xi_2 = \text{difference of damping} \tag{1b}$$

$$\epsilon = \frac{m_2}{m_1} = \text{mass ratio} \tag{1c}$$

$$\beta = \frac{\omega_1-\omega_2}{\omega_a} = \text{detuning parameter} \tag{1d}$$

where

$$\omega_a = \frac{\omega_1+\omega_2}{2} = \text{average frequency} \tag{1e}$$

3.2.2 Review of perturbation methods

A non-dimensional parameter β is defined to be small if its absolute value is much smaller than 1; this is written symbolically as

$$|\beta| << 1 \tag{2}$$

For example, the damping ratios in structural systems are generally small parameters. Similarly, a parameter β_1 is defined to be of a smaller order of magnitude than another parameter β_2 if the ratio $|\beta_1|/|\beta_2|$ satisfies

$$\frac{|\beta_1|}{|\beta_2|} << 1 \tag{3}$$

By multiplying both sides of the above inequality by $|\beta_2|$, the order relationship can be rewritten symbolically as

$$|\beta_1| << |\beta_2| \tag{4}$$

Finally, two parameters β_1 and β_2 are defined to be of the same order of magnitude if neither

$$|\beta_1| << |\beta_2| \quad \text{nor} \quad |\beta_2| << |\beta_1| \tag{5a}$$

are true. This is written symbolically as

$$\beta_1 = O(\beta_2) \quad \text{or} \quad \beta_2 = O(\beta_1) \tag{5b}$$

where $O(\beta_1)$ denotes a term of the order of magnitude of the parameter β_1. Note that the above relationship does not imply equality. For example, if the damping ratios ξ_1=5% and ξ_2=2%, they are not close to equality, yet they are considered to be of the same order of magnitude.

In engineering applications, the above relationships are put in the context of relative errors. In this study, the parameter e denotes the order of magnitude of the relative error that is allowed in the approximations.

Using the above definitions, a mathematical description can be given to equipment-structure systems. The system in Fig.3.1 is defined to be an equipment-structure system if the parameters ξ_a and $\sqrt{\epsilon}$ are small. The system is tuned if β is also small, otherwise the system is detuned. A more precise definition of detuning will be developed later in this chapter.

As mentioned in the introduction, the key to the analysis of the equipment-structure systems is the use of perturbation methods. Only the most elementary techniques of perturbation theory are used in this study. For instance, using Taylor's series the quantity $\xi_a(1+\xi_a)^{-1}$ can be expanded

$$\frac{\xi_a}{1+\xi_a} = \xi_a(1-\xi_a+\xi_a^2-\xi_a^3+\cdots) \tag{6a}$$

For small ξ_a, the above can be approximated to the following degrees of accuracy:

$$\frac{\xi_a}{1+\xi_a} \approx \xi_a(1-\xi_a+\xi_a^2) \quad \text{second order} \tag{6b}$$

$$\approx \xi_a(1-\xi_a) \quad \text{first order} \tag{6c}$$

$$\approx \xi_a \quad \text{lowest order} \tag{6d}$$

The accuracy of the above three approximations can be observed from the graph in Fig.3.2. Clearly the second order approximation is the most accurate; however the algebraic expression is also the most complicated. Since this is a study for engineering applications, a high level of accuracy is not required and simple, manageable results are sought, therefore lowest order approximations are used. Occasionally first and second order expressions are derived for obtaining intermediate results.

Most expressions encountered in this study involve a combination of several small parameters, and it is important to note the order relationships between the various parameters. In this chapter, it is assumed that ϵ and ξ_a are of the same order of magnitude, i.e.

$$\xi_a = O(\epsilon) \tag{7a}$$

and if the system is tuned, then

$$\beta = O(\epsilon) \tag{7b}$$

Thus, an expression such as

$$\frac{\beta}{1+\xi_a} + \epsilon = \epsilon + \beta(1-\xi_a+\xi_a^2-\cdots) \tag{8a}$$

in the case of tuning can be approximated to

$$\frac{\beta}{1+\xi_a} + \epsilon \approx \epsilon + \beta(1-\xi_a+\xi_a^2) \quad \text{second order} \tag{8b}$$

$$\approx \epsilon + \beta(1-\xi_a) \quad \text{first order} \tag{8c}$$

$$\approx \epsilon + \beta \quad \text{lowest order} \tag{8d}$$

One final note: In a real problem, the order relationships in Eqs.7a,b may not always appear to be valid. For instance, the detuning parameter β may happen to be exactly 0, in which case the order relationships would seem to be

$$\beta << \epsilon \quad \text{and} \quad \beta << \xi_a \tag{9}$$

Consequently, the lowest order approximation for the expression in Eq.8a would be

$$\frac{\beta}{1+\xi_a} + \epsilon \approx \epsilon \tag{10}$$

The difference between Eq.8d and the above expression lies in the generality of the approximation. Eq.8d is valid if either of the relationships Eq.9 or Eqs.7a,b are satisfied, however the above approximation is valid only if Eq.9 is satisfied. Therefore, in order to obtain the most general results, it is assumed that Eq.7a applies to detuned systems and Eqs.7a,b applies to tuned systems.

3.3 Frequency Response Function Approach for Tuned Systems

3.3.1 Introduction

The frequency response function approach is well-suited for deriving the response of the equipment for tuned systems. By using perturbation methods, second-order results are obtained. These results are the basis of the response of all tuned PS systems and are used in the remainder of this study. Detuned systems are evaluated more easily using the modal approach and are studied in the next section.

3.3.2 Frequencies of the System

Let **M**,**C**, and **K** be the mass, damping, and stiffness matrices of the system in Fig.3.1. Using the parameters defined previously,

$$\mathbf{M} = m_1\begin{bmatrix}1 & 0\\ 0 & \epsilon\end{bmatrix} \quad \mathbf{C} = 2m_1\begin{bmatrix}\xi_1\omega_1+\epsilon\xi_2\omega_2 & -\epsilon\xi_2\omega_2\\ -\epsilon\xi_2\omega_2 & \epsilon\xi_2\omega_2\end{bmatrix} \quad \mathbf{K} = m_1\begin{bmatrix}\omega_1^2+\epsilon\omega_2^2 & -\epsilon\omega_2^2\\ -\epsilon\omega_2^2 & \epsilon\omega_2^2\end{bmatrix} \tag{12}$$

The equation of the response of the system to base input is

$$\mathbf{M}\ddot{\mathbf{x}} + \mathbf{C}\dot{\mathbf{x}} + \mathbf{K}\mathbf{x} = -\mathbf{M}\mathbf{r}\ddot{x}_g(t) \tag{13}$$

where $\mathbf{x}=[x_1\ x_2]^T$ is the vector of displacements relative to the base and $\mathbf{r}=[1\ 1]^T$ is the influence vector coupling the input to the DOF of the system. Taking the Fourier transform of Eq.13 and rearranging terms

$$\mathbf{X}(\omega) = -\mathbf{H}(\omega)\mathbf{M}\mathbf{r}X_g(\omega) \tag{14}$$

where $\mathbf{X}(\omega)$ and $X_g(\omega)$ are Fourier transforms of $\mathbf{x}(t)$ and $\ddot{x}_g(t)$, respectively, and $\mathbf{H}(\omega)$ is the complex frequency response matrix

$$\mathbf{H}(\omega) = [-\omega^2\mathbf{M} + i\omega\mathbf{C} + \mathbf{K}]^{-1} \tag{15}$$

Substituting Eq.12 into the above,

$$\mathbf{H}(\omega) = \begin{bmatrix} G_1(\omega) & f_1(\omega) \\ f_1(\omega) & g_1(\omega) \end{bmatrix}^{-1} = \frac{1}{d(\omega)} \begin{bmatrix} g_1(\omega) & -f_1(\omega) \\ -f_1(\omega) & G_1(\omega) \end{bmatrix} \tag{16}$$

where

$$G_1(\omega) = m_1[-\omega^2 + 2i(\xi_1\omega_1 + \epsilon\xi_2\omega_2)\omega + (\omega_1^2 + \epsilon\omega_2^2)] \tag{17a}$$

$$g_1(\omega) = m_2[-\omega^2 + 2i\xi_2\omega_2\omega + \omega_2^2] \tag{17b}$$

$$f_1(\omega) = -m_2[2i\xi_2\omega_2\omega + \omega_2^2] \tag{17c}$$

$$d(\omega) = g_1(\omega)G_1(\omega) - f_1^2(\omega) \tag{17d}$$

Note that $g_1(\omega)$ is the reciprocal of the complex frequency response function of the secondary subsystem. The function $G_1(\omega)$ closely resembles the reciprocal of the complex frequency response function of the primary subsystem. The difference is in the terms with the parameter ϵ which arise from the small additional stiffness and damping contributed from the secondary subsystem. The function $f_1(\omega)$ represents the coupling between the two subsystems. Also, $d(\omega)$ is the characteristic polynomial of the system.

Using the frequency response function $\mathbf{H}(\omega)$ defined above many properties of the system can be derived. The first set of properties that will be investigated are the frequencies of the system, which are found by solving the quartic equation

$$d(\omega) = 0 \tag{18}$$

It is possible to find second-order approximations to this equation by a straightforward yet tedious application of Ferrari's formula for solving quartic equations [3]. However, a more elegant approach based on perturbation methods can be used to solve Eq.18. The derivation is presented in detail to illustrate how perturbation methods can be effectively applied to the equipment-structure problem. Other researchers have found other forms for the expressions for the frequencies of the 2-DOF ES system [37, 36], however the perturbation method, as it is applied in this chapter, yields expressions which are of the same level of accuracy, yet algebraically simpler than the previous formulations. These simple forms of the frequencies will be used to derive several new expressions of the response of the system.

It was stated that the parameters ξ_a, β, and ϵ are small for tuned systems. It is instruc-

tive to examine the properties of the system when the mass ratio ϵ is of a smaller order of magnitude than the other parameters, i.e.

$$\epsilon \ll \max(\xi_a, \beta) \tag{19}$$

In this case, the first term in Eq.17d dominates the expression for $d(\omega)$ and the second term can be neglected

$$d(\omega) \approx g_1(\omega) G_1(\omega) \tag{20}$$

It is well known [11] that this is equivalent to ignoring the interaction forces between the equipment and structure and this point will be discussed later in this chapter. The low-order approximation for the frequencies of this system can be obtained by solving Eq.18. Using the above approximation for $d(\omega)$, Eq.18 is equivalent to

$$G_1(\omega) = 0 \quad \text{or} \quad g_1(\omega) = 0 \tag{21}$$

The roots of $G_1(\omega)$ are approximately equal to the frequencies of the primary substructure and the frequency with positive real part can be written to first order as

$$\omega_1^* \approx \omega_1(1+i\xi_1) \tag{22a}$$

The superposed asterisk is used hereafter to indicate that these properties are associated with the combined system. Similarly, the roots of $g_1(\omega)$ are the frequencies of the secondary substructure and the frequency with positive real part can be written to first order as

$$\omega_2^* \approx \omega_2(1+i\xi_2) \tag{22b}$$

The frequencies in the left half plane, which are located symmetrically with respect to the imaginary axis, are not explicitly written for clarity of notation. This convention will be used throughout the study.

On physical grounds, the above result is not surprising: For very small values of the mass ratio, the secondary system would be very light relative to the primary system and the dynamic behavior of the two subsystems would be essentially independent of each other. Therefore, the frequencies of the combined ES system would be very close to the frequencies of each subsystem, which is the result obtained above.

If ϵ is of the same order of magnitude as ξ_a or β, the above analysis would no longer be

valid. Both terms of the characteristic polynomial $d(\omega)$ must be included in Eq.17d. As a result, the solutions for the frequencies of the system would be slightly shifted or perturbed from the above values. To preserve the inherent symmetry of the problem, this perturbation will be measured from the average of the frequencies in Eqs.22a,b. If μ is defined to be the perturbation variable, the frequency ω can be written in the following form

$$\omega = \omega_a(1+i\xi_a+\mu) \tag{23}$$

By rearranging terms, the variable μ can be expressed in terms of ω

$$\mu = \frac{\omega}{\omega_a} - 1 - i\xi_a \tag{24}$$

Reformulating Eqs.17a-c in terms of μ and retaining only the lowest order terms, the new expressions are

$$G_1(\omega) \approx \omega_a^2 m_1(\beta + i\xi_a - 2\mu) \tag{25a}$$

$$g_1(\omega) \approx -\omega_a^2 m_2(\beta + i\xi_a + 2\mu) \tag{25b}$$

$$f_1(\omega) \approx -\omega_a^2 m_2 \tag{25c}$$

Substitution of the above into Eq.17d yields

$$\begin{aligned} d(\omega) &\approx \omega_a^4 m_1 m_2[(-\beta - i\xi_a - 2\mu)(\beta + i\xi_a - 2\mu) - \epsilon] \\ &= \omega_a^4 m_1 m_2[4\mu^2 - (\beta + i\xi_a)^2 - \epsilon] \end{aligned} \tag{26}$$

and its roots are readily found. The usefulness of the perturbation analysis becomes clear: The original quartic polynomial $d(\omega)$ has been reduced to a simple quadratic polynomial in terms of μ. Denoting the solutions for μ by μ_i^*, the lowest order result is

$$\mu_i^* \approx \pm\frac{1}{2}\sqrt{\epsilon + (i\xi_a + \beta)^2} \tag{27}$$

It follows from Eq.23 that the frequencies ω_i^* are

$$\omega_i^* \approx \omega_a[1 + i\xi_a \pm \frac{1}{2}\sqrt{\epsilon + (i\xi_a + \beta)^2}] \tag{28}$$

The accuracy of the above solution is shown numerically in Table 1.

In Figs.3.3a-c, the exact values of ω_i^* which are found from solving Eq.18 are plotted along with the above approximation for various values of the parameters. Figure 3.3a represents a general illustration of the behavior of the frequencies. The natural frequencies and damping ratios of the two subsystems are chosen to be unequal, and the location of these

frequencies on the complex plane are indicated by the solid squares. Then, for several values of the mass ratio ϵ, the corresponding pairs of frequencies of the complete system are plotted and labeled by the letters $A-D$. Figures 3.3b and 3.3c are similar, except in the former the frequencies ω_1 and ω_2 are chosen to be equal, and in the latter the damping ratios ξ_1 and ξ_2 are equal.

It is instructive to explore the meaning of Eq.28 and the corresponding characteristics that can be observed in Figs.3.3a-c. The following are some of the more revealing facts

1. The frequencies of the combined system are located symmetrically with respect to the average frequency $\omega_a(1+i\xi_a)$ on the complex plane. This is apparent in all of the Figures 3.3a-c.

2. For very small values of ϵ, the value of μ' is approximately

$$\mu' \approx \pm\frac{1}{2}\sqrt{(i\xi_d+\beta)^2} = \pm\frac{1}{2}(i\xi_d+\beta) \tag{29a}$$

which, when substituted in Eq.23, yields the same result obtained earlier in Eqs.22a,b. However, if ϵ is not negligible, it was explained earlier in hueristic terms that the frequencies become displaced or perturbed from the frequencies in Eqs.22a,b. This perturbation is accounted for mathematically by the presence of the parameter ϵ in the radical in Eq.28. This phenomena can be observed in Figs.3.3a-c, where for ϵ=.0005, the frequencies of the combined system nearly coincide with the subsystem frequencies, whereas they become displaced for larger values of the mass ratio.

3. If the frequencies ω_1 and ω_2 are equal, then β=0 which is usually referred to as the "perfect tuning" condition [37]. In this case, the frequencies of the combined system can be in one of two configurations.

   a. If $\xi_d^2<\epsilon$, then the frequencies would be

$$\omega_i' \approx \omega_a\left[1 \pm \frac{1}{2}\sqrt{\epsilon-\xi_d^2}+i\xi_a\right] \tag{29b}$$

which, on the complex plane, would lie to the right and left of the average at a distance of $\sqrt{\epsilon-\xi_d^2}$. The damping ratios would both be equal to ξ_a and the natural fre-

quencies would be unequal

b. If $\xi_1 > \epsilon$, then the frequencies would be

$$\omega' \approx \omega_n[1 + i(\xi_n \pm \frac{1}{2}\sqrt{-\epsilon + \xi_n^2})] \tag{29c}$$

which, on the complex plane, would lie above and below the average at a distance $\sqrt{-\epsilon+\xi_n^2}$. In this case, the frequencies would both be equal to ω_n and the damping ratios would be unequal

These characteristics are visible in Fig.3.3b; for points A and B, Eq.29b applies, and for points C and D, Eq.29c applies.

4. If the damping ratios ξ_1 and ξ_2 are equal, then the frequencies would be

$$\omega' \approx \omega_n[1 \pm \frac{1}{2}\sqrt{\epsilon + \beta^2} + i\xi_n] \tag{29d}$$

which, on the complex plane, would always lie parallel to the real axis at a distance $\sqrt{\epsilon+\beta^2}$ from the average frequency, as shown in Fig.3.3c.

3.3.3 Spectral Density of Equipment Response

Next consider the PSD of the response to stationary input. The primary response variable of interest is the displacement $y(t)$ of the equipment relative to the structure and is given by

$$y(t) = x_2(t) - x_1(t) = \mathbf{q}^t \mathbf{x}(t) \tag{30}$$

where $\mathbf{q}=[-1\ 1]^t$. The Fourier transform $Y(\omega)$ of the response $y(t)$ is found by taking the transform of both sides of the above equation and using Eq.14

$$Y(\omega) = \mathbf{q}^t \mathbf{X}(\omega) = -\mathbf{q}^t \mathbf{H}(\omega)\mathbf{M}\mathbf{r} X_1(\omega) \tag{31}$$

By definition, the frequency response function $H_1(\omega)$ for the response $y(t)$ to the input $\ddot{x}_1(t)$ satisfies the relation:

$$Y(\omega) = H_1(\omega) X_1(\omega) \tag{32}$$

It follows from the previous two equations that $H_1(\omega)$ is given by:

$$H_1(\omega) = -\mathbf{q}^t \mathbf{H}(\omega)\mathbf{M}\mathbf{r} \tag{33}$$

It is well known [10,28] that the PSD function $G_{11}(\omega)$ of the response can be found in terms of the frequency response function by the relation

$$G_{yy}(\omega) = T_{yy}(\omega) G_{xx}(\omega) \tag{34a}$$

where $T_{yy}(\omega)$ is the transfer function

$$T_{yy}(\omega) = |h_{yy}(\omega)|^2 \tag{34b}$$

and $G_{xx}(\omega)$ is the PSD of the input $\ddot{x}_g(t)$. By expanding $T_{yy}(\omega)$ through the use of Eqs.16 and 33 and keeping second order terms, the following is obtained

$$T_{yy}(\omega) \approx \frac{\omega_1^4 + 4\xi_1^2\omega_1^2\omega^2}{d(\omega)d(-\omega)} m_1^2 m_2^2 \tag{35}$$

A plot for $T_{yy}(\omega)$ is shown in Fig 3.4 for $\omega_1=1.0$, $\omega_2=1.04$, $\varepsilon=.001$, and two sets of values for the damping ratios. It is apparent that $T_{yy}(\omega)$ is highly peaked for values of ω that lie in a small neighborhood of ω_a and that the peak is higher for smaller damping values. The explanation of this phenomena can be seen by examining the denominator of the transfer function. The polynomial $d(\omega)$ can be factored

$$\begin{aligned} d(\omega) = {} & [\omega_a(1+i\xi_a+\mu_1^2)-\omega][\omega_a(1+i\xi_a+\mu_2^2)-\omega] \\ & [\omega_a(-1+i\xi_a-\bar{\mu}_1^2)-\omega][\omega_a(-1+i\xi_a-\bar{\mu}_2^2)-\omega]m_1^2 m_2^2 \end{aligned} \tag{36}$$

When ω lies near the average frequency ω_a, then the order of $d(\omega)$ is

$$d(\omega) = O(\xi_a^2)\omega_a^8 m_1^2 m_2^2 \tag{37}$$

From Eq.36, it is clear that the same order relationship holds for $d(-\omega)$. Returning to the expression for the transfer function, it follows that

$$T_{yy}(\omega) = O(\xi_a^{-4}) \quad \text{for } \omega \approx \omega_a \tag{38}$$

This characteristic of $T_{yy}(\omega)$ will be useful in making approximations

3.3.4 Spectral Moments of Response

The spectral moments λ_m of the response of the secondary system can be obtained by integrating the PSD function $G_{yy}(\omega)$

$$\lambda_m = \int_0^\infty \omega^m G_{yy}(\omega)\,d\omega = \int_0^\infty \frac{\omega_1^4 + 4\xi_1^2\omega_1^2\omega^2}{d(\omega)d(-\omega)} \omega^m G_{xx}(\omega)\,d\omega \tag{39}$$

For general forms of the input PSD $G_{xx}(\omega)$, the above integral can be evaluated numerically. However, for the important case of white-noise input closed form second-order approximations can be derived. For $m=0$ and 2 the following integration formula is used [11]:

$$\int_0^\infty \frac{p(\omega)\,d\omega}{q(\omega)q(-\omega)} = \frac{\pi}{2}\,\frac{a_3(-a_1b_3+a_3b_2)+b_3(a_2-a_1a_3)}{a_4(a_1^2+a_3^2a_4-a_1a_2a_3)} \tag{40a}$$

where the polynomials $p(\omega)$ and $q(\omega)$ are given by

$$p(\omega) = b_1\omega^2 + b_2\omega^2 + b_3 \tag{40b}$$

$$q(\omega) = a_1\omega^3 + a_2\omega^2 + a_3\omega + a_4 \tag{40c}$$

and the roots of $q(\omega)$ are required to be in the upper half plane. Since $G_{11}(\omega) \equiv G_{ww}$ is a constant for white-noise input and the roots of $d(\omega)$ all lie in the upper half plane, the formula above can be used directly to solve Eq.39 for λ_0 and λ_2. The calculations are fairly extensive yet straightforward with the following results:

$$\lambda_0 = \frac{\pi G_{ww}}{\omega_a^3 D}\left[2\xi_a+3\beta\xi_a+10\beta^2\xi_a+\epsilon(4\xi_a+\xi_a)+16\xi_a^2\xi_1\right] \tag{41a}$$

$$\lambda_2 = \frac{\pi G_{ww}}{\omega_a D}\left[2\xi_a+\beta\xi_a+\epsilon\xi_2+8\xi_a\xi_1^2\right] \tag{41b}$$

where the denominator D is

$$D = 16\left[\xi_1\xi_2(4\xi_a^2+\beta^2)+\epsilon\xi_a^2\right] \tag{41c}$$

Note that second order approximations are derived for the numerators in the above expressions. These are necessary to derive further results in this section.

For the first moment λ_1, the integrand in Eq 39 is an odd-powered polynomial, therefore Eqs.40a-c cannot be used. The obvious alternative is the method of residues; using the frequencies derived in the preceding section with some mathematical manipulation, the second-order approximation for λ_1 can be found [23]

$$\lambda_1 = \frac{\pi G_{ww}}{\omega_a^2 D}\left[2\xi_a+2\beta\xi_a+\frac{3}{4}\epsilon(3\xi_a+\xi_a)+8\xi_1\xi_a(5\xi_1+3\xi_2)\right] \tag{41d}$$

It is noted that the lowest order expressions for the three moments are very similar:

$$\lambda_m \approx \frac{2\pi\xi_a G_{ww}\omega_a^{m-3}}{D} \qquad \text{for } m = 0,1,2 \tag{41e}$$

Graphs comparing the expressions for λ_m in Eqs.41a-d with exact results obtained by numerical integration are presented in Figs.3.5a-c.

As stated in the Introduction, the first three spectral moments can be used to derive several important response quantities. The first of these quantities to be examined are the

mean squares of the displacement response σ_1^2 and the velocity response σ_2^2 which are given by λ_0 and λ_2, respectively

$$\sigma_1^2 \approx \frac{\pi \xi_a G_{ww}}{8\omega_a^3[\xi_1\xi_2(4\xi_a^2+\beta^2)+\epsilon\xi_a^2]} \tag{42a}$$

$$\sigma_2^2 \approx \frac{\pi \xi_a G_{ww}}{8\omega_a[\xi_1\xi_2(4\xi_a^2+\beta^2)+\epsilon\xi_a^2]} \tag{42b}$$

Note the presence of the parameter ϵ. The response of the equipment to ground motion is not independent of the mass ratio as is commonly assumed in the current design practice. In fact, as the value for ϵ increases, the mean square of the response decreases, as shown in Fig.3.5d. This behavior is a consequence of the interaction between the equipment and the structure, as was described by Newmark [33] and others [31,37].

For perfectly tuned systems, Eq.42a reduces to

$$\sigma_1^2 \approx \frac{\pi G_{ww}}{8\omega_a^3\xi_a(4\xi_1\xi_2+\epsilon)} \tag{43}$$

This can be compared with the expression derived by Der Kiureghian, et. al. [19]

$$\sigma_1^2 \approx \frac{\pi G_{ww}}{8\omega_a^3\xi_a(4\xi_a^2+\epsilon)} \tag{44}$$

which was based on the assumption that the system was classically damped. The two expressions are in agreement only when $\xi_1=\xi_2$, which, as noted in the previous chapter, corresponds to the classical damping condition. As the difference between the damping ratios increases, the system becomes non-classically damped, and Eq.44 tends to underestimate the true value for σ_1^2, particularly for small values of ϵ. The plots of σ_1^2 in Fig.3.5e using the above formulae demonstrate this phenomena. This was also shown in Chapter 2 using modal decomposition methods (see Fig.2.5). Note that for small differences of damping ratios, the formula based on classical damping will yield reasonable results.

For systems that are not perfectly tuned, the square of the detuning parameter β appears in the denominator in Eq.42a. Thus, as the system becomes increasingly detuned, the mean square of the response will decrease, as is expected. This behavior was exhibited in Figs.3.5a-c; note that σ_1^2 is symmetric with respect to β.

Other useful quantities that can be derived from the spectral moments are the mean zero crossing rate $\nu = \sqrt{\lambda_2/\lambda_0}/\pi$ and the shape factor $\delta = \sqrt{1-\lambda_1^2/(\lambda_0\lambda_2)}$. Using the second order expressions for λ_n in Eqs.41a-d, the following are derived

$$\nu = \frac{\omega_o}{\pi}\left[1-\frac{\beta\xi_o}{2\xi_o}\right] \tag{45a}$$

$$\delta = \left[\frac{\beta^2}{4}\left(1-\frac{\xi_o^2}{4\xi_o^2}\right)+\frac{1}{4}\epsilon+\xi_1\xi_2\right] \tag{45b}$$

The accuracies of the above formulae are shown in Figs.3.6a-c. The factor ν is physically interpreted as the average frequency of zero crossings of the response process [44] and the above expression is in agreement with this interpretation. The shape factor δ is a measure of the band-width of the response process [44]. For a SDOF oscillator with frequency ω and damping ratio ξ,

$$\delta \approx 2\sqrt{\frac{\xi}{\pi}} \tag{46}$$

For small values of ξ, δ is small reflecting the fact that the response process is very narrowly banded. For the 2-DOF ES system, δ is a more complex function of the parameters β, ξ, and ϵ. The general behavior of δ is as follows:

1. For perfectly tuned systems and very small mass ratios, $\delta \approx \sqrt{\xi_1\xi_2}$ which is an order of magnitude smaller than the shape factor for a SDOF oscillator in Eq 46.
2. As ϵ increases, δ increases (see Fig.3.6b). This reflects the fact that the frequencies of the system are moving apart which increases the band-width of the response.
3. As β increases, δ increases for the same reason as above (see Fig.3.6c).

All of the results derived in this section are based on white-noise input. For a general input specified by an arbitrary PSD $G_{ww}(\omega)$, two alternative methods can be used to find the response. The most straightforward method is numerical integration: the spectral moments can be computed using Eq.39 for any input PSD. However, if $G_{ww}(\omega)$ is a smoothly varying and wide-banded function such as the PSD for the Kanai-Tajimi filtered white-noise input [24], the highly peaked property of the transfer function $T_{11}(\omega)$ permits the approximate use of the same

expressions for λ_{jj} as those for white-noise input. The only difference is that the term G_{jj} in Eqs.41a-e is replaced by the value of the PSDF at the peak of $T_{jj}(\omega)$, i.e. $G_{jj}(\omega_{jj})$.

3.4 Modal Decomposition Approach

3.4.1 Introduction

An alternative method of deriving the spectral moments of response of general 2-DOF systems is through the modal decomposition approach for non-classically damped systems, as developed in Chapter 2. The analysis will begin with tuned systems and the results compared with those of the previous section. It will be shown that the two sets of results are equivalent, the primary difference being the order of the approximation: Only lowest order expressions can be readily calculated in the modal approach. The analysis of the equipment-structure system is extended to detuned systems with results similar to those of previous investigators [18, 19, 35].

To conclude the modal analysis, general expressions which apply for both tuned and detuned systems are formulated using matching techniques from perturbation theory.

3.4.2 Tuned Systems

3.4.2.1 Mode shapes

The basic relationship between the mode shapes $\boldsymbol{\phi}_j$ and frequencies ω_j of a general structural system is given by the eigenvalue problem

$$[-\omega_j^2\mathbf{M} + i\omega_j\mathbf{C} + \mathbf{K}]\boldsymbol{\phi}_j = 0 \tag{47}$$

For the 2-DOF system, the frequencies ω_j have been derived earlier by solving the characteristic equation. Consequently, the mode shapes can be computed readily by substituting the expressions in Eq.12 for the mass, damping, and stiffness matrices and the expressions in Eq.28 for the frequencies. Using the notation $\boldsymbol{\phi}_j = [\alpha_j \;\; 1]^t$, the equations for the eigenvectors are

$$\begin{bmatrix} G_1(\omega_j) & f_1(\omega_j) \\ f_1(\omega_j) & g_1(\omega_j) \end{bmatrix} \begin{bmatrix} \alpha_j \\ 1 \end{bmatrix} = \begin{bmatrix} 0 \\ 0 \end{bmatrix} \qquad j=1,2 \tag{48}$$

Solving for α_j and taking lowest order terms yields

$$\alpha_j = -\frac{g_j(\omega_j)}{f_j(\omega_j)} \approx \frac{2[\omega_s(1+i\xi_s)-\omega_j]}{\omega_{ss}} \tag{49}$$

Note that the numerator is simply the difference between the frequency of the fixed base secondary subsystem and the frequency of the combined system. Substituting Eq.28 for ω_j, the eigenvalue, eigenvector solution pairs for Eq.47 are

$$\omega_1 = \omega_s[1 + i\xi_s + \frac{1}{2}\sqrt{\epsilon + (i\xi_s+\beta)^2}], \quad \alpha_1 = -\beta - i\xi_s - \sqrt{\epsilon + (i\xi_s+\beta)^2} \tag{50a}$$

$$\omega_2 = \omega_s[1 + i\xi_s - \frac{1}{2}\sqrt{\epsilon + (i\xi_s+\beta)^2}], \quad \alpha_2 = -\beta - i\xi_s + \sqrt{\epsilon + (i\xi_s+\beta)^2} \tag{50b}$$

The component α_2 is compared with exact values, computed by numerically solving the eigenvalue problem, in Table 2. The exact and approximate values of α are also plotted in Figs.3.7a-c using the same values for the parameters used in Figs.3.3a-c. The key relationships between the mode shapes ϕ_j and the system parameters are:

1. For very small values of the mass ratio ϵ, α_2 is very nearly zero, and the mode shape ϕ_2 is dominated by equipment motion. Similarly, mode 1 is associated with the structure subsystem and α_1 is approximately $-2(\beta+i\xi_{ss})$. This is indicated in Figs.3.7a,b, where α are shown to converge to the limiting values 0 and $-2(\beta+i\xi_{ss})$ for small values of ϵ. This corresponds to the convergence of the frequencies of the combined system to those of the subsystems for increasingly smaller values of the mass ratio, ϵ.

2. If the system is perfectly tuned and $\xi_s^2 < \epsilon$, then α_1 and α_2 would be given by

$$\alpha_1 = -i\xi_{ss} - \sqrt{\epsilon - \xi_s^2} \tag{51a}$$

$$\alpha_2 = -i\xi_{ss} + \sqrt{\epsilon - \xi_s^2} \tag{51b}$$

which have the same absolute value. Thus, the characteristics of the two subsystems would be distributed equally to both modes; it is no longer possible to associate a mode with either subsystem. This demonstrates some of the symmetry of the system. This is shown graphically in Fig.3.7b for points A and B, where the coordinates α lie to each side of the imaginary axis at a distance of approximately $\sqrt{\epsilon - \xi_s^2}$.

3. The mode shapes will be real-valued only when the damping ratios of the equipment and structure are equal. This follows since the damping matrix would be proportional to the

stiffness matrix to lowest order terms, and the system, by definition, attains classical damping. This can be observed in Fig.3.7c, where the imaginary components of α_r are relatively small.

4 Finally, the product of α_1 and α_2 is

$$\alpha_1 \alpha_2 \approx -\epsilon \tag{52}$$

which is constant with respect to β, ξ_1, and ξ_2. This relation will be used in the next section.

3.4.2.2 Spectral Moments

The modal decomposition method can be applied directly to the results in Eqs.50a,b to obtain the spectral moments of response.

First, new notation will be introduced. Following the convention in Chapter 2, the frequencies ω_r' can be rewritten

$$\omega_r' = \tilde{\omega}_r \sqrt{1-\tilde{\xi}_r^2} + i\tilde{\xi}_r \tilde{\omega}_r \tag{53a}$$

where $\tilde{\omega}_r$ and $\tilde{\xi}_r$ are the undamped frequencies and the damping ratios, respectively, which are associated with ω_r' and are given by

$$\tilde{\omega}_r = |\omega_r'| \approx \mathrm{Re}\omega_r' \text{ and } \tilde{\xi}_r = \frac{\mathrm{Im}\omega_r'}{\tilde{\omega}_r} \tag{53b}$$

In general, the system parameters $\tilde{\omega}_r$ and $\tilde{\xi}_r$ are not related to the original parameters ω_r and ξ_r, however, the averages are the same. This fact is verified by referring to the expressions in Eq.50a,b

$$\frac{\tilde{\omega}_1+\tilde{\omega}_2}{2} \approx \frac{\mathrm{Re}(\omega_1'+\omega_2')}{2} \approx \omega_a \tag{54a}$$

$$\frac{\tilde{\xi}_1+\tilde{\xi}_2}{2} = \frac{1}{2}\left[\frac{\mathrm{Im}\omega_1'}{\tilde{\omega}_1} + \frac{\mathrm{Im}\omega_2'}{\tilde{\omega}_2}\right] \approx \frac{1}{2}\left[\frac{\mathrm{Im}(\omega_1'+\omega_2')}{\omega_a}\right] \approx \xi_a \tag{54b}$$

It is useful to define the differences

$$\beta = \frac{(\tilde{\omega}_1-\tilde{\omega}_2)}{\omega_a} \text{ and } \tilde{\xi}_d = \tilde{\xi}_1-\tilde{\xi}_2 \tag{55}$$

From Eqs.50a,b and Eq.53b, it can be shown by direct substitution that

$$|\tilde{\beta}^2+\tilde{\xi}_j| \approx |\epsilon+(i\xi_j+\beta)^2| \tag{56}$$

This relation will be useful in computing the spectral moments

The first step in the modal decomposition method is the evaluation of the three sets of constants C_j, D_j, and E_j defined in Eqs.2.26 and 2.34. In order to obtain these quantities, some preliminary expressions must be computed as outlined in Chapter 2

The quantities A and b defined by Eqs.2.17a and 2.20 can be obtained in terms of α_j and ϵ

$$A = \hat{\boldsymbol{\phi}}^T\mathbf{A}\hat{\boldsymbol{\phi}} \approx 2i\boldsymbol{\phi}^T\mathbf{M}\boldsymbol{\phi}\omega_j - 2i(\alpha_j^2+\epsilon)m_j\omega_j \tag{57a}$$

$$b = -\left[\frac{\boldsymbol{\phi}^T\mathbf{M}\mathbf{r}}{A}\right]\mathbf{q}^T\boldsymbol{\phi}^j \approx -\frac{i(\alpha_j+\epsilon)}{2(\alpha_j^2+\epsilon)\omega_j} \approx -\frac{i}{2(\alpha_j+\alpha_j^{-1}\epsilon)\omega_j} \tag{57b}$$

The formula for b_j can be expressed in terms of α_1 and α_2 by using Eq.52

$$b_j \approx \frac{i(-1)^j}{2\omega_j(\alpha_1-\alpha_2)} \tag{58}$$

Note that $b_1 = -b_2$. The constants a_j and c_j defined by Eq.2.26 can be evaluated in terms of b_j using the relation $s=i\omega$

$$C_j \approx 4\omega_j^2(\mathrm{Im}b_j)(\mathrm{Im}b_j) \quad D_j \approx 0 \quad E_j \approx 4(\mathrm{Re}b_j)(\mathrm{Re}b_j) \tag{60}$$

$$c_j = 2\mathrm{Re}b_j \tag{59b}$$

The lowest order terms for C_j, D_j, and E_j are calculated using Eq.2.34

$$C_j \approx 4\omega_j^2(\mathrm{Im}b_1)^2 \quad D_j \approx 0 \quad E_j \approx 4(\mathrm{Re}b_1)^2 \tag{60}$$

It was noted in Chapter 2 that the coefficient D_j was always nearly equal to zero in the numerical studies of the tuned 2-DOF equipment-structure system. The expressions above confirm that result.

The next step in the modal decomposition method is the evaluation of the cross spectral moments λ_{jk}, for white-noise input. By using the parameters $\tilde{\omega}_j$ and $\tilde{\xi}_j$, the computation is straightforward using Eqs.2.49a-h. The imaginary parts of λ_{jk} are nearly zero due to the fact that the frequencies $\tilde{\omega}_j$ are closely spaced for tuned systems. Therefore, only the real parts of the cross moments are needed. The zeroeth cross moments are

$$\mathrm{Re}\lambda_{0jk} \approx \frac{\pi G_{ss}}{4\omega_j^2\tilde{\xi}_j} \qquad j=1,2 \tag{61a}$$

$$\mathrm{Re}\lambda_{n,n+1} = \frac{2\pi G_{xx}(\tilde{\xi}_n\tilde{\omega}_n+\tilde{\xi}_{n+1}\tilde{\omega}_{n+1})}{(\tilde{\omega}_n^2-\tilde{\omega}_{n+1}^2)^2+4(\tilde{\xi}_n\tilde{\omega}_n+\tilde{\xi}_{n+1}\tilde{\omega}_{n+1})(\tilde{\xi}_n\tilde{\omega}_{n+1}+\tilde{\xi}_{n+1}\tilde{\omega}_n)\tilde{\omega}_n\tilde{\omega}_{n+1}} \approx \frac{\pi G_{xx}}{\omega_n}\frac{\xi_n}{\tilde{\beta}^2+4\xi_n^2} \tag{61b}$$

As an initial low-order approximation, higher cross moments can be obtained by using the following

$$\mathrm{Re}\lambda_{n,n+r} \approx \omega_n^r \mathrm{Re}\lambda_{n,n} \tag{62}$$

which will yield low order expressions for $\lambda_{n,n}$.

The final step in the modal decomposition method is the evaluation of $\lambda_{n,n}$ by substituting the preceding results into Eq.2.36. The lowest order expression for $\lambda_{n,n}$ is

$$\lambda_{n,n} \approx \sum_{r}\sum_{s}\left\{4\omega_n^2\mathrm{Im}b_r\,\mathrm{Im}b_s\,\mathrm{Re}\lambda_{n,n+r-s} + 4\mathrm{Re}b_r\,\mathrm{Re}b_s\,\omega_n^2\mathrm{Re}\lambda_{n,n+r-s}\right\}$$

$$= 4\omega_n^2|b_1|^2[\mathrm{Re}\lambda_{n,n} + \mathrm{Re}\lambda_{n,n} - 2\mathrm{Re}\lambda_{n,n}] \tag{63}$$

The term $|b_1|^2$ is found by substituting Eqs.50a,b into Eq.58 and utilizing Eq.56

$$|b_1|^2 \approx \frac{1}{16}\left|\omega_n\sqrt{\epsilon+(\epsilon\xi_n+\beta)^2}\right|^2 = \frac{1}{16\omega_n^2}\left[\tilde{\beta}^2+\tilde{\xi}_n^2\right] \tag{64}$$

After substituting Eqs.61a,b and 64 into Eq.63, the expression for the moment $\lambda_{n,n}$ reduces to

$$\lambda_{n,n} \approx \frac{\pi G_{xx}}{8\omega_n^3}\frac{\xi_n}{\tilde{\xi}_n\tilde{\xi}_{n+1}(\tilde{\beta}^2+4\xi_n^2)} \tag{65a}$$

This can be compared with the formula for $\lambda_{n,n}$ in the preceding section which, to lowest order is

$$\lambda_{n,n} \approx \frac{\pi G_{xx}}{8\omega_n^3}\frac{\xi_n}{[\xi_n\xi_{n+1}(\beta^2+4\xi_n^2)+\epsilon\xi_n^2]} \tag{65b}$$

The latter expression is entirely in terms of the original parameters ω_n, ξ_n, and ϵ while the former is in terms of the derived parameters $\tilde{\omega}_n$ and $\tilde{\xi}_n$. The mass ratio ϵ, which is present in Eq.65b is implicitly included in Eq.65a in the derived parameters. It can be shown that the two expressions are equivalent by rewriting the derived parameters in terms of the original parameters.

Higher order refinements can be made to the expression in Eq.65a for $m>0$ by using the results of Section 3.3.4. From the definitions of the factors ν and δ, it is possible to derive the following relationships between the first three moments:

$$\lambda_1 = \pi\nu\sqrt{1-\delta^2}\lambda_0, \quad \lambda_2 = \pi\nu\lambda_0 \tag{66}$$

Substituting the expressions for ν and δ from Eqs.45a,b into the above, higher order relations are obtained which are equivalent to the expressions in Eqs 41

3.4.3 Detuned Systems

3.4.3.1 Introduction

Thus far, the analysis of the 2-DOF equipment-structure system has been restricted to tuned systems. For detuned systems, the parameter β is large and can not be treated as a perturbation variable, consequently a new set of expressions must be developed. The analysis is straightforward through the application of the modal decomposition method.

3.4.3.2 Frequencies and Mode Shapes

The eigenvalue problem for the 2-DOF system can be rewritten as

$$\Gamma(\omega^*)\phi^* = 0 \tag{67a}$$

where

$$\Gamma(\omega^*) = \begin{bmatrix} G_1(\omega^*) & f_2(\omega^*) \\ f_1(\omega^*) & g_2(\omega^*) \end{bmatrix} \tag{67b}$$

To begin the analysis, the following approximations for the frequencies and mode shapes are used.

$$\omega^{*(0)} = \omega\,(\sqrt{1-\xi^2}+i\xi) \tag{68a}$$

$$\phi_1^{(0)} = \begin{bmatrix} 1 \\ 0 \end{bmatrix} \quad \phi_2^{(0)} = \begin{bmatrix} 0 \\ 1 \end{bmatrix} \tag{68b}$$

The 0 superscript is used to indicate that the above are initial approximations. Low-order refinements of these rough estimates are possible using perturbation techniques. Details are presented for mode 1 which is associated with the structure mode.

The above approximations have errors, which are found by direct substitution into the left-hand-side of Eq.67a

$$\Gamma(\omega_1^{*(0)})\phi_1^{(0)} = \begin{bmatrix} G_1(\omega_1^{*(0)}) & f_2(\omega_1^{*(0)}) \\ f_1(\omega_1^{*(0)}) & g_1(\omega_1^{*(0)}) \end{bmatrix} \begin{bmatrix} 1 \\ 0 \end{bmatrix} = \begin{bmatrix} G_1(\omega_1^{*(0)}) \\ f_1(\omega_1^{*(0)}) \end{bmatrix} \tag{69}$$

Using Eqs.17a-c to evaluate the above polynomials, the order of magnitude of the above errors can be found

$$\Gamma(\omega_1^{(0)})\phi_1^{(0)} \sim \begin{bmatrix} O(\epsilon) \\ O(\epsilon) \end{bmatrix} m_1\omega_1^2 \tag{70}$$

To reduce the above errors, a refined mode shape and frequency, which will be denoted $\phi^{(1)}$ and $\omega^{(1)}$, will be derived.

The first step in reducing the errors is finding a suitable value for the equipment component of $\phi_1^{(1)}$. By examining Eq.69, it is clear that if the following value is given to the refined mode shape

$$\phi_1^{(1)} = \begin{bmatrix} 1 \\ -\dfrac{f_1(\omega_1^{(0)})}{g_1(\omega_1^{(0)})} \end{bmatrix} \tag{71a}$$

the error in the second coordinate in Eq.69 would be zero and the new error terms would be

$$\Gamma(\omega_1^{(0)})\phi_1^{(1)} = \begin{bmatrix} G_1(\omega_1^{(0)}) - \dfrac{f_1^2(\omega_1^{(0)})}{g_1(\omega_1^{(0)})} \\ 0 \end{bmatrix} \tag{71b}$$

The error in the first coordinate can be reduced by finding the refined frequency $\omega_1^{(1)}$ that satisfies

$$G_1(\omega_1^{(1)}) = \frac{f_1^2(\omega_1^{(0)})}{g_1(\omega_1^{(0)})} \tag{72}$$

Let $\Delta\omega_1 = \omega_1^{(1)} - \omega_1^{(0)}$. Then $G_1(\omega)$ can be reduced to a linear function in $\Delta\omega_1$ by using the derivative approximation

$$\begin{aligned} G_1(\omega_1^{(1)}) - G_1(\omega_1^{(0)}) &\approx \frac{d}{d\omega} G_1(\omega_1^{(0)})\Delta\omega_1 \\ &\approx 2m_1[-\omega_1^{(0)} + i\xi_1\omega_1]\Delta\omega_1 \\ &\approx -2m_1\omega_1\Delta\omega_1 \end{aligned} \tag{73}$$

The solution to $\Delta\omega_1$ is found by combining Eqs.72 and 73

$$\Delta\omega_1 = -\frac{1}{2m_1\omega_1}\left[\frac{f_1^2(\omega_1^{(0)})}{g_1(\omega_1^{(0)})} - G_1(\omega_1^{(0)})\right] \tag{74}$$

It is clear that $\Delta\omega_1 = O(\epsilon)\omega_1$ from the definitions of f_1, g_1, and G_1. By comparing each ele-

ment of the matrix $\Gamma(\omega_1^{(0)})$ with the corresponding element in $\Gamma(\omega_1^{(0)})$, it can be shown that

$$\Gamma(\omega^{(1)})\phi^{(1)} = \begin{bmatrix} O(\epsilon^3) \\ O(\epsilon^3) \end{bmatrix} m_1\omega_1^2 \tag{75}$$

Thus, the refined mode shape and frequency have errors an order of magnitude smaller than those of the initial solutions. Further refinements are possible, however the small second order improvements in accuracy generally does not warrant the increased analytical and computation effort, particularly in engineering applications. Using the * notation for the final low-order approximations, the above expressions reduce to

$$\phi_1^* \approx \begin{bmatrix} 1 \\ \dfrac{\omega_1^2}{\omega_1^2 - \omega_2^2} \end{bmatrix} \qquad \omega_1^* \approx \omega_1(1+\epsilon\xi_1) \tag{76}$$

Although the expression for $\omega_1^{(1)}$ is not used in the final result, its derivation is necessary to prove that the solutions $\phi^{(1)}$ and $\omega_1^{(1)}$ reduce the error in the eigenvalue problem. This proof justifies that the solutions in Eq.76 are valid low-order approximations.

In a very similar procedure, refined solutions can be obtained for the mode shape and the frequency of mode 2, which is associated with the equipment mode. The high-order expressions are:

$$\phi_2^{(1)} = \begin{bmatrix} \dfrac{f_1(\omega_2^{(0)})}{G_1(\omega_2^{(0)})} \\ 1 \end{bmatrix} \qquad \omega_2^{(1)} = \omega_2^{(0)} + \frac{f_1^2(\omega_2^{(0)})}{2m_1\epsilon\omega_2 G_1(\omega_2^{(0)})} \tag{77}$$

which reduce to the following, final low-order approximations

$$\phi_2^* \approx \begin{bmatrix} \dfrac{\epsilon\omega_2^2}{\omega_1^2 - \omega_2^2} \\ 1 \end{bmatrix} \qquad \omega_2^* \approx \omega_2(1+\epsilon\xi_2) \tag{78}$$

Note the similarity between the above results for mode 2 and those for mode 1.

The mode shapes and frequencies for detuned systems have an entirely different character than those of tuned systems. The mode shapes are real, indicating that detuned systems are classically damped. Also, the frequencies of the combined system are close to the fixed base frequencies of each subsystem indicating that interaction plays a negligible role in detuned systems.

3.4.3.3 Spectral Moments of Response

As in Section 3.4.2.2, the modal decomposition approach can be applied directly to the above mode shapes and frequencies to obtain the spectral moments of response. Since detuned systems are classically damped, the method for classically damped systems, as developed by Der Kiureghian [16], can be used. The effective participation factor ψ is given by

$$\psi = \frac{(q'\phi)(\phi'\mathbf{M}r)}{M} \tag{79}$$

where $M = \phi'\mathbf{M}\phi$ is the modal mass. By substituting the preceding expressions for ϕ into Eq.79 and taking lowest-order terms, the result is

$$\psi_1 \approx -\frac{\omega_1^2}{\omega_1^2-\omega_2^2} \quad \psi_2 \approx -\psi_1 \tag{80}$$

The expressions for the moments $\lambda_{n,0}$ are easily found in terms of ω_i

$$\lambda_{n,0} \approx \frac{\pi G_{ii}\omega_i^{n+1}}{4\xi_i} \tag{81}$$

As for the cross-spectral moments $\lambda_{n,r}$, it has been established that the cross spectral moments $\lambda_{n,r} \approx 0$ for well-spaced modes [15]. It will be shown in Section 3.4.4.3 that detuned modes are well-spaced; therefore this approximation for $\lambda_{n,r}$ is applicable here.

The spectral moments are calculated using the formula Eq.2.38

$$\lambda_n = \sum_{i=1}^{2}\sum_{j=1}^{2}\psi_i\psi_j\lambda_{n,0} \approx \left[\frac{\omega_1^2}{\omega_1^2-\omega_2^2}\right]^2 \frac{\pi G_{ii}}{4}\left[\frac{\omega_1^{n+1}}{\xi_1} + \frac{\omega_2^{n+1}}{\xi_2}\right] \tag{82}$$

The most notable characteristic of the above expression is that λ_n decreases as the system becomes increasingly detuned. This is illustrated in Fig.3.8.

3.4.4 Comparison between Tuned and Detuned Systems

3.4.4.1 Introduction

The 2-DOF system has been considered as being either tuned or detuned with different sets of expressions derived for each case. However, for practical applications a general expression applicable for all systems would be more useful, particularly for those systems which lie between the tuned and detuned categories. This is accomplished by matching, which is a

standard procedure from perturbation methods [32]. Also, guidelines are established to determine if a system is characterized by tuning or detuning.

3.4.4.2 A General Expression for λ_1

The idea behind matching is to combine two expressions into one general expression that would apply for all values of a perturbation parameter. In this case, the expression that will be evaluated is the spectral moment λ_1, and the perturbation parameter is the detuning, β.

For systems with large values of β, the detuned moment in Eq.82 would be used, and for systems with small values of β, the tuned moment in Eq.65b would be used. However, for systems with values of β which are large enough to be considered detuned yet small enough to be considered tuned, both expressions for λ_1 would be applicable. The detuned version can be rewritten in terms of β

$$\lambda_1^d = \frac{\omega_n^4 \pi G_0 \left(\omega_1^2 + \omega_2^2\right)\xi_1 \xi_2}{16\beta^2 \omega_n^4 \left(\omega_1^2 + \omega_2^2\right)\xi_1 \xi_2} \tag{83}$$

where the d superscript denotes detuning. The tuned version can be rewritten to account for the relatively large value for β

$$\lambda_1^t = \frac{\pi G_0 \left(\xi_1 + \xi_2\right)}{16\beta^2 \omega_n^3 \xi_1 \xi_2} \tag{84}$$

where the t superscript denotes tuning. Since the two expressions above are derived using different assumptions on the parameter β, they are slightly different. However, it is clear that small modifications can be made to λ_1^t so that the expressions would agree, or match. If these modifications are applied to the original expression for λ_1^t in Eq.65b, the result would be

$$\lambda_1 = \frac{\pi G_0}{16\omega_n^4} \frac{\omega_1^4}{\omega_1^2 + \omega_2^2} \frac{\left(\omega_1^2 + \omega_2^2\right)\xi_1 \xi_2}{\left[\xi_1 \xi_2 \left(4\xi_n^2 + \beta^2\right) + \epsilon \xi_n^2\right]} \tag{85}$$

Note that when β is small, $\omega_1 \approx \omega_2$ and the above expression reduces to the original expression in Eq.65b. For larger values of β, the one above will closely approximate the detuned moment λ_1^d. This can be clearly seen in Fig.3.9.

3.4.4.3 Detuning Criteria

For systems with large values for the parameter β, the detuned moment λ_m^d in Eq.83 would be in close agreement with the general expression for λ_m in Eq 85. However, systems with sufficiently small values for β would be characterized by tuning and λ_m^d and λ_m would no longer be in agreement.

If the relative error tolerance is e, then a system will be defined to be detuned if the difference between λ_m^d and λ_m is less than e, i.e.

$$\text{relative error} = \frac{\lambda_m^d - \lambda_m}{\lambda_m} < e \tag{86}$$

Substituting Eqs.83 and 85 into the above yields

$$\text{relative error} = \frac{\xi_a^2(4\xi_1\xi_2 + \epsilon)}{\xi_1\xi_2\beta^2} < e \tag{87}$$

This error is plotted in Fig.3.10; clearly in the vicinity of perfect tuning (β=0) the error becomes very large. Rewriting the above in terms of β yields

$$\beta^2 > \frac{4\xi_1\xi_2 + \epsilon}{\xi_1\xi_2 e}\xi_a^2 = \frac{1}{e}\left[4 + \frac{\epsilon}{\xi_1\xi_2}\right]\xi_a^2 \tag{88}$$

which will be used hereafter to define detuning.

It was noted earlier that detuned systems have widely-spaced modes. This hypothesis will be proven, presently. In the context of the present study, two modes are defined to be widely spaced if the correlation coefficients for white noise input $\rho_{m,ij} \ll 1$ for m=0,1,2 and $i \neq j$. This relation will be shown to be true for the 2-DOF detuned system for m=0; similar proofs hold for m=1 and 2.

Using Eq.2.56a, the expression for $\rho_{0,12}$ can be written in terms of the parameters of the PS system:

$$\rho_{0,12} = \frac{\sqrt{\xi_1\xi_2}(4\xi_a + \beta\xi_d)}{4\xi_a^2 + \beta^2} \tag{89}$$

The relation in Eq.88 can be simplified to

$$\beta > \frac{2\xi_a}{\sqrt{e}} \tag{90}$$

which, when substituted for the first summand in the numerator of Eq.89, yields

$$\rho_{0,12} < \frac{\sqrt{\xi_1 \xi_2}(2\sqrt{e} + \xi_a)\beta}{4\xi_a^2 + \beta^2} \tag{91}$$

Dividing through by β, dropping the first summand in the denominator, and substituting Eq 90 to the remaining summand in the denominator, the above simplifies to

$$\rho_{0,12} < \frac{\sqrt{\xi_1 \xi_2}(2\sqrt{e} + \xi_a)}{\frac{2\xi_a}{\sqrt{e}}} \tag{92}$$

Finally, using the fact that the geometric mean is less than or equal to the arithmetic mean, the above reduces to the following inequality

$$\rho_{0,12} < e + \tfrac{1}{2}\sqrt{e}\,\xi_a << 1 \tag{93}$$

which proves that detuned modes are widely spaced.

3.5 Non-Interaction Results

All of the results derived thus far in this chapter correctly account for the effect of interaction between the structure and the equipment. A question with practical implications is: What is the difference between these results and the results which would be obtained if interaction was neglected?

In the derivation of non-interaction results the response is first found for the structure alone without accounting for the equipment. Then the structural motion is used as the base input to the equipment. In mathematical terms, the equations for the system response which were coupled in Eq.13 for the interaction study are decoupled in the non-interaction analysis.

The structural response $x_1^{(non)}$ relative to the ground is given by

$$m_1\ddot{x}_1^{(non)} + c_1\dot{x}_1^{(non)} + k_1 x_1^{(non)} = -m_1\ddot{x}_g(t) \tag{94a}$$

where the superscript (non) indicates that the variables are the results of the non-interaction analysis. The motion at the base of the equipment is $x_1^{(non)} + x_g$, therefore the equipment response $y^{(non)}$ relative to the attachment point is

$$m_2\ddot{y}^{(non)} + c_2\dot{y}^{(non)} + k_2 y^{(non)} = -m_2(\ddot{x}_1^{(non)} + \ddot{x}_g) \tag{94b}$$

The Fourier transform $X_1^{(non)}(\omega)$ and $Y^{(non)}(\omega)$ of the displacements $x_1^{(non)}(t)$ and $y^{(non)}(t)$ are

3.4.4.3 Detuning Criteria

For systems with large values for the parameter β, the detuned moment λ_m'' in Eq.83 would be in close agreement with the general expression for λ_m in Eq.85. However, systems with sufficiently small values for β would be characterized by tuning and λ_m'' and λ_m would no longer be in agreement.

If the relative error tolerance is e, then a system will be defined to be detuned if the difference between λ_m'' and λ_m is less than e, i.e

$$\text{relative error} = \frac{\lambda_m'' - \lambda_m}{\lambda_m} < e \tag{86}$$

Substituting Eqs.83 and 85 into the above yields

$$\text{relative error} = \frac{\xi_a^2(4\xi_1\xi_2+\epsilon)}{\xi_1\xi_2\beta^2} < e \tag{87}$$

This error is plotted in Fig.3.10; clearly in the vicinity of perfect tuning (β=0) the error becomes very large. Rewriting the above in terms of β yields

$$\beta^2 > \frac{4\xi_1\xi_2+\epsilon}{\xi_1\xi_2 e}\xi_a^2 = \frac{1}{e}\left(4+\frac{\epsilon}{\xi_1\xi_2}\right)\xi_a^2 \tag{88}$$

which will be used hereafter to define detuning.

It was noted earlier that detuned systems have widely-spaced modes. This hypothesis will be proven, presently. In the context of the present study, two modes are defined to be widely spaced if the correlation coefficients for white noise input $\rho_{m,ij} \ll 1$ for m=0,1,2 and $i \neq j$. This relation will be shown to be true for the 2-DOF detuned system for m=0; similar proofs hold for m=1 and 2.

Using Eq.2.56a, the expression for $\rho_{0,12}$ can be written in terms of the parameters of the PS system:

$$\rho_{0,12} = \frac{\sqrt{\xi_1\xi_2}(4\xi_a + \beta\xi_a)}{4\xi_a^2 + \beta^2} \tag{89}$$

The relation in Eq.88 can be simplified to

$$\beta > \frac{2\xi_a}{\sqrt{e}} \tag{90}$$

which when substituted for the first summand in the numerator of Eq.89, yields

$$\rho_{a,12} < \frac{\sqrt{\xi_1 \xi_2}(2\sqrt{e} + \xi_a)\beta}{4\xi_a^2 + \beta^2} \tag{91}$$

Dividing through by β, dropping the first summand in the denominator, and substituting Eq.90 to the remaining summand in the denominator, the above simplifies to

$$\rho_{a,12} < \frac{\sqrt{\xi_1 \xi_2}(2\sqrt{e} + \xi_a)}{\frac{2\xi_a}{\sqrt{e}}} \tag{92}$$

Finally, using the fact that the geometric mean is less than or equal to the arithmetic mean, the above reduces to the following inequality

$$\rho_{a,12} < e + \tfrac{1}{2}\sqrt{e}\,\xi_a << 1 \tag{93}$$

which proves that detuned modes are widely spaced.

3.5 Non-Interaction Results

All of the results derived thus far in this chapter correctly account for the effect of interaction between the structure and the equipment. A question with practical implications is: What is the difference between these results and the results which would be obtained if interaction was neglected?

In the derivation of non-interaction results the response is first found for the structure alone without accounting for the equipment. Then the structural motion is used as the base input to the equipment. In mathematical terms, the equations for the system response which were coupled in Eq.13 for the interaction study are decoupled in the non-interaction analysis.

The structural response $x_1^{(non)}$ relative to the ground is given by

$$m_1\ddot{x}_1^{(non)} + c_1\dot{x}_1^{(non)} + k_1 x_1^{(non)} = -m_1\ddot{x}_g(t) \tag{94a}$$

where the superscript (non) indicates that the variables are the results of the non-interaction analysis. The motion at the base of the equipment is $x_1^{(non)} + x_g$, therefore the equipment response $y^{(non)}$ relative to the attachment point is

$$m_2\ddot{y}^{(non)} + c_2\dot{y}^{(non)} + k_2 y^{(non)} = -m_2(\ddot{x}_1^{(non)} + \ddot{x}_g) \tag{94b}$$

The Fourier transform $X_1^{(non)}(\omega)$ and $Y^{(non)}(\omega)$ of the displacements $x_1^{(non)}(t)$ and $y^{(non)}(t)$ are

$$X_1^{(non)}(\omega) = -h_1(\omega) m_1 X_g(\omega) \tag{95a}$$

$$\begin{aligned} Y^{(non)}(\omega) &= -h_2(\omega) m_2 [-\omega^2 X_1^{(non)}(\omega) + X_g(\omega)] \\ &= -h_2(\omega) m_2 [\omega^2 h_1(\omega) m_1 + 1] X_g(\omega) \end{aligned} \tag{95b}$$

where $h_1(\omega)$ and $h_2(\omega)$ are the complex frequency response functions of the structure and equipment subsystems, respectively, given by

$$h_i(\omega) = (-\omega^2 m + i\omega c_i + k_i)^{-1} \tag{96}$$

Using this definition, the expression for $Y^{(non)}(\omega)$ can be reduced

$$\begin{aligned} Y^{(non)}(\omega) &= -h_1(\omega) h_2(\omega) m_2 [\omega^2 m_1 + h_1^{-1}(\omega)] X_g(\omega) \\ &= -h_1(\omega) h_2(\omega) m_2 [i\omega c_1 + k_1] X_g(\omega) \\ &= -h_1(\omega) h_2(\omega) m_1 m_2 [2i\omega_1 \xi_1 \omega + \omega_1^2] X_g(\omega) \end{aligned} \tag{97}$$

It follows from Eq 32 and Eq.34b that the transfer function $T_{11}^{(non)}(\omega)$ for the relative displacement response is

$$T_{11}^{(non)}(\omega) = \frac{(\omega_1^4 + 4\xi_1^2 \omega_1^2 \omega^2) m_1^2 m_2^2}{d^{(non)}(\omega) d^{(non)}(-\omega)} \tag{98a}$$

where

$$d^{(non)}(\omega) = h_1^{-1}(\omega) h_2^{-1}(\omega) \tag{98b}$$

Note the similarity between Eq.98a and the corresponding expression which includes interaction, Eq.35. The difference is in the denominator: in the non-interaction analysis $d(\omega)$ is replaced by $d(\omega)^{(non)}$. Comparing Eq.17d with Eq.98b, it can be seen that

$$d(\omega) = d(\omega)^{(non)} + \epsilon(\text{additional terms}) \tag{99}$$

where the additional terms account for the interaction between the equipment and the structure. As the mass ratio becomes very small, the additional interaction term in the above equation becomes negligible and $d(\omega)$ approaches $d(\omega)^{(non)}$, i.e.

$$\lim_{\epsilon \to 0} d(\omega) = d(\omega)^{(non)} \tag{100a}$$

It follows that a similar relation holds for the transfer function

$$\lim_{\epsilon \to 0} T_{11}(\omega) = T_{11}^{(non)}(\omega) \tag{100b}$$

Using the above fact, the rederivation of the spectral moments and other related quantities for the non-interaction study becomes trivial. Most of the results found earlier can be adjusted to yield results that do not account for interaction by setting ϵ to zero, i.e., modeling

the equipment as a subsystem with negligible mass. This makes sense intuitively - such equipment is not expected to affect the motion of the structure.

As an example, the formula for the moments given in Eq.85 would simplify to

$$\lambda_n^{(non-i)} = \frac{\pi G_{xx}}{16\omega_n^3} \frac{\omega_1^4}{\omega_1^{n-1}\omega_2^{3-n}} \frac{(\omega_1^{n-1}\xi_1+\omega_2^{3-n}\xi_2)}{\xi_1\xi_2(4\xi_n^2+\beta^2)} \tag{101}$$

Note that the non-interaction expression tends to overestimate the true value for λ_n, particularly for tuned systems due to the absence of the ϵ term in the denominator of Eq.101 (see Fig.3.11).

It is instructive to investigate how small ϵ must be in order to insure that the non-interaction expressions will yield reasonable approximations. The simplest measure of the difference between the non-interaction and exact approaches is the ratio

$$r_n = \frac{\lambda_n^{(non-i)}}{\lambda_n} \tag{102}$$

which, for white-noise input, can be calculated from Eqs.85 and 101

$$r_n = \frac{(4\xi_n^2+\beta^2)\xi_1\xi_2+\epsilon\xi_n^2}{(4\xi_n^2+\beta^2)\xi_1\xi_2} \tag{103}$$

If the error tolerance is e, then the non-interaction results can be used if

$$r_n - 1 < e \tag{104}$$

or equivalently,

$$\epsilon < (4\xi_n^2+\beta^2)\frac{\xi_1\xi_2}{\xi_n^2}e \tag{105}$$

For detuned systems where β is large, the above condition will usually be satisfied and $\lambda_n^{(non-i)}$ will be a good approximation for λ_n as was stated earlier. However, for tuned systems, β is small, and Eq.105 will be satisfied only if ϵ is sufficiently small. A conservative upper bound for ϵ is made by setting $\beta=0$, in which case Eq.105 simplifies to

$$\epsilon < 4\xi_1\xi_2 e \tag{106}$$

The relationship between the error in non-interaction analysis and the size of the mass ratio ϵ is illustrated Fig.3.12.

3.6 Summary

3.6.1 Discussion

A thorough study of the 2-DOF ES system was made. The mode shapes and frequencies were derived for tuned and detuned systems and physical interpretations of these quantities were given to elucidate the dynamic characteristics of these systems. Two different methods of analysis were used to find the response of the ES system to stationary input. In the first approach, the frequency response function method was used for tuned systems, and second order expressions were derived for the spectral moments λ_m for m=0,1,2. These expressions were subsequently used to find the shape factors ν and δ. In the second approach, the modal decomposition method was used in analyzing both tuned and detuned systems. The results for tuned systems were compared with those from the frequency response function analysis and the two expressions were found to be equivalent. Then the results for detuned systems were combined with those for tuned systems to form a general expression applicable for all systems and to develop a criteria for detuning. Finally, the commonly used decoupled equations of motion for the ES systems were analyzed. It was shown that the results of this analysis can be obtained directly from the results which included interaction by setting the mass ratio ϵ to zero. Also, a criterion for the use of the decoupled approximation was established.

The emphasis of this chapter was to understand the underlying mathematical relationships that exists in the 2-DOF system in preparation of the study of more general and complex PS systems.

3.6.2 Results

For future reference, the important results derived in this chapter are listed below:

Detuning Criteria

$$\beta^2 > \frac{1}{e}\left(4+\frac{\epsilon}{\xi_1\xi_2}\right)\xi_2^2 \tag{88}$$

Non-interaction Criteria

Detuned Systems

$$\epsilon < (4\xi_a^2+\beta^2)\frac{\xi_1\xi_2}{\xi_a^2}\epsilon \tag{105}$$

Tuned Systems

$$\epsilon < \xi_1\xi_2\epsilon \tag{106}$$

Frequencies and Mode Shapes

Tuned Systems

$$\boldsymbol{\phi}_j = \begin{Bmatrix} \alpha \\ 1 \end{Bmatrix}$$

$$\omega_1' = \omega_a\left[1 + i\xi_a + \frac{1}{2}\sqrt{\epsilon + (i\xi_a+\beta)^2}\right], \quad \alpha_1 = \left[-\beta - i\xi_a - \sqrt{\epsilon + (i\xi_a+\beta)^2}\right] \tag{50a}$$

$$\omega_2' = \omega_a\left[1 + i\xi_a - \frac{1}{2}\sqrt{\epsilon + (i\xi_a-\beta)^2}\right], \quad \alpha_2 = \left[-\beta - i\xi_a + \sqrt{\epsilon + (i\xi_a+\beta)^2}\right] \tag{50b}$$

Detuned Systems

$$\boldsymbol{\phi}_1 \approx \begin{Bmatrix} 1 \\ \dfrac{\omega_1^2}{\omega_1^2-\omega_2^2} \end{Bmatrix} \qquad \omega_1' \approx \omega_1(1+i\xi_1) \tag{76}$$

$$\boldsymbol{\phi}_2 \approx \begin{Bmatrix} \dfrac{\epsilon\omega_2^2}{\omega_1^2-\omega_2^2} \\ 1 \end{Bmatrix} \qquad \omega_2' \approx \omega_2(1+i\xi_2) \tag{78}$$

Spectral Moments

Tuned Systems

$$\lambda_{jn} \approx \frac{\pi\xi_a G_{ee}}{8\omega_a^{4-n}[\xi_1\xi_2(4\xi_a^2+\beta^2)+\epsilon\xi_a^2]} \tag{41e}$$

Detuned Systems

$$\lambda_{jn} = \sum_{i=1}^{2}\sum_{j=1}^{2}\psi_{ij}\psi_{ij}\lambda_{mij} \approx \left[\frac{\omega_1^2}{\omega_1^2-\omega_2^2}\right]^2\frac{\pi G_{ee}}{4}\left[\frac{\omega_1^{2n-1}}{\xi_1} + \frac{\omega_2^{2n-1}}{\xi_2}\right] \tag{82}$$

All Systems

$$\lambda_{jn} = \frac{\pi G_{ee}}{16\omega_a^4}\frac{\omega_1^4}{\omega_1^4-\omega_2^4}\frac{\omega_1^{2n-1}\xi_1+\omega_2^{2n-1}\xi_2}{\xi_1\xi_2(4\xi_a^2+\beta^2)+\epsilon\xi_a^2} \tag{85}$$

Mean zero crossing rate and shape factors for tuned systems

$$\nu = \frac{\omega_a}{\pi}\left[1-\frac{\beta\xi_a}{2\xi_a}\right] \tag{45a}$$

$$\delta = \left[\frac{\beta^2}{4}\left(1-\frac{\xi_d^2}{4\xi_0^2}\right)+\frac{1}{4}\epsilon+\xi_1\xi_2\right] \qquad (45b)$$

Table 3.1 Frequencies for Example System
ω_a=1.0, β=0.04, ξ_a=0.03, ξ_d=0.04

ϵ	Mode	Exact Frequency		Computed Frequency		Error
		Real Part	Imag. Part	Real Part	Imag. Part	%
0.01	1	0.949	0.022	0.951	0.021	0.3
	2	1.050	0.037	1.050	0.038	0.1
0.005	1	0.963	0.019	0.964	0.018	0.2
	2	1.036	0.040	0.036	0.041	0.1
0.001	1	0.976	0.012	0.976	0.012	0.0
	2	1.023	0.047	1.023	0.047	0.0

Table 3.2 Mode Shape Component α_i of Example System
ω_a=1.0, β=0.04, ξ_a=0.03, ξ_d=0.04

ϵ	Mode	Exact α_i		Computed α		Error
		Real Part	Imag. Part	Real Part	Imag. Part	%
0.01	1	0.061	-0.024	0.058	-0.022	8.9
	2	-0.141	-0.055	-0.148	-0.063	7.0
0.005	1	0.033	-0.018	0.032	-0.017	3.8
	2	-0.113	-0.061	-0.118	-0.068	6.7
0.001	1	0.006	-0.005	0.006	-0.005	0.0
	2	-0.086	-0.074	-0.088	-0.080	5.6

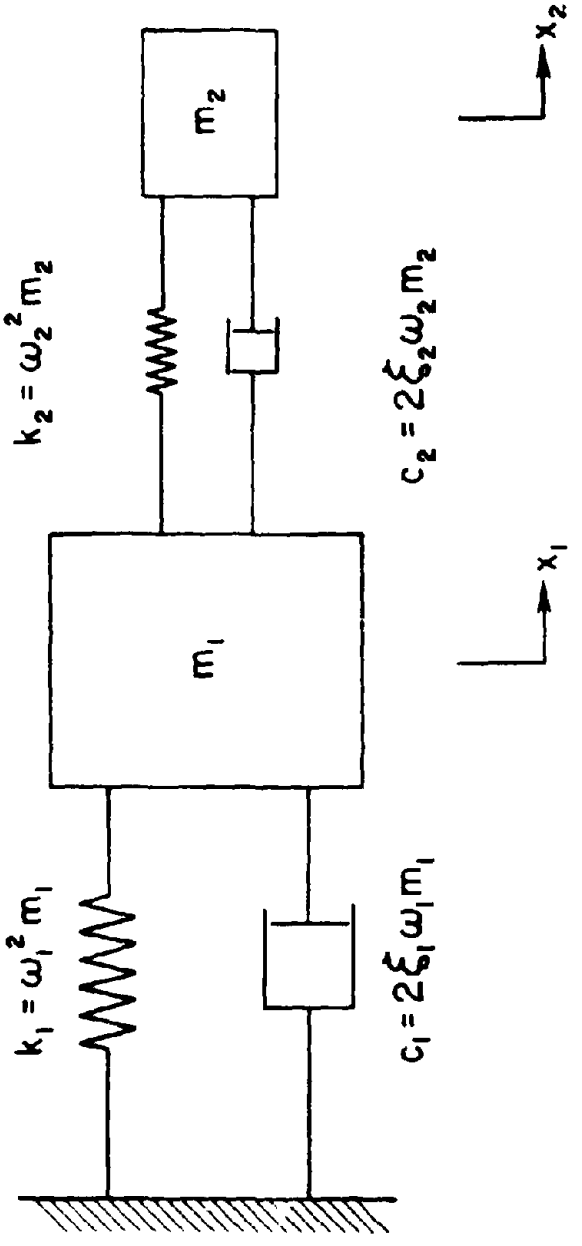

Fig.3.1. Two Degree-of-Freedom Equipment-Structure System

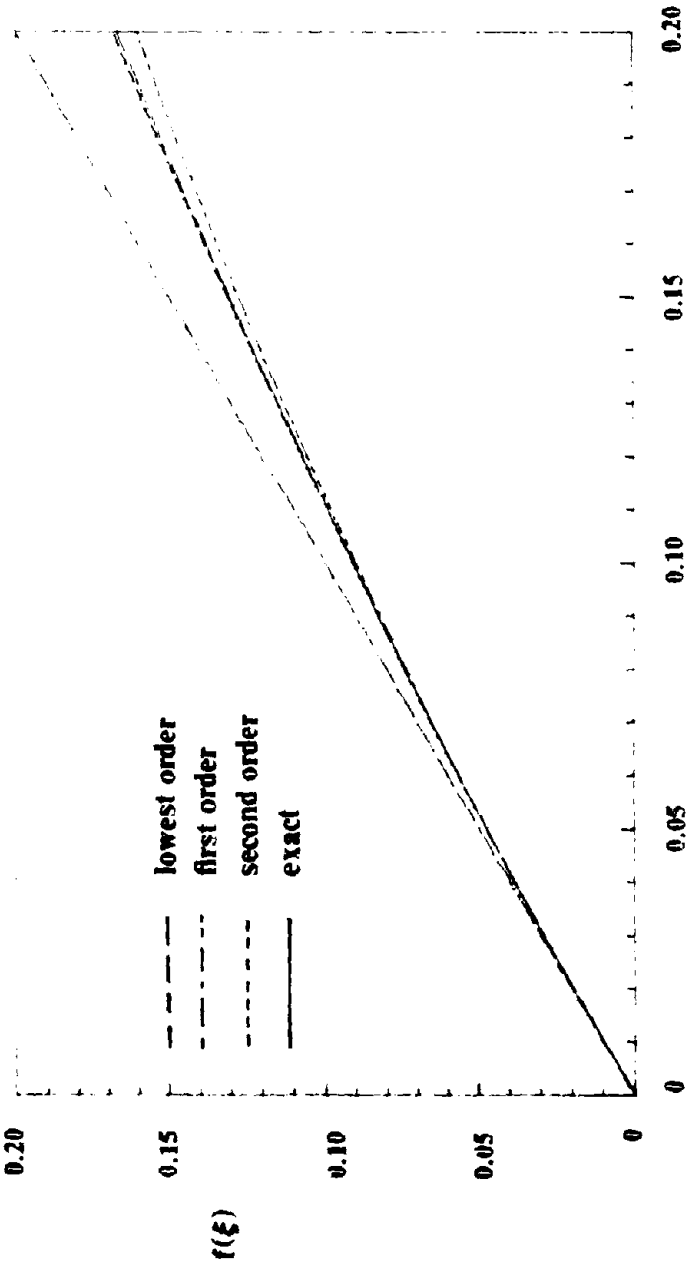

Fig.3.2. Perturbation Approximations

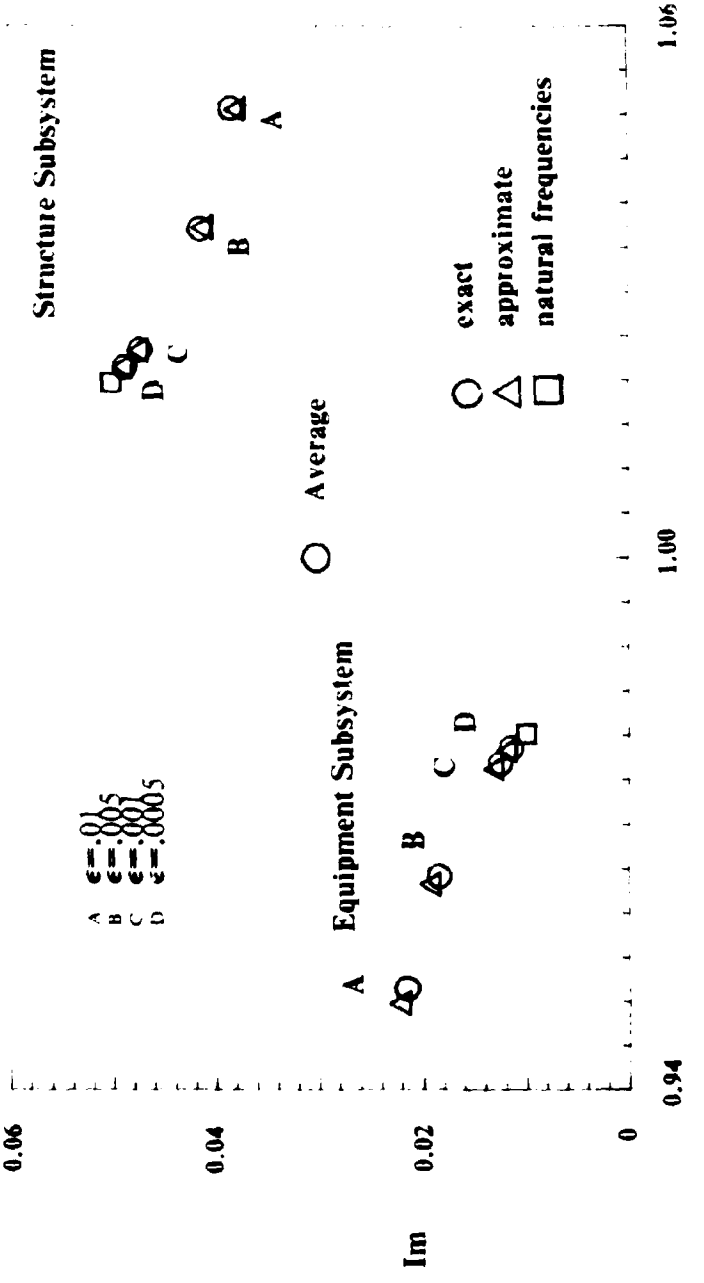

Fig.3.3a. Tuned Complex Frequencies: General Configuration
β=0.04, ξ_d=0.04, ξ_s=0.03, ω_s=1 rad/sec

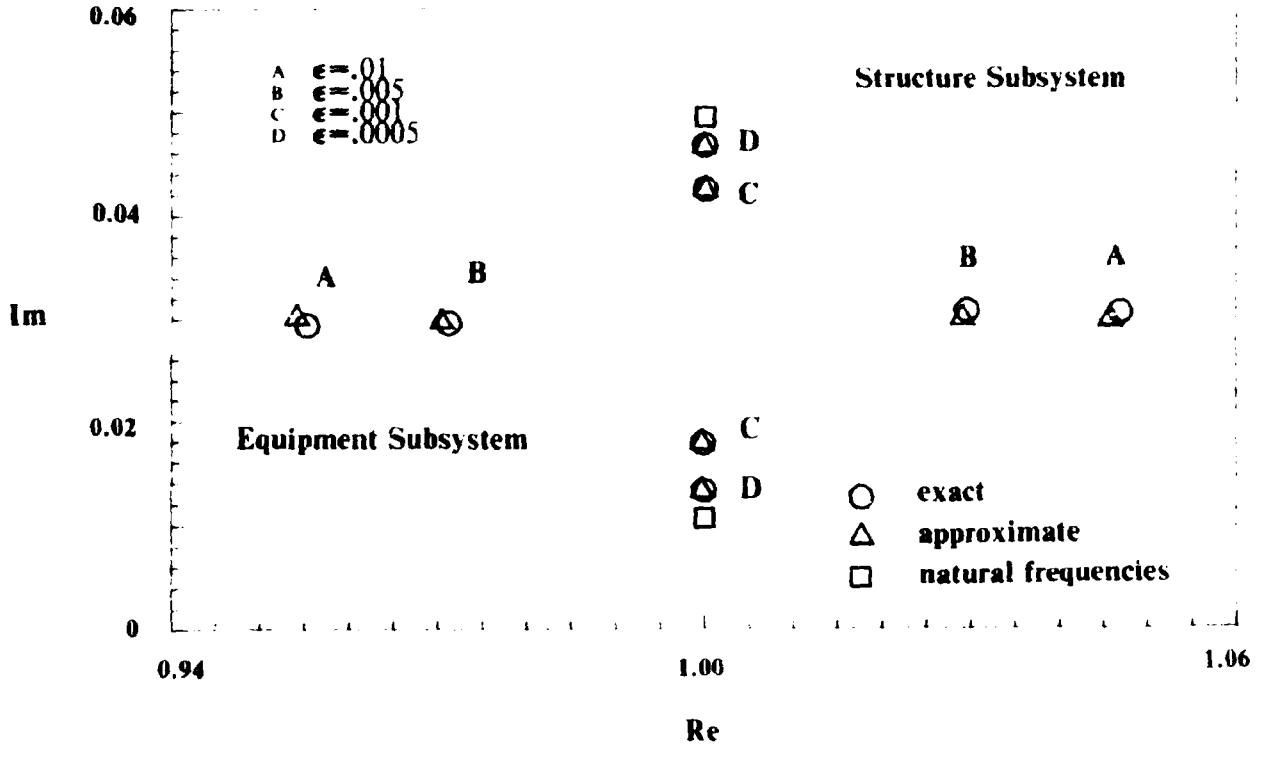

Fig.3.3b. Tuned Complex Frequencies: Perfect Tuning
β=0.00, ξ_d=0.04 ξ_a=0.03, ω_a=1 rad/sec

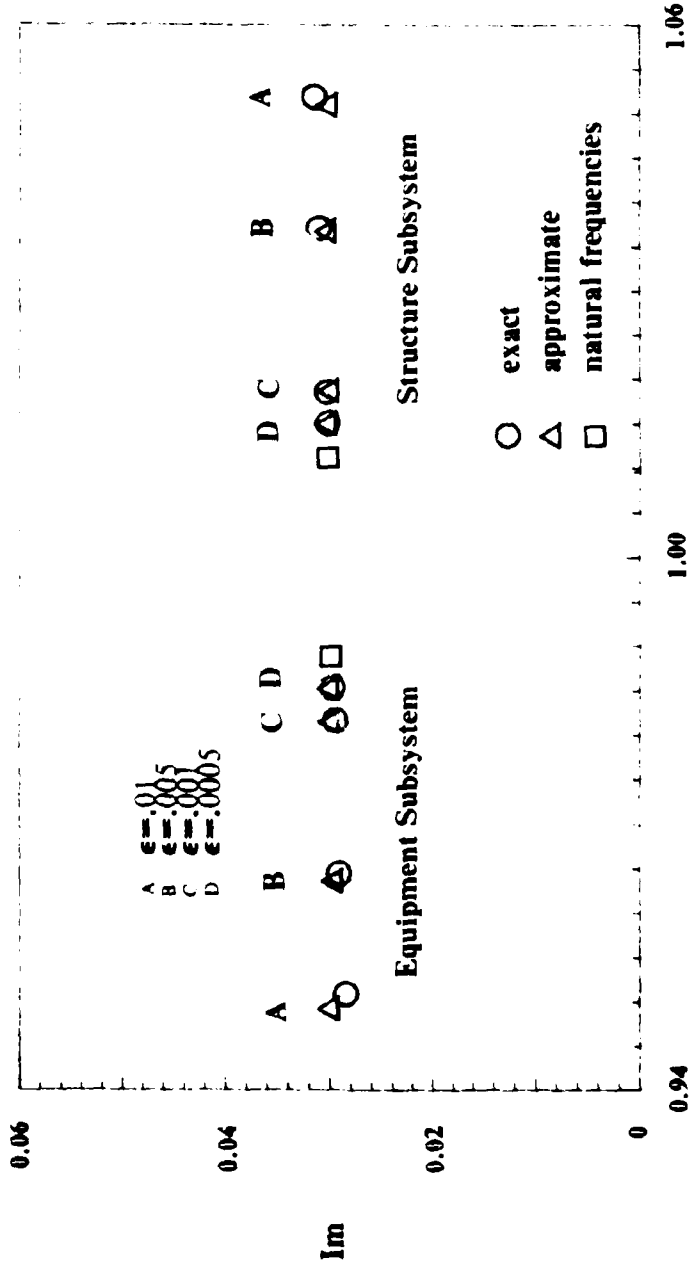

Fig.3.3c. Tuned Complex Frequencies: Equal Damping
β=0.02, ξ_d=0.00, ξ_s=0.03, ω_s=1 rad/sec

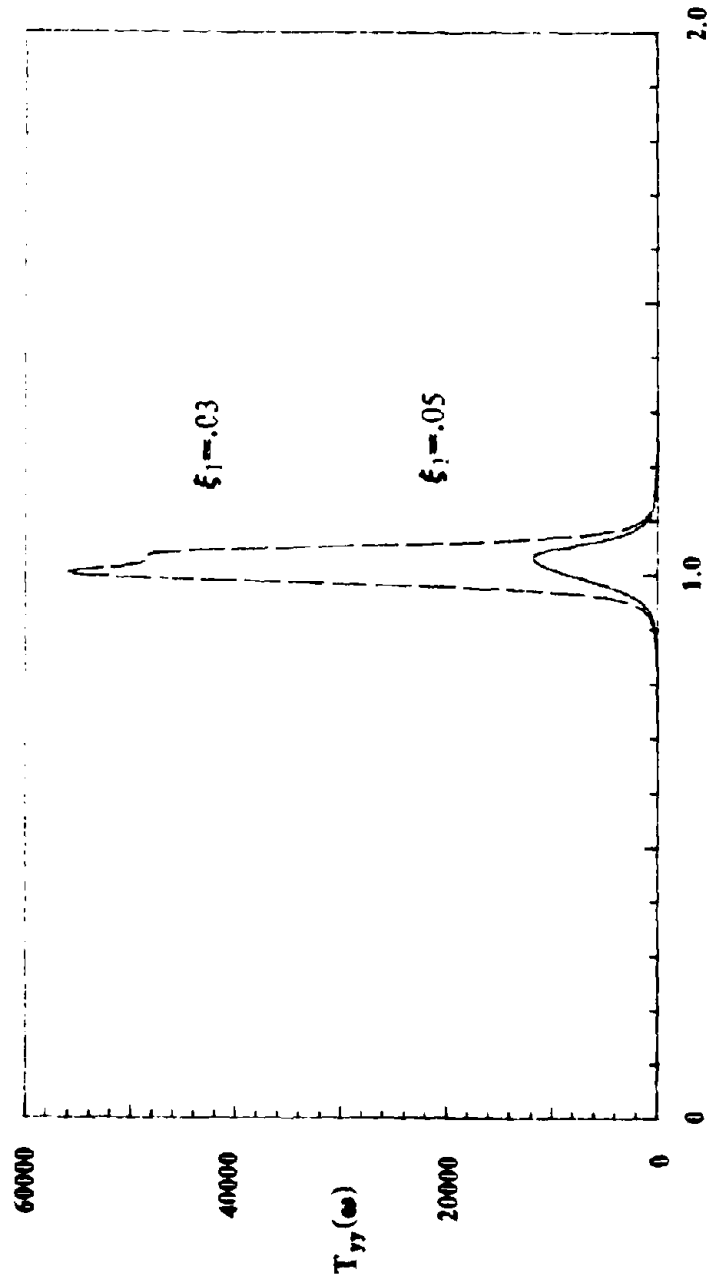

Fig.3.4. Transfer Function $T_{yy}(\omega)$: Tuned System
ω_1=1 rad/sec, ω_2=1.04 rad/sec, ϵ=.001, ξ_2=.02

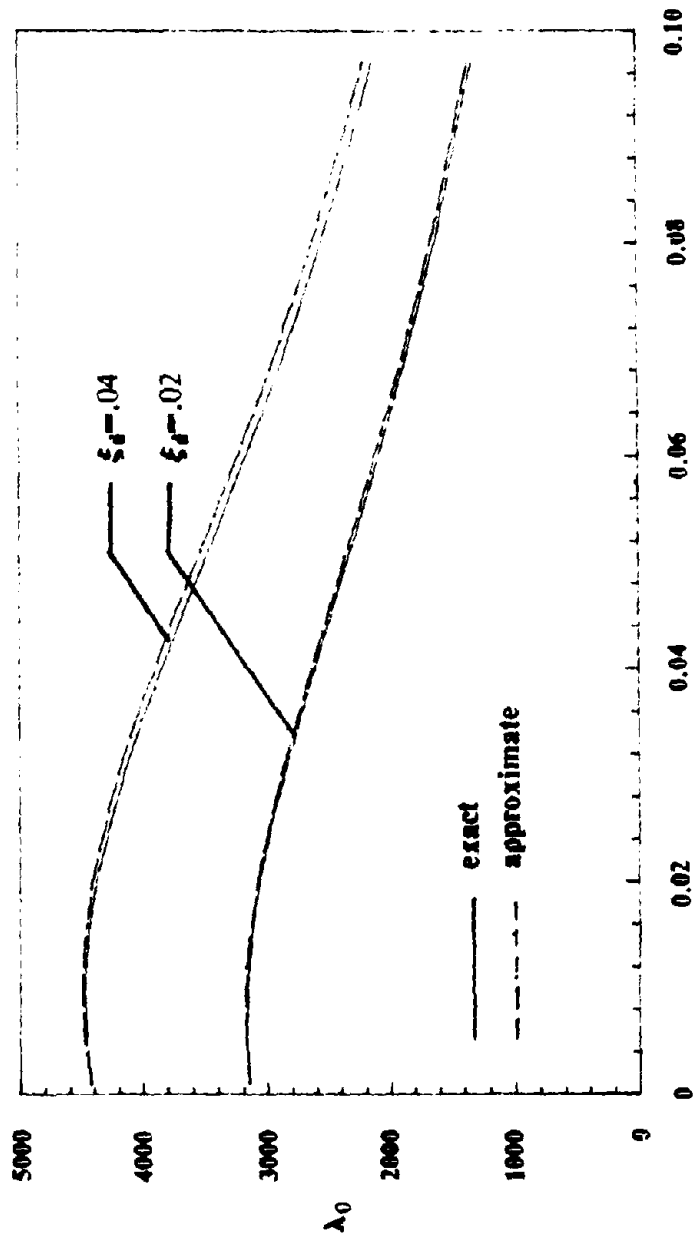

Fig.3.5.a. Spectral Moment λ_0
ω_e=1 rad/sec, ξ_s=.03, ϵ=.001

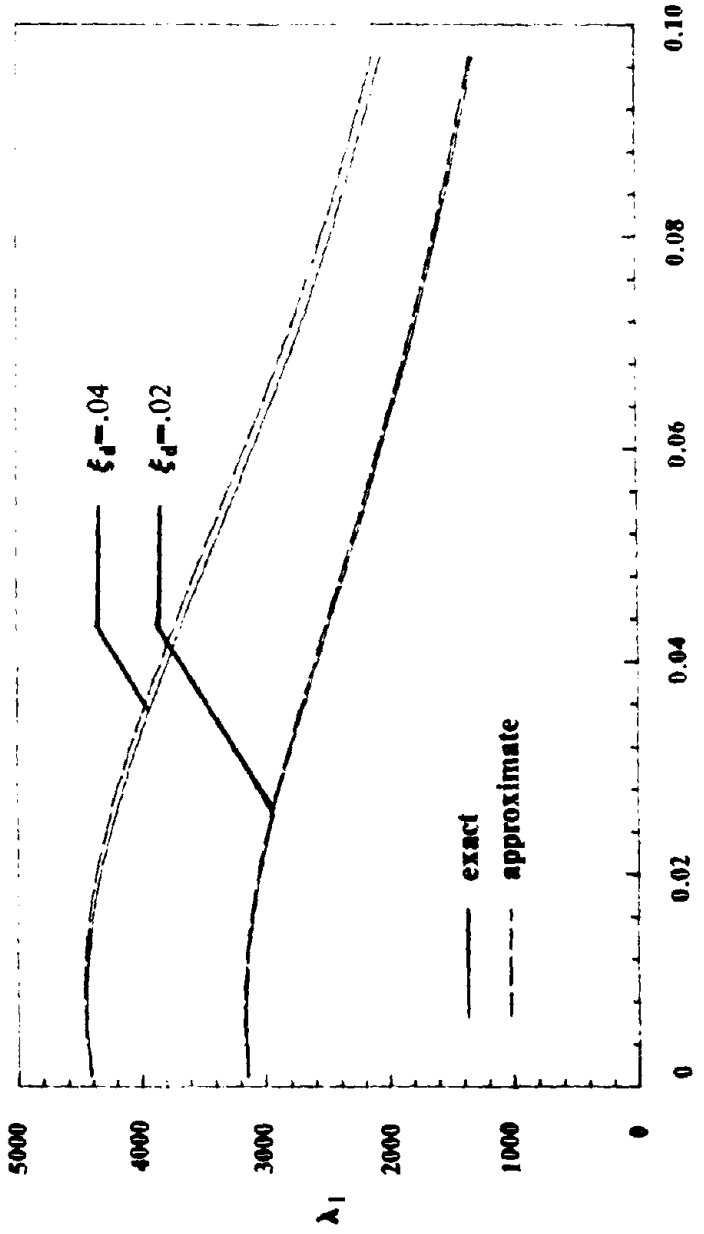

Fig.3.5.b. Spectral Moment λ_1
ω_n=1 rad/sec, ξ_s=.03, ϵ=.001

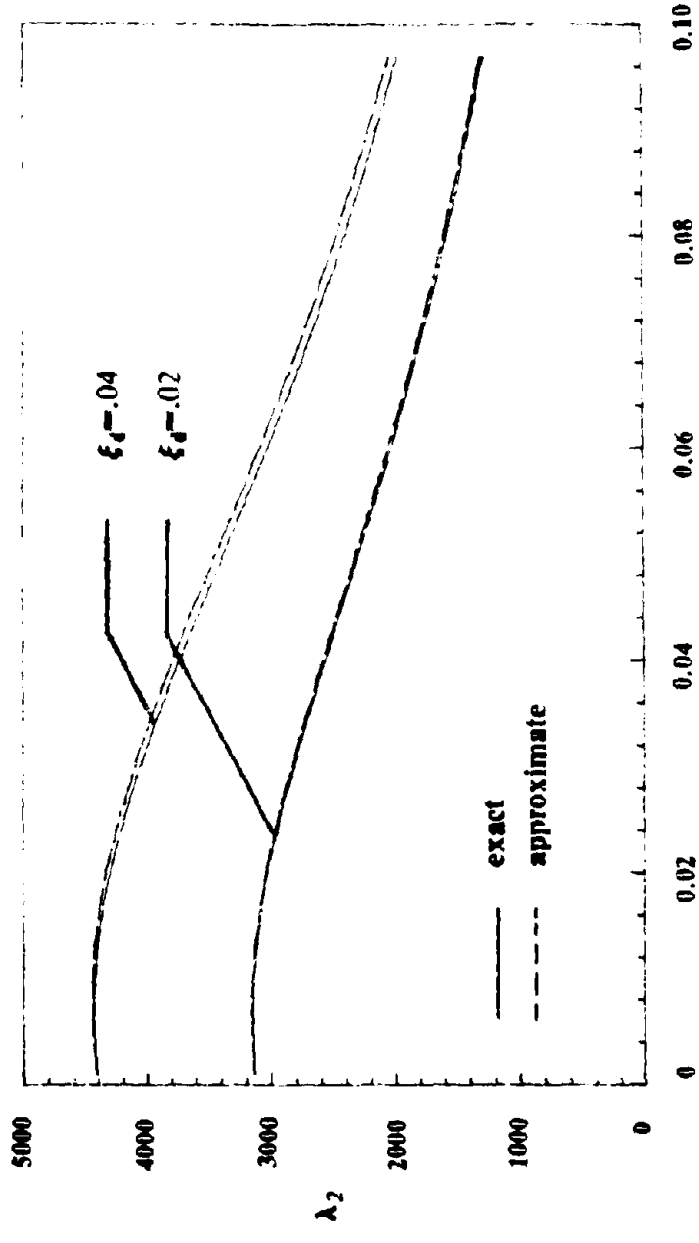

Fig.3.5.c. Spectral Moment λ_2
ω_s=1 rad/sec, ξ_s=.03, ϵ=.001

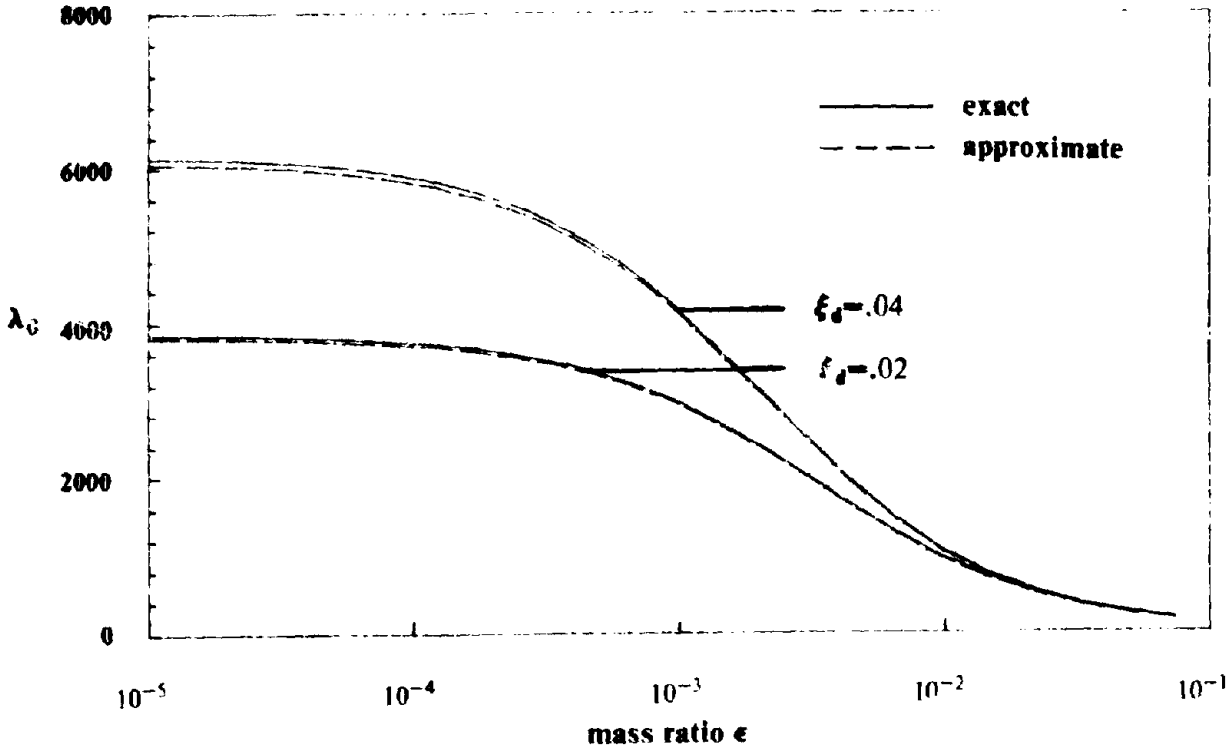

Fig.3.5.d. Spectral Moment λ_0 versus Mass Ratio ϵ
ω_n=1 rad/sec, ξ_s=.03, β=0

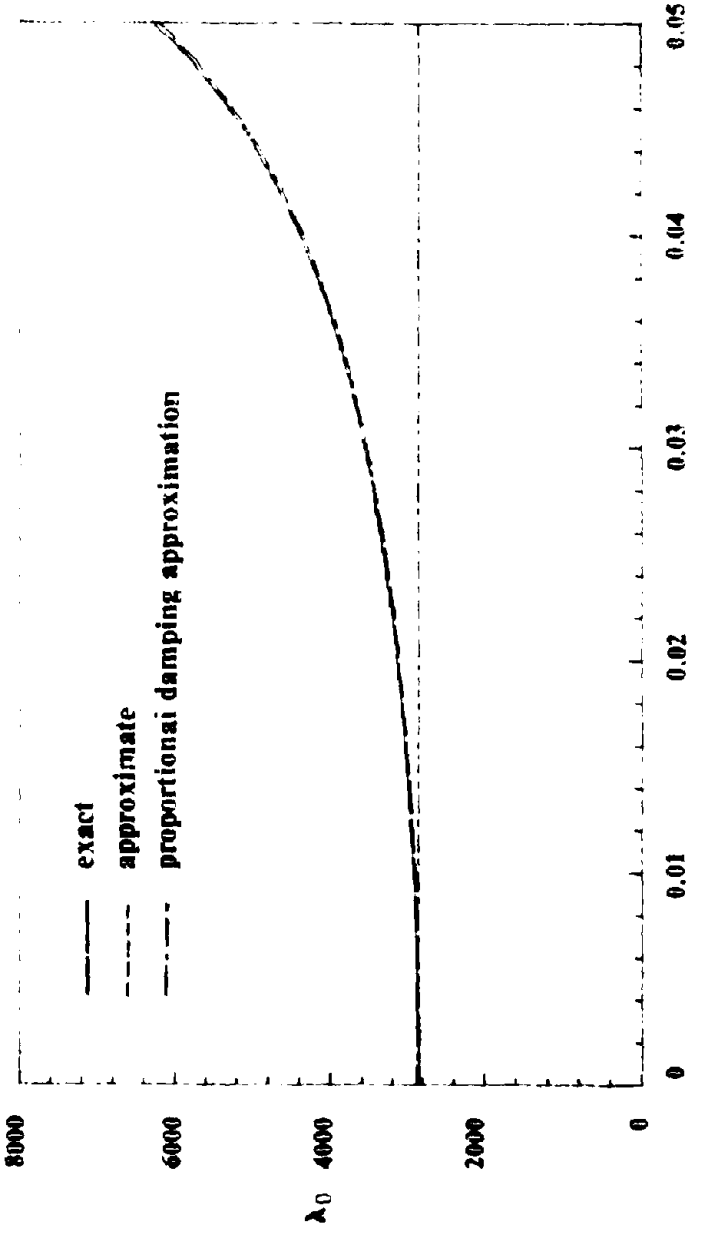

Fig.3.5.e. Spectral Moment λ_0 versus Damping Difference ξ_d
ω_s=1 rad/sec, ξ_s=.03, ϵ=.25

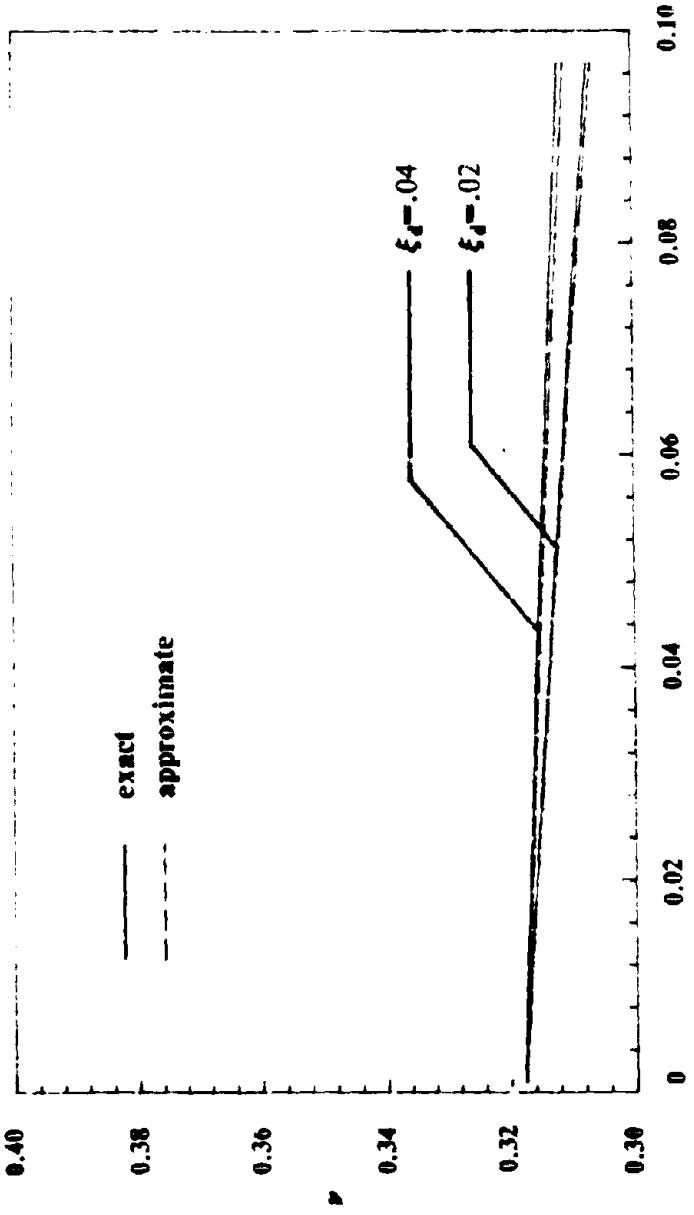

Fig.3.6a. Mean Zero-Crossing Rate ν
ω_n=1 rad/sec, ξ_n=0.03, ϵ=.001

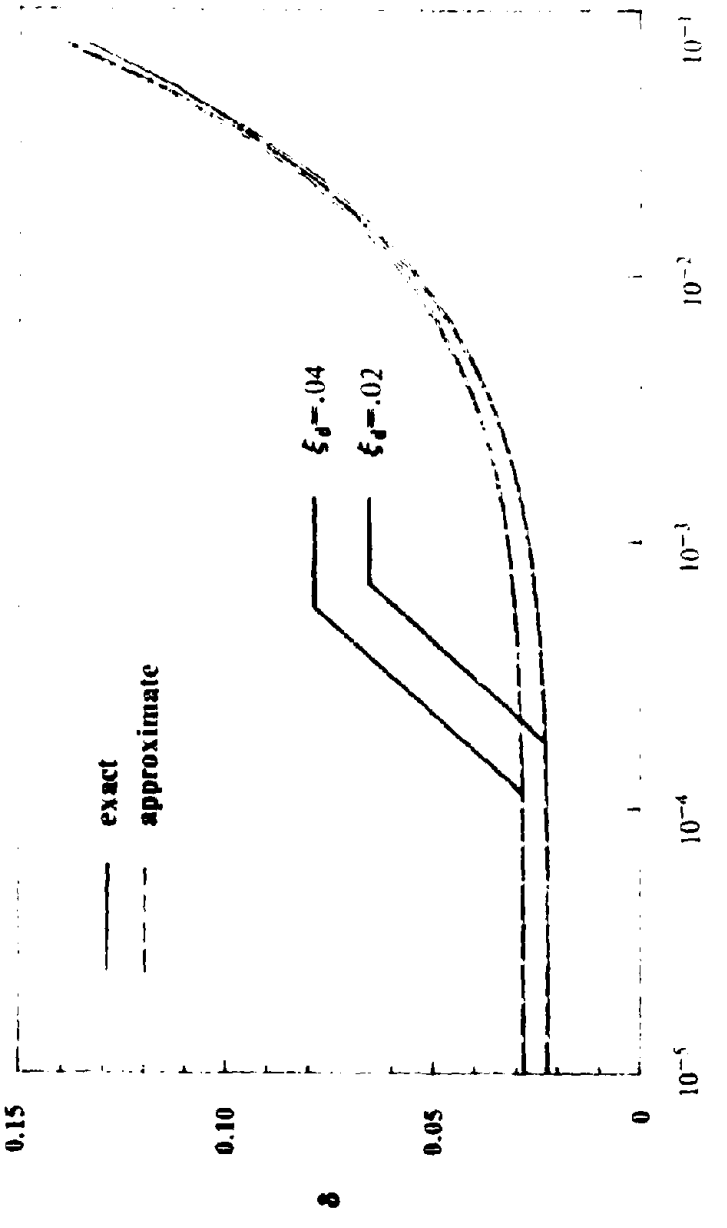

Fig.3.6b. Shape Factor δ versus Mass Ratio ε
ω_n=1 rad/sec, ξ_n=0.03, β=0.0

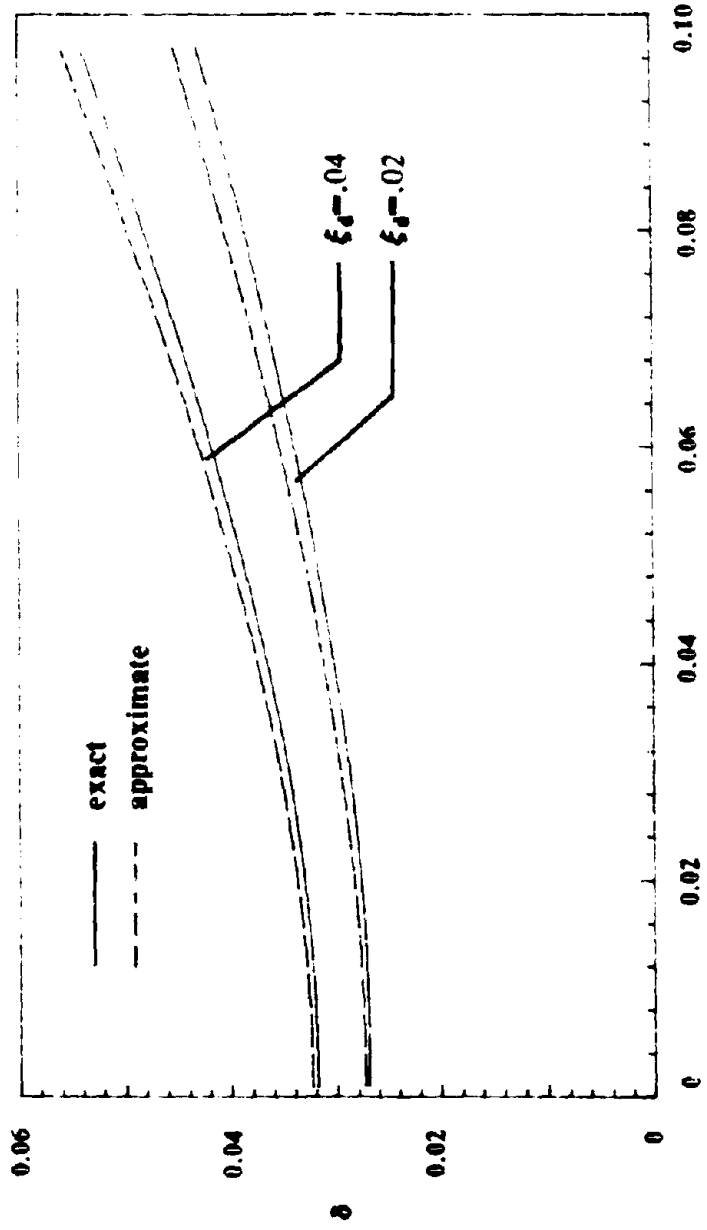

Fig.3.6c. Shape Factor δ versus Detuning β
ω_n=1 rad/sec, ξ_n=0.03, ϵ=.001

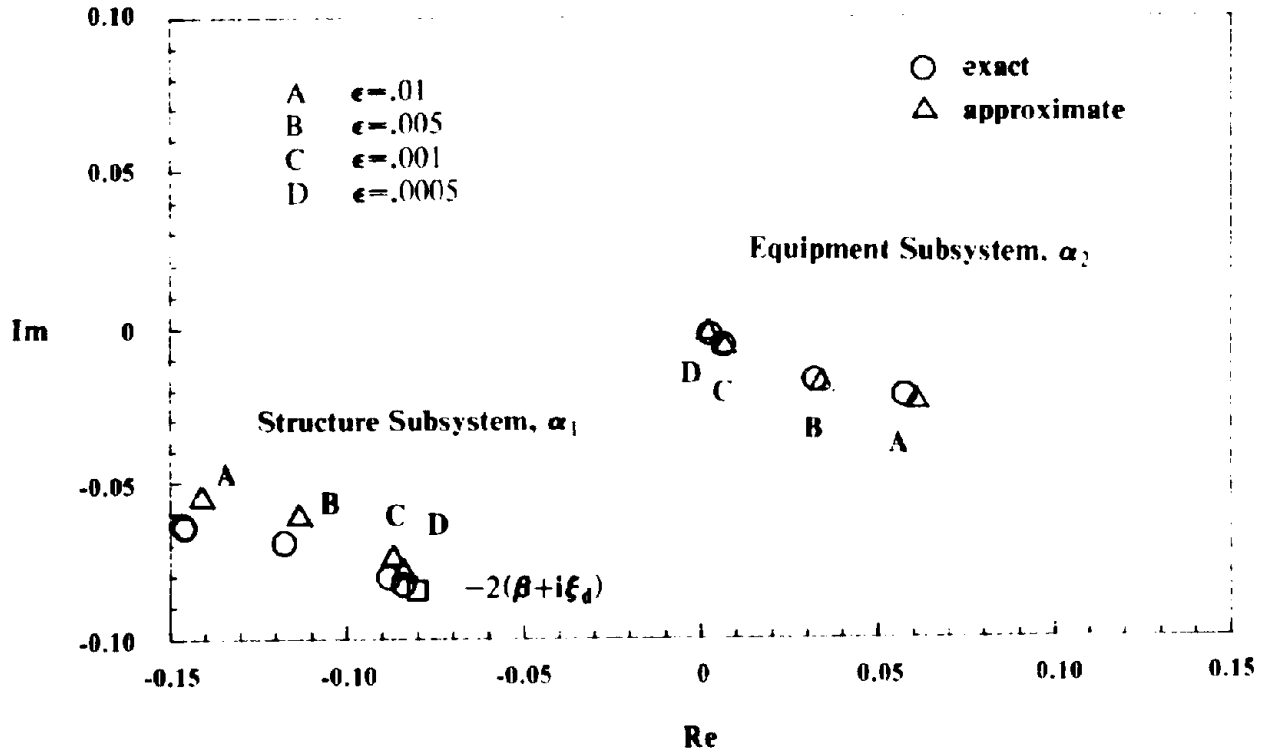

Fig.3.7a. Mode Shape Component α_i: General Configuration
β=0.04, ξ_d=0.04, ξ_s=0.03, ω_s=1 rad/sec

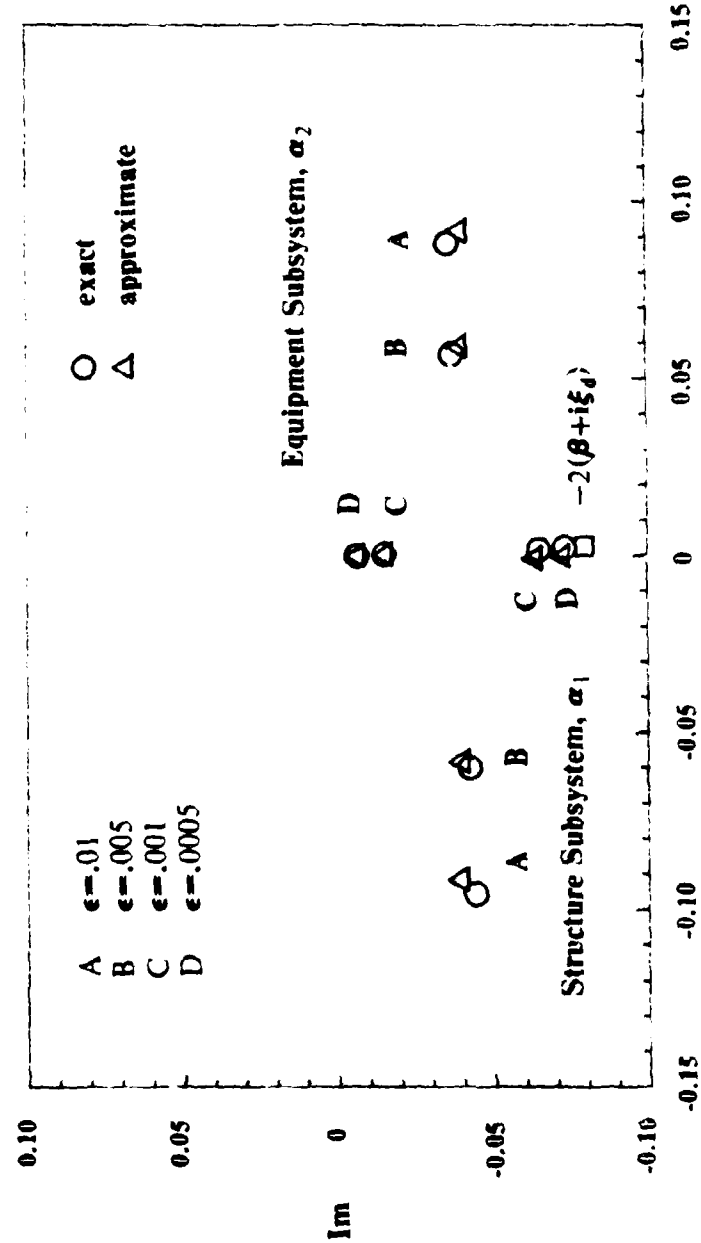

Fig.3.7b. Mode Shape Component α_1: Perfect Tuning
β=0.00, ξ_d=0.04, ξ_s=0.03, ω_s=1 rad/sec

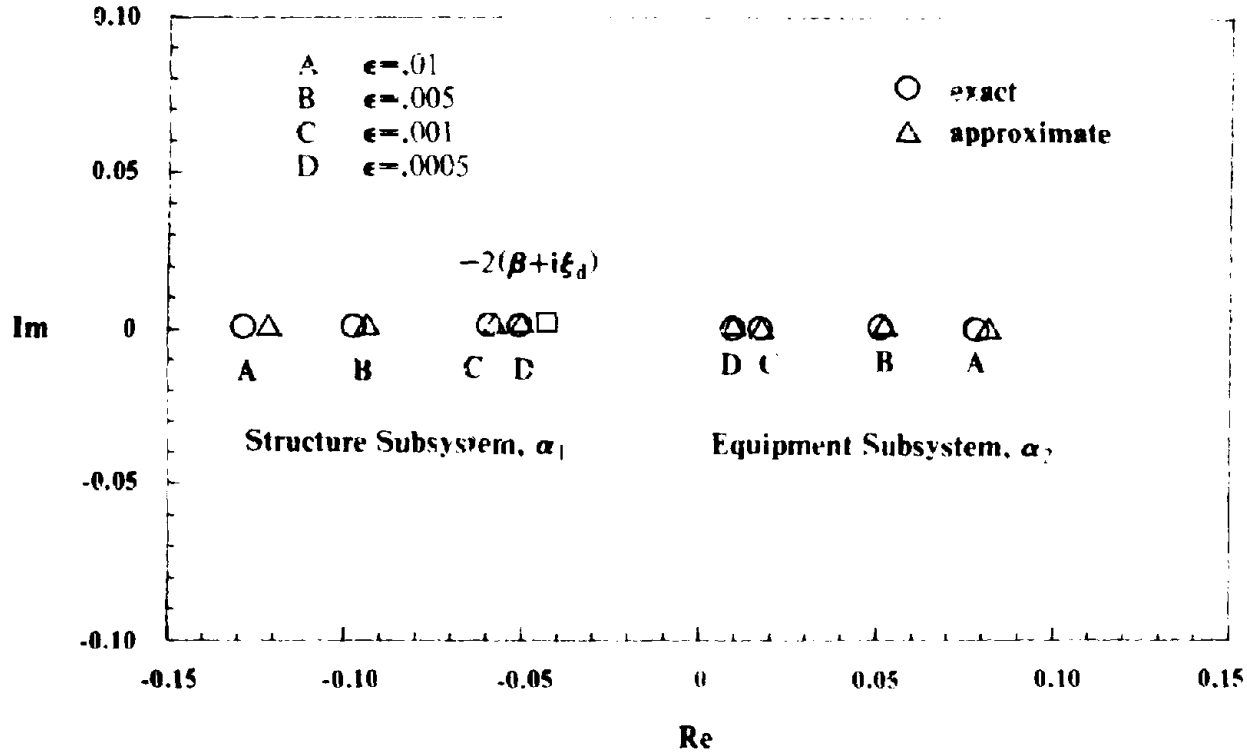

Fig.3.7c. Mode Shape Component α_1: Equal Damping
β=0.02, ξ_d=0.00, ξ_s=0.03, ω_s=1 rad/sec

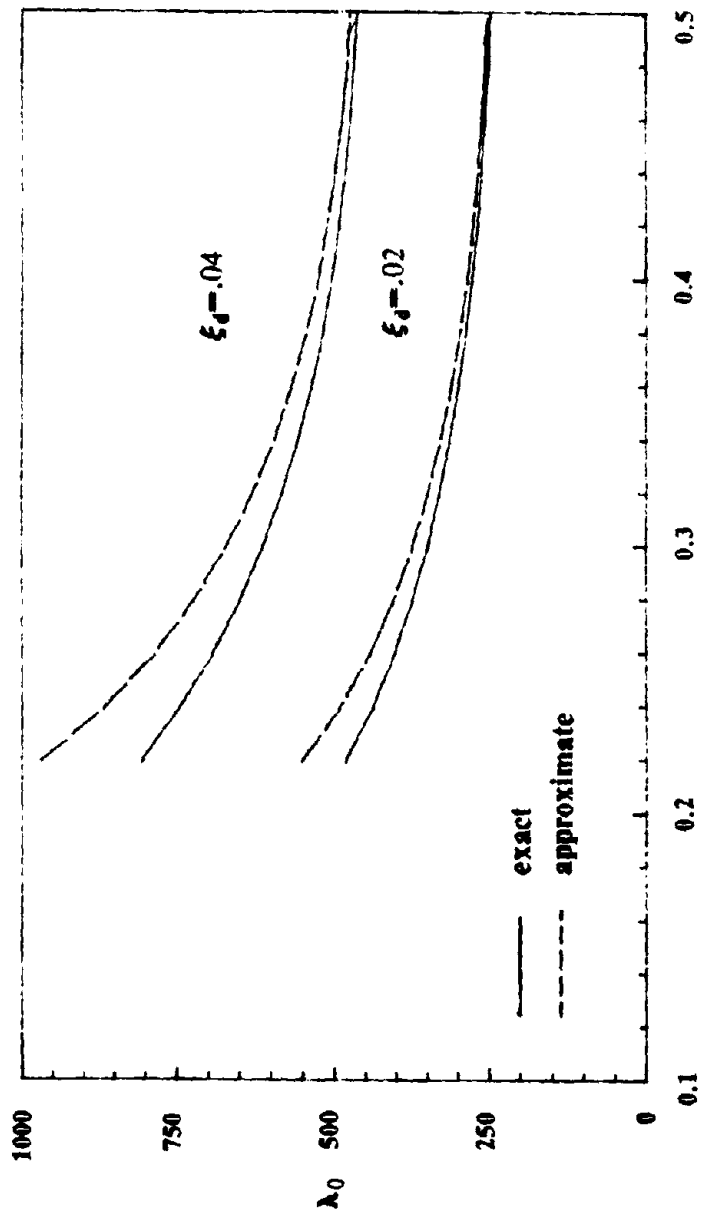

Fig.3.8. Spectral Moment λ_0: Detuned System
ω_n=1 rad/sec, ξ_s=0.03, ϵ=.01

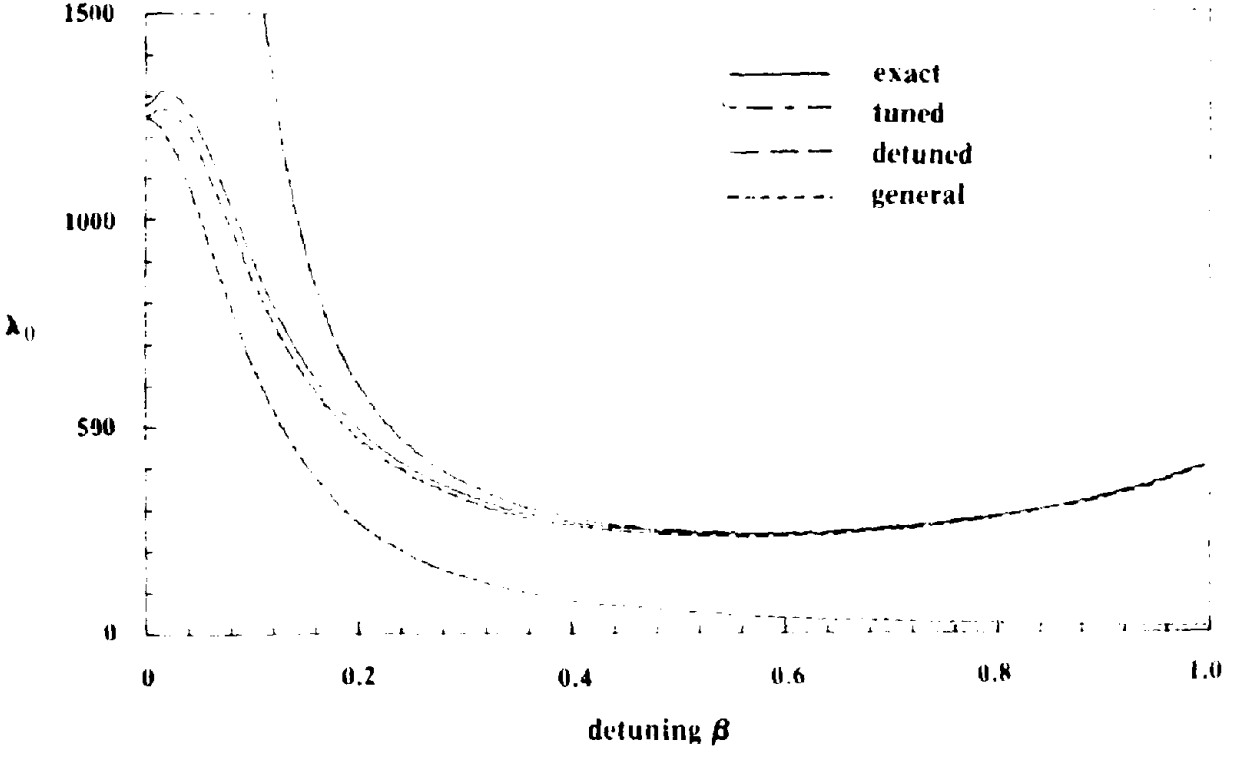

Fig.3.9. General Formula for Spectral Moments
ω_n=1 rad/sec, ξ_1=0.05, ξ_2=0.02, ϵ=.005

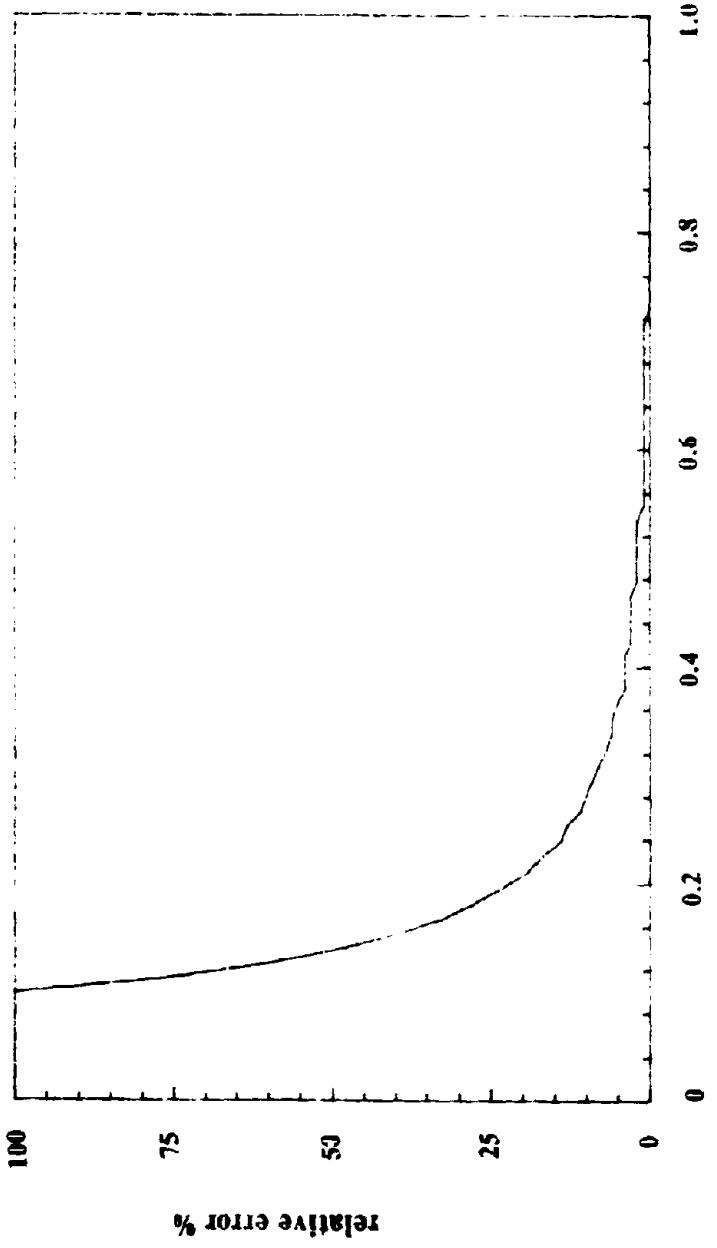

Fig.3.10. Error for Detuned Spectral Moments
ω_n=1 rad/sec, ξ_1=0.05, ξ_2=0.02, ϵ=.005

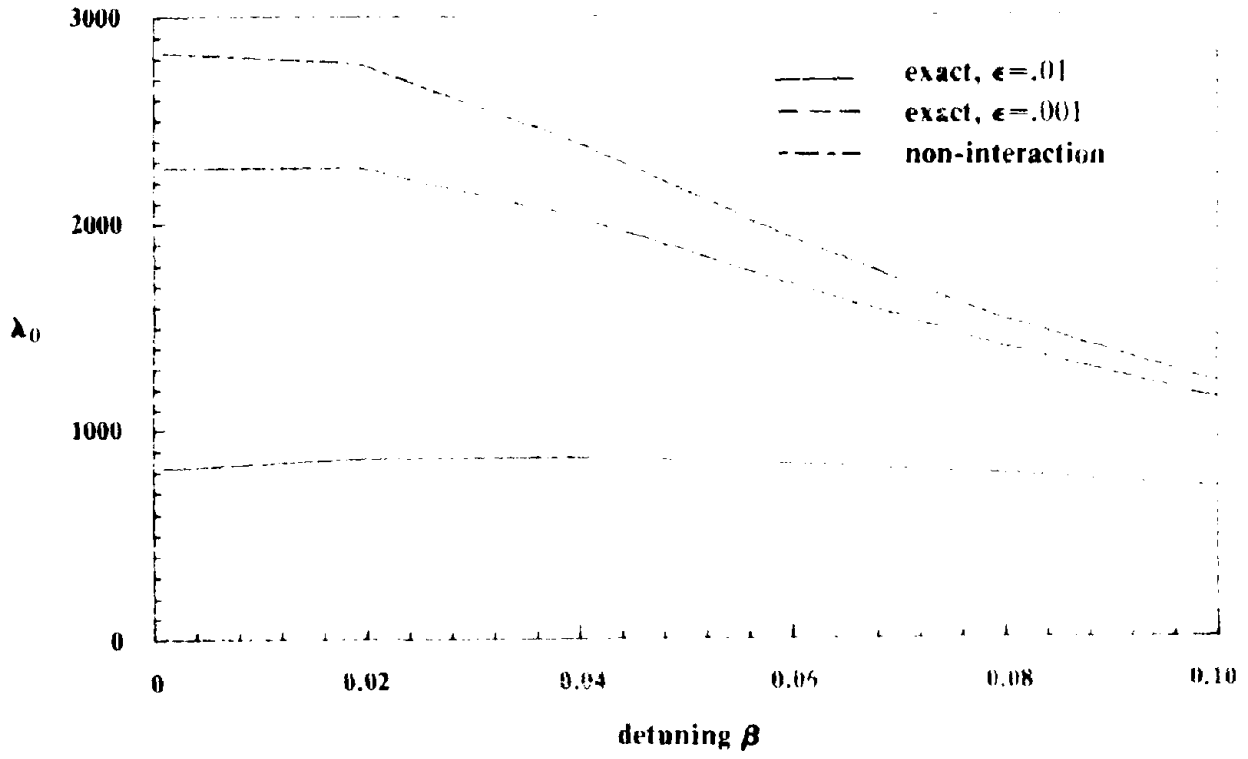

Fig.3.11. Spectral Moments for Non-Interaction
ω_n=1 rad/sec, ξ_1=0.05, ξ_2=0.02

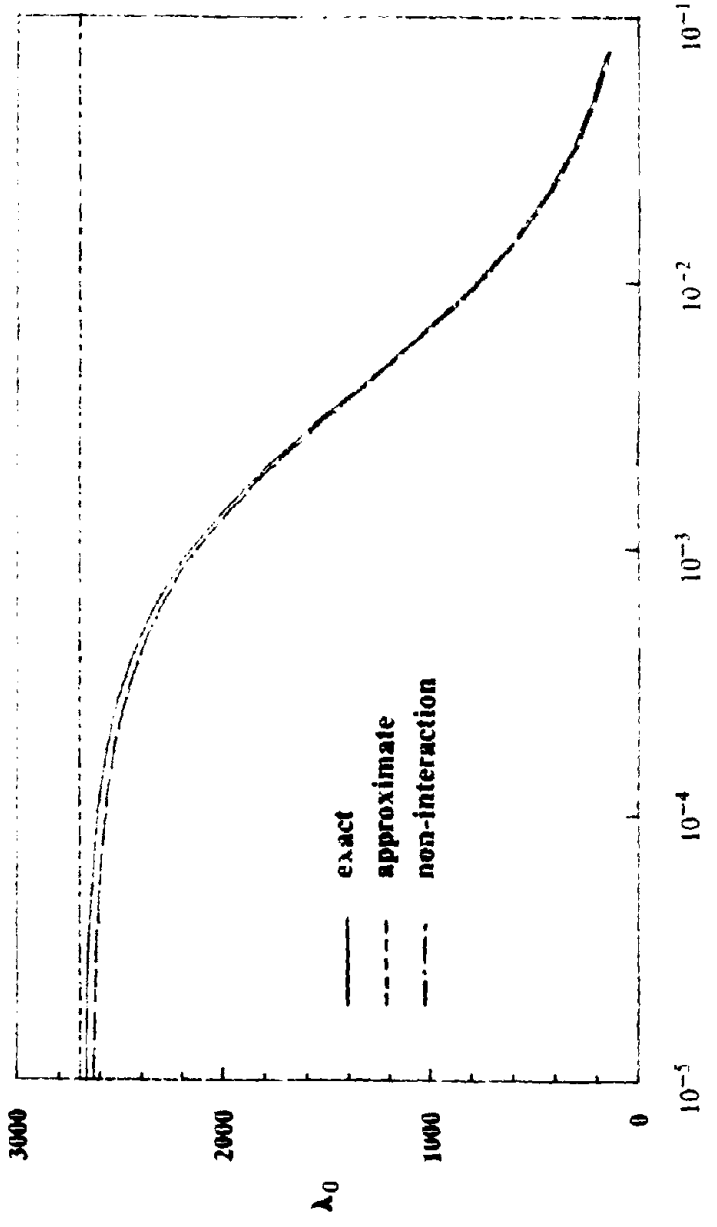

Fig.3.12. Non-interaction Error in Spectral Moment λ_0
ω_n=1 rad/sec, ξ_1=0.05, ξ_2=0.02, β=0

CHAPTER 4

ANALYSIS OF SINGLE-DEGREE-OF-FREEDOM EQUIPMENT ATTACHED TO MULTI-DEGREE-OF-FREEDOM STRUCTURES

4.1 Introduction

In this chapter, MDOF/SDOF PS systems will be analyzed, where the structure studied in the previous chapter is generalized to one with multiple degrees of freedom and an arbitrary configuration. The equipment remains to have a single degree of freedom; however, it can be attached to the structure at more than one node; it may also be attached to the base.

The methods of analysis of the MDOF/SDOF PS system will follow the same approach developed in the previous chapter. It will be shown that the basic characteristics and properties of equipment-structure systems, such as tuning, interaction, non-classical damping, and closely-spaced, correlated modes that were found earlier are also present in the MDOF/SDOF system. However, the results in Chapter 3 will be generalized to account for the more complex inter-relationships that are possible between the multiple structure modes and the equipment mode.

It has been recognized that the analysis of certain MDOF/SDOF PS systems can be reduced to the analysis of the 2-DOF equipment-structure system [37, 36]. However, it is shown that this reduction can not be utilized in many MDOF/SDOF systems, therefore more general methods of analysis will be developed.

The analysis will begin with a discussion of tuning and multiple tuning. Then, the frequency response function will be derived for the response of the secondary subsystem. Next, expressions for the mode shapes and frequencies will be derived which are suitable for use in many dynamic analysis techniques such as those described in the Introduction. For further insight to the behavior of the MDOF/SDOF system, these expressions are used directly in the

modal decomposition method developed earlier for finding algebraic formulations for the spectral moments of response to white-noise input. In the final part of this chapter, non-interaction is considered. The results derived earlier in the chapter reduce to simple, closed form expressions for all arbitrary configurations of the two subsystems.

4.2 Definitions

4.2.1 Parameters

In this section a set of matrices will be developed to describe the MDOF/SDOF system which will be used in the remainder of this study.

First, the parameters of the primary subsystem will be defined. Let N be the number of degrees-of-freedom of this subsystem and $x_1, \ldots, x_N$ be the displacement coordinates relative to the base. Then define the primary subsystem matrices

$$\mathbf{K}_{pp} = \text{stiffness matrix } (N \times N) \tag{1a}$$

$$\mathbf{C}_{pp} = \text{damping matrix } (N \times N) \tag{1b}$$

$$\mathbf{M}_{pp} = \text{mass matrix } (N \times N) \tag{1c}$$

which are associated with the displacements x_i.

It is assumed that the primary subsystem in itself is classically damped. Therefore by standard eigenvalue analysis the following properties can be derived:

$$\omega_{pi} = \text{natural frequencies} \tag{2a}$$

$$\xi_{pi} = \text{damping ratios} \tag{2b}$$

$$\boldsymbol{\phi}_{pi} = \text{mode shapes} \tag{2c}$$

In general, it is not required to obtain all N mode shapes and frequencies; it is assumed that the above parameters are obtained for $i = 1, \ldots, n \leq N$. From the orthogonal properties of the mode shapes, the mass, stiffness, and damping matrices can be diagonalized using the $(N \times n)$ transformation matrix

$$\boldsymbol{\Phi}_p = \left[\boldsymbol{\phi}_{p1} \cdots \boldsymbol{\phi}_{pn}\right] \tag{3}$$

with the following result

$$\boldsymbol{\Phi}_p^T \mathbf{M}_{pp} \boldsymbol{\Phi}_p = \text{diag}[m_{p1} \cdots m_{pn}] \tag{4a}$$

$$\boldsymbol{\Phi}_p^t \mathbf{C}_{pp} \boldsymbol{\Phi}_p = \text{diag}[2m_{p1}\omega_{p1}\xi_{p1} \quad \cdots \quad 2m_{pN}\omega_{pN}\xi_{pN}] \tag{4b}$$

$$\boldsymbol{\Phi}_p^t \mathbf{K}_{pp} \boldsymbol{\Phi}_p = \text{diag}[m_{p1}\omega_{p1}^2 \quad \cdots \quad m_{pN}\omega_{pN}^2] \tag{4c}$$

For the single DOF secondary subsystem, let m_{s1}, ξ_{s1}, and ω_{s1} be the mass, damping ratio, and natural frequency of this subsystem, respectively. Then the 1×1 mass, damping, and stiffness matrices are simply

$$\mathbf{M}_{ss} = [m_{s1}], \quad \mathbf{C}_{ss} = [2m_{s1}\omega_{s1}\xi_{s1}], \text{ and } \mathbf{K}_{ss} = [m_{s1}\omega_{s1}^2], \tag{5}$$

The parameters of the two subsystems will now be used to describe the properties of the combined $N+1$ DOF PS system. The first N DOF will correspond to the primary subsystem and the $N+1$ DOF will correspond to the secondary subsystem. Thus, the displacements are defined by the $N+1$ vector

$$\mathbf{x}_0 = [x_{p1} \quad \cdots \quad x_{pN} \quad x_{s1}]^t \tag{6}$$

where x_{s1} is the displacement of the secondary subsystem relative to the base of the combined system. The $N+1\times N+1$ mass, damping, and stiffness matrices are

$$\mathbf{M}_{ss} = \begin{bmatrix} \mathbf{M}_{pp} & \mathbf{M}_{ps} \\ \mathbf{M}_{sp} & \mathbf{M}_{ss} \end{bmatrix} \quad \mathbf{C}_{ss} = \begin{bmatrix} \mathbf{C}_{pp} & \mathbf{C}_{ps} \\ \mathbf{C}_{sp} & \mathbf{C}_{ss} \end{bmatrix} \quad \mathbf{K}_{ss} = \begin{bmatrix} \mathbf{K}_{pp} & \mathbf{K}_{ps} \\ \mathbf{K}_{sp} & \mathbf{K}_{ss} \end{bmatrix} \tag{7}$$

where $\mathbf{C}_{sp} = \mathbf{C}_{ps}^t$, $\mathbf{M}_{sp} = \mathbf{M}_{ps}^t$, and $\mathbf{K}_{sp} = \mathbf{K}_{ps}^t$ are $1\times N$ matrices representing the physical coupling between the primary and secondary subsystems. The $N+1$ vector $\mathbf{r}_0$ is defined to be the influence vector coupling the base input to the displacements x_{s0}. From these matrices, the equations of motion for the combined system is given by

$$\mathbf{M}_{ss}\ddot{\mathbf{x}}_0 + \mathbf{C}_{ss}\dot{\mathbf{x}}_0 + \mathbf{K}_{ss}\mathbf{x}_0 = -\mathbf{M}_{ss}\mathbf{r}_0\ddot{x}_0(t) \tag{8}$$

where $\ddot{x}_0(t)$ is the base input acceleration.

To be precise, the primary subsystem matrices $\mathbf{M}_{pp}$, $\mathbf{C}_{pp}$, and $\mathbf{K}_{pp}$ should be replaced by more complicated matrices to account for the small added mass, damping, and stiffness terms arising from the influence of the secondary subsystem. However, these terms are of second-order magnitude in relation to the original primary subsystem matrix elements. Therefore, the use of the original primary matrices in the above equations is consistent with the lowest and first-order perturbation analysis that will be performed.

The damping and stiffness matrices $\mathbf{C}_{sp}$ and $\mathbf{K}_{sp}$ have a simple physical interpretation: For secondary subsystems with a single attachment point at, say, the l-th DOF of the primary subsystem, these matrices are given by

$$\mathbf{C}_{sp} = \left[0 \cdots 0 \; -2m_{s1}\omega_{s1}\xi_{s1} \; 0 \cdots 0\right] \tag{10a}$$

$$\mathbf{K}_{sp} = \left[0 \cdots 0 \; -m_{s1}\omega_{s1}^2 \; 0 \cdots 0\right] \tag{10b}$$

where the non-zero terms are at the l-th coordinate. For multiply attached secondary subsystems, stiffness and damping terms would be found in the coordinates corresponding to each attachment point. On the other hand, the mass matrix $\mathbf{M}_{sp}$ is assumed to be zero since PS systems are usually modeled with lumped masses.

In general, $\mathbf{C}_{ss}$ and $\mathbf{K}_{ss}$ are full matrices and are difficult to utilize for analysis. For this reason dynamic analysis of the combined PS system has been avoided in the past. However, from the above discussion it is clear that these matrices can be reduced using the transformation matrix

$$\mathbf{\Phi} = \begin{bmatrix} \mathbf{\Phi}_p & 0 \\ 0 & \mathbf{\Phi}_s \end{bmatrix} \tag{11a}$$

where $\mathbf{\Phi}_s = [1]$ is the 1×1 identity matrix. Using this transformation a new coordinate vector $\mathbf{z}$, given by the $n+1$ modal coordinates

$$\mathbf{z} = [z_{p1}, \ldots, z_{pn}, z_{s1}] \tag{11b}$$

is obtained through the relation $\mathbf{\Phi z} = \mathbf{x}_{ss}$. The mass, damping, and stiffness matrices in terms of these modal coordinates are, to lowest order,

$$\mathbf{M} = \mathbf{\Phi}^t \mathbf{M}_{ss} \mathbf{\Phi} = \mathrm{diag}\left[m_{p1} \cdots m_{pn} \; m_{s1}\right] \tag{12a}$$

$$\mathbf{C} = \mathbf{\Phi}^t \mathbf{C}_{ss} \mathbf{\Phi} = \begin{bmatrix} 2m_{p1}\omega_{p1}\xi_{p1} & 0 & c_{1l} \\ \cdots & \cdots & \cdots \\ 0 & 2m_{pn}\omega_{pn}\xi_{pn} & c_{nl} \\ c_{1l} & c_{nl} & 2m_{s1}\omega_{s1}\xi_{s1} \end{bmatrix} \tag{12b}$$

$$\mathbf{K} = \mathbf{\Phi}^t \mathbf{K}_{ss} \mathbf{\Phi} = \begin{bmatrix} m_{p1}\omega_{p1}^2 & 0 & k_{1l} \\ \cdots & \cdots & \cdots \\ 0 & m_{pn}\omega_{pn}^2 & k_{nl} \\ k_{1l} & k_{nl} & m_{s1}\omega_{s1}^2 \end{bmatrix} \tag{12c}$$

where

$$c_j = \boldsymbol{\phi}_j^T \mathbf{C}_{jj} \quad k_j = \boldsymbol{\phi}_j^T \mathbf{K}_{jj} \tag{12d}$$

Note the simplicity of the form of the above matrices as compared with the original system matrices, Eqs 7. The original equations of motion that were given in Eq 8 for the nodal coordinates $\mathbf{x}_s$ has the following form for the modal coordinates $\mathbf{z}$

$$\mathbf{M}\ddot{\mathbf{z}} + \mathbf{C}\dot{\mathbf{z}} + \mathbf{K}\mathbf{z} = -\mathbf{M}\mathbf{r}\ddot{y}_g(t) \tag{13}$$

where the vector of modal participation factors $\mathbf{r}$ are given in terms of $\mathbf{M}_{ss}$ and $\mathbf{r}_s$ by the standard formulation [10]

$$\mathbf{r} = \mathbf{M}_{ss}^{-1} \boldsymbol{\Phi}^T \mathbf{M}_{ss} \mathbf{r}_s \tag{14}$$

It is worthwhile to examine the terms in Eqs.12d more closely. For secondary subsystems with only a single attachment point at the j-th DOF, these equations reduce to

$$k_j = -m_j \omega_j^2 \{\boldsymbol{\phi}_{sj}\} \tag{15a}$$

$$c_j = -2m_j \omega_j \xi_j \{\boldsymbol{\phi}_{sj}\} \tag{15b}$$

where $\{\boldsymbol{\phi}_{sj}\}$ denotes the j-th coordinate of the vector $\boldsymbol{\phi}_j$. For more general support configurations, similar expressions can be obtained. Let ζ_j be the ratio

$$\zeta_j = -\frac{k_j}{m_j \omega_j^2} \tag{16}$$

Then k_j and c_j can be written as

$$k_j = -m_j \omega_j^2 \zeta_j \qquad c_j \approx -2m_j \omega_j \xi_j \zeta_j \tag{17}$$

where the first equation is exact by the definition of ζ_j, and the second is an approximation. The approximation is justified for obtaining low-order results for two reasons: (1) it is exact in the important case of single attachment point, as shown in Eq 15b, (2) this relatively small term has been neglected altogether in previous research work without much loss of accuracy.

Before going further, a physical interpretation of the term ζ_j will be investigated. For systems with a single attachment point, $\zeta_j = \{\boldsymbol{\phi}_{sj}\}$ is the displacement that the mass of the secondary subsystem experiences when the primary subsystem is statically displaced into its mode shape $\boldsymbol{\phi}_j$. For multiply supported secondary subsystems, the meaning for ζ_j remains the same. This is clear from the static equilibrium equation $\mathbf{Kz}=0$, which can be rewritten in

terms of the equipment DOF

$$\sum_{j} k_{ij} z_j = -\omega^2 m_{si} z_{si} \tag{18}$$

Given a unit displacement of the i-th primary mode, i.e., $z_i = 1$ and $z_j = 0$ for $j \neq i$, the corresponding displacement for the equipment is

$$z_{si} = -\frac{k_{ii}}{\omega^2 m_{si}} = \zeta_{si} \tag{19}$$

As an example, consider the 3-DOF system in Fig.4.1. By following the matrix analysis outlined in this section, it can be shown that

$$\boldsymbol{\phi}_{p1} = \begin{bmatrix} 1 \\ .5 \end{bmatrix} \quad \boldsymbol{\phi}_{p2} = \begin{bmatrix} 1 \\ -.5 \end{bmatrix} \quad \mathbf{K}_{sp} = \begin{bmatrix} -\frac{1}{2}\omega_1^2 m_{s1} & -\frac{1}{2}\omega_2^2 m_{s1} \end{bmatrix} \tag{20a}$$

from which it follows, by definition, that

$$\zeta_{s1} = -.75 \quad \text{and} \quad \zeta_{s2} = -.25 \tag{20b}$$

The deflections of the primary subsystem into its mode shapes are shown, and it is observed that the corresponding static displacement of the equipment are given exactly by ζ_{si}.

Before continuing, it is useful to introduce notation for mass ratios. Let ϵ_i be the ratio

$$\epsilon_i = \frac{m_{si}}{m_p} \tag{21}$$

Also, let γ_i be the effective mass ratio

$$\gamma_i = \zeta_{si}^2 \frac{m_{si}}{m_p} \tag{22}$$

which is a generalization of the effective mass ratio defined by Der Kiureghian, et al. [18] for the case of a single attachment point, i.e., where $\zeta_{si} = [\boldsymbol{\phi}_{si}]_i$.

4.2.2 Classifications for MDOF/SDOF Systems

The 2-DOF PS system has only two simple classifications: tuned and detuned. However, the MDOF/SDOF PS system has a larger number of possible relationships between the modes of the structure and the mode of the equipment, therefore more classifications are necessary for an organized, well-defined analysis of this system.

First, a definition of tuning for MDOF/SDOF systems will be presented. For the 2-DOF

system the structure mode was found to be tuned to the equipment mode if

$$\beta^2 = \left[\frac{\omega_{j1} - \omega_{s1}}{\omega_a}\right]^2 < \frac{\xi_a^2}{e}\left[4 + \frac{\epsilon}{\xi_{s1}\xi_{j1}}\right] \tag{23}$$

where ω_a is the average of ω_{j1} and ω_{s1}. This definition can be extended to MDOF/SDOF systems: mode i of the structure is said to be tuned to the equipment mode if

$$\left[\frac{\omega_{ji} - \omega_{s1}}{\omega_a}\right]^2 < \frac{\xi_a^2}{e}\left[4 + \frac{\gamma_1}{\xi_{s1}\xi_{ji}}\right] \tag{24}$$

where ω_a is the average of ω_{s1} and ω_{ji} and γ_1 is the effective mass ratio defined earlier.

The above definition is used to define several types of tuning classifications. Let I_t and I_d denote the sets of structure modes tuned and detuned from the equipment, respectively, i.e.

$$I_t = \left\{ i : \omega_{ji} \text{ is tuned to } \omega_{s1} \right\} \tag{25a}$$

$$I_d = \left\{ i : \omega_{ji} \text{ is detuned from } \omega_{s1} \right\} \tag{25b}$$

For the 2-DOF system, $n=1$ and only two classification are possible:

$$I_t = \{ 1 \},\ I_d = \{ \} \quad \text{for tuned systems} \tag{26a}$$

$$I_t = \{ \},\ I_d = \{ 1 \} \quad \text{for detuned systems} \tag{26b}$$

For MDOF structures where $n > 1$, several relationships must be considered. If all primary modes are detuned from the equipment, the system is totally detuned. Otherwise the system is singly or multiply tuned, according to the number of primary modes tuned to the secondary subsystem. Using the above notation,

$$I_t = \{ \},\ I_d = \{ 1, \cdots, n \} \quad \text{for detuned systems} \tag{27a}$$

$$I_t = \{ l \} \quad \text{for singly tuned systems} \tag{27b}$$

$$I_t = \{ k, k+1, \cdots, k+l-1 \} \quad \text{for multiply tuned systems} \tag{27c}$$

In the last case, l primary modes, beginning with the k-th mode, are tuned to the equipment.

4.2.3 Example System

To illustrate the major characteristics of MDOF/SDOF systems and check the accuracy of the formulations derived in this chapter, the example system shown in Fig.4.2 is used. The primary subsystem is composed of two parts, a SDOF oscillator and a 2-DOF subsystem, both

attached to a common base. The SDOF secondary subsystem is attached to both parts of the primary subsystem as well as the base.

The dynamic properties of the subsystems are described in Tables 1 and 2 and are chosen so that the combined system would exhibit important characteristics found in general MDOF/SDOF systems. For instance, the frequency of the equipment is a variable parameter, which allows for an investigation of tuning. For $\omega = .38$ rad/sec, the system is singly tuned as shown in Fig 4.3a, and for $\omega = 1.0$ rad/sec, the system becomes multiply tuned as shown in Fig 4.3b. The mass ratio, ϵ, is also chosen to be a variable parameter in order to study the influence of interaction. Finally, the damping ratio of the equipment is unequal to the damping ratios of the primary subsystem, thus the combined system is, in general, non-proportionally damped.

The response quantity that will be investigated is the relative displacement between the mass of the secondary subsystem and the upper mass of the primary subsystem 2.

4.3 Frequency Response Function Approach

4.3.1 Introduction

The complex frequency response matrix will be derived for general MDOF/SDOF PS systems. The transfer function is obtained which is used to find the power spectral density function and its moments for the response of the system to random excitation. The exact form of the transfer function is complicated; however, perturbation methods are used to reduce the expressions to a relatively simple closed form rational polynomial.

4.3.2 The Complex Frequency Response Matrix

The complex frequency response matrix for the system described by Eq 3.15 is found by substituting the expressions Eqs.12a-c for the matrices **M**, **C**, and **K** into the definition Eq.3.15. The result is

$$\mathbf{H}(\omega) = \begin{bmatrix} G_1(\omega) & \cdots & 0 & f_{11}(\omega) \\ \cdots & \cdots & \cdots & \cdots \\ 0 & \cdots & G_n(\omega) & f_{n1}(\omega) \\ f_{11}(\omega) & \cdots & f_{n1}(\omega) & g_1(\omega) \end{bmatrix}^{-1} \tag{28a}$$

where

$$g_1(\omega) = m_{s1}(-\omega^2 + 2i\omega_{s1}\xi_{s1}\omega + \omega_{s1}^2) \tag{28b}$$

$$G_i(\omega) = m_{pi}(-\omega^2 + 2i\omega_{pi}\xi_{pi}\omega + \omega_{pi}^2) \tag{28c}$$

$$f_{i1}(\omega) = -\zeta_{i1}m_{s1}(2i\omega_{s1}\xi_{s1}\omega + \omega_{s1}^2) \tag{28d}$$

for $i=1, \cdots, n$. As in the analysis of the 2-DOF system, $G_i(\omega)$ and $g_1(\omega)$ are the reciprocals of the complex frequency response functions for the i-th mode of the primary subsystem and the secondary subsystem, respectively. The function $f_{i1}(\omega)$ represents the coupling between these two modes. Due to the simple form of the matrix in Eq 28a, a closed form expression can be found for the inverse

$$\mathbf{H}(\omega) = \frac{\prod_{i=1}^{n} G_i}{d(\omega)} \begin{vmatrix} \frac{1}{G_1}\left[g_1 - \sum_{j\neq 1}\frac{f_{j1}^2}{G_j}\right] & & & & \text{(sym)} \\ \frac{f_{11}f_{21}}{G_1G_2} & \frac{1}{G_2}\left[g_1 - \sum_{j\neq 2}\frac{f_{j1}^2}{G_j}\right] & & & \\ \cdots & \cdots & \cdots & & \\ \frac{f_{11}f_{n1}}{G_1G_n} & \frac{f_{21}f_{n1}}{G_2G_n} & \cdots & \frac{1}{G_n}\left[g_1 - \sum_{j\neq n}\frac{f_{j1}^2}{G_j}\right] & \\ -\frac{f_{11}}{G_1} & -\frac{f_{21}}{G_2} & \cdots & -\frac{f_{n1}}{G_n} & 1 \end{vmatrix} \tag{28e}$$

where $d(\omega)$ is the characteristic polynomial of the system

$$d(\omega) = \prod_{i=1}^{n} G_i\left[g_1 - \sum_{i=1}^{n}\frac{f_{i1}^2}{G_i}\right] \tag{28f}$$

The frequencies of the system are the roots of the $2(n+1)$ order equation

$$d(\omega) = 0 \tag{29}$$

Unlike the study of 2-DOF systems, general closed form solutions for the above equation do not exist.

Most response variables can be expressed as linear combinations of the original DOF $\mathbf{x}(t)$. Following the notation of chapter 3, a response variable $y(t)$ can be written

$$y(t) = \mathbf{q}_0^T\mathbf{x}(t) \tag{30}$$

For example, if the response of interest is the displacement of the equipment relative to the attachment point, the vector $\mathbf{q}_0$ is given by

$$\mathbf{q}_0 = [\,0 \;\cdots\; 0 \;-1\; 0 \;\cdots\; 0\; 1\,]^T$$

where the position of the -1 corresponds to the attachment DOF. Transforming to the modal coordinates $\mathbf{z}(t)$, the expressions for $y(t)$ becomes

$$y = \mathbf{q}_0^T\mathbf{x} = \mathbf{q}_0^T\boldsymbol{\Phi}\mathbf{z} = \mathbf{q}^T\mathbf{z} \tag{31}$$

where $\mathbf{q}=\boldsymbol{\Phi}^T\mathbf{q}_0$.

The formula for the frequency response function $H_i(\omega)$ for the response $y(t)$ is (see Eq.3.33)

$$H_i(\omega) = -\mathbf{q}^T\mathbf{H}(\omega)\mathbf{M}\mathbf{r} \tag{32}$$

By substituting Eq.28e into the above, the exact solution for $H_i(\omega)$ can be obtained; however, this expression is rather cumbersome for frequency response analysis. By using perturbation methods, it will be shown that the dominant terms of the frequency response matrix are along the diagonal and the last row.

The order relationships between the elements of the complex frequency response matrix $\mathbf{H}(\omega)$ are examined for various values of the frequency ω. For values of ω in a neighborhood of each of the detuned primary frequencies ω_{pj} for $j \in J_0$, the order of magnitude of the polynomials $f_i(\omega)$, $g_i(\omega)$, and $G_i(\omega)$ are estimated by setting $\omega=\omega_{pj}$:

$$g_i(\omega_{pj}) = O(e^2) \qquad f_{ij}(\omega_{pj}) = O(e^2) \tag{33a}$$

$$G_i(\omega_{pj}) = \begin{cases} O(e) & \text{for } i=j \\ O(1) & \text{for } i\neq j \end{cases} \tag{33b}$$

where e represents the order of the problem. Substituting the above into Eq.28e,

$$\mathbf{H}(\omega) = \frac{1}{O(e^2)} \begin{vmatrix} O(e^2) & & & & \text{(sym)} \\ O(e^3) & O(e^2) & & & \\ \cdots & \cdots & \cdots & & \\ O(e^3) & O(e^3) & \cdots & O(e^2) & \\ O(e^2) & O(e^2) & \cdots & O(e^2) & O(1) \end{vmatrix} \tag{33c}$$

where only the j-th terms of the diagonal and of the last row are of order $O(e)$.

For values of ω that are not in the neighborhood of any of the primary or secondary frequencies,

$$g_i(\omega) = O(e^2) \qquad f_{ij}(\omega) = O(e^2) \qquad G_i(\omega) = O(1) \tag{34a}$$

and $\mathbf{H}(\omega)$ is of the same form as Eq.33c except that all of the terms of the diagonal and the last row are of order $O(e^2)$.

Next, consider ω near the secondary subsystem frequency ω_{s1} for detuned systems. In this case, $g_1(\omega) = O(e^2)$, $f_{i1}(\omega)$ and $G_i(\omega)$ are as in Eq.34a, and the order relationships for $\mathbf{H}(\omega)$ are

$$\mathbf{H}(\omega) = \frac{1}{O(e^3)} \begin{vmatrix} O(e^3) & & & & & (\text{sym}) \\ O(e^4) & O(e^3) & & & & \\ \cdots & \cdots & \cdots & & & \\ O(e^4) & O(e^4) & \cdots & O(e^3) & & \\ O(e^2) & O(e^2) & \cdots & O(e^2) & O(1) & \end{vmatrix} \tag{34b}$$

Finally, consider tuned systems, where for the sake of notational convenience it is assumed that the first l primary subsystem modes (not necessarily having the lowest l frequencies) are the tuned modes, i.e. $I_t = \{1, \ldots, l\}$ and $I_d = \{l+1, \ldots, n\}$. For values of ω in a neighborhood of the equipment frequency ω_{s1}

$$g_1(\omega_{s1}) = O(e^2) \quad f_{i1}(\omega_{s1}) = O(e^2) \tag{35a}$$

$$G_i(\omega_{s1}) = \begin{cases} O(e) & \text{for } 1 \leqslant i \leqslant l \\ O(1) & \text{for } l < i \leqslant n \end{cases} \tag{35b}$$

and

$$\mathbf{H}(\omega) = \frac{1}{O(e^3)} \begin{vmatrix} O(e^2) & & & & & (\text{sym}) \\ O(e^2) & O(e^2) & & & & \\ \cdots & \cdots & \cdots & & & \\ O(e^2) & O(e^2) & \cdots & O(e^2) & & \\ O(e) & O(e) & \cdots & O(e^2) & O(1) & \end{vmatrix} \tag{35c}$$

where, in the last row, the first l terms are of order $O(e)$ and the l+1-st through the n-th terms are of order $O(e^2)$.

In the calculation of $H_s(\omega)$, the matrix $\mathbf{H}(\omega)$ is post multiplied by $\mathbf{M}\mathbf{r}$. In this process, the last column of the matrix is multiplied by a term of order $O(e^2)$ smaller than the multiplier for the first l columns. It follows from the order relations above that the reduced expression for $H_s(\omega)$ is obtained from the diagonal and last row of $\mathbf{H}(\omega)$

$$H_s(\omega) \approx \frac{g_1(\omega) \prod_{i=1}^{n} G_i(\omega)}{d(\omega)} \left[\sum_{i=1}^{n} \frac{q_{n+1} m_{pi} r_{i1} f_{i1}(\omega)}{g_1(\omega) G_i(\omega)} - \frac{q_{n+1} m_{s1} r_{n+1}}{g_1(\omega)} - \sum_{i=1}^{n} \frac{q_i m_{pi} r_i}{G_i(\omega)} \right] \tag{36}$$

where r_i is the i-th component of the influence vector $\mathbf{r}$ and q_i is the i-th component of $\mathbf{q}$.

By giving similar considerations to the characteristic polynomial $d(\omega)$, it can be shown that only the terms corresponding to the tuned frequencies are needed for the summation in the expression in Eq.28f. Thus, for the multiply tuned case,

$$d(\omega) = \prod_{i} G_i(\omega) \left[g_1(\omega) - \sum_{i \in I_d} \frac{f_i^2(\omega)}{G_i(\omega)} \right] \tag{37}$$

The above constitutes a considerable simplification for the expression for the frequency response function $H_1(\omega)$ and by observing the order relationships and keeping all dominant terms, first-order accuracy is maintained. The transfer function $T_{11}(\omega)$ and spectral density function $G_{11}(\omega)$ are obtained using Eqs.3.34a,b. From the order relationships above, it can be shown that for tuned systems the transfer function has a peak of order $O(\epsilon^{-3})$ at $\omega=\omega_{s1}$ as for the 2-DOF system. There are also smaller peaks of order $O(\epsilon^{-1})$ at the detuned frequencies ω_{pi} for $i \in I_d$.

A plot of $T_{11}(\omega)$ for the example system in Fig.4.2 is shown in Figs.4.4a,b. In Fig.4.4a, the equipment frequency, ω_{s1} = .38 rad/sec, is tuned to the first primary frequency, ω_{p1} = .374 rad/sec, thus a sharp peak is found for $\omega = \omega_{s1}$. There is also a small peak corresponding to the detuned primary modes near ω = 1.00 rad/sec, however it is considerably smaller than the first peak and is not visible on the plot. In Fig.4.4b, the equipment frequency, ω_{s1} = 1.00 rad/sec, is multiply tuned to two primary frequencies, ω_{p2} = .98 rad/sec and ω_{p3} = 1.02 rad/sec, and a peak is found for $\omega = \omega_{s1}$. For this case, a smaller peak is also found for the detuned primary mode at $\omega = \omega_{p1}$.

4.3.3 Spectral Moments of Response

The spectral moments λ_n of the response variable $y(t)$ are given by the integral Eq.2.1

$$\lambda_n = \int_0^\infty \omega^n G_{11} \, d\omega \tag{38}$$

For general forms of the input power spectral density this integral can be obtained by numerical integration. This method of finding the moments was used to find the response of the example

system in Fig.4.2 to white-noise base excitation. The results obtained from the approximate and exact forms of the complex frequency response function $H_{,}(\omega)$ derived above are plotted as a function of the equipment frequency, $\omega_{,1}$, and compared in Figs.4.5a-c. The peaks correspond to the responses for singly tuned systems ($\omega_{,1} \approx \omega_{p1}$) and multiply tuned systems ($\omega_{,1} \approx \omega_{p2}, \omega_{p3}$). The difference between approximate and exact results are slight, illustrating the accuracy of the perturbation methods.

Also, an integration formula which is a generalization of Eq.3.40a-c can be used to find $\lambda_{,}$ for m=0 and 2 for a white noise input. However, this formula does not yield simple closed form solutions as in the previous chapter and the method is difficult to implement into a computer.

4.4 Modal Decomposition Approach

4.4.1 Mode Shapes and Frequencies

First, mode shapes and frequencies will be derived for each set of modes classified earlier in this chapter. An analysis of the system requires the solutions to an $n+1 \times n+1$ order complex eigenvalue problem, however, this problem is reduced significantly using perturbation principles. For most modes, simple closed form solutions exist for the eigenvalues and eigenvectors; only the multiply tuned case requires the solution of an eigenvalue problem. In the latter case, if l is the number of modes tuned to the equipment, the size of the problem is $l+1 \times l+1$ which, in general, is far smaller than the original $n+1 \times n+1$ problem. Thus, given any MDOF/SDOF PS system, the expressions for the mode shapes and frequencies can be evaluated numerically, and the results used directly in the modal decomposition method developed in Chapter 2, or in any other suitable dynamic analysis method.

In this chapter, the algebraic form of the mode shapes and frequencies are used in the modal decomposition method to form general approximate expressions for the spectral moments for response to white noise input. Closed form solutions are obtained for all but the multiply tuned case. The results are less accurate than the numerical application of the

method, and is not recommended for computer applications. However, the closed form expressions are useful in gaining further insight into the behavior of PS systems. For computer applications, the direct modal decomposition approach mentioned above is more appropriate.

4.4.1.1 Primary Detuned Modes

The modes shapes and frequencies detuned from the secondary subsystem are found by solving the eigenvalue problem

$$\mathbf{\Gamma}(\omega)\boldsymbol{\phi} = 0 \tag{39a}$$

where

$$\mathbf{\Gamma}(\omega) = \begin{bmatrix} G_1(\omega) & \cdots & 0 & f_{s1}(\omega) \\ \cdots & \cdots & \cdots & \cdots \\ 0 & \cdots & G_s(\omega) & f_{ss}(\omega) \\ f_{s1}(\omega) & \cdots & f_{ss}(\omega) & g_s(\omega) \end{bmatrix} \tag{39b}$$

This problem is similar to the eigenvalue problem in Section 3.4.3.2 and the method of analysis developed in detail in that section is used here.

For notational convenience, assume that primary mode 1 is detuned, i.e. $1 \in I_p$. Also, assume that mode 1 is widely spaced from the other primary subsystem modes. (This analysis will be repeated without this assumption in a later section.) The initial approximation for the mode shape and frequency are similar to those given in Eqs.3.68

$$\boldsymbol{\phi}_1^{(0)} = [\,1\ 0\ \cdots\ 0\,]^t \tag{40a}$$

$$\omega_1^{(0)} = \omega_{n1}(\sqrt{1-\xi_{n1}^2} + i\xi_{n1}) \tag{40b}$$

By applying the same error analysis developed in Eqs.3.69-71a and using the more general form for the matrix $\mathbf{\Gamma}(\omega)$, a higher order approximation for $\boldsymbol{\phi}_1$ can be found. The resulting mode shape corresponding to Eq.3.71a is

$$\boldsymbol{\phi}_1^{(1)} = \left[\,1\ \frac{f_{11}f_{21}}{g_1G_2}\ \cdots\ \frac{f_{11}f_{s1}}{g_1G_s}\ -\frac{f_{11}}{g_1}\,\right]^t \tag{41}$$

where the polynomials f_{s1}, g_1, and G_s are evaluated at $\omega=\omega_1^{(0)}$. Note that if the s-th primary mode is closely spaced to mode 1, $G_s(\omega_1^{(0)})$ would be relatively small and the corresponding coordinate in $\boldsymbol{\phi}_1^{(1)}$ would be relatively large, invalidating the perturbation analysis used to derive

$\phi_1^{(1)}$. Therefore, the widely spaced assumption for the detuned mode is necessary in this analysis.

As for the 2-DOF system, the low-order approximations for the mode shape and frequency are found from $\omega_1^{(0)}$ and $\phi_1^{(1)}$:

$$\phi_1 \approx \left[1\ 0\ \cdots\ 0\ \frac{\zeta_{11}\omega_{s1}^2}{\omega_{s1}^2-\omega_{p1}^2} \right]^t \tag{42a}$$

$$\omega_1 = \omega_{p1}(1 + i\xi_{p1}) \tag{42b}$$

Note the similarity between the above results and the results for the 2-DOF system in Eq.3.76. The only significant difference is in the appearance of the coefficient ζ_{11}. This coefficient reflects the more general form of the physical coupling between the primary and secondary subsystems in MDOF/SDOF systems.

4.4.1.2 Secondary Detuned Mode

If the secondary subsystem mode is detuned from the primary subsystem modes, i.e. if $I_s=\{\}$, then the mode shape and frequency for mode $n+1$ which is associated with the secondary subsystem can be derived in a manner parallel to the preceding analysis. The initial approximations for ϕ_{n+1} and ω_{n+1} are

$$\phi_{n+1}^{(0)} = [\,0\ 0\ \cdots\ 1\,]^t \tag{43a}$$

$$\omega_{n+1}^{(0)} = \omega_{s1}(\sqrt{1-\xi_{s1}^2} + i\xi_{s1}) \tag{43b}$$

The higher order expression for ϕ_{n+1} corresponding to Eq.41 is

$$\phi_{n+1}^{(1)} = \left[-\frac{f_{11}}{G_1}\ \cdots\ -\frac{f_{n1}}{G_n}\ 1 \right]^t \tag{44}$$

where the polynomials are evaluated at $\omega=\omega_{n+1}^{(0)}$. The final, low-order results are

$$\phi_{n+1} = \left[\zeta_{11}\epsilon_{11}\frac{\omega_1^2}{\omega_{p1}^2-\omega_{s1}^2}\ \cdots\ \zeta_{n1}\epsilon_{n1}\frac{\omega_{s1}^2}{\omega_{pn}^2-\omega_{s1}^2}\ 1 \right]^t \tag{45a}$$

$$\omega_{n+1} = \omega_{s1}(1 + i\xi_{s1}) \tag{45b}$$

where ϵ_{11} are the mass ratios defined in Eq.21. Note the similarities between the above results and the results for the 2-DOF system in Eq.3.78. Again, the only difference is in the appearance of the coupling coefficient ζ_{11}.

4.4.1.3 Singly Tuned Modes

The eigenvalue analysis of singly tuned systems is similar to that of tuned 2-DOF systems presented in section 3.4.2.1. For notational convenience, assume that primary subsystem mode 1 is tuned to the secondary subsystem, i.e. $I_t = \{ 1 \}$, $I_u = \{ 2, \cdots, n \}$.

The initial approximations for the tuned modes are obtained by neglecting the effect of the detuned modes and considering only the first and $n+1$ coordinates of the eigenvalue problem in Eqs.39a,b. The resulting problem is essentially the same as that solved for the 2-DOF system in Eq.3.48. The parameters β, ξ_u, ξ_v, and ω_u which were defined in Eqs.3.1a,b,d,e for the 2-DOF system are redefined here by setting $\xi_1=\xi_{p1}$, $\xi_2=\xi_{s1}$, $\omega_1=\omega_{p1}$, and $\omega_2=\omega_{s1}$. Using this notation, the initial approximations for the mode shapes and frequencies are nearly identical to the expressions in Eq.3.50a,b. The only difference is that the mass ratio ϵ is replaced by the more general effective mass ratio γ_{11}

$$\omega_1^{(0)} = \omega_u \left\{ 1 + \imath\xi_u + \frac{1}{2}[\gamma_{11}+(\imath\xi_u+\beta)^2] \right\} \tag{46a}$$

$$\omega_2^{(0)} = \omega_u \left\{ 1 + \imath\xi_u - \frac{1}{2}[\gamma_{11}+(\imath\xi_u+\beta)^2] \right\} \tag{46b}$$

$$\phi_1^{(0)} = [\, \alpha_1^{(0)} \; 0 \; \cdots \; 0 \; 1 \,]^T \tag{46c}$$

$$\phi_2^{(0)} = [\, \alpha_2^{(0)} \; 0 \; \cdots \; 0 \; 1 \,]^T \tag{46d}$$

$$\alpha_1^{(0)} = \frac{1}{\zeta_{11}} \left\{ -\beta - \imath\xi_u - [\gamma_{11}+(\imath\xi_u+\beta)^2] \right\} \tag{46e}$$

$$\alpha_2^{(0)} = \frac{1}{\zeta_{11}} \left\{ -\beta - \imath\xi_u + [\gamma_{11}+(\imath\xi_u+\beta)^2] \right\} \tag{46f}$$

Higher order approximations for the mode shapes are obtained using the error analysis developed in Eqs.3.69-71a. The first and $n+1$ coordinates remain unchanged and the coordinates corresponding to the detuned modes are similar to those in Eq.44

$$\phi_i^{(1)} = \left[\alpha_i^{(0)} \; -\frac{f_{21}}{G_2} \; \cdots \; -\frac{f_{n1}}{G_n} \; 1 \right]^T \tag{47}$$

From the above solutions, the final low-order approximations are

$$\omega_i^* = \omega_i^{(0)} \tag{48a}$$

$$\phi_i^* = \left[\alpha_i^{(0)} \; \epsilon_{21}\zeta_{21}\frac{\omega_{s1}^2}{\omega_{p2}^2-\omega_{s1}^2} \; \cdots \; \epsilon_{n1}\zeta_{n1}\frac{\omega_{s1}^2}{\omega_{pn}^2-\omega_{s1}^2} \; 1 \right]^T \tag{48b}$$

where $r=1,2$ denotes the two modes arising from the single tuning.

4.4.1.4 Multiply Tuned Modes

The eigenvalue analysis of a multiply tuned MDOF/SDOF system is a generalization of the analysis of singly tuned systems. Although simple closed form expressions can not be obtained for this system, it is possible to reduce the analysis to a small eigenvalue problem.

Let l modes of the primary subsystem be tuned to the secondary subsystem; for notational convenience assume that the first l primary subsystem modes (not necessarily having the lowest l frequencies) are the tuned modes, i.e. $I_t = \{1, \ldots, l\}$ and $I_d = \{l+1, \ldots, n\}$. Initial approximations are obtained for the mode shapes by neglecting the effect of the detuned modes, as in the previous section. When the detuned coordinates $l+1,\ldots,n$ are eliminated from the original $n+1\times n+1$ order eigenvalue problem given in Eq.39a, the result is a relatively small $l+1\times l+1$ problem

$$\mathbf{\Gamma}_t(\omega^{(0)})\begin{Bmatrix}\boldsymbol{\phi}_t^{(0)}\\ 1\end{Bmatrix}=0 \tag{49}$$

where $\mathbf{\Gamma}_t(\omega)$ is the submatrix of $\mathbf{\Gamma}(\omega)$ corresponding to the coordinates $\{1,2,\ldots,l,n+1\}$. The l-vector $\boldsymbol{\phi}_t^{(0)}$ corresponds to the first l coordinates of the r-th mode shape $\boldsymbol{\phi}_r^{(0)}$ and is used in the initial approximation

$$\boldsymbol{\phi}_r^{(0)}=\begin{Bmatrix}\boldsymbol{\phi}_t^{(0)}\\ 0\\ 1\end{Bmatrix} \tag{50}$$

A higher order approximation is found through an error analysis, as before. The result is

$$\boldsymbol{\phi}_r^{(1)}=\begin{Bmatrix}\boldsymbol{\phi}_t^{(0)}\\ \boldsymbol{\phi}_d^{(0)}\\ 1\end{Bmatrix} \tag{51a}$$

where $\boldsymbol{\phi}_d^{(0)}$ is the $n-l$ vector

$$\boldsymbol{\phi}_d^{(0)}=\left[-\frac{f_{l+1,r}}{G_{l+1}}\quad\cdots\quad-\frac{f_{nr}}{G_n}\right]^T \tag{51b}$$

and the polynomials are evaluated at the frequencies $\omega_r^{(0)}$ found from Eq.49. Finally, the above can be reduced to the following low-order expressions

$$\boldsymbol{\phi}_j = \begin{bmatrix} \boldsymbol{\phi}_j^{(0)} \\ \boldsymbol{\phi}_{sj} \\ 1 \end{bmatrix} \tag{52a}$$

$$\omega_j = \omega_j^{(0)} \tag{52b}$$

where

$$\boldsymbol{\phi}_{sj} = \left[\epsilon_{s+1} \zeta_{s+1} \frac{\omega_{s1}^2}{\omega_{p\,s+1}^2 - \omega_{s1}^2} \quad \cdots \quad \epsilon_{sn} \zeta_{sn} \frac{\omega_{s1}^2}{\omega_{pn}^2 - \omega_{s1}^2} \right] \tag{52c}$$

Note the similarity between the above expressions and Eqs.48a,b.

4.4.1.5 Closely Spaced Primary Detuned Modes

As noted in Section 4.4.1.1, the analysis of closely spaced detuned modes may require special attention. The theoretical method for deriving these mode shapes which is consistent with the results of the previous sections would require the solution of a small eigenvalue problem and is outlined below. However, it is shown in Section 4.4.2.5 that this derivation is unnecessary if the quantity of interest is the response of the secondary subsystem. If the expressions for the detuned mode shapes and frequencies in Eqs.42a,b are used directly, the results for the system response are shown to be the same as those obtained from the theoretical mode shapes. Therefore, the mode shapes and frequencies derived in Section 4.4.1.1 can be used for all detuned modes, regardless of the spacing of the frequencies. If the mode shapes of closely spaced detuned modes are themselves of interest, the derivation for the theoretical low-order expressions given below can be used.

The analysis of systems with closely spaced detuned modes is similar to the analysis in the preceding section. Assume the first l primary modes are closely spaced and detuned from the secondary subsystem. The initial approximations for these l modes are obtained by neglecting the effect of those primary modes that are not among the closely spaced modes. Thus, the original $n+1 \times n+1$ order eigenvalue problem reduces to the same $l+1 \times l+1$ problem in Eq.49. There are $l+1$ solutions to this equation, however only the l solutions associated with the primary subsystem are used. The subsequent analysis is essentially the same as in the previous section and the final low-order expression for the mode shapes and frequencies are given by

Eqs.52a-c.

4.4.1.6 Example Study

The complex modal properties of the example system in Fig.4.2 were computed using the formulations developed in this section and were compared with exact results obtained by using a complex eigenvalue solver from the IMSL library [1]. The frequencies are shown in Table 3 and are plotted in Figs.4.6a-c for various values of the equipment frequency ω_{s_1}, and the mode shapes for the multiply tuned case (i.e., ω_{s_1} = 1.00 rad/sec) are shown in Table 4. The non-classical damping character of the multiply tuned system is apparent in the mode shapes, which have imaginary components. Good agreement between approximate and exact values is found in all cases.

The effect of the equipment mass is illustrated in Fig.4.6b, where the frequencies corresponding to ϵ = .01, .005, and .001 are represented by points A, B, and C, respectively (which can be compared with Fig.3.3a-c from the 2-DOF system study). Mode 1 is not affected by the mass ratio because it is detuned. The frequencies corresponding to the other modes converge to the subsystem natural frequencies as was observed in the study of the 2-DOF system.

4.4.2 Spectral Moments

As stated earlier, the most direct method for finding the moments is through numerical computation. The mode shapes and frequencies of any MDOF/SDOF system can be calculated using the formulae developed above and the results substituted into the modal decomposition method developed in Chapter 2. It is straightforward to implement this procedure into a computer; the complex eigenvalue solution, which is of small order and is only required for multiply tuned systems, can be solved by routines found in standard libraries such as the IMSL [1].

For the example system in Fig.4.2, the results of this numerical computation are compared with exact results obtained by integrating the complex frequency response function in

Figs.4.7a-c. Also, the mean zero-crossing rate, ν, and the shape factor, δ, are computed and plotted in Figs.4.8a,b. All plots show good comparison between exact and the proposed approximate results.

At tuning, the response of the equipment is dominated by oscillatory motion at the equipment frequency, thus the mean zero-crossing rate is close to $\nu = \omega_{s1}/\pi$ [19]. The line representing this equation is plotted in Fig.4.8a and it can be seen that the actual values for ν approach this line at tuning. For other values of ω_{s1}, the contribution from the detuned modes of the primary system to the response motion becomes more significant, and the contribution from those modes with frequencies which are less than ω_{s1} tend to lower the values for the mean zero-crossing rate.

The shape factor, δ, which is a measure of the band-width of the response process, becomes small at tuning due to the predominance of the response of the tuned modes in the response motion. This is reflected by the marked decreased values of δ in Fig.4.8b at the two tuning frequencies, $\omega_{s1} = .38$ and 1.00 rad/sec. For $\omega_{s1} = .38$ rad/sec, it was noted that the complex frequency response function $H_1(\omega)$ has only a single peak, thus the power spectral density function is narrow-banded and δ has a very small value. For $\omega_{s1} = 1.00$ rad/sec, the complex frequency response function had two significant peaks, one at the tuned frequencies and another at the detuned frequencies, thus the power spectral density function is not as narrowly-banded and δ is not as small as in the previous case.

Although the numerical approach to finding the spectral moments is useful in practical applications, it is instructive to utilize the algebraic forms for the mode shapes and frequencies derived in the previous section in order to obtain expressions for the response. Closed form solutions will be derived for response to white noise input for all but the multiply tuned systems. Although these expressions are not as accurate as the numerical method outlined above, they provide important information about PS systems which would be hidden in a numerical or parametric analysis.

4.4.2.1 Totally Detuned Systems with Well-Spaced Modes

Totally detuned systems with well-spaced modes are the simplest and most basic to analyze. Since totally detuned systems are classically damped and the correlations between well-spaced modes are negligible, the modal decomposition method simplifies to the square-root-of-sum-of-squares (SRSS) method [16]. The expressions for the mode shapes and frequencies which were derived in Section 4.4.1.2 can be substituted directly into the formula for the effective participation factors given in Eq.3.79. The factors associated with the primary subsystem modes are

$$\psi_{p} = r_{p}\left[\frac{q_{p+1}\omega_{s1}^{2}\zeta_{s1}}{\omega_{s1}^{2}-\omega_{p}^{2}} + q_{p}\right] \qquad p=1,\cdots,n \tag{53a}$$

and that associated with the secondary subsystem mode is

$$\psi_{s1} = q_{n+1}\left[\sum_{p=1}^{n}\frac{r_{p}\omega_{s1}^{2}\zeta_{s1}}{\omega_{p}^{2}-\omega_{s1}^{2}} + r_{n+1}\right] \tag{53b}$$

The moments λ_{ij} are given by the expressions in Eq.2.48a-c. Substituting into the formula Eq.2.38 the final expressions for the spectral moments are

$$\lambda_{ij} = \frac{\pi G_{s0}}{4}\left\{\sum_{p=1}^{n} r_{p}^{2}\left[\frac{q_{p+1}\omega_{s1}^{2}\zeta_{s1}}{\omega_{s1}^{2}-\omega_{p}^{2}} + q_{p}\right]^{2}\frac{\omega_{p}^{i+j-3}}{\xi_{p}} + q_{n+1}^{2}\left[\sum_{p=1}^{n}\frac{r_{p}\omega_{s1}^{2}\zeta_{s1}}{\omega_{p}^{2}-\omega_{s1}^{2}} + r_{n+1}\right]^{2}\frac{\omega_{s1}^{i+j-1}}{\xi_{s1}}\right\} \tag{54}$$

Note that for $n = 1$ this reduces to a result similar to the expression for the 2-DOF system in Eq.3.82.

4.4.2.2 Singly Tuned Systems

In this section, singly tuned systems with well spaced primary subsystem modes are considered. The well-spaced assumption allows a separate analysis of the detuned modes and the tuned modes in the modal decomposition method. Thus, the spectral moment can be expressed as a sum of two additive components,

$$\lambda_{ij} = \lambda_{ij_{det}} + \lambda_{ij_{tun}} \tag{55}$$

where $\lambda_{ij_{det}}$ and $\lambda_{ij_{tun}}$ constitute the contributions of the detuned and tuned modes to the spectral moments, respectively. The detuned moment $\lambda_{ij_{det}}$ arises from the $n-1$ detuned primary mode shapes and is similar to the expression in Eq.54

$$\lambda_{jm} = \frac{\pi G_{cc}}{4} \sum_{i \in I_d} r^2 \left[\frac{q_{m+1} \omega_{i1}^2 \zeta_{i1}}{\omega_{i1}^2 - \omega_{jp}^2} + q \right]^2 \frac{\omega_{jp}^{m-1}}{\xi_i} \tag{56}$$

where the summation above is taken over the detuned modes I_d. Note that the second summation in Eq.54 arises from the contribution of the secondary subsystem mode in the totally detuned system, therefore it is not included here.

The tuned moment λ_{jm} is obtained from the two singly tuned mode shapes of the system and its derivation follows the analysis of tuned 2-DOF systems in Section 3.4.2.2. Taking lowest order terms for the moments, the result is identical to the low-order expression Eq.3.65a,b

$$\lambda_{jm} = \frac{\pi G_{cc}}{8} \frac{q_{m+1} r^2 \zeta_{i1}^2 \xi_{j2} \omega_{j2}^{m-1}}{\xi_{j1} \xi_{i1} (4\xi_{j2}^2 \beta^2) + \gamma_{i1} \xi_{j2}^2} \tag{57}$$

The detuned moment λ_{jm} is small in comparison with the tuned moment λ_{jm}. However, this term is not ignored since it is important for the calculation of the factors ν and b.

4.4.2.3 Multiply Tuned Systems

The analysis of multiply tuned systems follows the same line of reasoning as used for singly tuned systems. The expression for the detuned moment λ_{jm} is identical to Eq.56, however, there is no simple closed form algebraic solution for the tuned moment λ_{jm}. This quantity must be computed numerically by solving for the tuned mode shapes using the reduced eigenvalue problem in Section 4.4.1.4 and substituting the results directly into the modal decomposition method.

4.4.2.4 Systems with Closely Spaced Primary Modes

In the above, it was assumed that the detuned primary modes are widely spaced from each other, therefore the relatively small correlations between these modes were ignored. However, if these modes are closely spaced, the correlations become significant and another term λ_{cm} must be included in the expressions for the moments λ_m:

$$\lambda_m = \lambda_{dm} + \lambda_{tm} + \lambda_{cm} \tag{58}$$

This term would have the general form

$$\lambda_{m+1} = \sum_{(i,j)\in I} [\, C_i \lambda_{m-1} - D_i \lambda_{m+1,i} + E_i \lambda_{m+2,i} \,] \tag{59}$$

where

$$I = \left\{ \begin{array}{l} \text{pairs of closely spaced modes } (i,j) \\ \text{excluding pairs of tuned modes} \end{array} \right\} \tag{60}$$

and the sum includes correlations between detuned primary modes and singly or multiply tuned modes.

Closed form expressions for λ_{m+1} can be obtained only for closely spaced detuned modes. Such modes are classically damped, therefore, $D_i = E_i = 0$ and $C_i = a\, a_i$ and the cross term between modes i and j reduces to

$$C_i \lambda_{m-1} = \psi_i \psi_j \rho_{m-1,ij} \sqrt{\lambda_{m-1,i} \lambda_{m-1,j}} \tag{61}$$

where ψ_i are the effective participation factors given in Eq.53a and $\rho_{m-1,ij}$ are the correlation coefficients defined in Chapter 2 (e.g., see Eqs.2.56 for wide-band inputs). For detuned modes closely spaced to a tuned mode, such simple forms for C_i, D_i, and E_i do not exist, and the corresponding cross terms in Eq.59 must be evaluated numerically.

4.4.2.5 Systems with Closely Spaced Primary Modes

Assume that the first l primary subsystem modes are detuned from the secondary subsystem and are very closely spaced and the damping ratios of these modes are approximately equal. From physical considerations, it is expected that modes with nearly identical frequencies and damping ratios respond to a common input as a collective unit. This can be shown rigorously using an argument based on frequency response methods. Thus, these modes can be replaced by a single equivalent mode containing their essential properties. The frequency ω_l and damping ratio ξ_l of the equivalent mode are given by the averages

$$\omega_l = \frac{1}{l} \sum_{i=1}^{l} \omega_{ji}, \quad \xi_l = \frac{1}{l} \sum_{i=1}^{l} \xi_{ji} \tag{62}$$

The effective participation factor ψ_l is given by the sum of the modal participation factors ψ_i given in Eq.53a

$$\psi_l = \sum_{i=1}^{l} \psi_i = \sum_{i=1}^{l} r_i \left[\frac{q_{n+1} \omega_{n+1}^2 \zeta_{n+1}}{\omega_{n+1}^2 - \omega_{ji}^2} + q_i \right] \tag{63}$$

It follows that the detuned moment λ_{dm} is simply

$$\lambda_{dm} = |\psi_l|^2 \lambda_{m,ll} + \text{contribution from other detuned modes} \tag{64}$$

where $\lambda_{m,ll}$ is the spectral moment corresponding to the frequency ω_l and damping ratio ξ_l.

The same solutions for the response is obtained if the mode shapes and frequencies for widely spaced detuned modes are used. Using the participation factors ψ obtained in Section 4.4.2.1, the expression for the moment λ_{dm} is

$$\lambda_{dm} = \sum_{i=1}^{l}\sum_{j=1}^{l} \psi_i \psi_j \lambda_{m,ij} + \text{other contributions} \tag{65}$$

Since the modes are closely spaced and the damping ratios are assumed to be approximately equal,

$$\lambda_{m,ij} \approx \lambda_{m,ll} \qquad \text{for all } i,j \leq l \tag{66}$$

Then the above expression for λ_{dm} simplifies to

$$\begin{aligned} \lambda_{dm} &\approx \left\{\sum_{i=1}^{l}\sum_{j=1}^{l} \psi_i \psi_j\right\} \lambda_{m,ll} + \text{other contributions} \\ &= |\psi_l|^2 \lambda_{m,ll} + \text{other contributions} \end{aligned} \tag{67}$$

which is the same result as Eq.64. The latter approach is more suitable for computer implementation since the same solutions for the mode shapes, frequencies, and participation factors are used for closely spaced and widely spaced detuned modes.

4.5 Non-Interaction Results

4.5.1 Introduction

The effect of interaction between the primary and secondary subsystems has been included in both the frequency response function analysis in Section 4.3 and the modal decomposition method in Section 4.4. However, for many PS systems, the mass of the secondary subsystem is considerable smaller than the masses of the primary subsystem and the results from Section 3.5 for 2-DOF systems suggest that the interaction effect would be negligible for such systems. Although the results of the preceding sections would remain valid for this case, it is worthwhile to reanalyze the system without accounting for interaction for several reasons:

1. The results are simpler than the results which include interaction.
2. Closed form expressions will be derived for results that were not obtainable in that form in the previous sections.
3. Comparisons can be made between interaction and non-interaction results.

The frequency response analysis is presented first. Then, after deriving closed form solutions for the mode shapes, the modal decomposition method is presented.

4.5.2 Frequency Response Function Approach

The procedure in Section 3.5 is used to obtain the complex frequency response function $H_1(\omega)$. The equations of motion are decoupled into two sets of equations. The first set corresponds to the response of the primary subsystem to the base input and is given by

$$\ddot{z}_{pi}^{(mod)} + 2\omega_{pi}\xi_{pi}\dot{z}_{pi}^{(mod)} + \omega_{pi}^2 z_{pi}^{(mod)} = -r_i\ddot{x}_g \qquad i=1,\cdots,n \tag{68}$$

and the second set is an equation for the response of the secondary subsystem to the motions at the support points,

$$\ddot{z}_{s1}^{(mod)} + 2\omega_{s1}\xi_{s1}\dot{z}_{s1}^{(mod)} + \omega_{s1}^2 z_{s1}^{(mod)} = \sum_{i=1}^{n}[\omega_{s1}^2 z_i + 2\xi_{s1}\omega_{s1}\dot{z}_i]\zeta_{i1} - r_{n+1}\ddot{x}_g \tag{69}$$

where the secondary DOF z_{s1} is identical to the nodal coordinate x_{n+1}. The Fourier transforms $Z_{pi}^{(mod)}(\omega)$ and $Z_{s1}^{(mod)}(\omega)$ of the subsystem responses $z_{pi}^{(mod)}(t)$ and $z_{s1}^{(mod)}(t)$ are

$$Z_{pi}^{(mod)}(\omega) = -\frac{X_g(\omega)\, m_{pi} r_i}{G_i(\omega)} \qquad i=1,\cdots,n \tag{70a}$$

$$Z_{n+1}^{(mod)}(\omega) = \frac{X_g(\omega)}{g_1(\omega)}\left[\sum_{i=1}^{n}\frac{f_{i1}(\omega)\, m_{pi} r_i}{G_i(\omega)} - m_{s1} r_{n+1}\right] \tag{70b}$$

From these expressions, the Fourier transform $Y^{(mod)}(\omega)$ of the response variable $y(t) = \mathbf{q}'\mathbf{z}$ is obtained

$$\begin{aligned} Y^{(mod)}(\omega) &= \sum_{i=1}^{n} q_i Z_{pi}^{(mod)}(\omega) + q_{n+1} Z_{s1}^{(mod)}(\omega) \\ &= X_g(\omega)\left\{\sum_{i=1}^{n}\frac{q_{n+1} f_{i1}(\omega)\, m_{pi} r_i}{g_1(\omega) G_i(\omega)} - \sum_{i=1}^{n}\frac{q_i m_{pi} r_i}{G_i(\omega)} - \frac{q_{n+1} m_{s1} r_{n+1}}{g_1(\omega)}\right\} \end{aligned} \tag{71}$$

It follows that the frequency response function is

$$H_1^{(mod)}(\omega) \approx \frac{g_1 \prod_{i=1}^{n} G_i}{d^{(mod)}(\omega)}\left\{\sum_{i=1}^{n}\frac{q_{n+1} f_{i1}(\omega)\, m_{pi} r_i}{g_1(\omega) G_i(\omega)} - \sum_{i=1}^{n}\frac{q_i m_{pi} r_i}{G_i(\omega)} - \frac{q_{n+1} m_{s1} r_{n+1}}{g_1(\omega)}\right\} \tag{72a}$$

$$= \sum_{r=1}^{n} \frac{q_{n+1} f_{r+1}(\omega) m_{ir} r_r}{g_1(\omega) G_r(\omega)} - \sum_{r=1}^{n} \frac{q_r m_{ir} r_r}{G_r(\omega)} - \frac{q_{n+1} m_{n+1} r_{n+1}}{g_1(\omega)} \tag{72b}$$

where

$$d^{(non-int)}(\omega) = g_1(\omega) \prod_{r=1}^{n} G_r(\omega) \tag{72c}$$

Note the similarity between Eq.72a with Eq.36, in the latter case γ_{r1} order terms are included in the polynomial $d^1(\omega)$ to account for interaction. This important fact is expressed mathematically as

$$\lim_{m_{r1} \to 0} H_i(\omega) = H_i^{(non-int)}(\omega) \tag{73}$$

which indicates that all of the closed form results previously obtained in this chapter can be applied to the non-interaction study by taking the limit $m_{r1} \to 0$, as was done for the 2-DOF system.

For the example system in Fig.4.2, a comparison between the transfer function $T_i(\omega) = |H_i(\omega)|^2$ for interaction and non-interaction analysis is shown in Fig.4.9 for various values of the secondary subsystem mass. The differences are most notable for values of ω near the tuned mode particularly for larger values of the secondary mass where interaction is more prominent. For other values of ω, the transfer function is insensitive to interaction. This can be shown analytically simply by examining the order relationships in the expressions for the functions $H_i(\omega)$ and $H_i^{(non-int)}(\omega)$.

The spectral moments of the response of the system is found by integrating the transfer function $T_{ii}^{(non-int)}(\omega)$ directly with the input power spectral density function as in Section 4.3.3. In Fig.4.10, plots of the non-interaction and interaction moments are given for the system in Fig.4.2 with varying values for the mass and frequency of the secondary subsystem. The result is similar to the findings in Chapter 3: the difference between λ_0 and $\lambda_0^{(non-int)}$ are greatest at tuning and diminish at detuning.

4.5.3 Modal Decomposition Method

4.5.3.1 Introduction

The approach taken here is essentially the same as in Section 4.4: the expression for the mode shapes and frequencies are derived for the combined system and the results substituted into the modal decomposition method of Chapter 2. However, by neglecting interaction, it is possible to obtain closed form expressions for all mode shapes and frequencies, including multiply tuned modes due to the simplicity of decoupled PS systems. Furthermore, closed form expressions are derived for the factors a_i and c_i, defined in Eq.2.26, which are key factors for the modal decomposition method. The final results for the spectral moments are easily obtainable from the expressions for a_i and c_i and the original parameters of the two subsystems.

4.5.3.2 Closed Form Expressions for the Mode Shapes

The original eigenvalue problem

$$\mathbf{\Gamma}(\omega_i)\boldsymbol{\phi}_i = 0 \tag{74}$$

from Eqs.39a,b is reinvestigated. First, the modes associated with the primary subsystem are analyzed. It is intuitively clear that the frequencies associated with these n modes are given by the original primary subsystem frequencies

$$\omega_i = \omega_{pi}(\sqrt{1-\xi_{pi}^2} + i\xi_{pi}) \qquad i = 1, \ldots, n \tag{75}$$

The corresponding mode shapes are derived by substituting ω_i into Eq.74 and solving the eigenvalue problem. The solution is

$$\boldsymbol{\phi}_i = \left[0 \cdots 0\ 1\ 0 \cdots 0 - \frac{f_{i1}(\omega_i)}{g_1(\omega_i)}\right]^T$$
$$\approx \left[0 \cdots 0\ 1\ 0 \cdots 0 - \frac{\zeta_{i1}\omega_{i1}^2}{2(\beta_{i1}+i\xi_{di1})\omega_{ai1}^2}\right]^T \tag{76}$$

where the unit term is at the ith coordinate and the parameters ω_{ai1}, β_{i1}, and ξ_{di1} are generalizations of the average frequency, detuning, and damping difference parameters used in the analysis of the 2-DOF system

$$\omega_{ai1} = \frac{\omega_{pi}+\omega_{s1}}{2} \qquad \beta_{i1} = \frac{\omega_{pi}-\omega_{s1}}{\omega_{ai1}} \quad \text{and} \quad \xi_{di1} = \xi_{pi}-\xi_{s1} \tag{77}$$

The derivation of the modal properties associated with the equipment is similar to the

above analysis. The frequency is given by the equipment subsystem frequency

$$\omega_{n+1}^{*} = \omega_{s1}(\sqrt{1-\xi_{s1}^2} + i\xi_{s1}) \tag{78}$$

which, when substituted into Eq.74, yields the following expression for the mode shapes

$$\begin{aligned}\boldsymbol{\phi}_{n+1}^{*} &= \left\{ -\frac{f_{s1}(\omega_{n+1}^{*})}{G_1(\omega_{n+1}^{*})} \quad \cdots \quad -\frac{f_{sn}(\omega_{n+1}^{*})}{G_n(\omega_{n+1}^{*})} \quad 1 \right\}^t \\ &\approx \left\{ \frac{\epsilon_{11}\zeta_{11}\omega_{s1}^2}{2(\beta_{11}+i\xi_{d,n1})\omega_{d,11}^2} \quad \cdots \quad \frac{\epsilon_{n1}\zeta_{n1}\omega_{s1}^2}{2(\beta_{n1}+i\xi_{d,n1})\omega_{d,n1}^2} \quad 1 \right\}^t \end{aligned} \tag{79}$$

These expressions reduce to the results in Sections 4.4.1.1 and 4.4.1.2 for the detuned cases.

It appears that the expression for the mode shape $\boldsymbol{\phi}_{n+1}^{*}$ is indeterminate since it involves an arbitrarily small parameter ϵ_{s1} and the terms β_{s1} and $\xi_{d,s1}$ in the denominator may also be small or zero. However, the limit $m_{s1} \to 0$ is not taken until after the coefficients a_i and c_i of the modal decomposition rule are derived. Also, the problem arising from the condition $\beta_{s1} = \xi_{d,s1} = 0$ is resolved after the modal quantities are combined, as will be shown subsequently.

4.5.3.3 Spectral Moments

As stated earlier, closed form expressions will be obtained for the factors a_i and c_i, defined in Eq.2.26, which are the key factors of the modal decomposition method. Due to the simplicity of the expressions for the mode shapes and frequencies, the derivation is straightforward.

By following the matrix multiplications in Eqs.2.17a,c and 2.20 and taking the limit $m_{s1} \to 0$, the following expressions for the factors b_i are obtained, which are independent of the mass ratio ϵ_{s1}:

$$b_i = \frac{ir_i}{2\omega_{pi}}\left[q_i - \frac{q_{n+1}\zeta_{s1}\omega_{s1}^2}{2(\beta_{s1}+i\xi_{d,s1})\omega_{d,s1}^2}\right] \quad \text{for } i = 1, \ldots, n \tag{80a}$$

$$b_{n+1} = \frac{iq_{n+1}}{2a_{s1}}\left[r_{n+1} + \sum_{i=1}^{n}\frac{r_i\zeta_{s1}\omega_{s1}^2}{2(\beta_{s1}+i\xi_{d,s1})\omega_{d,s1}^2}\right] \tag{80b}$$

The factor a_i and c_i are found from Eq.2.26

$$a_i \approx 2\omega_{pi}\mathrm{Im}b_i = -\frac{q_{n+1}\zeta_{s1}r_i\beta_{s1}\omega_{s1}^2}{2(\beta_{s1}^2+\xi_{d,s1}^2)\omega_{d,s1}^2} + r_i q_i \tag{81a}$$

$$a_{n+1} \approx 2\omega_{s1}\mathrm{Im}b_{n+1} = \sum_{i=1}^{n}\frac{q_{n+1}\zeta_{s1}r_i\beta_{s1}\omega_{s1}^2}{2(\beta_{s1}^2+\xi_{d,s1}^2)\omega_{d,s1}^2} + r_{n+1}q_{n+1} \tag{81b}$$

$$c \approx 2\mathrm{Re}b = -\frac{q_{n+1}\zeta_{n+1}r_i\xi_{n+1}\omega_{n+1}^2}{2\omega_n(\beta_{n+1}^2+\xi_{n+1}^2)\omega_{n+1}^2} \tag{81c}$$

$$c_{n+1} \approx 2\mathrm{Re}b_{n+1} = -\sum_{i=1}^{n}\frac{\omega_{pi}}{\omega_{n+1}}c \tag{81d}$$

From these expressions, the spectral moments are easily obtained from Eqs.2.34 and 2.36, which are repeated here:

$$C_i = a_i a_i \quad D_i = a_i c_i + a_i c \quad E_i = c_i c_i \tag{82a}$$

$$\lambda_m = \sum_{i=1}^{n}\sum_{j=1}^{n}(C_i\lambda_{m-2,ij} - D_i\lambda_{m-1,ij} + E_i\lambda_{m-2,ij}) \tag{82b}$$

The frequencies and damping ratios needed to calculate the cross-spectral moments are given by the original subsystem parameters as indicated in Eqs.75 and 78. Equations 81a-d and the above combination rule are in a form suitable for computer implementation. The moments calculated by the above expressions are compared with exact results for various values of the secondary masses in Fig.4.11. The results are similar to those observed in Fig.4.10.

For the case where ξ_{n+1} and β_{n+1} are small or zero, it suffices to give ξ_{n+1} an arbitrary residual number (for computer applications, this number would depend on the precision of the hardware). After combining modal responses, the end result would be consistent with previous results and would be independent of the parameter ξ_{n+1}; this will be shown presently with an example for the important case of perfect tuning.

4.5.3.4 Multiply Tuned Example

Consider a primary subsystem with all modes perfectly tuned to the secondary system and sharing the same damping ratio, i.e. $\xi_{n+1} = \beta_{n+1} = 0$ for all i. As mentioned earlier, a residual value $\Delta << 1$ is given to ξ_{n+1} to keep all terms well-defined. Then, the factors a_i and c_i become

$$a_i \approx 0 \qquad i = 1, \ldots, n \tag{83a}$$

$$c_i = -\frac{r_i\zeta_{n+1}}{2\omega_n\Delta} \qquad i = 1, \ldots, n \tag{83b}$$

$$c_{n+1} = \frac{\sum_{i=1}^{n} r_i\zeta_{n+1}}{2\omega_n\Delta} \tag{83c}$$

where ω_n is the common frequency of the system modes. Substituting into Eqs.82a,b, the

expression for λ_{rr} is obtained

$$\lambda_{rr} = \sum_{i=1}^{r-1}\sum_{j=1}^{r-1} E_{ij}\lambda_{rr,ij}$$

$$= \omega_r^2\left(\sum_{i=1}^{r-1}\sum_{j=1}^{r-1} E_{ij}\lambda_{rr,ij} + 2\sum_{j=1}^{r-1} E_{r,r+1}\lambda_{rr,r,r+1} + E_{r+1,r+1}\lambda_{rr,r+1,r+1}\right)$$

$$= \frac{\pi G_{ss}\left(\sum_{i=1}^{n} r_i\zeta_i\right)^2}{16\omega_r^3 m_r\Delta^2}\left[\frac{1}{\xi_{r-1}} - \frac{4}{\xi_{r-1}+\xi_r} + \frac{1}{\xi_r}\right] = \frac{\pi G_{ss}\left(\sum_{i=1}^{n} r_i\zeta_i\right)^2}{16\omega_r^3 m_r\xi_{r-1}\xi_r(\xi_{r-1}+\xi_r)} \tag{84}$$

The final result does not include the residual term Δ and is very similar to the result for the 2-DOF system in Eq.3.65b. The main difference is that the factor $\sum_{i=1}^{n} r_i\zeta_i$ which represents the general physical coupling between the primary and secondary subsystems is included in the above expression for λ_{rr}.

4.6 Floor Spectra

The floor spectrum for a primary subsystem and a given ground input, is the response spectrum associated with the motion of the system at a selected attachment point. More precisely, it is defined as the mean of the peak displacements of a set of oscillators with variable values for damping ratios and frequencies subjected to the motion of the primary subsystem at the selected attachment point.

Clearly, floor spectra are special cases of the results developed in this chapter. Since the secondary subsystem is attached to the primary subsystem at a single attachment point, the vector $\mathbf{q}_0$ is of the form

$$\mathbf{q}_0 = [\,0 \;\cdots\; 0 \;-1\; 0 \;\cdots\; 0\;1\,]^t \tag{85}$$

where the -1 is located at the coordinate associated with the attachment point.

The remainder of the analysis is based on the results derived in this chapter. Frequency response analysis or the modal decomposition method can be employed, and for the latter approach, input specified by its response spectrum can be used. Finally, interaction can be included or ignored, according to the particular application of the problem.

Table 4.1. Physical Properties of the MDOF/SDOF Example System

Subsystem	Parameter Relationships
Primary	$k_1 = (1.02)^2 m_1$ (radians/sec)^2 $k_2 = (.6057)^2 m_2$ (radians/sec)^2 $m_2 = m_1$
Secondary	$k = \omega_s^2 m$ (ω_s variable) $m = \epsilon m_1$ (ϵ variable)

Table 4.2. Modal Properties of the Fixed Base Subsystems

Subsystem	Modal DOF	Frequency (rad/s)	Damping Ratio
Primary 1	1	1.02	0.02
Primary 2	2	0.374	0.023
	3	0.98	0.06
Secondary	4	ω_{s1}	0.01

Table 4.3 Frequencies for Example System (ϵ_{11}=0.01)

ω_{s1} (rad/sec)	Mode	Exact Frequency		Computed Frequency		Error
		Real Part	Imag. Part	Real Part	Imag. Part	%
0.38	1	0.371	0.007	0.371	0.007	0.0
	2	0.382	0.005	0.382	0.005	0.0
	3	0.978	0.058	0.980	0.058	0.2
	4	1.019	0.020	1.020	0.020	0.1
1.00	1	0.376	0.008	0.374	0.008	0.5
	2	0.991	0.013	0.991	0.013	0.0
	3	0.978	0.057	0.977	0.057	0.1
	4	1.029	0.018	1.028	0.018	0.1
1.40	1	0.378	0.008	0.374	0.008	0.2
	2	0.978	0.058	0.980	0.058	0.2
	3	1.020	0.020	1.020	0.020	0.0
	4	1.402	0.014	1.400	0.014	0.2

Table 4.4 Mode Shapes of Example System (ϵ_{11}=0.01, ω_{n1}=1.0)

Mode	DOF	Exact Mode Shape		Computed Mode Shape		Error
		Real Part	Imag. Part	Real Part	Imag. Part	%
1	1	1.000	0.000	1.000	0.000	0.0
	2	0.000	0.000	0.000	0.000	0.0
	3	0.000	0.000	0.000	0.000	0.0
	4	0.388	0.002	0.387	0.000	0.3
2	1	-0.002	0.000	-0.002	0.000	0.0
	2	0.110	-0.300	0.110	-0.300	0.0
	3	0.022	0.019	0.022	0.019	0.0
	4	1.000	0.000	1.000	0.000	0.0
3	1	-0.002	0.000	-0.002	0.000	0.0
	2	-0.002	-0.009	-0.002	-0.009	0.0
	3	0.053	-0.011	0.054	-0.011	0.1
	4	1.000	0.000	1.000	0.000	0.0
4	1	-0.002	0.000	-0.002	0.000	0.0
	2	-0.005	-0.004	-0.005	-0.004	0.0
	3	-0.175	-0.043	-0.171	-0.043	0.4
	4	1.000	0.000	1.000	0.000	0.0

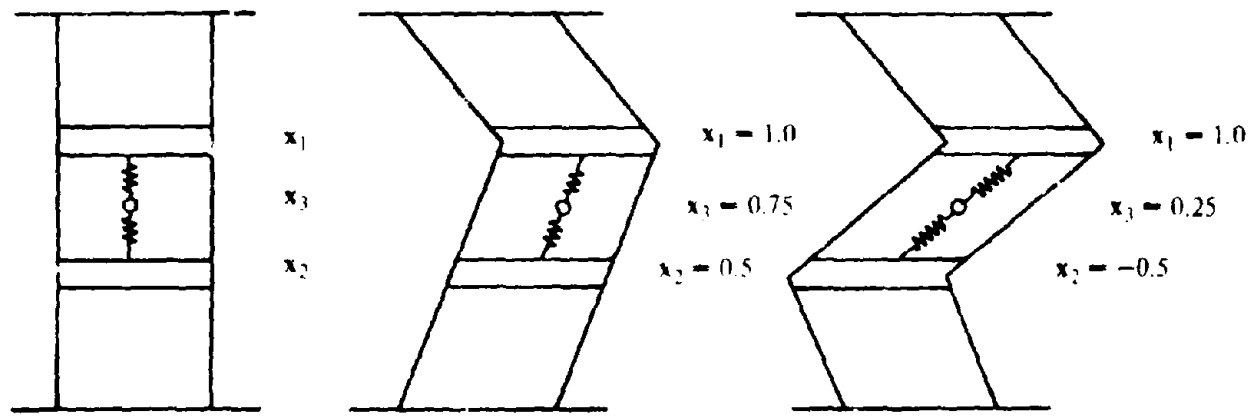

Example System

Primary Mode 1 ζ_{11}=0.75

Primary Mode 2 ζ_{21}=0.25

Fig. 4.1. Example of ζ_{ij} Calculation

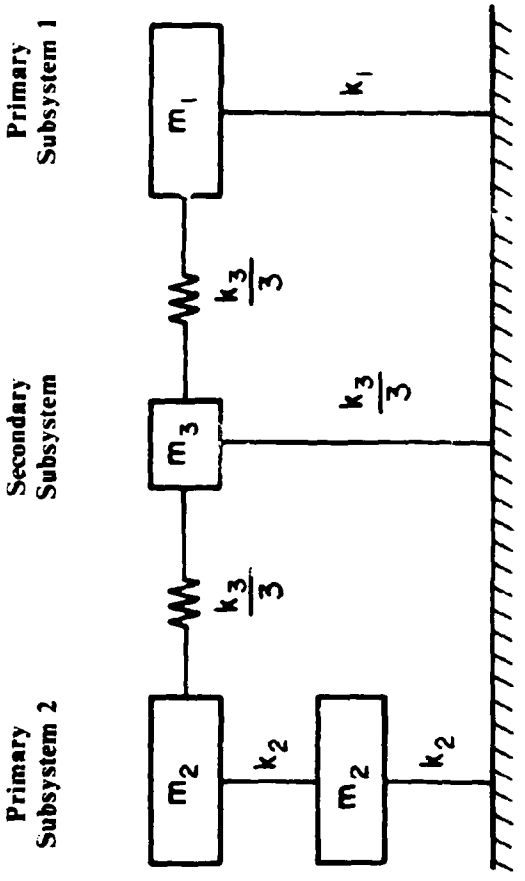

Figure 4.2. Example MDOF/SDOF System

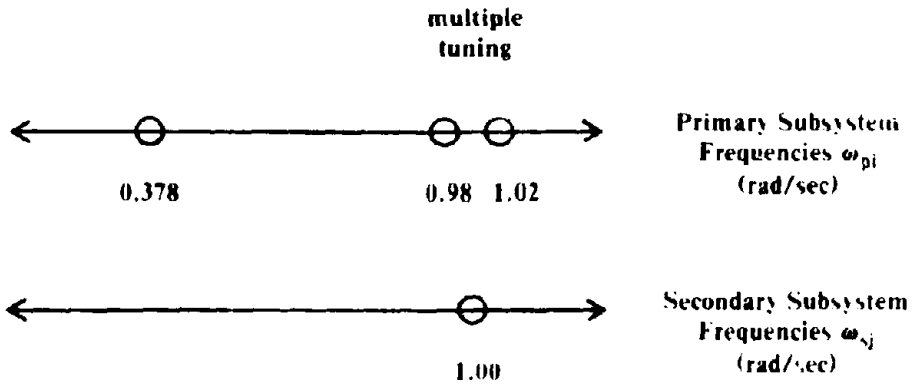

Multiply Tuned System, ω_{s1}=1.0 rad/sec

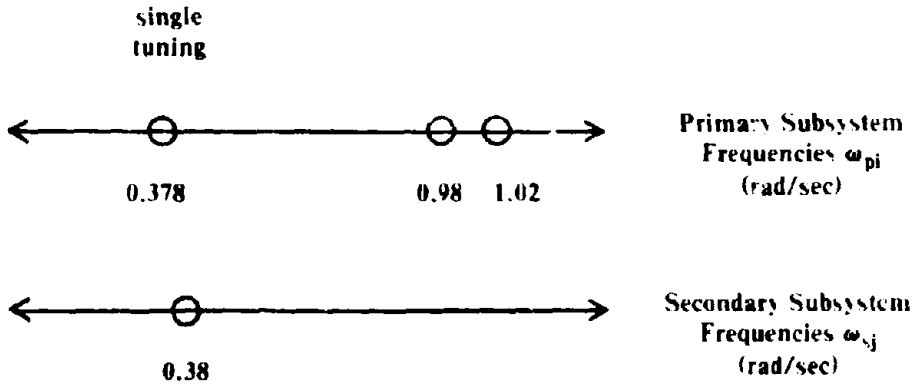

Singly Tuned System, ω_{s1}=0.38 rad/sec

Fig.4.3. Distribution of Subsystem Free Vibration Frequencies

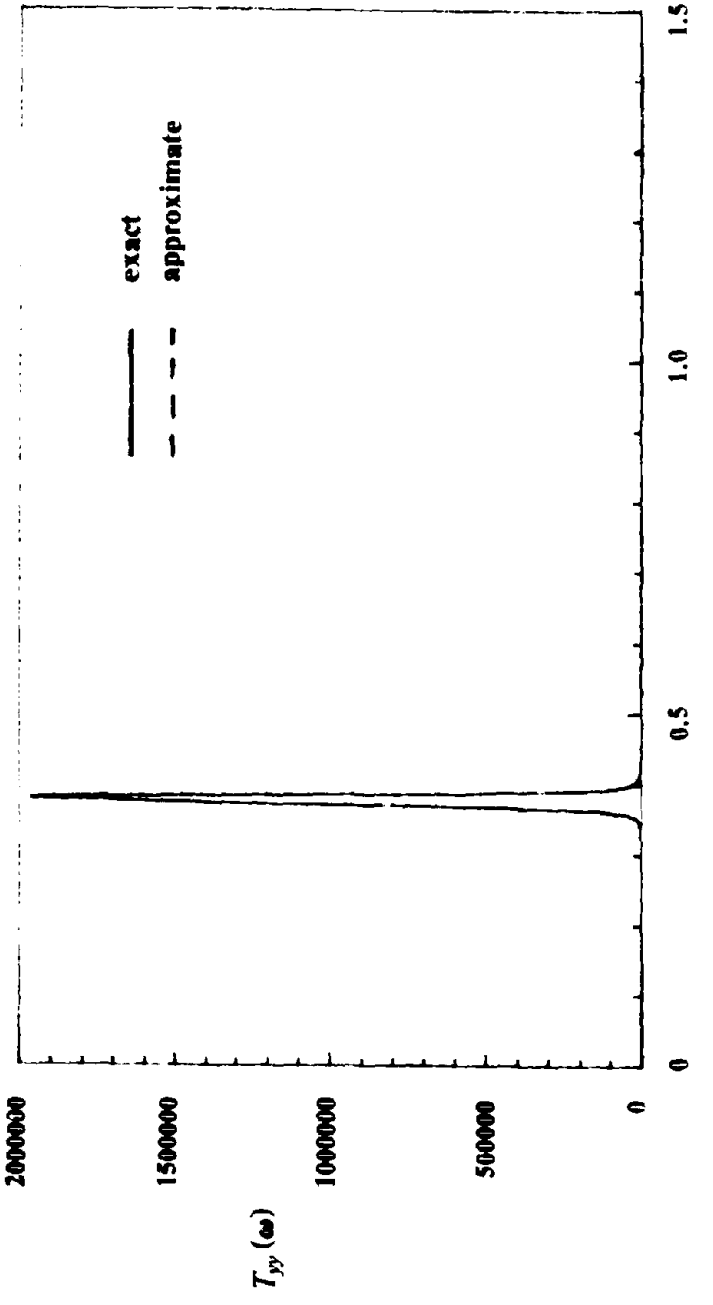

Fig.4.4a. Transfer Function $T_{yy}(\omega)$: Singly Tuned System
ω_{n1}=0.38 rad/sec, ϵ_{11}=0.01

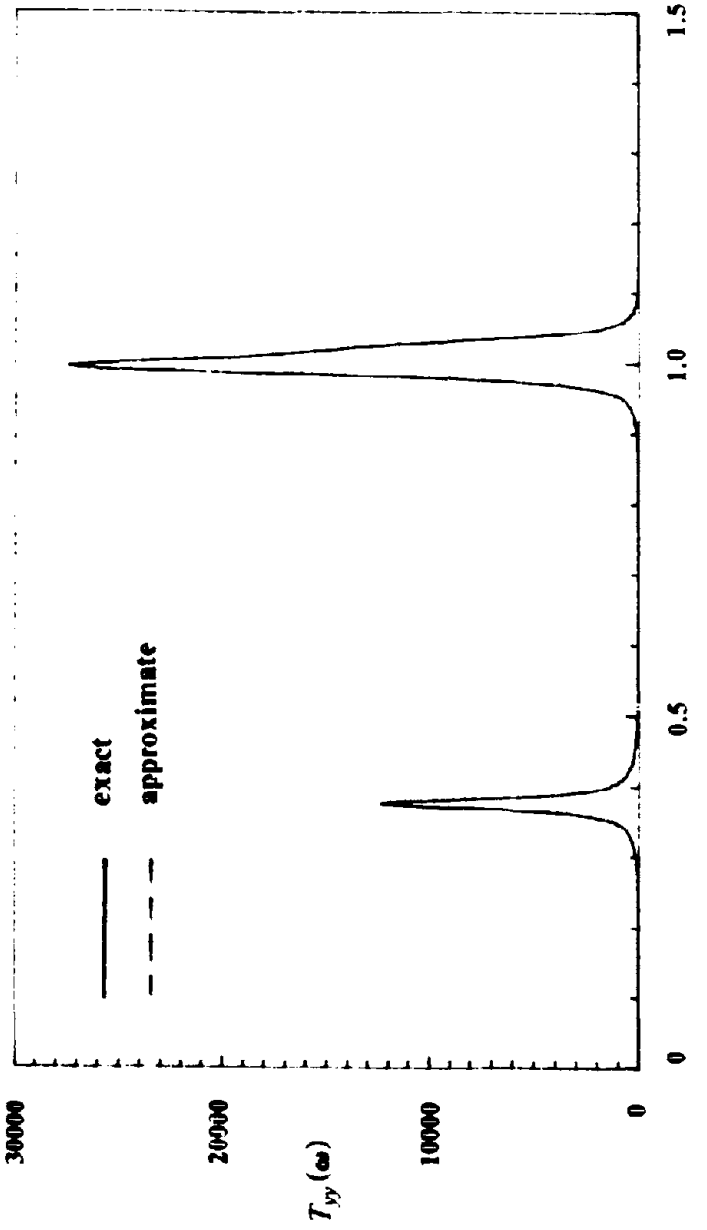

Fig.4.4b. Transfer Function $T_{yy}(\omega)$: Multiply Tuned System
$\omega_{n1}=1.0$ rad/sec, $\epsilon_{11}=0.01$

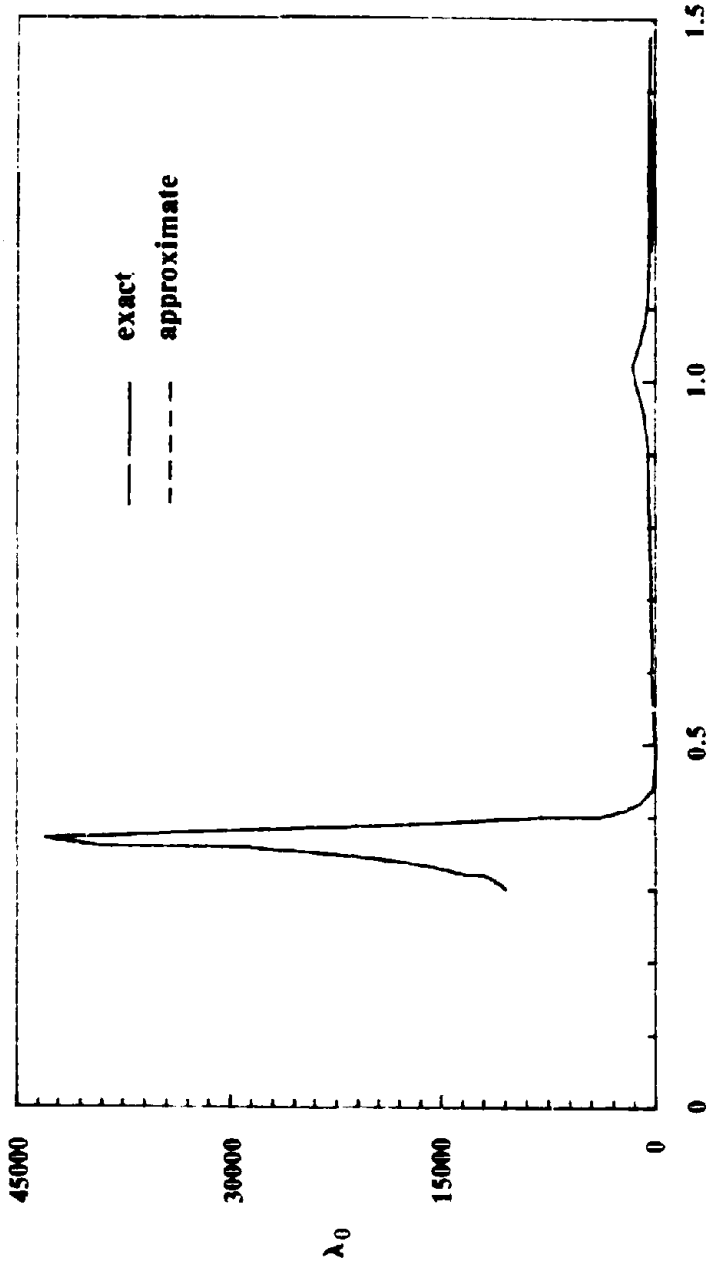

Fig4.5a. Spectral Moment λ_0 derived from $H_1(\omega)$, ϵ_{11}=0.01

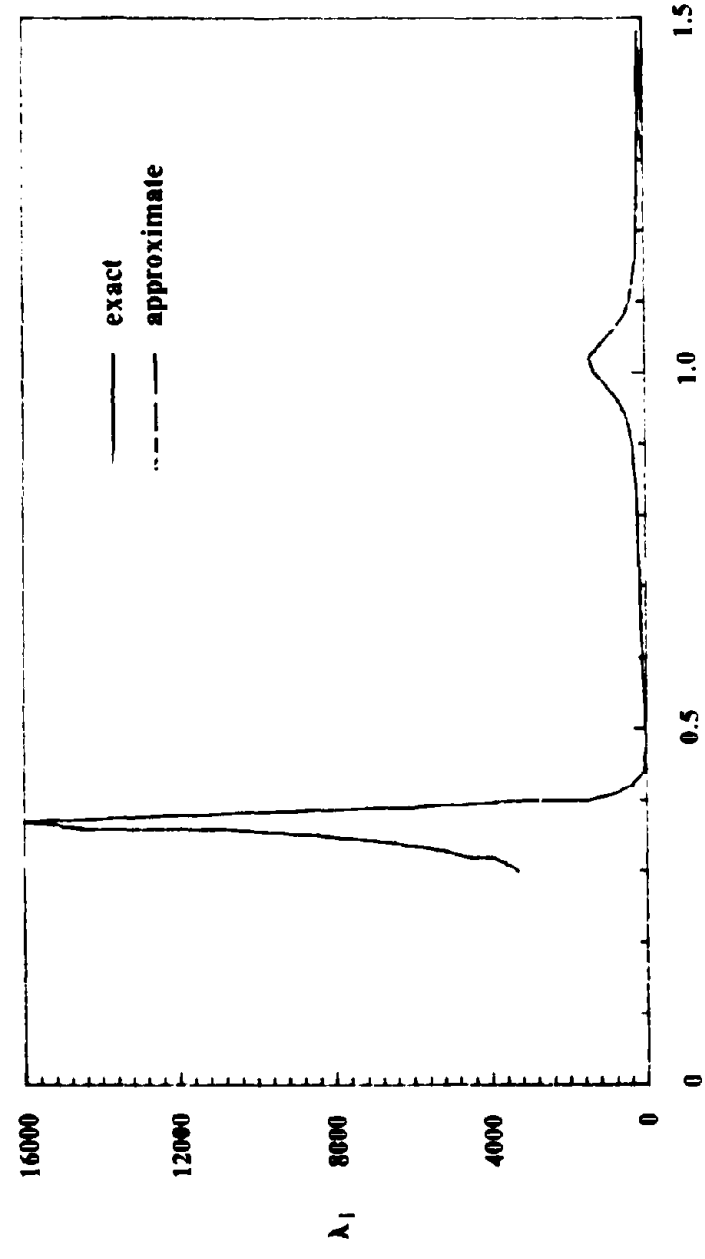

Fig4.5b. Spectral Moment λ_1 derived from $H_1(\omega)$, ϵ_{11}=0.01

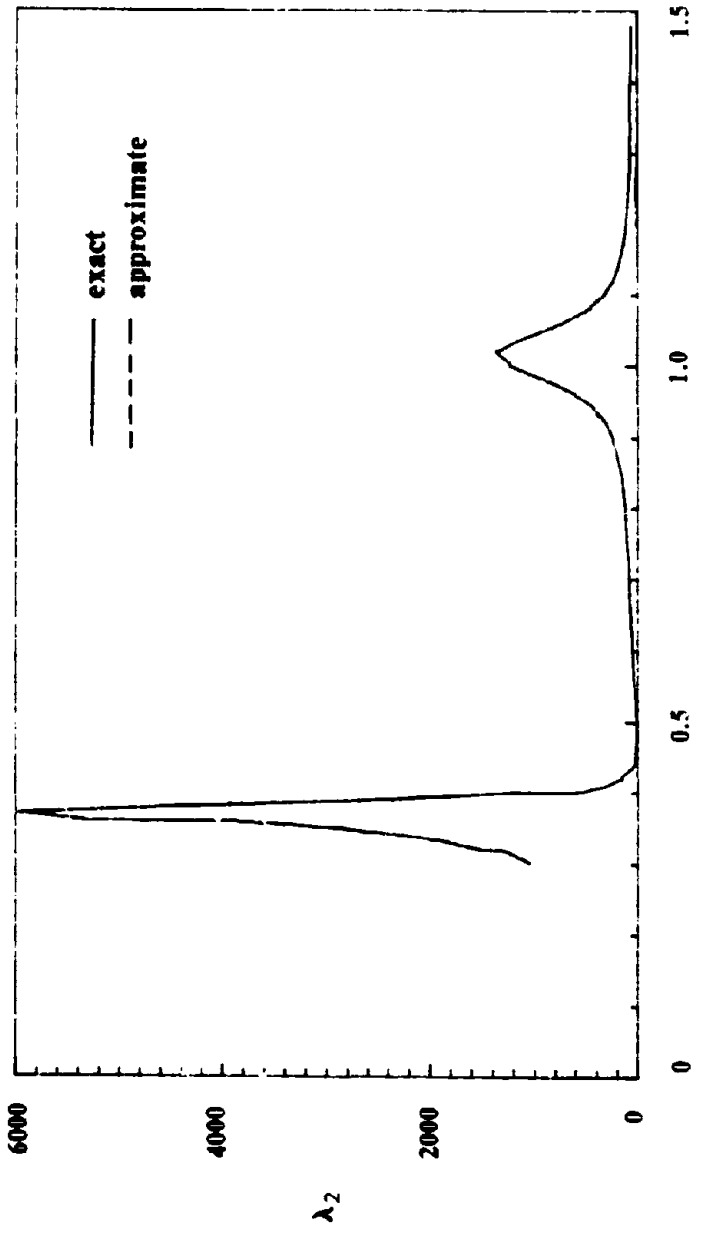

Fig4.5c. Spectral Moment λ_2 derived from $H_1(\omega)$, ϵ_{11}=0.01

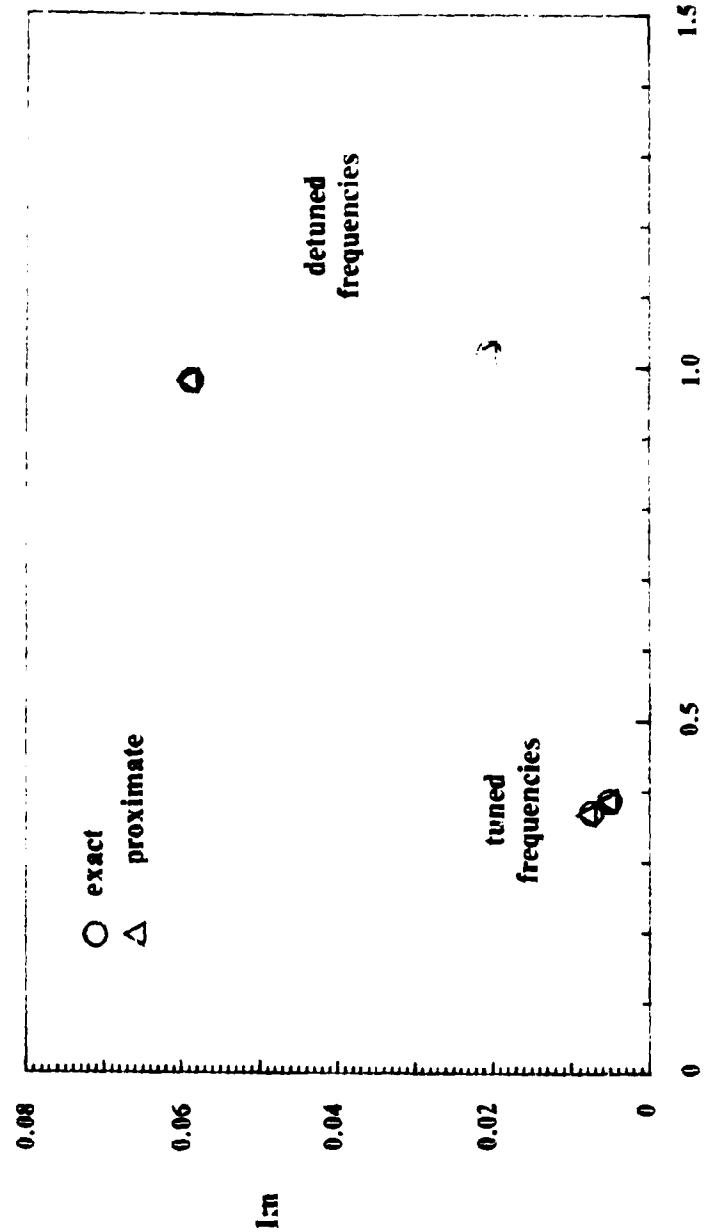

Fig.4.6a. Complex Frequencies: Singly Tuned System
ω_{s1}=0.38 rad/sec, ϵ_{11}=0.01

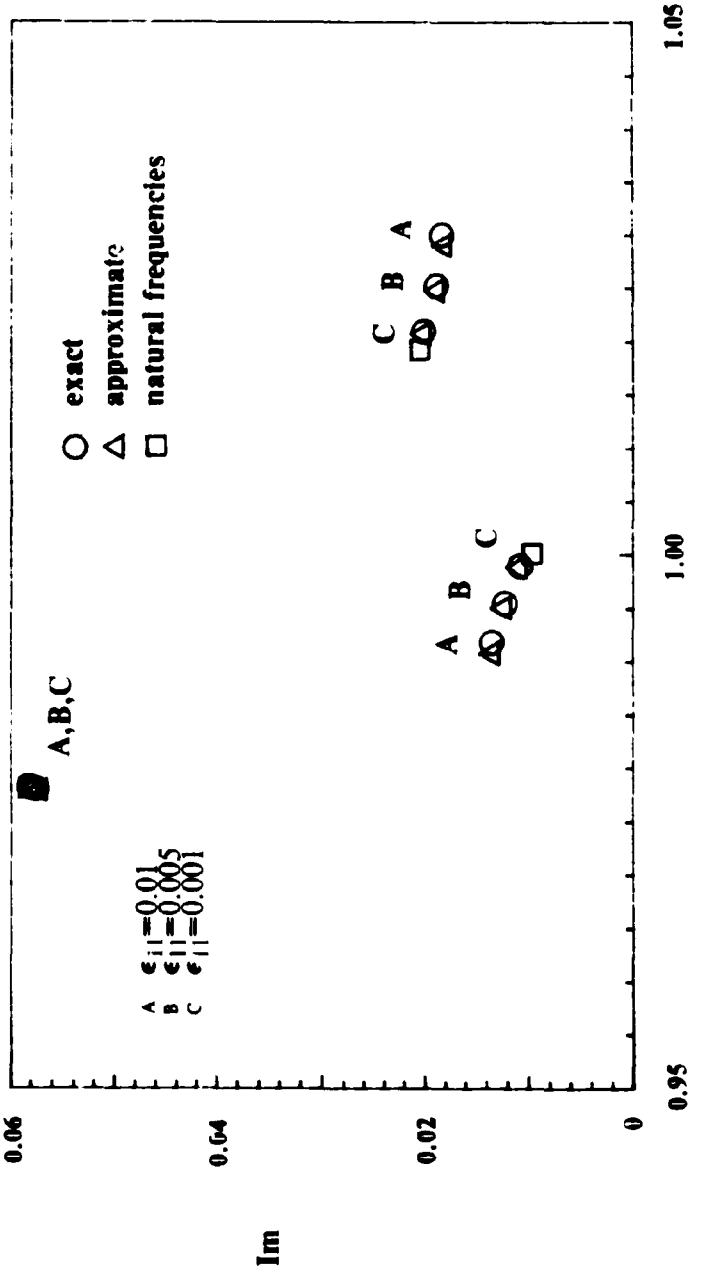

Fig.4.6b. Complex Frequencies: Multiply Tuned System
ω_{s1}=1.0 rad/sec, ϵ_{11}=0.01, 0.005, 0.001

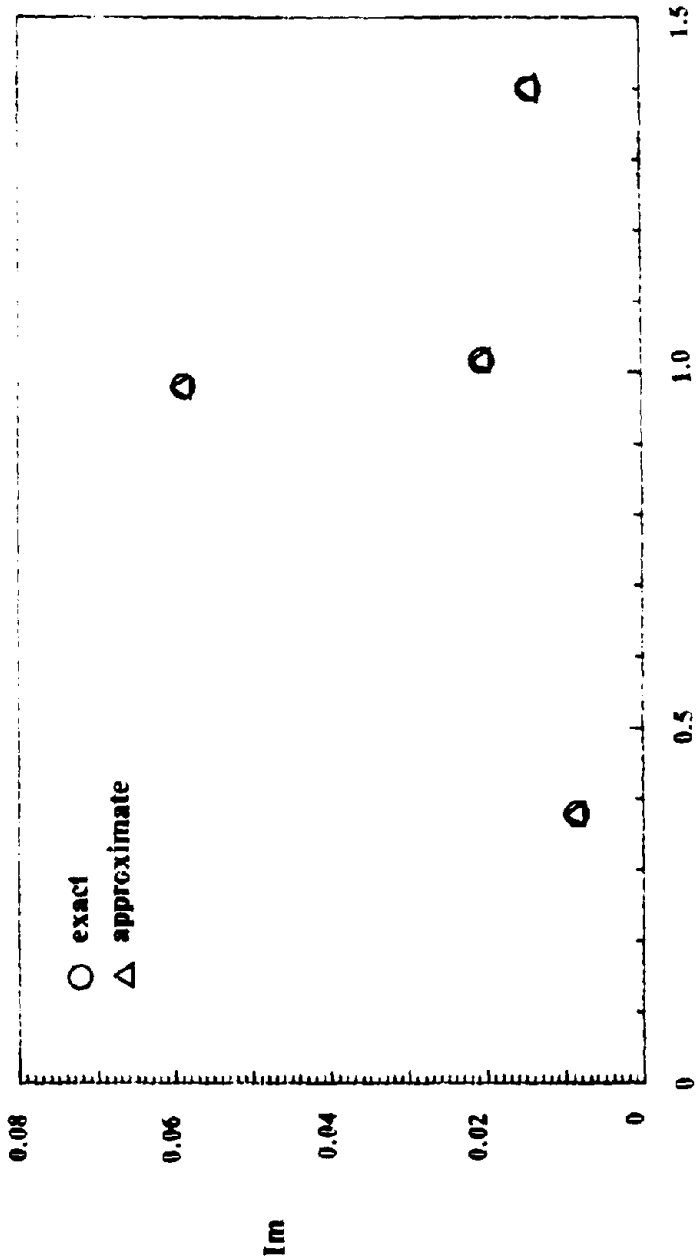

Fig.4.6c. Complex Frequencies: Detuned System
ω_{s1}=1.4 rad/sec, ϵ_{11}=0.01

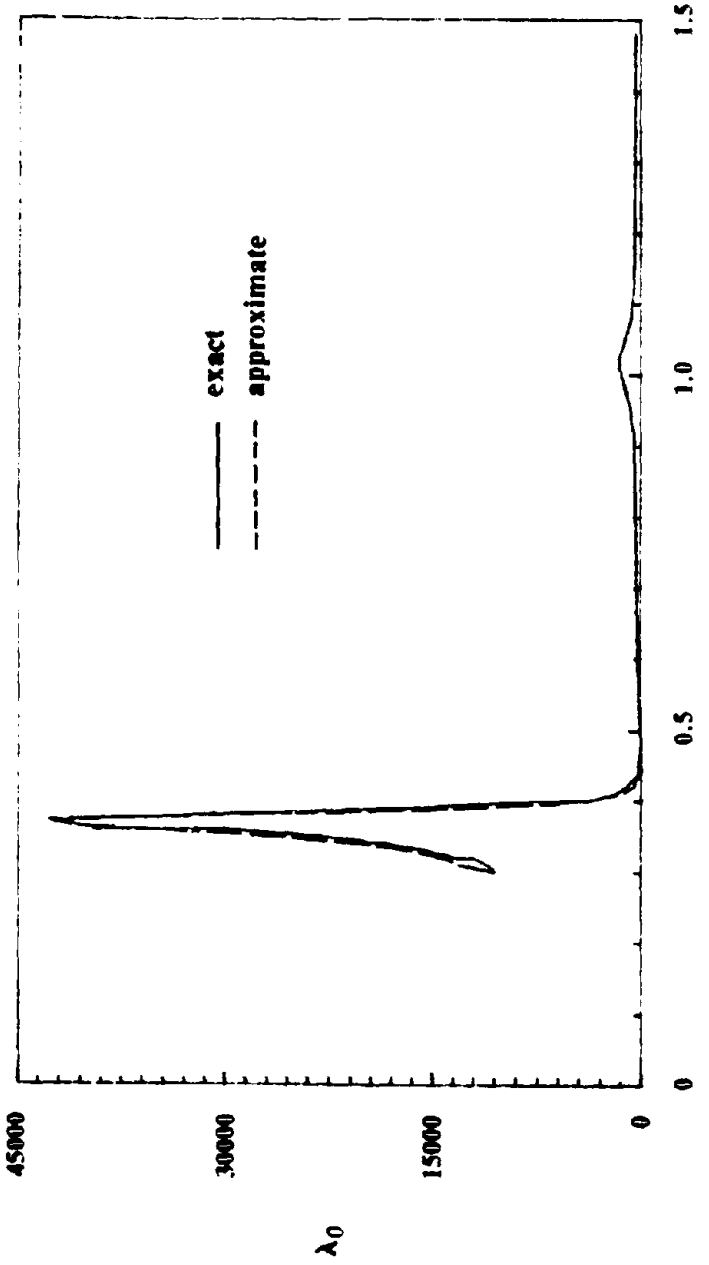

Fig4.7a. Spectral Moment λ_0, ϵ_{11}=0.01

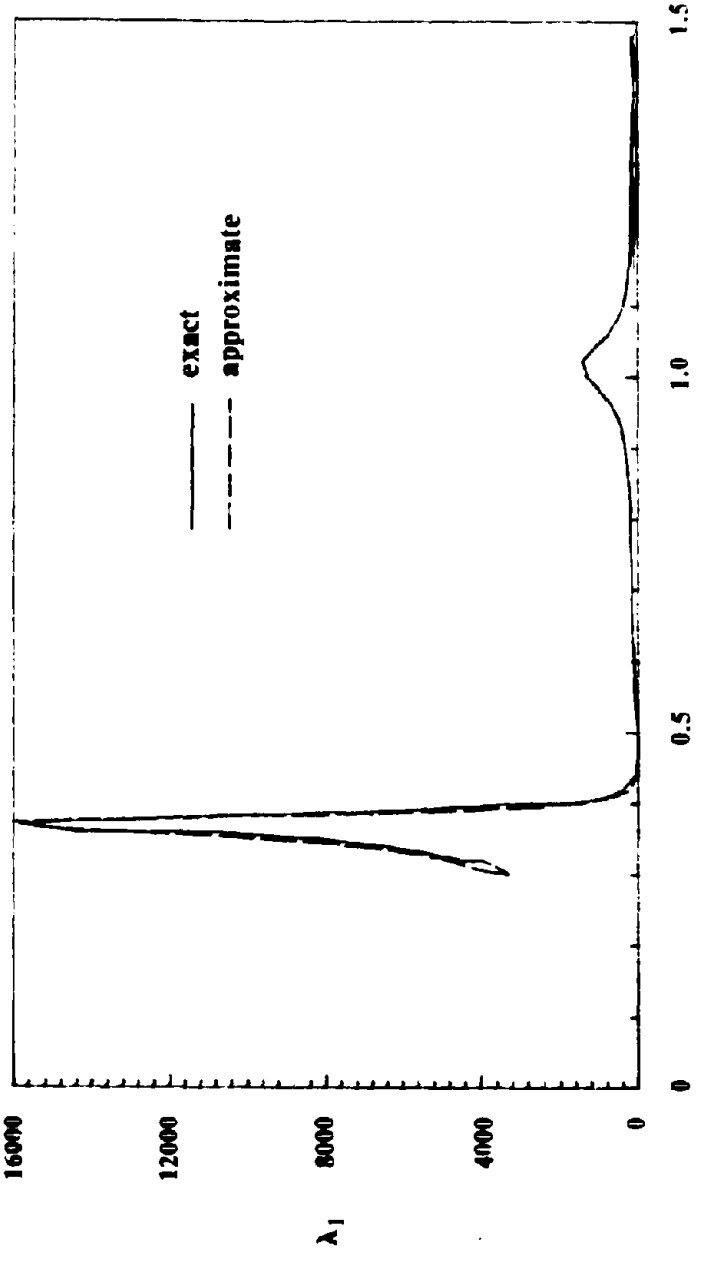

Fig4.7b. Spectral Moment λ_1, ϵ_{11}=0.01

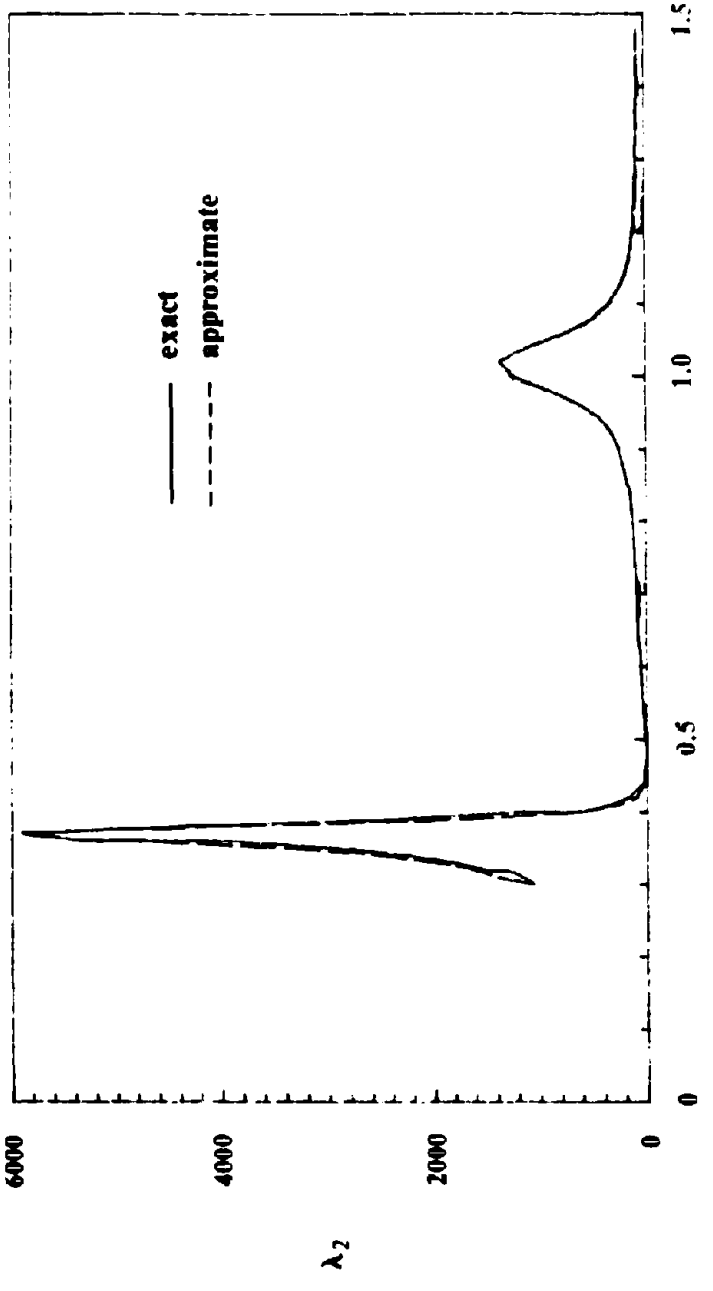

Fig4.7c. Spectral Moment λ_2, ϵ_{11}=0.01

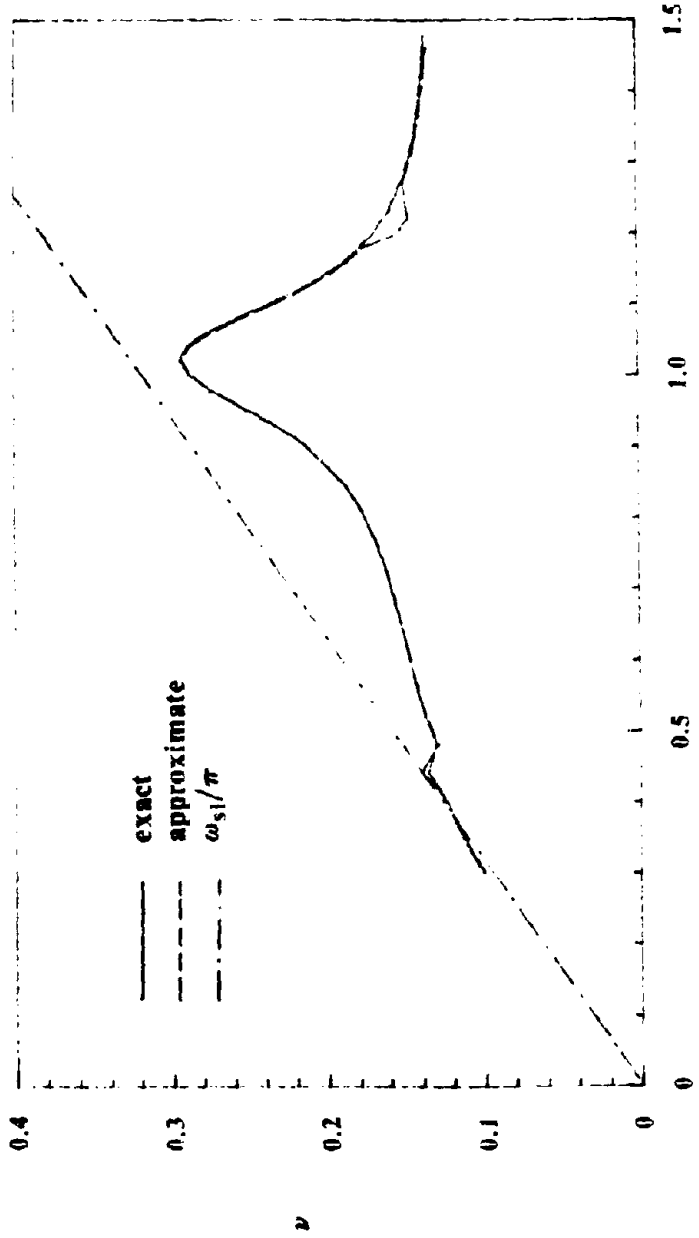

Fig4.8a. Mean Zero-Crossing Rate ν, ϵ_{11}=0.01

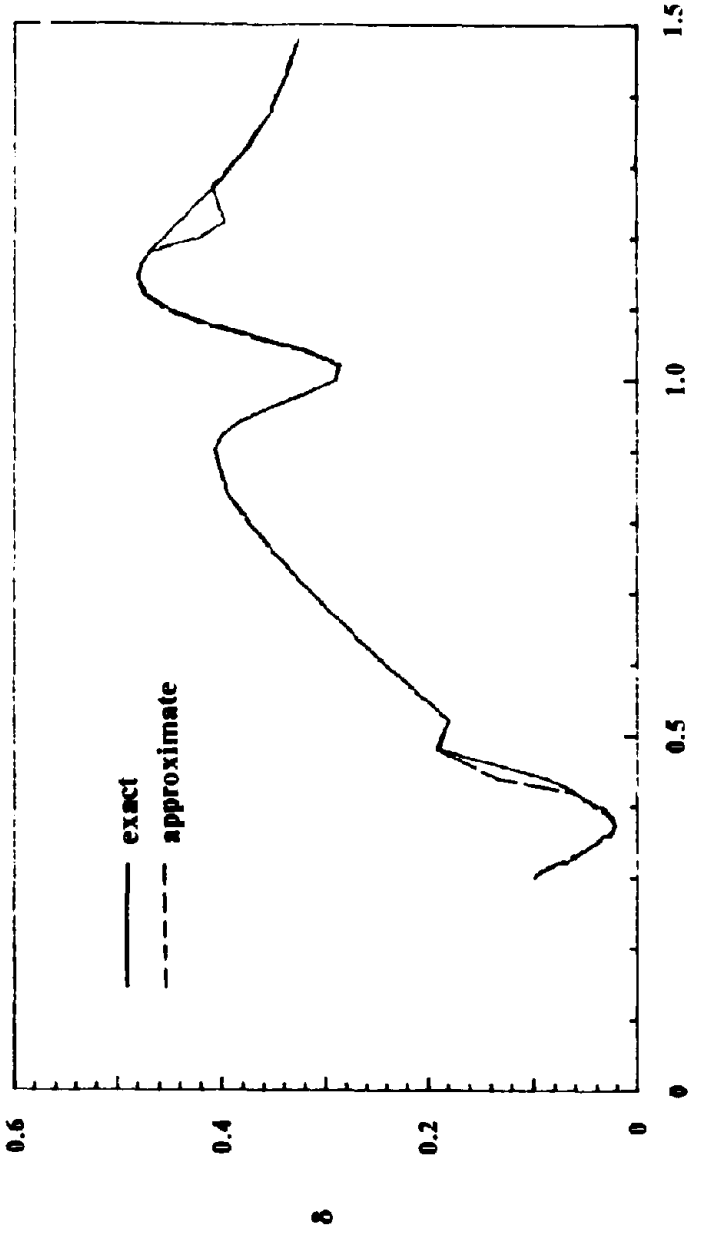

Fig4.8b. Shape Factor δ, ϵ_{11}=0.01

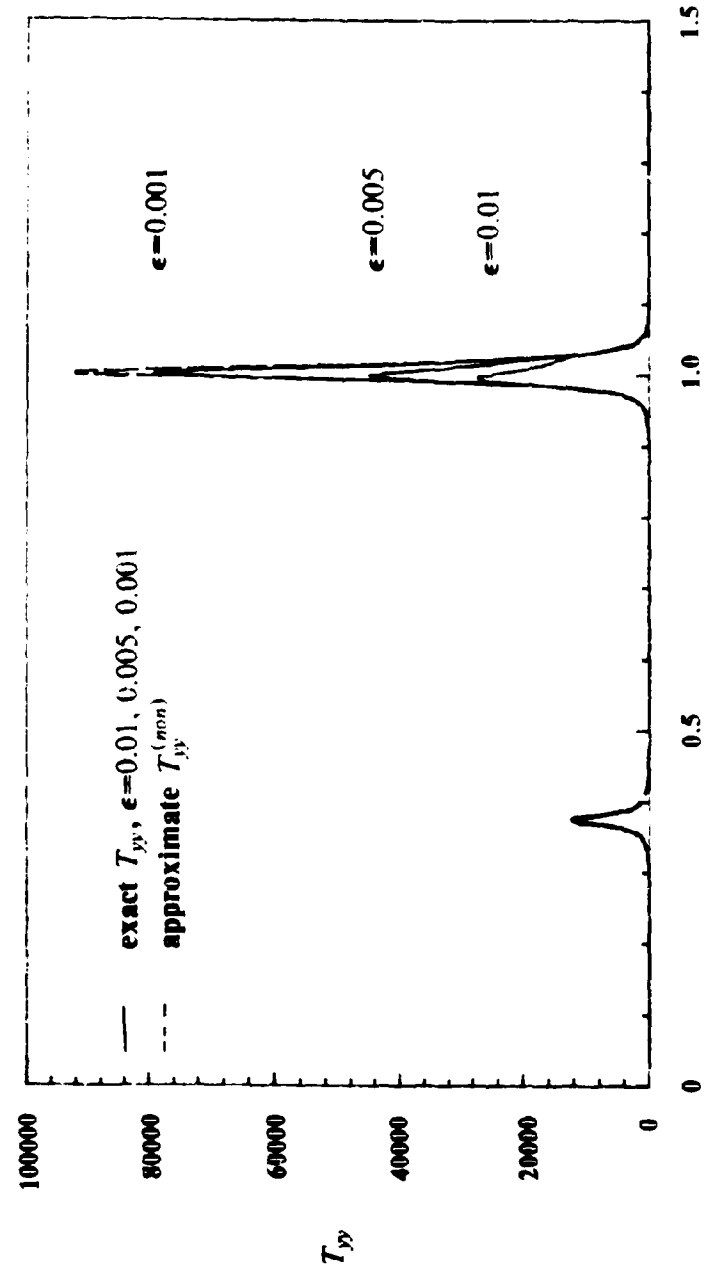

Fig4.9. Transier Function $T_{yy}^{(mon)}(\omega)$ without Interaction

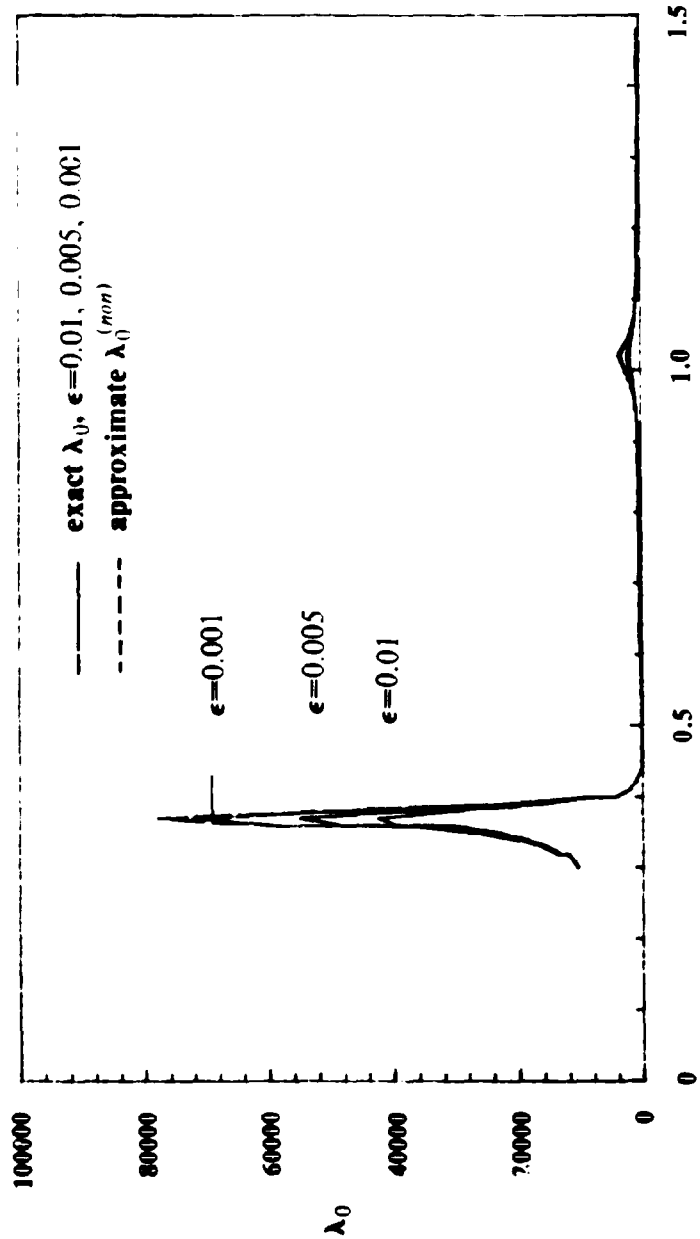

Fig4.10. Spectral Moment $\lambda_0^{(mon)}$ without Interaction Calculated from $H_1^{(mon)}(\omega)$

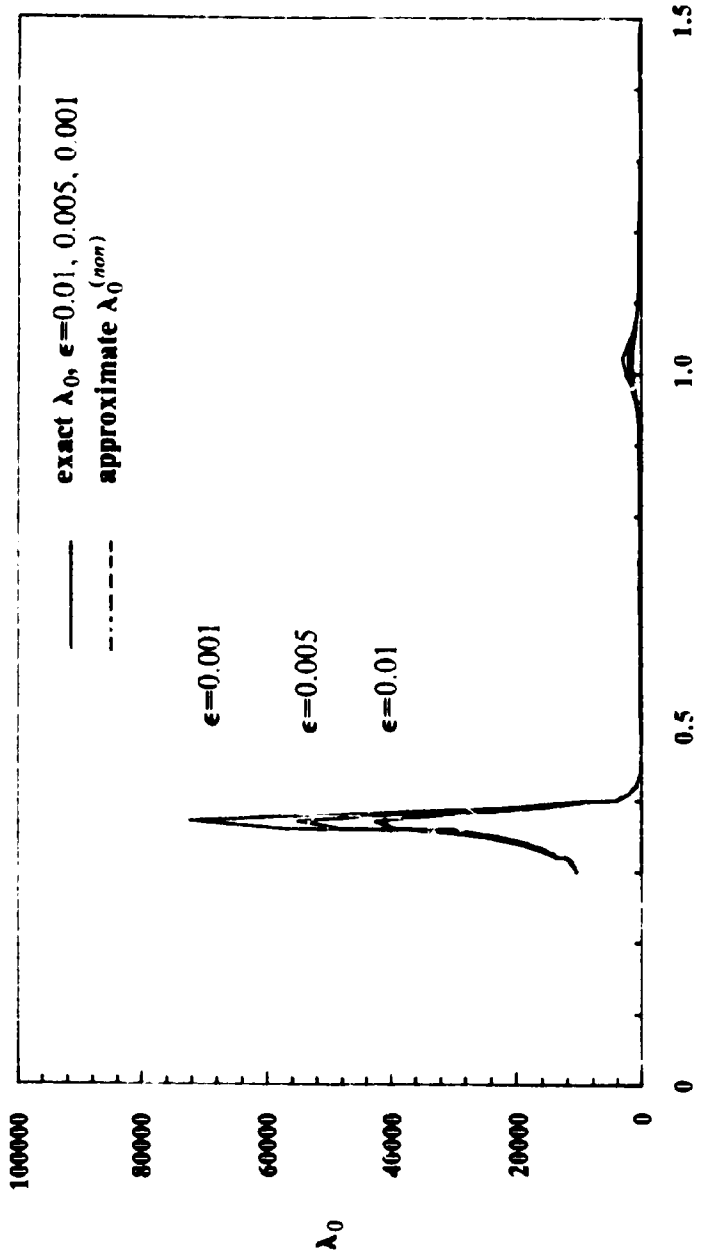

Fig4.11. Spectral Moment $\lambda_0^{(non)}$ without Interaction Calculated from Modal Combination

CHAPTER 5

ANALYSIS OF MULTI-DEGREE-OF-FREEDOM SECONDARY SYSTEMS ATTACHED TO SINGLE-DEGREE-OF-FREEDOM PRIMARY SYSTEMS

5.1 Introduction

In this chapter systems consisting of a SDOF primary subsystem supporting a MDOF secondary subsystem as shown in Fig.5.1 will be studied. Although this system appears to be entirely different from the MDOF/SDOF system studied in the previous chapter, the two systems are, in fact, strongly related. In mathematics, this relationship is called duality: every formula or theorem derived for one system has a nearly identical dual counterpart for the other system. Once this dual relationship between the two systems has been established, all of the results obtained for the MDOF/SDOF system in the previous chapter can be directly reformulated for the SDOF/MDOF system without further analytical derivation.

5.2 Definitions

5.2.1 Parameters

The first step in defining a duality relationship is to establish a one-to-one correspondence between the parameters of the two systems. In this case, the parameters defined for the n primary modes and the single secondary mode of the MDOF/SDOF system are associated with the parameters defined for the n secondary modes and the single primary mode of the SDOF/MDOF system, respectively. For instance, the natural frequencies for the subsystems of the MDOF/SDOF system, which were

$$\omega_{p1}, \omega_{p2}, \cdots, \omega_{pn}, \omega_{s1} \tag{1a}$$

are associated with the frequencies

$$\omega_{s1}, \omega_{s2}, \cdots, \omega_{sn}, \omega_{p1} \tag{1b}$$

for the SDOF/MDOF system. To maintain the above correspondence, the numbering of the

modal degrees-of-freedom for the SDOF/MDOF system is as follows: the first n degrees of freedom correspond to the modes of the secondary subsystem and the $n+1$-th degree of freedom corresponds with the primary subsystem.

Most of the definitions of the previous chapter are applied in this chapter with obvious modifications. For instance, I_i is the set of all secondary subsystem modes tuned to the primary subsystem mode.

There were several expressions used in the previous chapter with two indices, the first associated with the primary subsystem and the second with the secondary subsystem. This convention is maintained in this chapter. Thus, the mass ratios are defined as

$$\epsilon_{ij} = \frac{m_{sj}}{m_{pi}} \qquad i=1,\cdots,n. \tag{2a}$$

Also, the terms ζ_{ij} are defined as

$$\zeta_{ij} = \frac{k_{ij}}{m_{sj}\omega_{sj}^2} \qquad \text{for } i = 1,\ldots,n. \tag{2b}$$

and are interpreted as the displacement of the ith mode of the secondary subsystem produced by a static unit displacement of the primary subsystem. Similar definitions apply for the constants c_{ij}, k_{ij}, and the polynomial $f_{ij}(\omega)$. It follows that the complex frequency response matrix $\mathbf{H}(\omega)$ is

$$\mathbf{H}(\omega) = \begin{bmatrix} g_1(\omega) & \cdots & 0 & f_{11}(\omega) \\ \cdots & \cdots & \cdots & \cdots \\ 0 & \cdots & g_n(\omega) & f_{1n}(\omega) \\ f_{11}(\omega) & \cdots & f_{1n}(\omega) & G_1(\omega) \end{bmatrix}^{-1} \tag{3a}$$

where

$$g_i(\omega) = m_{si}(-\omega^2 + 2i\omega_{si}\xi_{si}\omega + \omega_{si}^2) \tag{3b}$$

$$G_1(\omega) = m_{p1}(-\omega^2 + 2i\omega_{p1}\xi_{p1}\omega + \omega_{p1}^2) \tag{3c}$$

$$f_{1i}(\omega) = -k_{1i} - ic_{1i} \approx -\zeta_{1i}m_{si}(\omega_{si}^2 + 2i\omega_{si}\xi_{si}\omega) \tag{3d}$$

for $i=1,\cdots,n$.

5.2.2 Duality Relationships

The duality between the MDOF/SDOF and SDOF/MDOF systems is established by com-

paring their complex frequency response matrices $\mathbf{H}(\omega)$ in Eqs.4.28a and 3a. The matrix in Eq.3a has an identical form to that in Eq.4.28a with the polynomials

$G_i(\omega)$ replaced by $g_i(\omega)$, (4a)

$g_i(\omega)$ replaced by $G_i(\omega)$, (4b)

$f_i(\omega)$ replaced by $f_i(\omega)$. (4c)

For the MDOF/SDOF system, the matrix $\mathbf{H}(\omega)$ and its inverse were used to derive results in the frequency response and modal analysis, respectively. Consequently, the derivations for the SDOF/MDOF system would be essentially the same as those in the previous chapter with the replacements in Eqs.4a-c. Thus, a repetition of the analysis is unnecessary and only the final results will be presented through the use of the dual relationships defined above.

5.2.3 Example System

To illustrate the major characteristics of SDOF/MDOF systems and check the accuracy of the formulations derived in this chapter, the example system shown in Fig.5.1 is used. A 2-DOF secondary system is supported by the SDOF primary subsystem and the base of the combined system. The dynamic properties of the subsystems are described in Tables 1 and 2 and are chosen so that the combined system would exhibit important characteristics found in general MDOF/SDOF systems, as was done for the study of MDOF/SDOF systems. By varying the stiffnesses k_2 and k_3, it is possible to vary the frequencies of the secondary subsystem. One frequency of the secondary subsystem was chosen to be fixed at $\omega_{s2} = 1.0$ rad/sec, thus the secondary subsystem was always tuned to the primary system, which had a frequency of $\omega_{p1} = 1.02$ rad/sec. The other frequency of the secondary subsystem was variable. For $\omega_{s1} = 0.7$ rad/sec, the system is singly tuned as shown in Fig.5.2a, and for $\omega_{s1} = 1.0$ rad/sec, the system becomes multiply tuned as shown in Fig.5.2b. The mass ratio, ϵ, is also chosen to be a variable parameter, as in the MDOF/SDOF example system. Finally, the damping ratio of the equipment is unequal to the damping ratios of the primary subsystem, thus the combined system is, in general, non-proportionally damped.

The response quantity that will be investigated is the relative displacement between the

mass of the primary subsystem and the adjacent mass of the secondary subsystem.

5.3 Frequency Response Results

As a first application of the duality the expression for the complex frequency response function $H_1(\omega)$ of the response variable $y(t)=\mathbf{q}^T\mathbf{z}(t)$ is given. For the MDOF/SDOF system, $H_1(\omega)$ is given in Eq.4.36 and is repeated here

$$H_1(\omega) \approx \frac{g_1(\omega)\prod_1^n G_j(\omega)}{d(\omega)}\left[\sum_1^n \frac{q_{n+1}m_j r_j f_1(\omega)}{g_1(\omega)G_j(\omega)} - \frac{q_{n+1}m_{n+1}r_{n+1}}{g_1(\omega)} - \sum_1^n \frac{q_j m_j r_j}{G_j(\omega)}\right] \tag{5}$$

The dual form of the above is found through the relations in Eqs.1a,b and Eqs.4a-c

$$H_1(\omega) \approx \frac{G_1(\omega)\prod_1^n g_j}{d(\omega)}\left[\sum_1^n \frac{q_{n+1}m_j r_j f_1(\omega)}{G_1(\omega)g_j(\omega)} - \frac{q_{n+1}m_{n+1}r_{n+1}}{G_1(\omega)} - \sum_1^n \frac{q_j m_j r_j}{g_j(\omega)}\right] \tag{6a}$$

where $d(\omega)$ is the characteristic polynomial

$$d(\omega) = \prod_1^n g_j(\omega)\left[G_1(\omega) - \sum_{j\neq 1}\frac{f_1^2(\omega)}{g_j(\omega)}\right] \tag{6b}$$

These expressions are considerably simpler than the exact form of $H_1(\omega)$ which requires the inversion of an $n+1\times n+1$ matrix.

A plot of $T_{11}(\omega)$ for the example system in Fig.5.1 is shown in Figs.5.3a,b. In Fig.5.3a, the secondary subsystem frequency $\omega_{s1} = 0.7$ rad/sec is detuned, and a peak is found only for the tuned modes at $\omega = \omega_{p1}$. There is also a small peak corresponding to the detuned secondary mode near $\omega = 0.7$ rad/sec, however it is considerably smaller than the first peak and is not visible on the plot. In Fig.5.3b, both secondary subsystem frequencies are multiply tuned to the primary subsystem frequency, and a single peak is found at $\omega = \omega_{s1}$ which is slightly larger and broader than the corresponding peak of the singly tuned system, as expected.

As in Section 4.3.3, the approximate and exact forms of the complex frequency response function $H_1(\omega)$ derived above were used to calculate the power spectral density function for the response of the example system in Fig.5.1 to white-noise base excitation. From this result, the spectral moments of the response were obtained by numerical integration and plotted as a func-

tion of the equipment frequency, ω_{s1}, in Figs.5.4a-c. For values of ω_{s1} detuned from the primary subsystem frequency, the response of the system is dominated by the singly tuned modes which are relatively independent of the detuned secondary mode. Thus, the spectral moment maintains a large and nearly constant value. However, when the system is multiply tuned, an increase in the spectral moment arises at $\omega_{s1} = 1.0$ rad/sec from the additional tuned secondary mode. The values for λ_m for $m = 0$, 1, and 2 are nearly identical, due to the fact that the frequencies of the dominant modes in the response are all nearly equal to 1.0 rad/sec. Also, the difference between approximate and exact results are slight, illustrating the accuracy of the perturbation methods.

5.4 Modal Decomposition results

5.4.1 Mode Shapes and Frequencies

In this section, expressions for the mode shapes and frequencies of the SDOF/MDOF system are developed which are suitable for numerical evaluation and subsequent use in the modal decomposition analysis to provide accurate measures of the response. Approximate expressions for the spectral moments of response to white noise input are derived from the algebraic form of the mode shapes to provide further insight to the dynamic behavior of the system.

Due to the duality between the SDOF/MDOF and MDOF/SDOF systems, a derivation of the mode shapes and frequencies is unnecessary, and final expressions for these quantities are found directly from the results of Section 4.4.1 through the use of the relationships in Section 5.2.

5.4.1.1 Detuned Modes

For notational convenience, assume that the first secondary subsystem mode is detuned from the primary subsystem. Then, the first-order expressions for the frequency and mode shape of the combined system which are associated with mode 1 of the secondary subsystem are given by the dual forms of Eq.4.40b and 4.41, respectively:

$$\omega_1^{(0)} = \omega_{s1}(\sqrt{1-\xi_{s1}^2} + i\xi_{s1}) \tag{7a}$$

$$\boldsymbol{\phi}_1^{(0)} = \left[1 \quad \frac{f_{12}f_{12}}{G_1 g_2} \quad \cdots \quad \frac{f_{1n}f_{1n}}{G_1 g_n} \quad -\frac{f_{s1}}{G_1} \right]^t \tag{7b}$$

where all of the above polynomial are evaluated at $\omega = \omega_1^{(0)}$. The low-order approximations of the above are

$$\omega_1^{(1)} = \omega_{s1}(1 + i\xi_{s1}) \tag{8a}$$

$$\boldsymbol{\phi}_1^{(1)} \approx \left[1 \; 0 \quad \cdots \quad 0 \quad \frac{\zeta_{s1}\epsilon_{11}\omega_{s1}^2}{\omega_{p1}^2 - \omega_{s1}^2} \right]^t \tag{8b}$$

Similarly, if the primary subsystem mode is detuned from all of the secondary subsystem modes, the first-order expressions associated with the primary subsystem mode are found from Eqs.4.43b and 4.44

$$\boldsymbol{\phi}_{n+1}^{(1)} = \left[-\frac{f_{s1}}{g_1} \quad \cdots \quad -\frac{f_{sn}}{g_n} \quad 1 \right]^t \tag{9a}$$

$$\omega_{n+1}^{(1)} = \omega_{p1}(\sqrt{1-\xi_{p1}^2} + i\xi_{p1}) \tag{9b}$$

where the above polynomials are evaluated at $\omega = \omega_{n+1}^{(1)}$. To low-order, the above reduces to

$$\boldsymbol{\phi}_{n+1}^{(1)} = \left[\zeta_{11}\frac{\omega_{s1}^2}{\omega_{s1}^2 - \omega_{p1}^2} \quad \cdots \quad \zeta_{1n}\frac{\omega_{sn}^2}{\omega_{sn}^2 - \omega_{p1}^2} \quad 1 \right]^t \tag{10a}$$

$$\omega_{n+1}^{(1)} = \omega_{p1}(1 + i\xi_{p1}) \tag{10b}$$

The mode shapes $\boldsymbol{\phi}_1^{(1)}$ and $\boldsymbol{\phi}_{n+1}^{(1)}$ can be viewed as a MDOF generalization of Eq.2.78 and 2.76, respectively, which are for a SDOF secondary subsystem.

5.4.1.2 Singly tuned modes

Assume that the first secondary subsystem mode is tuned to the primary subsystem. The expressions for the frequencies $\omega_1^{(0)}$ given in Eqs.4.46a,b are not changed by the duality relationships due to the symmetry of the singly tuned modes.

$$\omega_1^{(0)} = \omega_a\left\{ 1 + i\xi_a - \frac{1}{2}[\gamma_{11} + (i\xi_a + \beta)^2] \right\} \tag{11a}$$

$$\omega_2^{(0)} = \omega_a\left\{ 1 + i\xi_a + \frac{1}{2}[\gamma_{11} + (i\xi_a + \beta)^2] \right\} \tag{11b}$$

The first-order solutions to the mode shapes are found from Eq.4.47 using the results of section 4.4.1.3

$$\boldsymbol{\phi}^{(1)} = \left[\alpha^{(1)} \quad -\frac{f_{12}}{g_2} \quad \cdots \quad -\frac{f_{1n}}{g_n} \quad 1 \right]^T \tag{12}$$

where $\alpha^{(1)}$ is given by Eqs.4.46e,f and the above polynomials are evaluated at the frequency $\omega^{(1)}$. Note that the reciprocal of $\alpha^{(1)}$ is used here since the roles of the secondary and primary degrees-of-freedom are reversed. From these solutions, the following low-order approximations are obtained

$$\omega^{(1)} = \omega^{(1)} \tag{13a}$$

$$\boldsymbol{\phi}^{(1)} = \left[\alpha^{(1)} \quad \frac{\zeta_{12}\omega_{s2}^2}{\omega_{s2}^2-\omega_{p1}^2} \quad \cdots \quad \frac{\zeta_{1n}\omega_{sn}^2}{\omega_{sn}^2-\omega_{p1}^2} \quad 1 \right]^T \tag{13b}$$

5.4.1.3 Multiply Tuned Modes

Assume the first l secondary subsystem modes are tuned to the primary subsystem. The first-order approximations for the mode shapes for a multiply tuned system are written in the same form as in Eq.4.51a

$$\boldsymbol{\phi}^{(1)} = \begin{bmatrix} \boldsymbol{\phi}_t^{(1)} \\ \boldsymbol{\phi}_d^{(1)} \\ 1 \end{bmatrix} \tag{14}$$

The tuned components $\boldsymbol{\phi}_t^{(1)}$ and the frequency $\omega^{(1)}$ are found by solving the $l+1 \times l+1$ eigenvalue problem in Eq.4.49. The detuned component $\boldsymbol{\phi}_d^{(1)}$ is found from the dual of Eq.4.51b

$$\boldsymbol{\phi}_d^{(1)} = \left[-\frac{f_{1,l+1}}{g_{l+1}} \quad \cdots \quad -\frac{f_{1n}}{g_n} \right]^T \tag{15}$$

which, to low-order, reduces to

$$\boldsymbol{\phi}_d^{(1)} = \left[\frac{\zeta_{1,l+1}\omega_{s,l+1}^2}{\omega_{s,l+1}^2-\omega_{p1}^2} \quad \cdots \quad \frac{\zeta_{1n}\omega_{sn}^2}{\omega_{sn}^2-\omega_{p1}^2} \right] \tag{16}$$

Note that the detuned components of the modes shapes are identical for multiply tuned, singly tuned, and detuned systems.

5.4.1.4 Very Closely Spaced Detuned Modes

It was shown in section 4.4.2.5 that the expressions for the mode shapes for widely spaced detuned modes can be used in obtaining results for the system response even for very closely spaced detuned modes. This fact continues to hold for SDOF/MDOF systems. If accurate

expressions for the mode shapes are required, then the same set of equations that were used in the multiple tuning problem are solved, as explained in Section 4.4.1.5.

5.4.1.5 Examples

The complex modal properties of the example system in Fig.5.1 were computed using the formulations developed in this section and was compared with exact results. The frequencies are shown in Table 3 and are plotted in Figs.5.5a,b for various values of the equipment frequency ω_{e_1}, and the mode shapes for the multiply tuned case (i.e., $\omega_{e_1} = 1.00$ rad/sec) are shown in Table 4. The non-classical damping character of the multiply tuned system is apparent in the mode shapes, which have imaginary components. Good agreement between approximate and exact values is found in all cases.

The effect of the equipment mass is illustrated in Fig.5.5b, where the frequencies corresponding to $\epsilon = .01$, .005, and .001 are represented by points A, B, and C, respectively, and are shown to be convergent to the subsystem natural frequencies.

5.4.2 Spectral Moments

As stated in the previous chapter the spectral moments can be calculated by evaluating the expressions for the mode shapes and frequencies and substituting the numerical results directly into the modal decomposition method. For the example system in Fig.5.1, the results of this numerical computation are compared with exact results obtained by integrating the complex frequency response function in Figs.5.6a-c. Also, the mean zero-crossing rate, ν, and the shape factor, δ, were computed and plotted in Figs.5.7a,b. All plots show good comparison between exact and the proposed approximate results.

It was noted in Section 4.4.2 that the mean zero-crossing rate of a tuned PS system was nearly equal to $\nu = \omega_{p1}/\pi$, where ω_{p1} is one of the tuned frequencies. Since the secondary subsystem is always tuned to the primary subsystem, ν would have a constant value of approximately $1.0/\pi \approx 0.318$ rad/sec, which is in agreement with Fig.5.7a. Also, it was observed in Section 5.3 that the complex frequency response function had only a single peak for both singly

and multiply tuned configurations of the example system, thus the shape factor would remain small and nearly constant for all values of the secondary frequency ω_{s1} as shown in Fig 5.7b.

Although the numerical approach to finding the spectral moments is useful in practical applications, it is instructive to derive general algebraic solutions for the spectral moments of response of arbitrary SDOF/MDOF PS systems to white-noise input. This is accomplished using the duality relationships and the results in section 4.4.2.

5.4.2.1 Totally Detuned Systems with Well-Spaced Modes

As before, the modal decomposition method simplifies to the SRSS method for totally detuned systems with well-spaced modes. The effective participation factors are found from Eqs.4.53a,b

$$\psi_i = q_i \left[\frac{r_{i-1}\omega_{i-1}^2\zeta_{i-1}}{\omega_{i-1}^2-\omega_i^2} + r_i \right] \qquad i=1,\cdots,n \tag{17a}$$

$$\psi_{n+1} = r_{n+1}\left[\sum_{1}^{n} \frac{q_i\omega_i^2\zeta_{i1}}{\omega_i^2-\omega_{i1}^2} + q_{n+1}\right] \tag{17b}$$

It follows that the spectral moments for response to white-noise are

$$\lambda_m = \frac{\pi G_{xx}}{4}\left\{\sum_{1}^{n} q_i^2 \left[\frac{r_{i-1}\omega_{i-1}^2\zeta_{i1}}{\omega_{i1}^2-\omega_i^2} + r_i\right]^2 \frac{\omega_i^{m-3}}{\xi_i} + r_{n+1}^2\left[\sum_{1}^{n} \frac{q_i\omega_i^2\zeta_{i1}}{\omega_i^2-\omega_{i1}^2} + q_{n+1}\right]^2 \frac{\omega_{i1}^{m-3}}{\xi_{i1}}\right\} \tag{18}$$

5.4.2.2 Singly Tuned Systems

Assuming the first secondary mode is tuned to the primary mode, the detuned moment corresponding to Eq.4.56 is

$$\lambda_{dm} = \frac{\pi G_{xx}}{4}\sum_{i\neq 1} q_i^2 \left[\frac{r_{i-1}\omega_{i-1}^2\zeta_{i-1}}{\omega_{i1}^2-\omega_i^2} + r_i\right]^2 \frac{\omega_i^{m-3}}{\xi_i} \tag{19}$$

and the tuned moment corresponding to Eq.4.57 is

$$\lambda_{tm} = \frac{\pi G_{xx}}{8}\frac{q_1 r_{n+1}\zeta_{11}\xi_{a}\omega_a^{m-3}}{\xi_{a1}\xi_{s1}(\beta^2+4\xi_a^2)} \cdot \gamma_{11}\xi_{s1}^2 \tag{20}$$

5.4.2.3 Multiply Tuned Systems

The procedure for finding λ_m for multiply tuned systems remains the same as in Section

4.4.2.3. The detuned component λ_{jj} is computed using Eq 19 and λ_{ij} is evaluated numerically by using the modal decomposition method

5.4.2.4 Systems with Closely Spaced Secondary Modes

The cross modal contribution λ_{ij} from closely spaced secondary subsystem modes is accounted for in the same manner as outlined in section 4.4.2.4. The expression for λ_{ij} is given by Eq 4.59.

5.4.2.5 Systems with Closely Spaced Detuned Secondary Modes

The two methods for considering closely spaced detuned modes derived in Section 4.4.2.5 can be applied to SDOF/MDOF systems. In the first method, the closely spaced modes are considered as a single collective mode. Assuming the first I secondary subsystem modes are very closely spaced, the frequency for this collective mode is given by the average ω_I of the I secondary frequencies, the damping ratio is given by the average ξ_I of the I modal damping ratios, and the effective participation factor ψ_I is given by

$$\psi_I = \sum_{j=1}^{I} q \left[\frac{r_{jj}(\omega_j \zeta_j}{\omega_{jj}^2 - \omega_j^2} + r \right] \qquad (21)$$

The alternative method is to consider the I modes separately. The mode shapes and frequencies are found from the formulae for widely spaced detuned modes, Eqs.8a,b; the effective participation factors are evaluated using Eq 17a; and the effect of close spacing is accounted for by using the approximation Eq.4.66 for the cross-spectral moments.

5.5 Non-Interaction Results

5.5.1 Introduction

Following the methods developed in Chapter 4, the SDOF/MDOF system is reanalyzed without accounting for interaction. The frequency response function and modal decomposition approaches are used and closed form results are obtained which are simpler than the corresponding expressions in the preceding sections.

5.5.2 Frequency Response Function Approach

The frequency response function for the response quantity $y(t)$ is given by the dual form of Eqs.4.72a-c

$$H^{(\infty)}(\omega) \approx \frac{G_i \prod g}{d^{(\infty)}(\omega)} \left[\sum_j \frac{q_{r-j} m_j r_j}{g G_j} - \sum_j \frac{q m_j r}{g} - \frac{q_{r-j} m_j r_{n-j}}{G_j} \right] \tag{22a}$$

$$= \sum_j \frac{q_{r-j} m_j r_j}{g G_j} - \sum_j \frac{q m_j r}{g} - \frac{q_{r-j} m_j r_{n-j}}{G_j}$$

where

$$d^{(\infty)}(\omega) = G_i(\omega) \prod g(\omega) \tag{22b}$$

As before, the above expression for $H_i(\omega)$ can be compared with that in Eq.6a which included interaction; the relationship between the two results is given by

$$\lim_{m_j \to 0} H_i(\omega) = H^{(\infty)}(\omega) \tag{23}$$

This indicates that the results previously obtained in this chapter can be converted to non-interaction results by taking the limit $m_j \to 0$.

For the example system in Fig.5.1, a comparison between the transfer function $T_{ii}(\omega) = |H_i(\omega)|^2$ for interaction and non-interaction analysis is shown in Fig.5.8 for various values of the secondary subsystem mass. As in Chapter 4, the differences are most notable for larger values of m_j and for ω near the tuned mode; for other values of ω, the transfer function is insensitive to interaction. A similar comparison is also made for the spectral moments of the system in Fig.5.9 with varying values for the mass and frequency of the secondary subsystem. As expected, the differences between λ_i and $\lambda_i^{(\infty)}$ are greatest at tuning and diminish at detuning.

5.5.3 Modal Decomposition Method

5.5.3.1 Introduction

Following the analysis in Section 4.5.3, closed form expressions are derived for the mode

shapes, frequencies and the factors a_i and c_i from the modal decomposition method. All of the results are obtained by duality.

5.5.3.2 Closed Form Expressions for the Mode Shapes

The frequencies and mode shapes associated with the secondary subsystem are given by the dual forms of Eqs.4.75 and 76:

$$\omega_i' = \omega_i' (\sqrt{1-\xi_i'^2} + i\xi_i') \qquad i = 1, \ldots, n \tag{24a}$$

$$\boldsymbol{\phi}_i' = \left[0 \cdots 0 - \frac{f_1(\omega_i')}{f_1(\omega_i')} 0 \cdots 0\ 1 \right]^t$$

$$\approx \left[0 \cdots 0 \frac{2(\beta_1 + i\xi_{d,1})\omega_{d,1}^2}{\epsilon_1 \zeta_1 \omega_i'^2} 0 \cdots 0\ 1 \right]^t \tag{24b}$$

where the first non-zero term is at the ith coordinate.

Similarly, the corresponding expressions associated with the primary subsystem are given by the dual forms of Eqs.4.78 and 4.79:

$$\omega_{i,s}' = \omega_{i,s} (\sqrt{1-\xi_{i,s}^2} + i\xi_{i,s}) \tag{25a}$$

$$\boldsymbol{\phi}_{i,s}' = \left[-\frac{f_{1,s}(\omega_{i,s}')}{g_{1,s}(\omega_{i,s}')} \cdots -\frac{f_{1,n}(\omega_{i,s}')}{g_{1,n}(\omega_{i,s}')} 1 \right]^t$$

$$\approx \left[\frac{-\zeta_{1,s}\omega_{i,s}'}{2(\beta_{1,s}+i\xi_{d,1,s})\omega_{d,1,s}^2} \cdots \frac{-\zeta_{1,n}\omega_{i,n}'}{2(\beta_{1,n}+i\xi_{d,1,n})\omega_{d,1,n}^2} 1 \right]^t \tag{25b}$$

For detuned modes, these expressions reduce to the results in Section 5.4.1.1. For the singly tuned modes, it can be shown that the above expressions are equivalent to the expressions derived in Section 5.4.1.2 in the limit $m_s \to 0$.

5.5.3.3 Spectral Moments

The key factors a_i and c_i which are used in the modal decomposition method are found simply by applying the duality relationships to Eqs.4.81a-d:

$$a_i \approx 2\omega_{s,i}\mathrm{Im}b_i = \frac{q_i\zeta_{1,i}r_{n+1}\beta_{1,i}\omega_{s,i}^2}{2(\beta_{1,i}^2+\xi_{d,1,i}^2)\omega_{d,1,i}^2} + r_i q_i \tag{26a}$$

$$a_{n+1} \approx 2\omega_{p,1}\mathrm{Im}b_{n+1} = -\sum_{i=1}^{n} \frac{q_i\zeta_{1,i}r_{n+1}\beta_{1,i}\omega_{s,i}^2}{2(\beta_{1,i}^2+\xi_{d,1,i}^2)\omega_{d,1,i}^2} + r_{n+1}q_{n+1} \tag{26b}$$

$$c_i \approx 2\mathrm{Re}b_i = \frac{q_i\zeta_{1,i}r_{n+1}\xi_{d,1,i}\omega_{s,i}^2}{2\omega_{s,i}(\beta_{1,i}^2+\xi_{d,1,i}^2)\omega_{d,1,i}^2} \tag{26c}$$

$$c_{n+1} \approx 2\mathrm{Re}\, b_{n+1} = -\sum_{i=1}^{n} \frac{\omega_{ni}}{\omega_{n1}} c_i \tag{26d}$$

which can be subsequently substituted into Eqs.4.82a,b to obtain the spectral moments λ_n. The moments calculated by the above expressions are compared with exact results for various values of the secondary masses in Fig.5.10. The results are similar to those observed in Fig.5.9.

Table 5.1. Physical Properties of the SDOF/MDOF Example System

Subsystem	Parameter Relationships
Primary	$k_1 = (1.02)^2 m_1$ (radians/sec)^2
Secondary	k_2, k_3 (variable) $m_2 = \epsilon m_1$ (ϵ variable)

Table 5.2. Modal Properties of the Fixed Base Subsystems

Subsystem	Modal DOF	Frequency (rad/s)	Damping Ratio
Primary 1	1	1.02	0.02
Secondary	2	ω_{s1}	0.03
	3	1.0	0.01

Table 5.3 Frequencies for Example System (ϵ_{11}=0.01)

ω_{s1} (rad/sec)	Mode	Exact Frequency		Computed Frequency		Error
		Real Part	Imag. Part	Real Part	Imag. Part	%
0.70	1	0.698	0.020	0.700	0.021	0.3
	2	0.991	0.011	0.990	0.012	0.1
	3	1.030	0.018	1.029	0.017	0.1
1.00	1	0.992	0.016	0.990	0.018	0.3
	2	0.992	0.022	0.994	0.020	0.3
	3	1.035	0.020	1.033	0.021	0.1

Table 5.4 Mode Shapes of Example System (ζ_{s1}=0.01, ω_{s1}=1.0)

Mode	DOF	Exact Mode Shape		Computed Mode Shape		Error
		Real Part	Imag. Part	Real Part	Imag. Part	%
1	1	0.006	0.000	0.003	0.000	0.3
	2	1.000	0.000	1.000	0.000	0.0
	3	0.003	0.000	0.000	0.000	0.3
2	1	0.050	-0.012	0.054	-0.014	0.5
	2	-0.034	0.006	0.005	0.001	3.2
	3	1.000	0.000	1.000	0.000	0.0
3	1	-0.186	-0.048	-0.172	-0.045	0.6
	2	0.197	0.031	0.017	0.004	10.3
	3	1.000	0.000	1.000	0.000	0.0

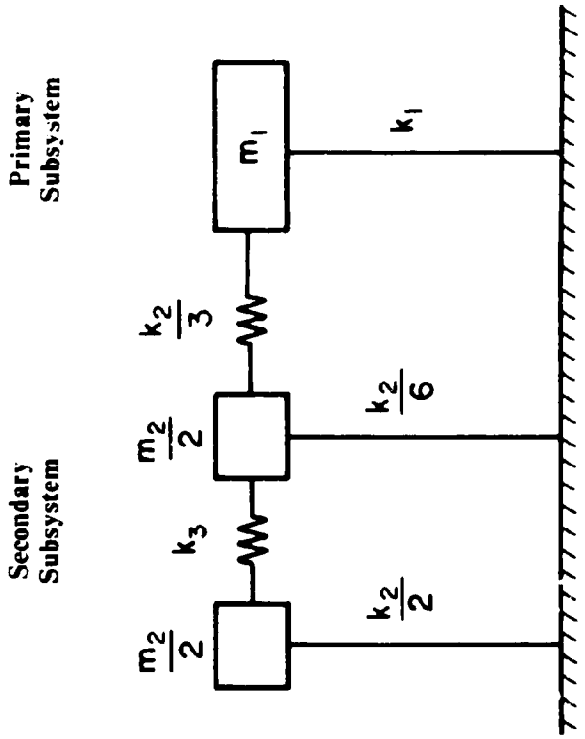

Figure 5.1. Example SDOF/MDOF System

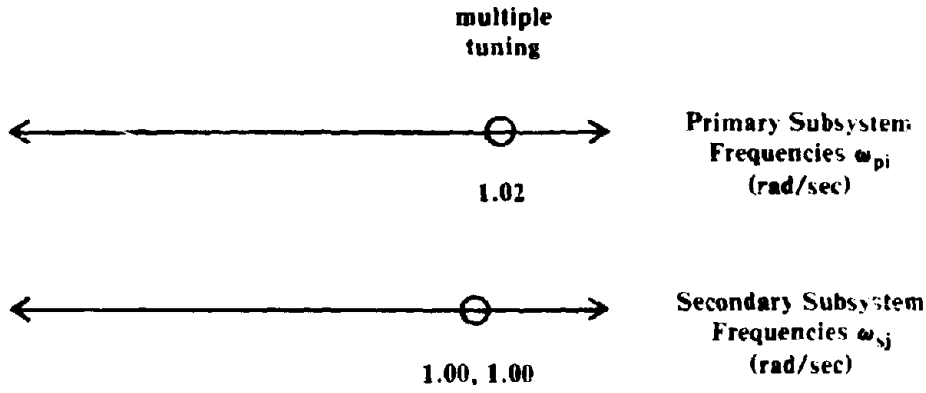

Multiply Tuned System, ω_{s1}=1.0 rad/sec

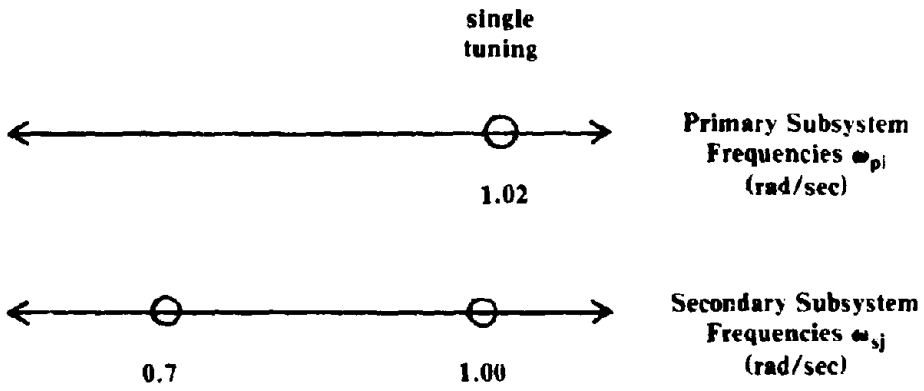

Singly Tuned System, ω_{s1}=0.7 rad/sec

Fig.5.2. Distribution of Subsystem Free Vibration Frequencies

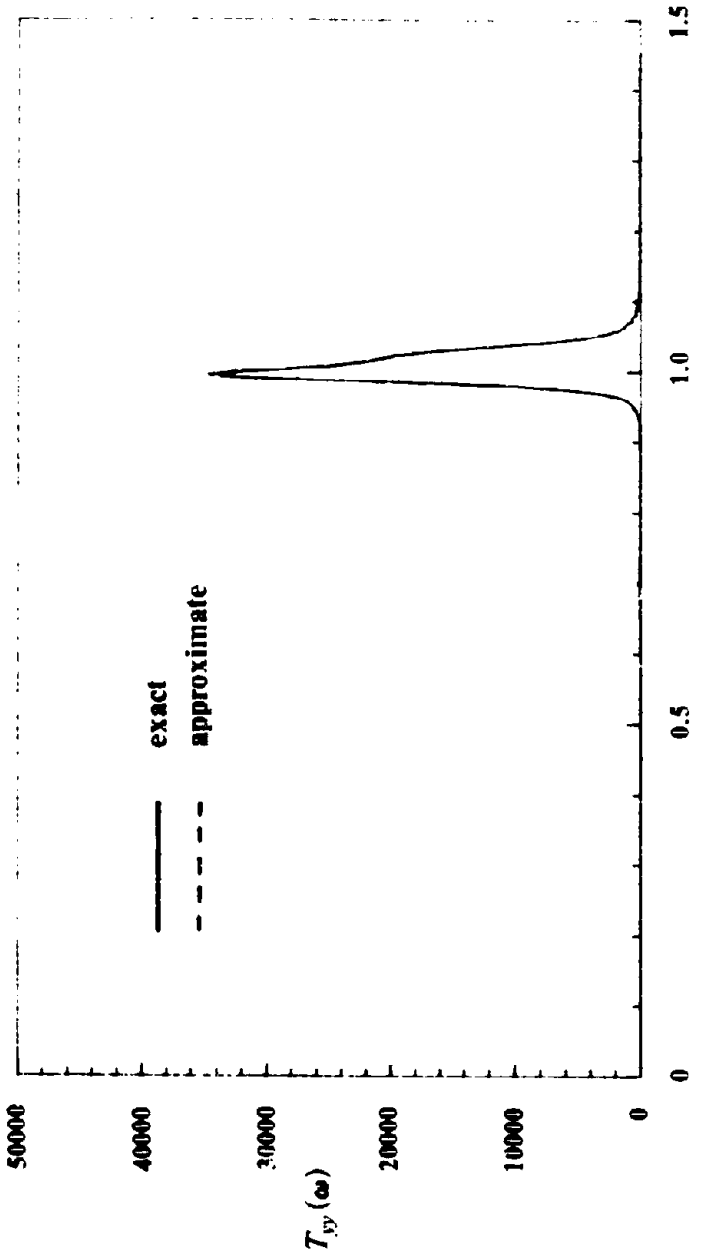

Fig.5.3a. Transfer Function $T_{yy}(\omega)$: Singly Tuned System
ω_{n1}=0.7 rad/sec, ϵ_{11}=0.01

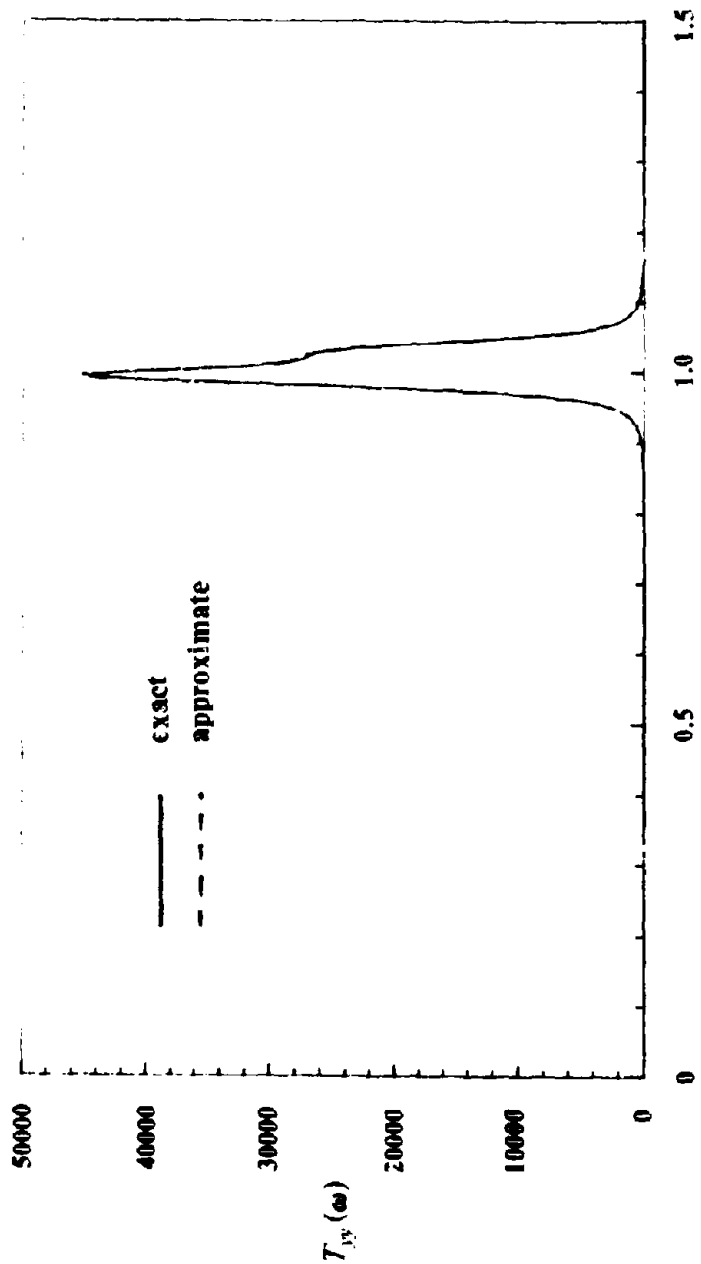

Fig.5.3b. Transfer Function $T_{yy}(\omega)$: Multiply Tuned System
ω_{n1}=1.0 rad/sec. ϵ_{11}=0.01

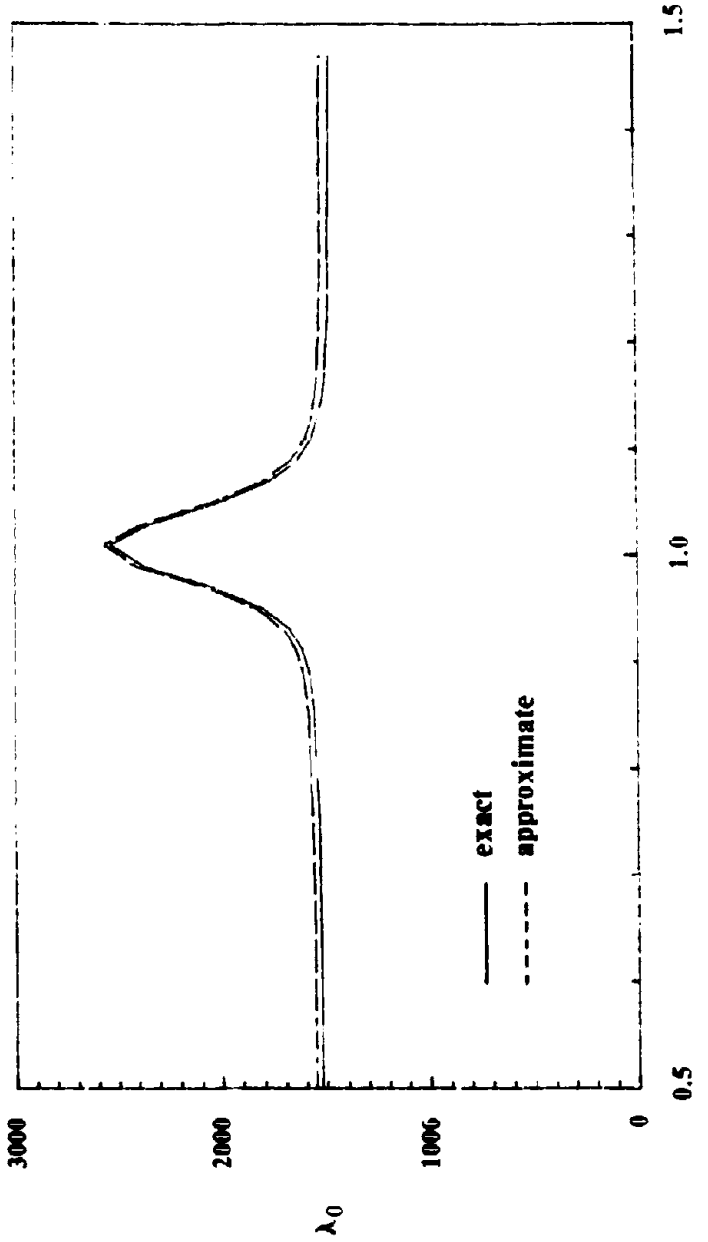

Fig5.4a. Spectral Moment λ_0 derived from $H_1(\omega)$, ϵ_{11}=0.01

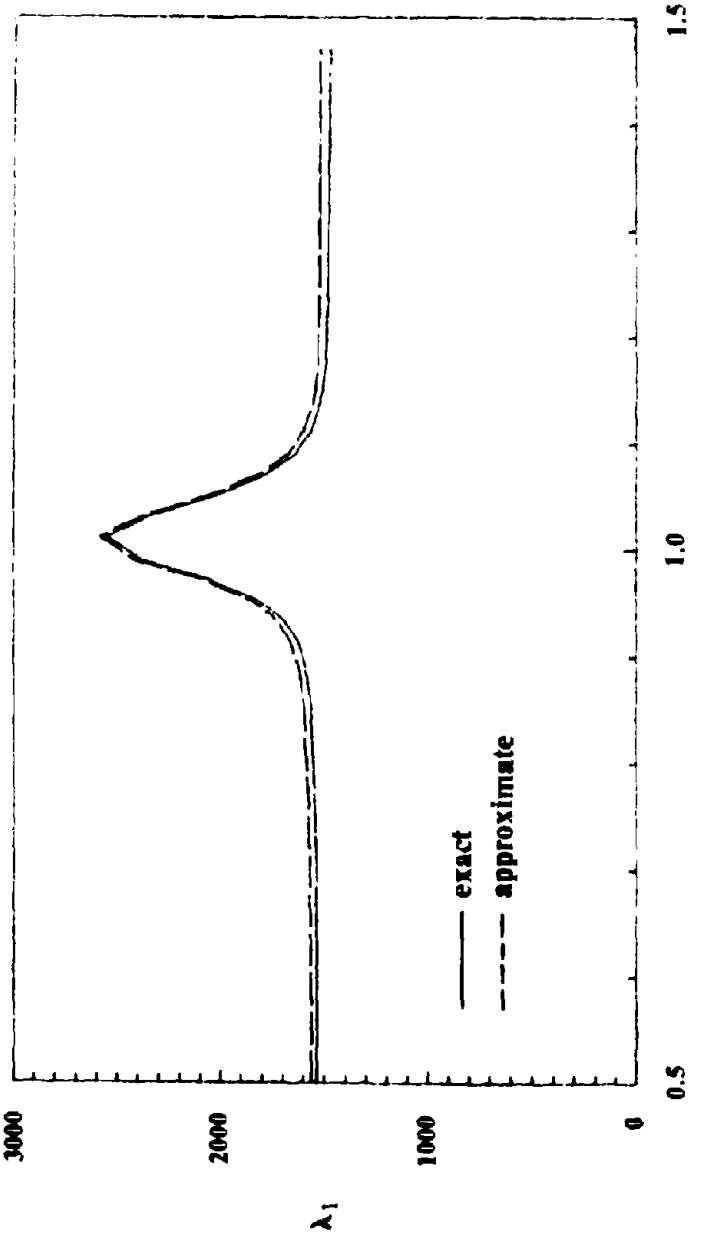

Fig5.4b. Spectral Moment λ_1 derived from $H_1(\omega)$, ϵ_{11}=0.01

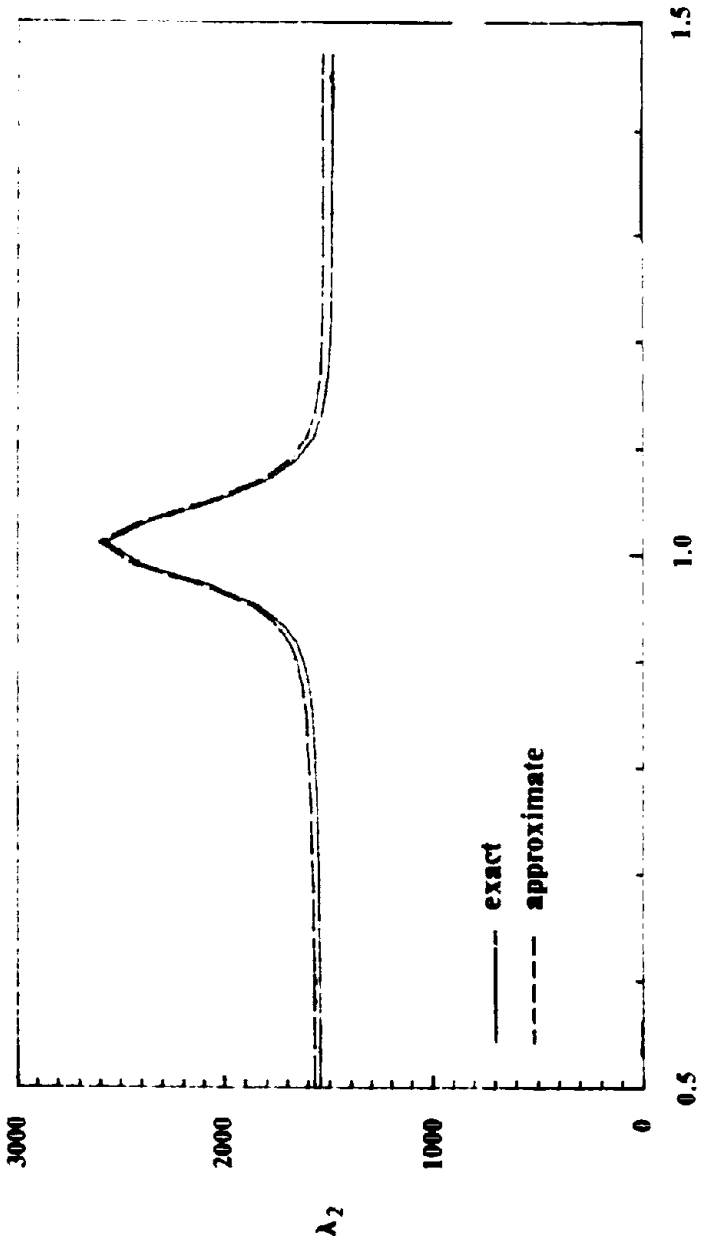

Fig5.4c. Spectral Moment λ_2 derived from $H_1(\omega)$, ϵ_{11}=0.01

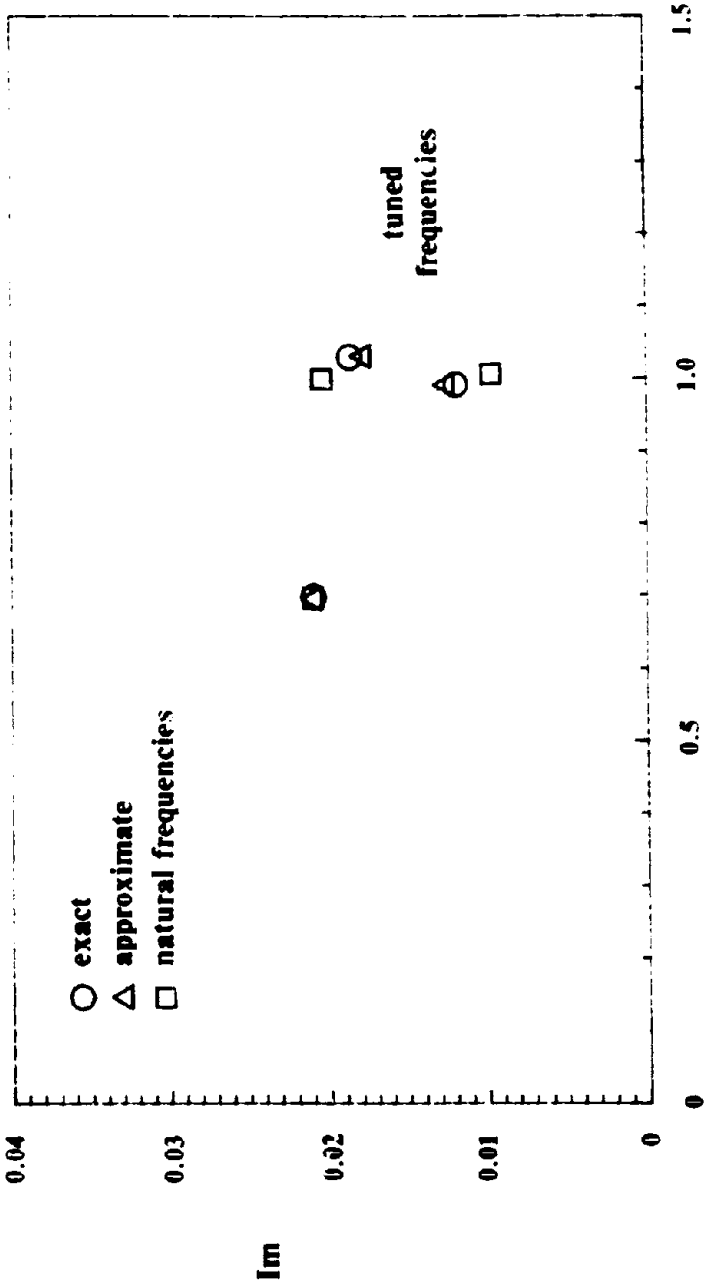

Fig.5.5a. Complex Frequencies: Singly Tuned System
ω_{n1}=0.7 rad/sec, ϵ_{11}=0.01

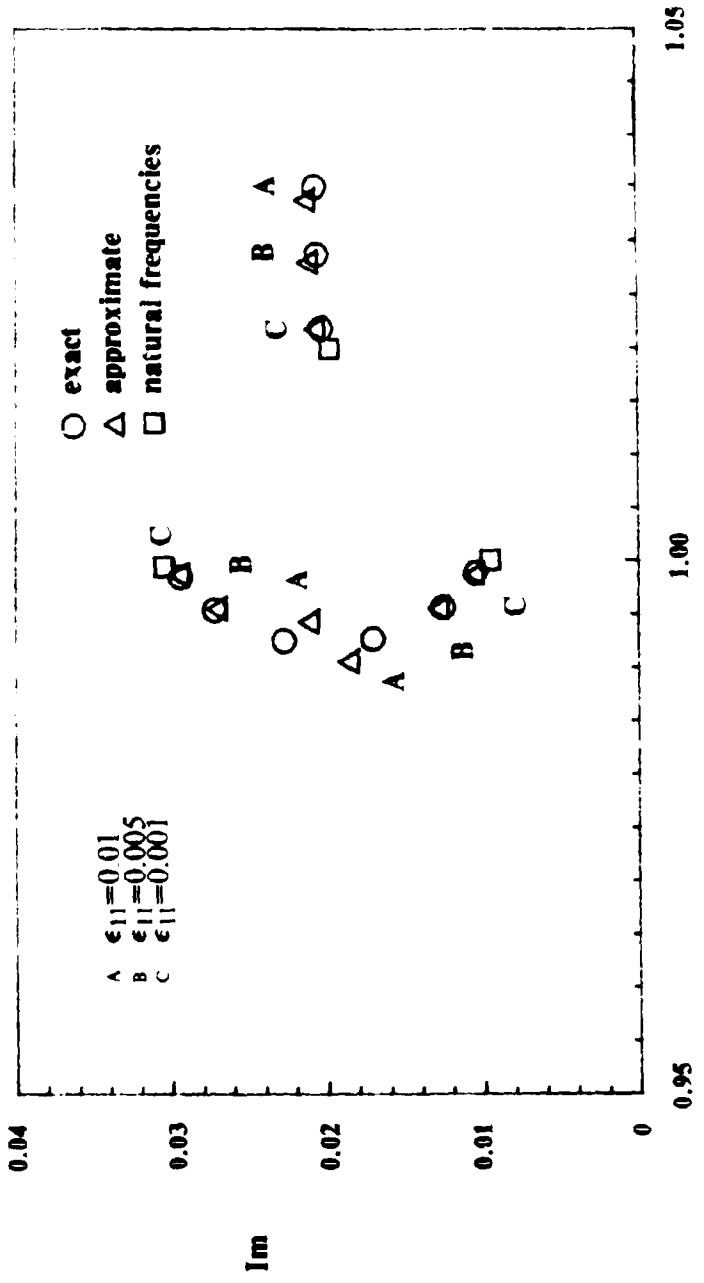

Fig.5.5b. Complex Frequencies: Multiply Tuned System
ω_{s1}=1.0 rad/sec, ϵ_{11}=0.01, 0.005, 0.001

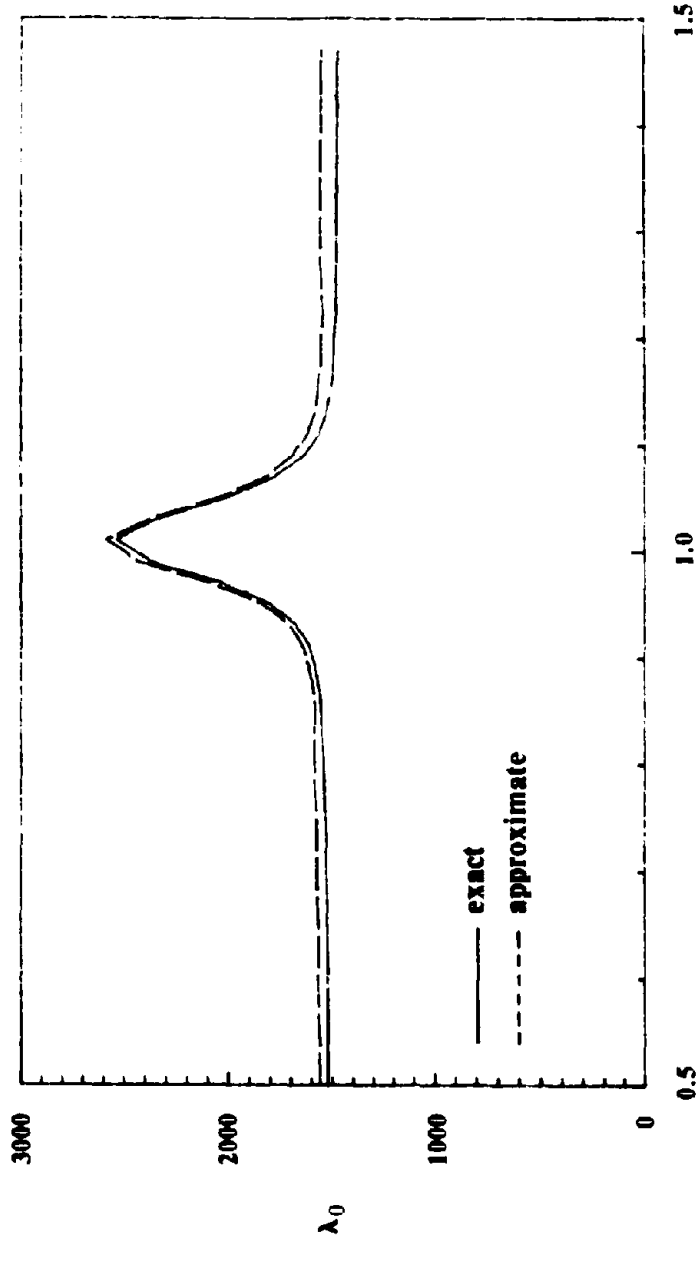

Fig5.6a. Spectral Moment λ_0, ϵ_{11}=0.01

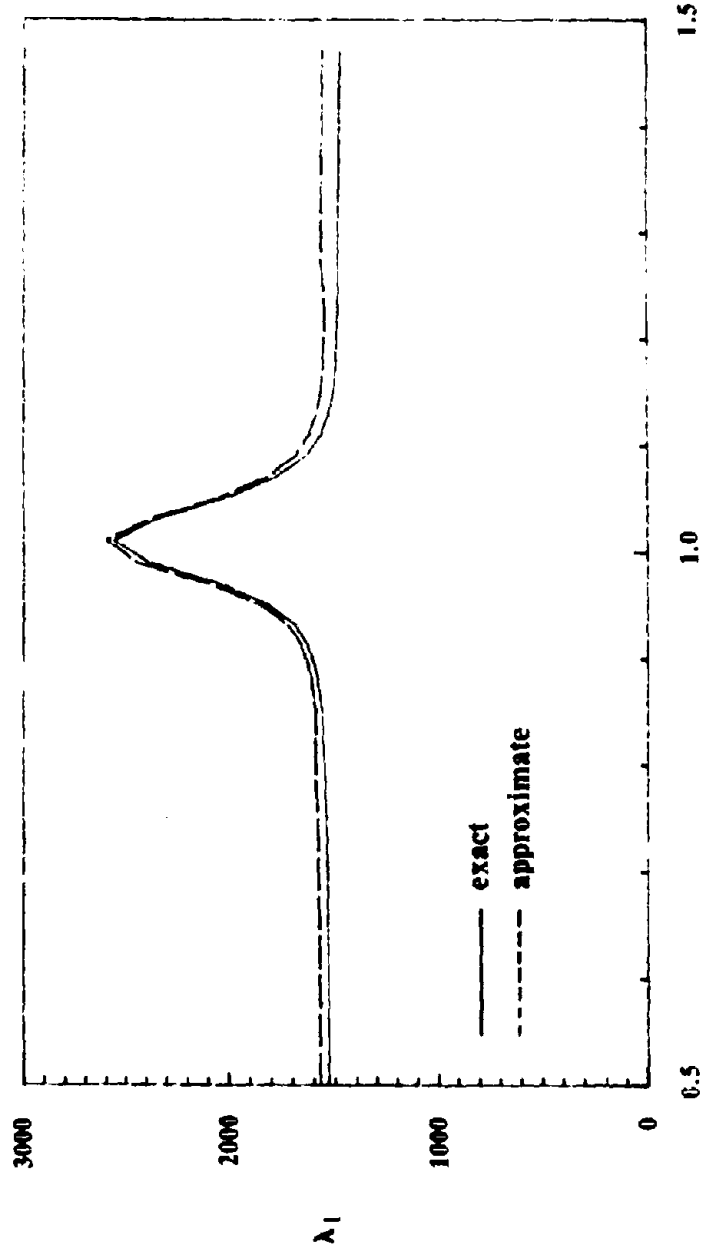

Fig5.6b. Spectral Moment λ_1, ϵ_{11}=0.01

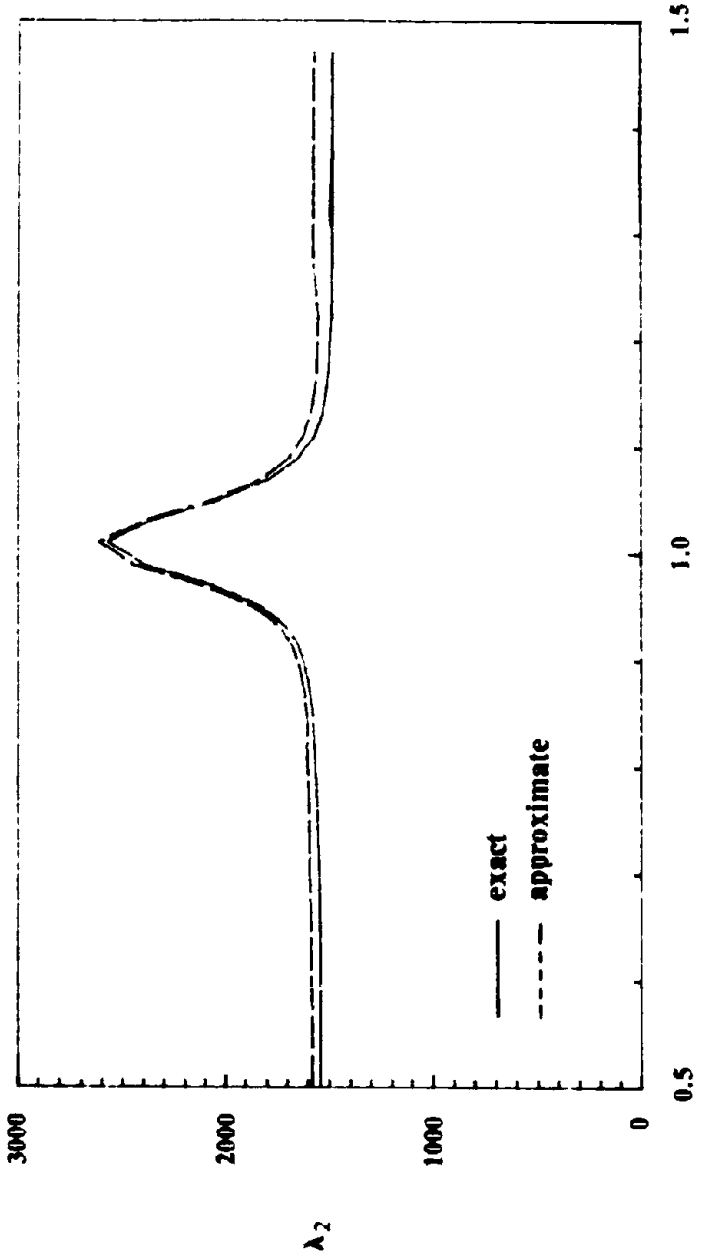

Fig5.6c. Spectral Moment λ_2, ϵ_{11}=0.01

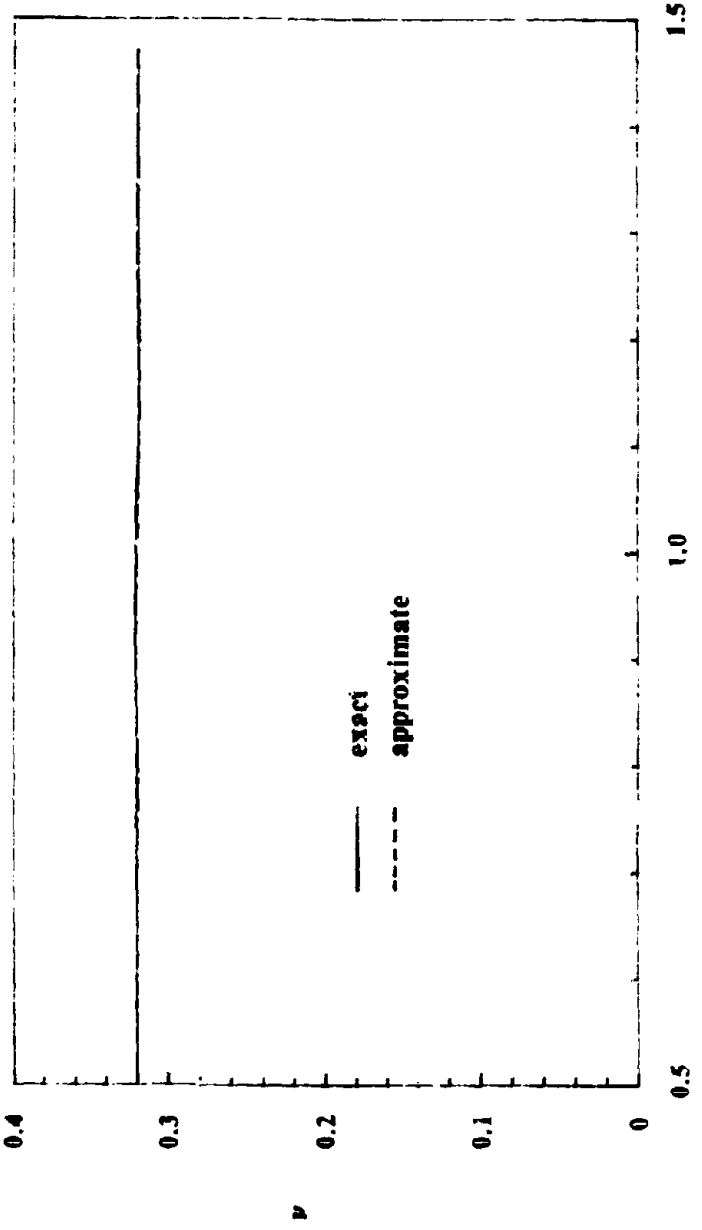

Fig5.7a. Mean Zero-Crossing Rate ν, ϵ_{11}=0.01

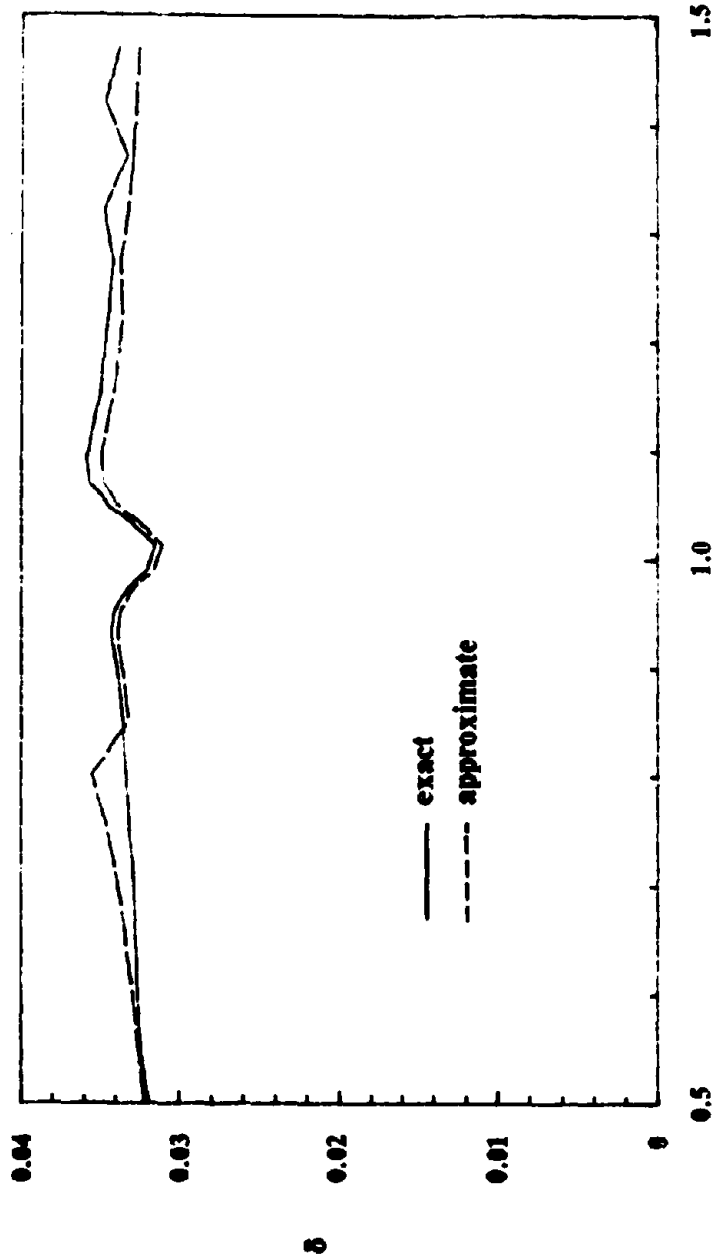

Fig5.7b. Shape Factor δ, ϵ_{11}=0.01

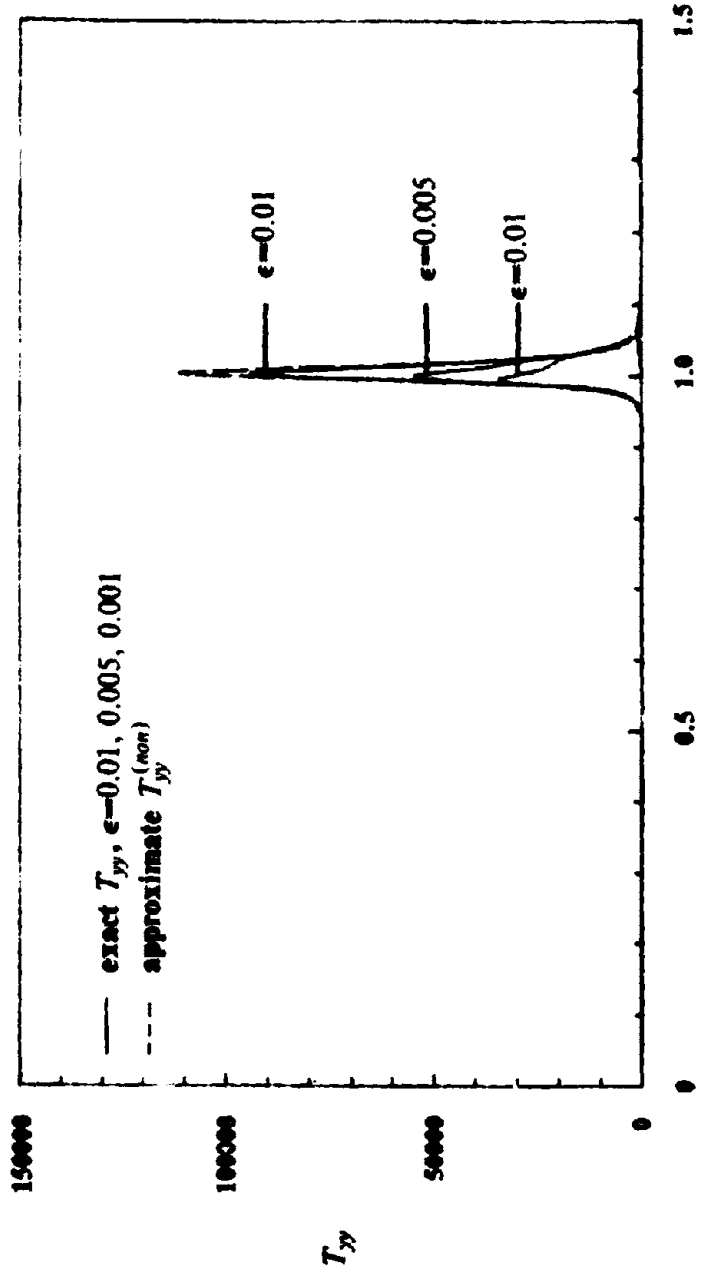

Fig5.8. Transfer Function $T_{yy}^{(non)}(\omega)$ without Interaction

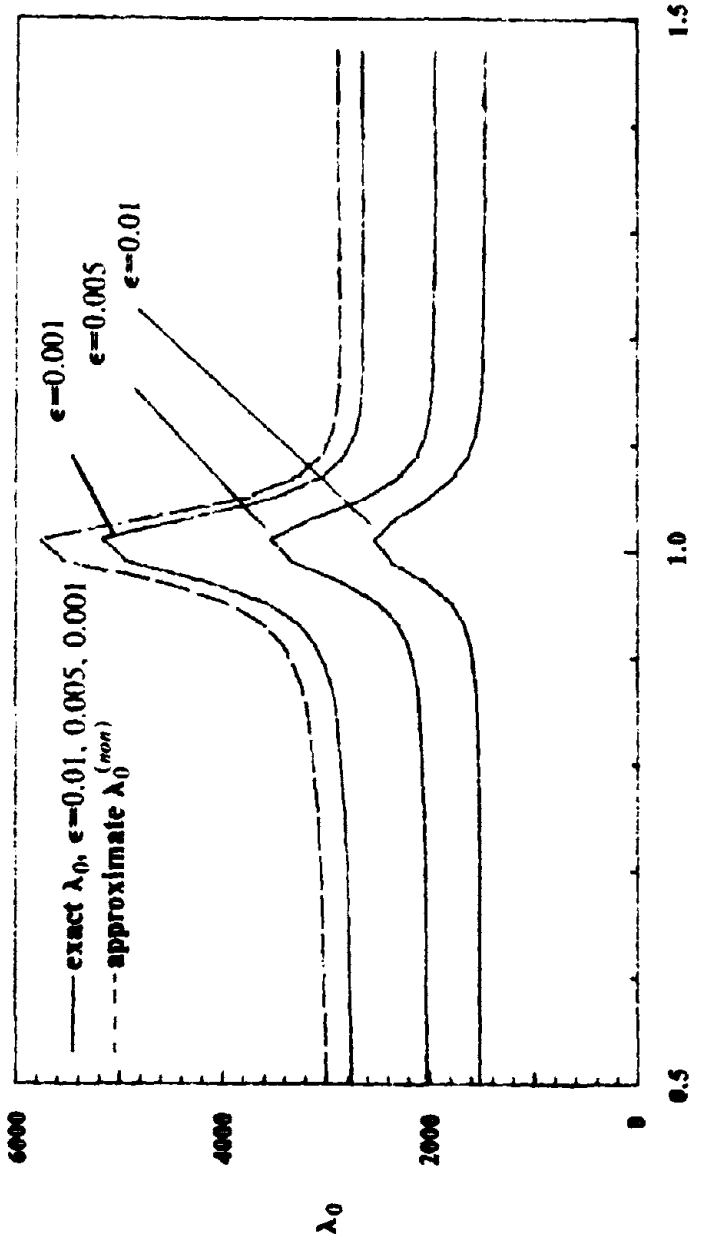

Fig5.9. Spectral Moment $\lambda_0^{(non)}$ without Interaction Calculated from $H_s^{(min)}(\omega)$

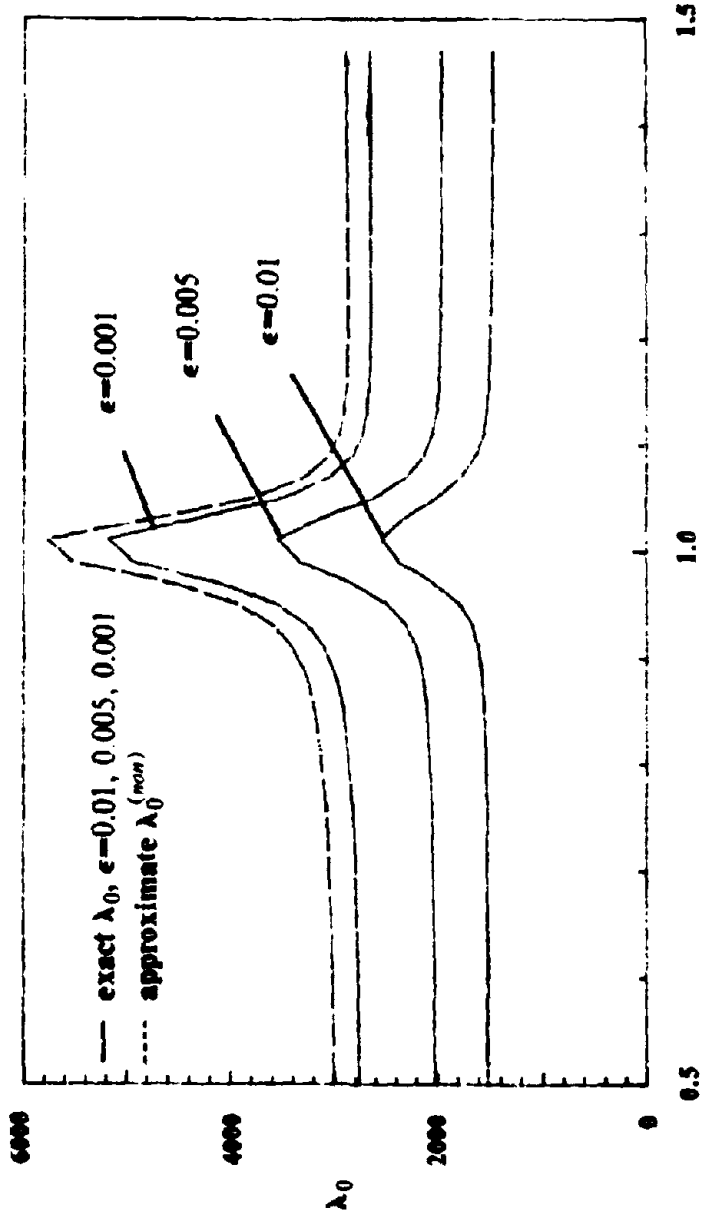

Fig5.10. Spectral Moment $\lambda_0^{(non)}$ without Interaction Calculated from Modal Combination

CHAPTER 6

ANALYSIS OF MULTI-DEGREE-OF-FREEDOM SECONDARY SYSTEMS ATTACHED TO MULTI-DEGREE-OF-FREEDOM PRIMARY SYSTEMS

6.1 Introduction

In this chapter, general PS systems consisting of an MDOF primary subsystem supporting an MDOF secondary subsystem in an arbitrary configuration are studied. Figure 6.1 provides a simple example of such a system. It will be shown that the expressions derived for MDOF/MDOF systems are combinations of the corresponding expressions for MDOF/SDOF and SDOF/MDOF systems analyzed in chapters 4 and 5, respectively.

The steps of the analysis will follow the same methodology used in chapter 4. Most of the results are new; previous research has not accounted for all of the dynamic properties for this general system, as was discussed in detail in the Introduction.

6.2 Definitions

6.2.1 Parameters

The matrices describing the MDOF/MDOF system are a generalization of those developed for the MDOF/SDOF system in Chapter 4. For the individual fixed base subsystems, the primary matrices $\mathbf{K}_{pp}$, $\mathbf{C}_{pp}$, and $\mathbf{M}_{pp}$ remain as before and the secondary matrices $\mathbf{M}_{ss}$, $\mathbf{C}_{ss}$, and $\mathbf{K}_{ss}$ are of order $M \times M$, where M is the number of degrees of freedom of the secondary subsystem.

The displacements of the combined system are defined by the $N+M$ vector

$$\mathbf{x}_0 = [x_1 \ \cdots \ x_N \ x_{N+1} \ \cdots \ x_{N+M}]^T \tag{1}$$

and the $N+M \times N+M$ mass, damping, and stiffness matrices $\mathbf{M}_{0ss}$, $\mathbf{C}_{0ss}$, and $\mathbf{K}_{0ss}$, respectively, are given by Eq.4.7. As noted in Chapter 4, these matrices are not precisely equal to the true

system matrices, however the approximation is consistent with the analysis that will be performed.

From these matrices, the equations of motion for the MDOF/MDOF system are given by Eq.4.8

$$\mathbf{M}_{ss}\ddot{\mathbf{x}}_0 + \mathbf{C}_{ss}\dot{\mathbf{x}}_0 + \mathbf{K}_{ss}\mathbf{x}_0 = -\mathbf{M}_{ss}\mathbf{r}_0\ddot{x}_g(t) \tag{2}$$

This equation can be transformed to modal coordinates by means of the $N+M\times n+m$ transformation matrix given by Eq.4.11a

$$\Phi = \begin{bmatrix} \Phi_p & 0 \\ 0 & \Phi_s \end{bmatrix} \tag{3}$$

where Φ_s is an $M\times m$ matrix consisting of the m mode shapes of interest for the fixed base secondary subsystem. The modal coordinate vector z is obtained through the relation $\Phi\mathbf{z}=\mathbf{x}_0$ and is given by

$$\mathbf{z}=[z_{p1} \ \ldots\ z_{pn}\ z_{s1} \ldots\ z_{sm}] \tag{4}$$

The transformed mass, damping, and stiffness matrices are generalizations of Eqs.4.12a-d:

$$\mathbf{M} = \mathrm{diag}\left[m_{p1} \ \cdots\ m_{pn}\ m_{s1} \ \cdots\ m_{sm}\right] \tag{5a}$$

$$\mathbf{C} = \begin{vmatrix} 2m_{p1}\omega_{p1}\xi_{p1} & & & & & (\mathrm{sym}) \\ \cdots & \cdots & & & & \\ 0 & \cdots & 2m_{pn}\omega_{pn}\xi_{pn} & & & \\ c_{11} & \cdots & c_{n1} & 2m_{s1}\omega_{s1}\xi_{s1} & \cdots & \\ \cdots & \cdots & \cdots & \cdots & \cdots & \\ c_{1m} & \cdots & c_{nm} & 0 & \cdots & 2m_{sm}\omega_{sm}\xi_{sm} \end{vmatrix} \tag{5b}$$

$$\mathbf{K} = \begin{vmatrix} m_{p1}\omega_{p1}^2 & & & & & (\mathrm{sym}) \\ \cdots & \cdots & & & & \\ 0 & \cdots & m_{pn}\omega_{pn}^2 & & & \\ k_{11} & \cdots & k_{n1} & m_{s1}\omega_{s1}^2 & & \\ \cdots & \cdots & \cdots & \cdots & \cdots & \\ k_{1m} & \cdots & k_{nm} & 0 & \cdots & m_{sm}\omega_{sm}^2 \end{vmatrix} \tag{5c}$$

where

$$c_{ij} = \boldsymbol{\phi}_{pi}^T\mathbf{C}_{ps}\boldsymbol{\phi}_{sj} \qquad k_{ij} = \boldsymbol{\phi}_{pi}^T\mathbf{K}_{ps}\boldsymbol{\phi}_{sj} \tag{5d}$$

The equations of motion in terms of the modal coordinates are given by Eq.4.13

$$\mathbf{M}\ddot{\mathbf{z}} + \mathbf{C}\dot{\mathbf{z}} + \mathbf{K}\mathbf{z} = -\mathbf{M}\mathbf{r}\ddot{x}_g(t) \tag{6}$$

where r is the vector of modal participation factors given by Eq.4.14. The form of the matrices

M, **C**, and **K** are more complicated than that for MDOF/SDOF systems, however, this does not pose any problems in the succeeding analysis.

To facilitate the analysis of the system, the terms k_{ij} and c_{ij} are rewritten in a form similar to Eq.4.17

$$k_{ij} = -m_{si}\omega_{sj}^2\zeta_{ij} \quad c_{ij} \approx -2m_{si}\omega_{si}\xi_{si}\zeta_{ij} \tag{7}$$

where ζ_{ij} is defined to be the ratio

$$\zeta_{ij} = -\frac{k_{ij}}{m_{si}\omega_{sj}^2} \tag{8}$$

The interpretation of ζ_{ij} is a generalization of that given in Section 4.2.1: It is the displacement of the jth mode of the secondary subsystem caused by a static unit displacement of the ith mode of the primary subsystem.

6.2.2 Notation

The classification of the modes of the MDOF/MDOF system is a generalization of the classification presented in Chapter 4. The definition of tuning remains as before: A primary mode i and a secondary mode j are considered to be tuned if

$$\left|\frac{\omega_{pi}-\omega_{sj}}{\omega_{avj}}\right|^2 < \frac{\xi_{avj}^2}{e}\left|4 + \frac{\gamma_{ij}}{\xi_{si}\xi_{pi}}\right| \tag{9}$$

A primary mode which is not tuned to any of the secondary modes is defined to be detuned; the same definition applies to secondary modes.

There are two sets of detuned modes, one for each subsystem:

$$I_{pd} = \left\{ \begin{array}{l} \text{set of indecies } i \text{ corresponding to} \\ \text{detuned primary subsystem modes} \end{array} \right\} \tag{10a}$$

$$I_{sd} = \left\{ \begin{array}{l} \text{set of indecies } j \text{ corresponding to} \\ \text{detuned secondary subsystem modes} \end{array} \right\} \tag{10b}$$

Tuned modes fall into two classifications, as discussed in Section 4.2.2: singly tuned modes and multiply tuned modes. The singly tuned modes form a set of ordered pairs

$$I_{st} = \left\{ (i,j) : \text{primary mode } i \text{ is singly tuned to secondary mode } j \right\} \tag{11}$$

Multiply tuned modes form a collection of sets. Assume there are a total of K clusters of

multiply tuned modes. Then for each $k \leqslant K$

$$I_{p2}^{(k)} = \left\{ \text{primary modes in the } k\text{-th multiply tuned cluster} \right\} \tag{12a}$$

$$I_{s2}^{(k)} = \left\{ \text{secondary modes in the } k\text{-th multiply tuned cluster} \right\} \tag{12b}$$

As an example, if the first k primary modes are all tuned to the first l secondary modes, then

$$I_{p2}^{(1)} = \{ 1, \ldots, k \} \quad I_{s2}^{(1)} = [1, \ldots, l] \tag{13}$$

It should be noted that each primary or secondary mode is included in one and only one of the above sets.

6.2.3 Example System

To illustrate the major characteristics of MDOF/MDOF systems and check the accuracy of the formulations derived in this chapter, the example system shown in Fig.6.1 is used. The primary subsystem is identical to the one used in the example system for MDOF/SDOF systems and the secondary subsystem is similar to that used in the example system for SDOF/MDOF systems.

The dynamic properties of the subsystems are described in Tables 1 and 2 and are chosen so that the combined system would exhibit important characteristics found in general MDOF/MDOF systems. For instance, the frequency of the equipment is a variable parameter, which allows for an investigation of tuning. For $\omega_s = .38$ rad/sec, the system is singly tuned as shown in Fig.6.2a, and for $\omega_s = 1.0$ rad/sec, the system becomes multiply tuned as shown in Fig.6.2b. The mass ratio, ϵ, is also chosen to be a variable parameter, as before. Finally, the damping ratio of the equipment is unequal to the damping ratios of the primary subsystem, thus the combined system is, in general, non-proportionally damped.

The response quantity that will be investigated is the relative displacement between the upper mass of primary subsystem 2 and the adjacent mass of the secondary subsystem.

6.3 Frequency Response Function Approach

6.3.1 The Complex Frequency Response Matrix

The complex frequency response matrix for the MDOF/MDOF system is a generalization of Eq.4.28a and Eq.5.3a

$$\mathbf{H}(\omega) = \begin{vmatrix} G_1(\omega) & & & & (\text{sym}) & -1 \\ \cdots & \cdots & & & & \\ 0 & \cdots & G_n(\omega) & & & \\ f_{11}(\omega) & \cdots & f_{n1}(\omega) & g_1(\omega) & & \\ \cdots & \cdots & \cdots & \cdots & \cdots & \\ f_{1m}(\omega) & \cdots & f_{nm}(\omega) & 0 & \cdots & g_m(\omega) \end{vmatrix} \tag{14a}$$

The polynomials $G_i(\omega)$ and $g_j(\omega)$ are given by Eqs.4.28c and 5.3b, respectively, and

$$f_{ij}(\omega) \approx -\zeta_{ij} m_{ij}(\omega_{ij}^2 + 2i\omega_{ij}\xi_{ij}\omega) \tag{14b}$$

for $i=1, \cdots, n$ and $j=1, \cdots, m$.

Unlike the previous chapters, the above inverse has no closed form solution. To find the complex frequency response function $H_i(\omega)$ for a response quantity $y(t)=\mathbf{q}^t\mathbf{z}(t)$, the equation Eq.4.32 must be solved numerically, which requires the reduction of an $n+m$ order system of equations for each value of the frequency ω. This is considerably more difficult than the evaluation of a rational polynomial, which is the computation required for $H_i(\omega)$ in the MDOF/SDOF and SDOF/MDOF systems. The modal decomposition method to be presented in the succeeding sections does not present such numerical difficulties and is the recommended method for analyzing MDOF/MDOF systems.

6.4 Modal Decomposition Approrch

6.4.1 Mode Shapes and Frequencies

The low-order approximations for the mode shapes and frequencies will be derived for the MDOF/MDOF system. The approach is similar to that of Section 4.4.1. The resulting expressions are a combination of those derived for MDOF/SDOF and SDOF/MDOF systems in Sections 4.4.1 and 5.4.1, respectively. These expressions can be evaluated numerically and used in the modal decomposition analysis to provide accurate measures of the response.

As before, approximate algebraic expressions for the spectral moments for response to white-noise input are obtained to investigate further the dynamic behavior of the system.

6.4.1.1 Detuned Modes

Assume that primary mode 1 is the detuned mode to be analyzed. Following the procedure in 4.4.1.1, the first-order solutions for the frequency and mode shape can be found

$$\omega_1^{(1)} = \omega_{p1}(\sqrt{1-\xi_{p1}^2} + i\xi_{p1}) \tag{15a}$$

$$\phi_1^{(1)} = \left[1 \sum_{j=1}^{m} \frac{f_{1j}f_{2j}}{g_j G_2} \cdots \sum_{j=1}^{m} \frac{f_{1j}f_{nj}}{g_j G_n} - \frac{f_{11}}{g_1} \cdots - \frac{f_{1m}}{g_m} \right]^T \tag{15b}$$

where the polynomials are evaluated at $\omega = \omega_1^{(0)}$. Note that the above expression for the mode shape is a combination of the results Eqs.4.41 and 5.9a. The low-order approximations are

$$\omega_1 = \omega_{p1}(1 + i\xi_{p1}) \tag{16a}$$

$$\phi_1 \approx \left[1\ 0 \cdots 0 \frac{\zeta_{s1}\omega_{s1}^2}{\omega_{s1}^2-\omega_{p1}^2} \cdots \frac{\zeta_{1m}\omega_{sm}^2}{\omega_{sm}^2-\omega_{p1}^2} \right]^T \tag{16b}$$

Likewise, if secondary mode 1 is detuned, the first-order approximations for the mode shape and frequency are

$$\omega_{n+1}^{(1)} = \omega_{s1}(\sqrt{1-\xi_{s1}^2} + i\xi_{s1}) \tag{17a}$$

$$\phi_{n+1}^{(1)} = \left[-\frac{f_{11}}{G_1} \cdots - \frac{f_{n1}}{G_n} 1 \sum_{i=1}^{n} \frac{f_{i1}f_{i2}}{g_2 G_i} \cdots \sum_{i=1}^{n} \frac{f_{i1}f_{im}}{g_m G_i} \right]^T \tag{17b}$$

where the polynomials are evaluated at $\omega = \omega_{n+1}^{(0)}$. In this case, the above expression for the mode shape is a combination of Eqs.4.44 and 5.7b. The low-order approximation is

$$\phi_{n+1} = \left[\zeta_{11}\epsilon_{11}\frac{\omega_{s1}^2}{\omega_{p1}^2-\omega_{s1}^2} \cdots \zeta_{n1}\epsilon_{n1}\frac{\omega_{s1}^2}{\omega_{pn}^2-\omega_{s1}^2} 1\ 0 \cdots 0 \right]^T \tag{18a}$$

$$\omega_{n+1} = \omega_{s1}(1 + i\xi_{s1}) \tag{18b}$$

6.4.1.2 Singly Tuned Modes

Assume that primary subsystem mode 1 and secondary subsystem mode 1 are tuned to each other. Applying the analysis of section 4.4.1.3, the resulting first-order approximations for the frequencies are given by the same expressions as in Eqs.4.46a,b:

$$\omega_1^{(0)} = \omega_{a,11}\left\{ 1 + i\xi_{a,11} \pm \frac{1}{2}[\gamma_{11}+(i\xi_{d,11}+\beta_{11})^2]^{\frac{1}{2}} \right\} \tag{19}$$

The mode shapes $\phi_r^{(1)}$ are

$$\phi_r^{(1)} = \left[\alpha_r^{(0)} - \frac{f_{r1}}{G_1} \quad \cdots \quad -\frac{f_{rl}}{G_l} \; 1 \; -\alpha_r^{(0)} \frac{f_{12}}{g_2} \quad \cdots \quad -\alpha_r^{(0)} \frac{f_{1m}}{g_m} \right]^t \tag{20a}$$

where the polynomials above are evaluated at $\omega=\omega_r^{(0)}$ and $\alpha_r^{(0)}$ are given by Eqs.4.46e,f

$$\alpha_r^{(0)} = \frac{1}{\zeta_{11}} \left\{ -\beta_{11} + i\xi_{d,11} \pm \frac{1}{2}[\gamma_{11} + (i\xi_{d,11} + \beta_{11})^2]^{\frac{1}{2}} \right\} \tag{20b}$$

The low-order approximations are

$$\phi_r^{(1)} = \left[\alpha_r^{(0)} \frac{\zeta_{21}\epsilon_{21}\omega_{s1}^2}{\omega_{p2}^2 - \omega_{s1}^2} \quad \cdots \quad \frac{\zeta_{nl}\epsilon_{nl}\omega_{s1}^2}{\omega_{pn}^2 - \omega_{s1}^2} \; 1 \; \alpha_r^{(0)} \frac{\zeta_{12}\omega_{s2}^2}{\omega_{s2}^2 - \omega_{p1}^2} \quad \cdots \quad \alpha_r^{(0)} \frac{\zeta_{1m}\omega_{sm}^2}{\omega_{sm}^2 - \omega_{p1}^2} \right]^t \tag{21}$$

Note that $\phi_r^{(1)}$ is a combination of Eqs.4.48b and 5.13b.

6.4.1.3 Multiply Tuned Modes

Assume the first k primary subsystem modes are tuned to the first l secondary subsystem modes, i.e., $I_{ps}^{(0)}$ and $I_{sp}^{(0)}$ are given by Eqs.13. The matrix $\Gamma(\omega) = \mathbf{H}^{-1}(\omega)$ can be partitioned into submatrices

$$\Gamma(\omega) = \begin{bmatrix} \Gamma_{pt} & 0 & \Gamma_{pt}^t & \Gamma_{pd}^t \\ 0 & \Gamma_{pd} & \Gamma_{td}^t & \Gamma_{dd}^t \\ \Gamma_{pt} & \Gamma_{td} & \Gamma_{st} & 0 \\ \Gamma_{pd} & \Gamma_{dd} & 0 & \Gamma_{sd} \end{bmatrix} \tag{22}$$

where the subscripts p, s, t, d refer to the primary subsystem, secondary subsystem, tuned modes, and detuned modes, respectively,

$$\Gamma_{pt}(\omega) = \text{diag}\{ G_1(\omega) \quad \cdots \quad G_k(\omega) \} \tag{23a}$$

$$\Gamma_{pd}(\omega) = \text{diag}\{ G_{k+1}(\omega) \quad \cdots \quad G_n(\omega) \} \tag{23b}$$

$$\Gamma_{st}(\omega) = \text{diag}\{ g_1(\omega) \quad \cdots \quad g_l(\omega) \} = \tag{23c}$$

$$\Gamma_{sd}(\omega) = \text{diag}\{ g_{l+1}(\omega) \quad \cdots \quad g_m(\omega) \} \tag{23d}$$

where diag $\{ \cdots \}$ denotes diagonal matrices, and Γ_{pt}, Γ_{td}, Γ_{dt}, and Γ_{dd} are full matrices.

Following the analysis in section 4.4.1.4, the initial approximations for the mode shapes are given by

$$\phi_r^{(0)} = \left[\phi_{tp}^{(0)} \; 0 \; \phi_{ts}^{(0)} \; 0 \right]^t \tag{24}$$

where the vectors $\phi_{tp}^{(0)}$ and $\phi_{ts}^{(0)}$ and the initial approximations for the frequencies are obtained

from the $k+l \times k+l$ order eigenvalue problem

$$\begin{bmatrix} \Gamma_{pp}(\omega_i^{(0)}) & \Gamma_{ps}(\omega_i^{(0)})^T \\ \Gamma_{ps}(\omega_i^{(0)}) & \Gamma_{ss}(\omega_i^{(0)}) \end{bmatrix} \begin{bmatrix} \phi_{ip}^{(0)} \\ \phi_{is}^{(0)} \end{bmatrix} = \begin{bmatrix} 0 \\ 0 \end{bmatrix} \tag{25}$$

This problem corresponds to Eq.4.49 and is relatively small compared to the order of the combined system $(n+m \times n+m)$. Referring back to the original matrix $\Gamma(\omega)$, the error is

$$\Gamma(\omega) \begin{bmatrix} \phi_{ip}^{(0)} \\ 0 \\ \phi_{is}^{(0)} \\ 0 \end{bmatrix} = \begin{bmatrix} 0 \\ \Gamma_{sp}^T \phi_{is}^{(0)} \\ 0 \\ \Gamma_{ds} \phi_{ip}^{(0)} \end{bmatrix} = \begin{bmatrix} 0 \\ O(\epsilon) \\ 0 \\ O(\epsilon^2) \end{bmatrix} \tag{26}$$

As before, the above error is reduced by introducing detuned components to the mode shapes. The resulting approximation ϕ_i^* which corresponds to Eqs.4.52a is

$$\phi_i^* = \begin{bmatrix} \phi_{ip}^{(0)} & \phi_{dp}^{(0)} & \phi_{is}^{(0)} & \phi_{ds}^{(0)} \end{bmatrix}^T \tag{27a}$$

where

$$\phi_{dp}^{(0)} = -\Gamma_{pd}^{-1} \Gamma_{sp}^T \phi_{is}^{(0)} \qquad \phi_{ds}^{(0)} = -\Gamma_{sd}^{-1} \Gamma_{ds} \phi_{ip}^{(0)} \tag{27b}$$

Note that Γ_{pd} and Γ_{sd} are diagonal matrices and are easily inverted.

6.4.1.4 Closely Spaced Detuned Modes

In sections 4.4.2.5 and 5.4.2.5 it was noted that the derivation of the mode shapes for closely spaced detuned modes is unnecessary if the quantity of interest is the response of the secondary subsystem. The solutions for the mode shapes derived for widely spaced detuned modes can be used in obtaining results for the system response even if the detuned modes are closely spaced. This method will be applied to MDOF/MDOF systems.

If precise solutions for the detuned modes is required, then considerable amount of computation is required. The analysis of the mode shapes for k very closely spaced detuned primary subsystem modes requires the solution of an $k+m \times k+m$ order eigenvalue problem. Similarly, for l detuned very closely spaced secondary subsystem modes the problem is of order $l+n \times l+n$. Since m and n are large integers, these eigenvalue problems are relatively large.

6.4.1.5 Examples

The complex modal properties of the example system in Fig.6.1 were computed using the formulations developed in this section and were compared with exact results obtained by using a complex eigenvalue solver from the IMSL library. The frequencies are shown in Table 3 and are plotted in Figs.6.3a,b for various values of the equipment frequency ω_{s1}, and the mode shapes for the multiply tuned case (i.e., $\omega_{s1} = 1.00$ rad/sec) are shown in Table 4. The non-classical damping character of the multiply tuned system is apparent in the mode shapes, which have imaginary components. Good agreement between approximate and exact values is found in all cases.

The effect of the equipment mass is illustrated in Fig.6.3b, where the frequencies corresponding to $\epsilon = .01$, .005, and .001 are represented by points A_i, B_i, and C_i, respectively. Mode 1 is not affected by the mass ratio because it is detuned. The frequencies corresponding to the other modes converge to the subsystem natural frequencies as was observed in the study of the 2-DOF system.

6.4.2 Spectral Moments

The spectral moments can be calculated using the preceding expressions for the modal properties and employing the modal decomposition method developed earlier. For the example system in Fig.6.1, such calculations are compared with exact results obtained by integrating the complex frequency response function in Figs.6.4a-c. Also, the mean zero-crossing rate, ν, and the shape factor, δ, were computed and plotted in Figs.6.5a,b. All plots show good comparison between exact and the proposed approximate results.

It was noted in Section 4.4.2 that the mean zero-crossing rate of a tuned PS system was nearly equal to $\nu = \omega_s/\pi$, where ω_s is one of the tuned frequencies. For $\omega_{s1} = .38$ rad/sec, it can be seen that ν approaches this theoretical value in Fig.6.5a (compare with Fig.4.8a for the MDOF/SDOF example study). For higher values of ω_{s1}, the tuned modes with frequencies at $\omega_{s2} = 1.0$ rad/sec are dominant in the response motion, and ν has a nearly constant value of

approximately $1.0/\pi \approx 0.318$ rad/sec (compare with Fig.5.7a for the SDOF/MDOF example study).

The shape factor is relatively large around $\omega_{s1} = .38$ rad/sec. This is due to the fact that the power spectral density function has two peaks, corresponding to the two sets of tuned modes of the system. For other values of ω_{s1}, there is only one peak at $\omega = 1.0$ rad/sec and the response process becomes narrow-banded with a small shape factor (see Fig.6.5b).

As in the previous chapters, general low-order algebraic expressions will be derived for the spectral moments for response to white-noise input. These results can be viewed as a combination of the results in Chapters 4 and 5.

6.4.2.1 Well-Spaced Detuned Modes

The treatment of well-spaced detuned modes is essentially the same as in Sections 4.4.2.1 and 5.4.2.1. Let mode i and mode $n+j$ correspond to detuned primary and secondary subsystem modes, respectively. The effective participation factors are

$$\psi_i = r_i \left[\sum_{j=1}^{m} \frac{q_{n+j}\omega_{sj}^2\zeta_{ij}}{\omega_{sj}^2-\omega_{pi}^2} + q_i \right] \tag{28a}$$

for the primary mode and

$$\psi_{n+j} = q_{n+j} \left[\sum_{i=1}^{n} \frac{r_i\omega_{sj}^2\zeta_{ij}}{\omega_{pi}^2-\omega_{sj}^2} + r_{n+j} \right] \tag{28b}$$

for the secondary mode. Note that the former expression is similar to Eq.5.17b and the latter is similar to Eq.4.53b, which is expected. The response contributed from the detuned modes is found from Eq.2.38, ignoring cross-modal terms due to well-spacing of modes:

$$\lambda_{dm} = \frac{\pi G_0}{4} \left\{ \sum_{i \in I_{pd}} r_i^2 \left[\sum_{j=1}^{m} \frac{q_{n+j}\omega_{sj}^2\zeta_{ij}}{\omega_{sj}^2-\omega_{pi}^2} + q_i \right]^2 \frac{\omega_{pi}^{m-3}}{\xi_{pi}} + \sum_{j \in I_{sd}} q_{n+j}^2 \left[\sum_{i=1}^{n} \frac{r_i\omega_{sj}^2\zeta_{ij}}{\omega_{pi}^2-\omega_{sj}^2} + r_{n+j} \right]^2 \frac{\omega_{sj}^{m-3}}{\xi_{sj}} \right\} \tag{29}$$

6.4.2.2 Singly Tuned Modes

For each pair of singly tuned modes there is a tuned contribution to the spectral moment of the form of Eq.4.57. To clarify notation, assume primary mode i and secondary mode j are

singly tuned and let

$$\omega_{a,ij} = \frac{\omega_{pi}+\omega_{sj}}{2} \tag{30a}$$

$$\xi_{a,ij} = \frac{\xi_{pi}+\xi_{sj}}{2} \tag{30b}$$

$$\beta_{ij} = \frac{\omega_{sj}-\omega_{pi}}{\omega_{a,ij}} \tag{30c}$$

Then, the moment term arising from these two modes is

$$\lambda_{mn}^{(i,j)} = \frac{\pi G_{xx}}{8} \frac{r_i q_{n+j} \zeta_{ij}^2 \xi_{a,ij} \omega_{a,ij}^{m-3}}{\xi_{pi}\xi_{sj}(\beta_{ij}^2+4\xi_{a,ij}^2) + \gamma_{ij}\xi_{a,ij}^2} \tag{31}$$

The total contribution from all pairs of singly tuned modes is simply the sum

$$\lambda_{s1m} = \sum_{(i,j)\in I_{s1}} \lambda_{mn}^{(i,j)} \tag{32}$$

6.4.2.3 Multiply Tuned Modes

The spectral moments for multiply tuned modes are derived numerically by the modal decomposition method, as before. For each k-th cluster of multiply tuned modes a moment term $\lambda_{l2m}^{(k)}$ is found, and, as in Eq.32 above, these moments are summed to find the total moment contribution

$$\lambda_{l2m} = \sum_{k=1}^{K} \lambda_{l2m}^{(k)} \tag{33}$$

6.4.2.4 Closely Spaced Modes

The correlation between closely spaced modes is accounted for in the same manner as detailed in section 4.4.2.4. The resulting expression for the total moment is

$$\lambda_m = \lambda_{dm} + \lambda_{s1m} + \lambda_{l2m} + \lambda_{cm} \tag{34}$$

6.4.2.5 Very Closely Spaced Modes

The two methods developed in the previous chapters for analyzing systems with closely spaced detuned modes can be applied directly to MDOF/MDOF systems. If the modes are to be considered separatedly, then the mode shapes and frequencies are found from the analysis of widely spaced detuned modes in Section 6.4.1.1. The effective participation factors are

subsequently evaluated using Eqs.28a or 28b, and the effect of close spacing is accounted for by the approximation Eq.4.66 for the cross spectral moments. If the set of very closely spaced modes are to be represented by one collective mode, the corresponding participation factor would be the sum of the participation factors in Eqs.28a or 28b and the frequency and damping ratio are given by their respective averages.

6.5 Non-Interaction Results

6.5.1 Introduction

The MDOF/MDOF system is reanalyzed without accounting for interaction in both the frequency response and the modal decomposition approaches. Unlike the outcome of Section 6.3, a simple closed form expression is available for the frequency response function $H_i(\omega)$ for the non-interaction case. Also, as in the previous chapters, closed form expressions are obtained for all mode shapes and the factors a_i and c_i which are used in the modal decomposition method.

6.5.2 Frequency Response Function Approach

The procedure developed in Section 3.5 is used to obtain the complex frequency response function $H_i(\omega)$. The equations of motion are decoupled into two sets of equations. The first set corresponds to the displacement response of the primary subsystem DOF to the base input and is given by

$$\ddot{z}_{pi}^{(non)} + 2\omega_{pi}\xi_{pi}\dot{z}_{pi}^{(non)} + \omega_{pi}^2 z_{pi}^{(non)} = -r_i\ddot{x}_g \qquad i=1,\cdots,n \tag{35}$$

and the remaining equations are for the resulting response of the secondary subsystem to the support motions,

$$\ddot{z}_{sj}^{(non)} + 2\omega_{sj}\xi_{sj}\dot{z}_{sj}^{(non)} + \omega_{sj}^2 z_{sj}^{(non)} = \sum_{i=1}^{n}[\omega_{sj}^2 z_{pi} + 2\xi_{sj}\omega_{sj}\dot{z}_{pi}]\zeta_{ij} - r_{n+j}\ddot{x}_g \tag{36}$$

The Fourier transforms $Z_{pi}^{(non)}(\omega)$ and $Z_{sj}^{(non)}(\omega)$ of the subsystem responses $z_{pi}^{(non)}(t)$ and $z_{sj}^{(non)}(t)$ are

$$Z_{pi}^{(non)}(\omega) = -\frac{X_g(\omega)\,m_{pi}\,r_i}{G_i(\omega)} \qquad i=1,\cdots,n \tag{37a}$$

$$Z_{sj}^{(mod)}(\omega) = \frac{X_g(\omega)}{g_j(\omega)}\left[\sum_{i=1}^{n}\frac{f_{ij}(\omega)m_{pi}r_i}{G_i(\omega)} - m_{sj}r_{n+j}\right] \tag{37b}$$

From these expressions, the Fourier transform $Y^{(mod)}(\omega)$ of the response variable $y(t)$ is obtained

$$Y^{(mod)}(\omega) = \sum_{i=1}^{n} q_i Z_{pi}^{(mod)}(\omega) + \sum_{j=1}^{m} q_{n+j} Z_{sj}^{(mod)}(\omega)$$

$$Y^{(mod)}(\omega) = X_g(\omega)\left\{\sum_{i=1}^{n}\sum_{j=1}^{m}\frac{q_{n+j}f_{ij}(\omega)m_{pi}r_i}{g_j(\omega)G_i(\omega)} - \sum_{i=1}^{n}\frac{q_i m_{pi}r_i}{G_i(\omega)} - \sum_{j=1}^{m}\frac{q_{n+j}m_{sj}r_{n+j}}{g_j(\omega)}\right\} \tag{38}$$

It follows that the frequency response function is

$$H_i^{(mod)}(\omega) = \sum_{i=1}^{n}\sum_{j=1}^{n}\frac{q_{n+j}f_{ij}(\omega)m_{pi}r_i}{g_j(\omega)G_i(\omega)} - \sum_{i=1}^{n}\frac{q_i m_{pi}r_i}{G_i(\omega)} - \sum_{j=1}^{m}\frac{q_{n+j}m_{sj}r_{n+j}}{g_j(\omega)} \tag{39}$$

A comparison between the transfer function $T_{11}(\omega) = |H_1(\omega)|^2$ for interaction and non-interaction analysis is shown in Fig.6.6 for various values of the secondary system mass. The differences are most notable for values of ω near the tuned mode; the differences increases for larger secondary masses due to the increased effect of interaction. For other values of ω, the transfer function is insensitive to interaction. A similar comparison is made for non-interaction and interaction moments in Fig.6.7 for the same system with varying values for the mass and frequency of the secondary system. The result is similar to the findings in Chapter 3: the difference between λ_0 and $\lambda_0^{(mod)}$ are greatest at tuning and diminish at detuning.

6.5.3 Modal Decomposition Method

6.5.3.1 Introduction

The approach taken here is essentially the same as in Section 4.5.3. Expressions for the mode shapes and frequencies are rederived for the non-interacting, combined system and the results substituted into the modal decomposition method of Chapter 2. Closed form expressions for all mode shapes and frequencies, including multiply tuned modes, and the factors a_i and c_i are obtained. The final results for the response of the system are easily obtainable from the expressions for a_i and c_i and the original parameters of the two subsystems.

6.5.3.2 Closed Form Expressions for the Mode Shapes

The original eigenvalue problem

$$\Gamma(\omega_i^*)\phi_i^* = 0 \tag{40}$$

is reinvestigated. First, the modes associated with the primary subsystem are analyzed. It is intuitively clear that the frequencies associated with these n modes are given by the original primary subsystem frequencies

$$\omega_i^* = \omega_{pi}(\sqrt{1-\xi_{pi}^2} + i\xi_{pi}) \qquad i = 1, \ldots, n \tag{41}$$

The corresponding mode shapes are derived by substituting ω_i^* into Eq.40 and solving the eigenvalue problem. The solutions are

$$\begin{aligned}\phi_i^* &= \left[0 \cdots 0\,1\,0 \cdots 0 - \frac{f_{i1}(\omega_i^*)}{g_1(\omega_i^*)} \cdots - \frac{f_{im}(\omega_i^*)}{g_n(\omega_i^*)}\right]^T \\ &\approx \left[0 \cdots 0\,1\,0 \cdots 0 - \frac{\zeta_{i1}\omega_{s1}^2}{2(\beta_{i1}+i\xi_{d,i1})\omega_{a,i1}^2} \cdots - \frac{\zeta_{im}\omega_{sm}^2}{2(\beta_{im}+i\xi_{d,im})\omega_{a,im}^2}\right]^T\end{aligned} \tag{42}$$

where the first non-zero term is at the ith coordinate and the parameters $\omega_{a,ij}$, β_{ij}, and $\xi_{d,ij}$ are generalizations of the average frequency, detuning, and damping difference parameters of the MDOF/SDOF system

$$\omega_{a,ij} = \frac{\omega_{pi}+\omega_{sj}}{2} \qquad \beta_{ij} = \frac{\omega_{pi}-\omega_{sj}}{\omega_{a,ij}} \qquad \xi_{d,ij} = \xi_{pi}-\xi_{sj} \tag{43}$$

The derivation of the modal properties associated with the equipment is similar to the above analysis. The frequency is given by the equipment subsystem frequency

$$\omega_{n+j}^* = \omega_{sj}(\sqrt{1-\xi_{sj}^2} + i\xi_{sj}) \tag{44}$$

which, when substituted into Eq.40, yields the following solution for the mode shape

$$\begin{aligned}\phi_{n+j}^* &= \left[-\frac{f_{1j}(\omega_{n+j}^*)}{G_1(\omega_{n+j}^*)} \cdots - \frac{f_{nj}(\omega_{n+j}^*)}{G_n(\omega_{n+j}^*)}\,0 \cdots 0\,1\,0 \cdots 0\right]^T \\ &\approx \left[\frac{\epsilon_{1j}\zeta_{1j}\omega_{sj}^2}{2(\beta_{1j}+i\xi_{d,1j})\omega_{a,1j}^2} \cdots \frac{\epsilon_{nj}\zeta_{nj}\omega_{sj}^2}{2(\beta_{nj}+i\xi_{d,nj})\omega_{a,nj}^2}\,0 \cdots 0\,1\,0 \cdots 0\right]^T\end{aligned} \tag{45}$$

These expressions reduce to the results in Section 6.4.1.1 for the detuned cases. For the singly tuned mode, it can be shown that the above expressions are equivalent to the expressions derived in Section 6.4.1.3 for the non-interaction case, where m_{sj} are small.

As in Section 4.5, the above expression appears to be indeterminate since it involves the small parameters ϵ_{ij}, β_{ij}, and $\xi_{d,ij}$. However, the limit $m_{sj} \to 0$ is taken after the coefficients a_i and c_i are derived and the problem with the β_{ij} and $\xi_{d,ij}$ terms are resolved when the modal responses are combined.

6.5.3.3 Spectral Moments

As stated earlier, closed form expressions will be obtained for the factors a_i and c_i, defined in Eq.2.26, which are the key factors of the modal decomposition method. Due to the simplicity of the expressions for the mode shapes and frequencies, the derivation is straightforward.

By following the matrix multiplication in Eqs.2.17a-c and 2.20 and taking the limit $m_{sj} \to 0$, the following expression for the factors b_i are obtained which are independent of the mass ratio ϵ_{ij}

$$b_i = \frac{ir_i}{2\omega_{pi}}\left[q_i - \sum_{j=1}^{m}\frac{q_{n+j}\zeta_{ij}\omega_{sj}^2}{2(\beta_{ij}+i\xi_{d,ij})\omega_{a,ij}^2}\right] \quad \text{for } i = 1, \ldots, n \tag{46a}$$

$$b_{n+j} = \frac{iq_{n+j}}{2\omega_{sj}}\left[r_{n+j} + \sum_{i=1}^{n}\frac{r_i\zeta_{ij}\omega_{sj}^2}{2(\beta_{ij}+i\xi_{d,ij})\omega_{a,ij}^2}\right] \quad \text{for } j = 1, \ldots, m \tag{46b}$$

The factor a_i and c_i are found from Eq.2.26

$$a_i \approx 2\omega_{pi}\mathrm{Im}b_i = -\sum_{j=1}^{m}\frac{q_{n+j}\zeta_{ij}r_i\beta_{ij}\omega_{sj}^2}{2(\beta_{ij}^2+\xi_{d,ij}^2)\omega_{a,ij}^2} + r_iq_i \tag{47a}$$

$$a_{n+j} \approx 2\omega_{sj}\mathrm{Im}b_{n+j} = -\sum_{i=1}^{n}\frac{q_{n+j}\zeta_{ij}r_i\beta_{ij}\omega_{sj}^2}{2(\beta_{ij}^2+\xi_{d,ij}^2)\omega_{a,ij}^2} + r_{n+j}q_{n+j} \tag{47b}$$

$$c_i \approx 2\mathrm{Re}b_i = -\sum_{j=1}^{m}\frac{q_{n+j}\zeta_{ij}r_i\xi_{d,ij}\omega_{sj}^2}{2\omega_{pi}(\beta_{ij}^2+\xi_{d,ij}^2)\omega_{a,ij}^2} \tag{47c}$$

$$c_{n+j} \approx 2\mathrm{Re}b_{n+j} = -\sum_{i=1}^{n}\frac{q_{n+j}\zeta_{ij}r_i\xi_{d,ij}\omega_{sj}^2}{2\omega_{sj}(\beta_{ij}^2+\xi_{d,ij}^2)\omega_{a,ij}^2} \tag{47d}$$

From these expressions, the spectral moments are easily found from Eqs.2.34 and 2.36, which are repeated here:

$$C_{ij} = a_ia_j \quad D_{ij} = a_ic_j - a_jc_i \quad E_{ij} = c_ic_j \tag{48a}$$

$$\lambda_m = \sum_{i=1}^{n}\sum_{j=1}^{n}(C_{ij}\lambda_{m,ij} - D_{ij}\lambda_{m+1,ij} + E_{ij}\lambda_{m+2,ij}) \tag{48b}$$

The frequencies and damping ratios needed to calculate the cross-spectral moments are given

by the original subsystem parameters as indicated in Eqs.41 and 44. The moments calculated by the above expressions are compared with exact results for various values of the secondary masses in Fig.6.8. The results are similar to those observed in Fig.6.7.

Table 6.1. Physical Properties of the MDOF/MDOF Example System

Subsystem	Parameter Relationships
Primary	$k_1 = (1.02)^2 m_1$ (radians/sec)^2 $k_2 = (.6057)^2 m_1$ (radians/sec)^2 $m_2 = m_1$
Secondary	k_3, k_4 (variable) $m_3 = \epsilon m_1$ (ϵ variable)

Table 6.2. Modal Properties of the Fixed Base Subsystems

Subsystem	Modal DOF	Frequency (rad/s)	Damping Ratio
Primary 1	1	1.02	0.02
Primary 2	2	0.374	0.023
	3	0.98	0.06
Secondary	4	ω_{s1}	0.03
	5	1.0	0.01

Table 6.3 Frequencies for Example System (ϵ_{11}=0.01)

ω_{s1} (rad/sec)	Mode	Exact Frequency		Computed Frequency		Error
		Real Part	Imag. Part	Real Part	Imag. Part	%
0.38	1	0.370	0.009	0.372	0.009	0.2
	2	0.382	0.011	0.383	0.010	0.1
	3	0.977	0.057	0.977	0.057	0.1
	4	0.991	0.013	0.991	0.013	0.0
	5	1.028	0.018	1.028	0.018	0.0
1.00	1	0.374	0.008	0.374	0.008	0.0
	2	0.976	0.055	0.976	0.055	0.0
	3	0.989	0.017	0.988	0.017	0.1
	4	0.998	0.025	0.998	0.025	0.0
	5	1.035	0.020	1.033	0.021	0.1

Table 6.4 Mode Shapes of Example System (ϵ_{11}=0.01, ω_{11}=1.0)

Mode	DOF	Exact Mode Shape		Computed Mode Shape		Error
		Real Part	Imag. Part	Real Part	Imag. Part	%
1	1	1.000	0.000	1.000	0.000	0.0
	2	0.000	0.000	0.000	0.000	0.0
	3	0.000	0.000	0.000	0.000	0.0
	4	0.387	-0.004	0.387	0.000	0.4
	5	0.387	0.002	0.387	0.000	0.4
2	1	-0.004	0.000	0.000	0.000	0.4
	2	0.130	-0.157	0.123	-0.163	2.1
	3	-0.009	-0.004	-0.008	-0.005	0.2
	4	1.000	0.000	1.000	0.000	0.0
	5	0.646	0.093	0.665	0.075	2.8
3	1	-0.002	-0.001	-0.003	0.001	0.3
	2	0.004	-0.009	0.004	-0.009	0.0
	3	0.060	-0.035	0.063	-0.035	0.3
	4	-0.215	0.620	-0.229	-0.600	3.4
	5	1.000	0.000	1.000	0.000	0.0
4	1	-0.004	0.001	-0.001	-0.001	0.5
	2	-0.014	-0.013	-0.013	-0.014	0.2
	3	-0.023	-0.041	-0.022	-0.042	0.2
	4	1.000	0.000	1.000	0.000	0.0
	5	0.562	-0.489	0.581	-0.440	7.3
5	1	0.000	0.001	-0.004	-0.001	0.4
	2	-0.003	0.002	-0.003	0.002	0.0
	3	-0.211	-0.065	-0.204	-0.066	0.7
	4	-0.804	-0.555	-0.777	-0.596	3.2
	5	1.000	0.000	1.000	0.000	0.0

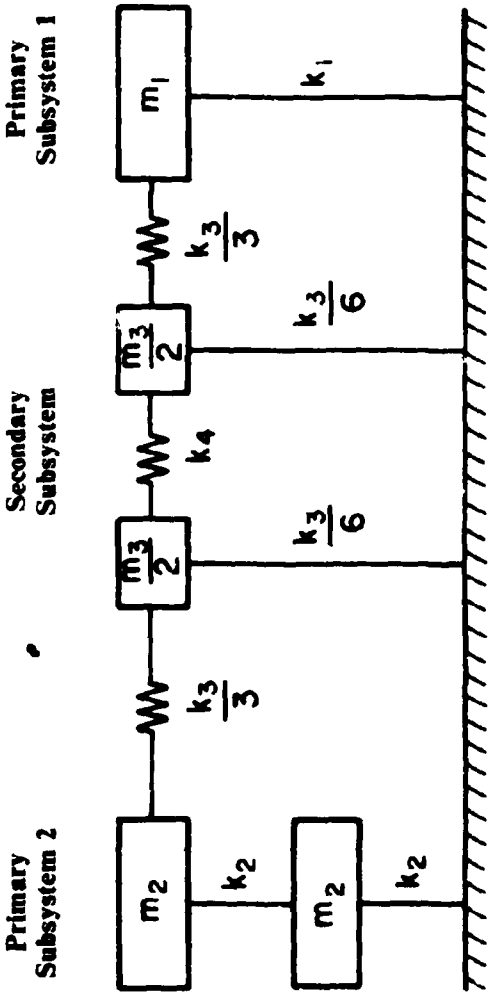

Figure 6.1. Example MDOF/MDOF System

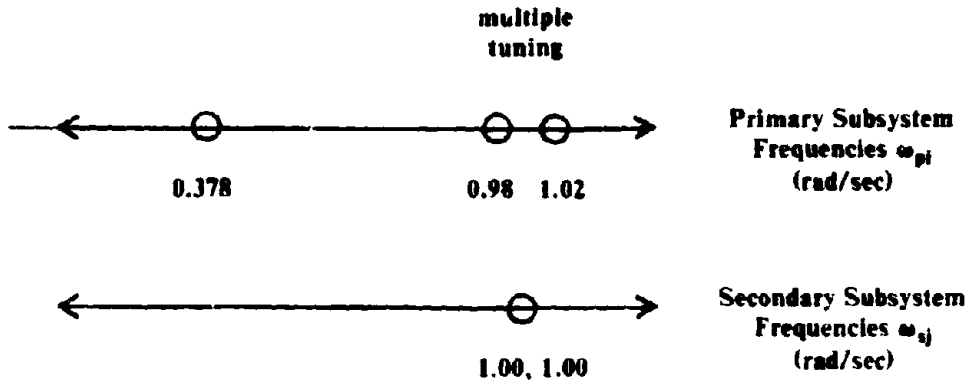

Multiply Tuned System, ω_{s1}=1.0 rad/sec

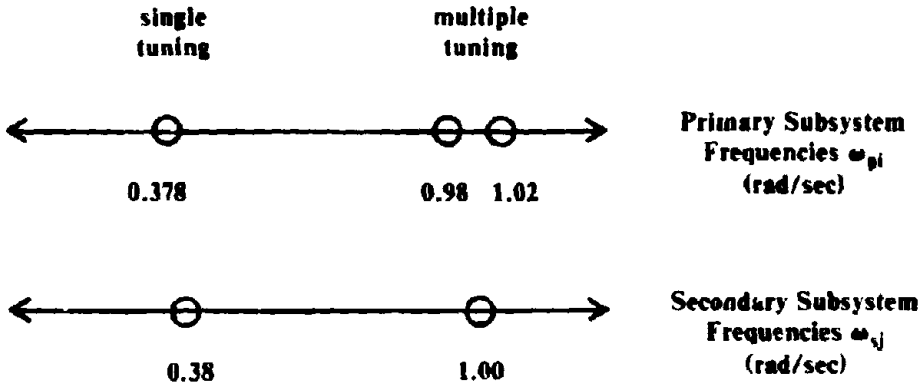

Multiply and Singly Tuned System, ω_{s1}=0.38 rad/sec

Fig.6.2. Distribution of Subsystem Free Vibration Frequencies

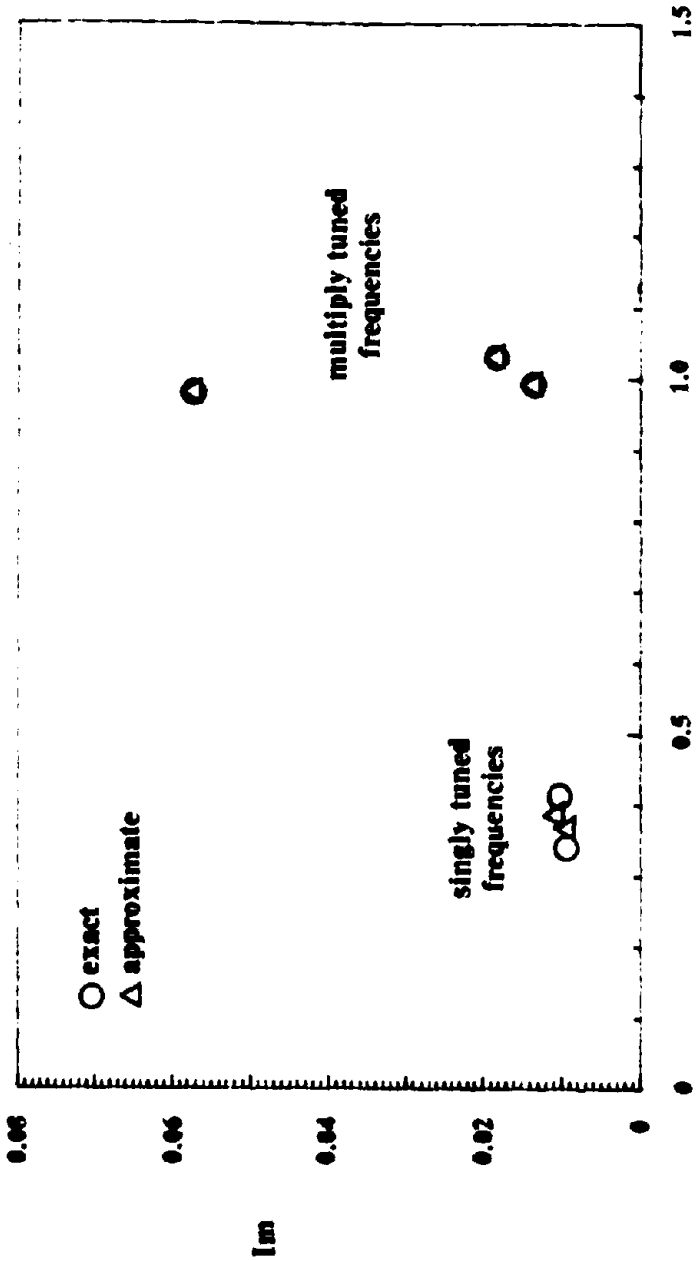

Fig.6.3a. Complex Frequencies: Singly Tuned System
ω_{n1}=0.38 rad/sec, ϵ_{11}=0.01

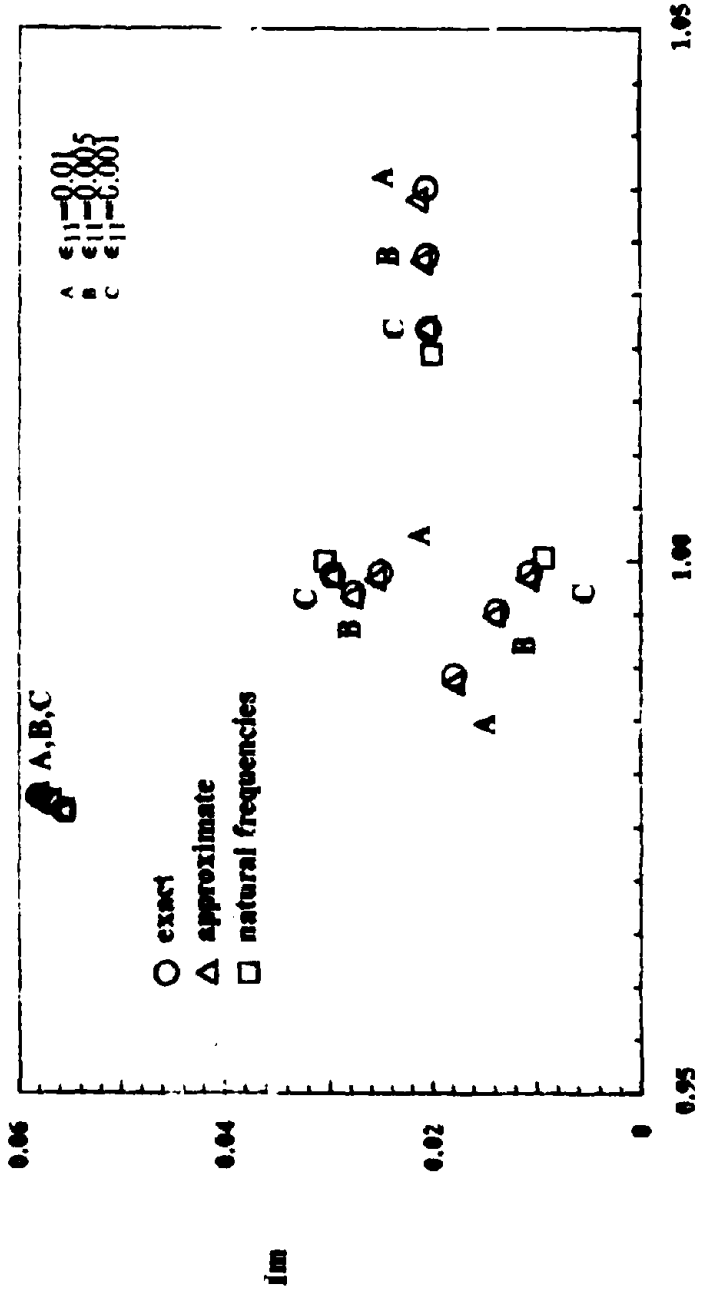

Fig.6.3b. Complex Frequencies: Multiply Tuned System
ω_{s1}=1.0 rad/sec, ϵ_{11}=0.01, 0.005, 0.001

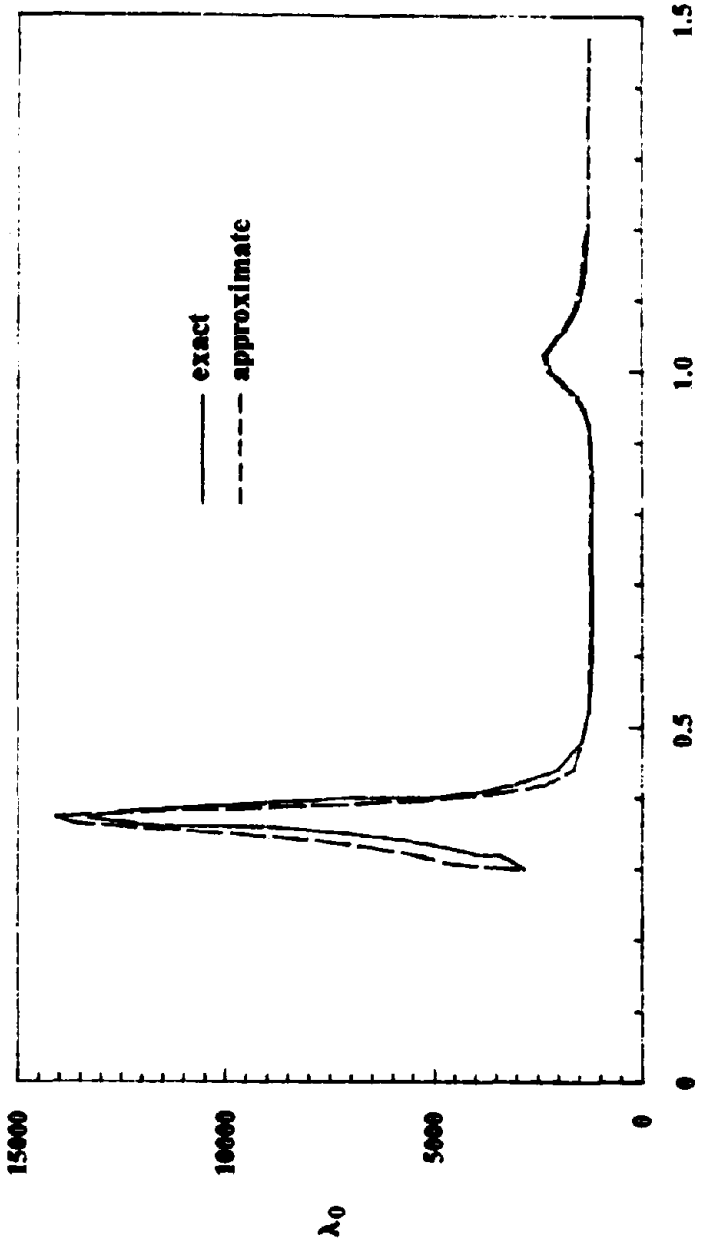

Fig6.4a. Spectral Moment λ_0, ϵ_{11}=0.01

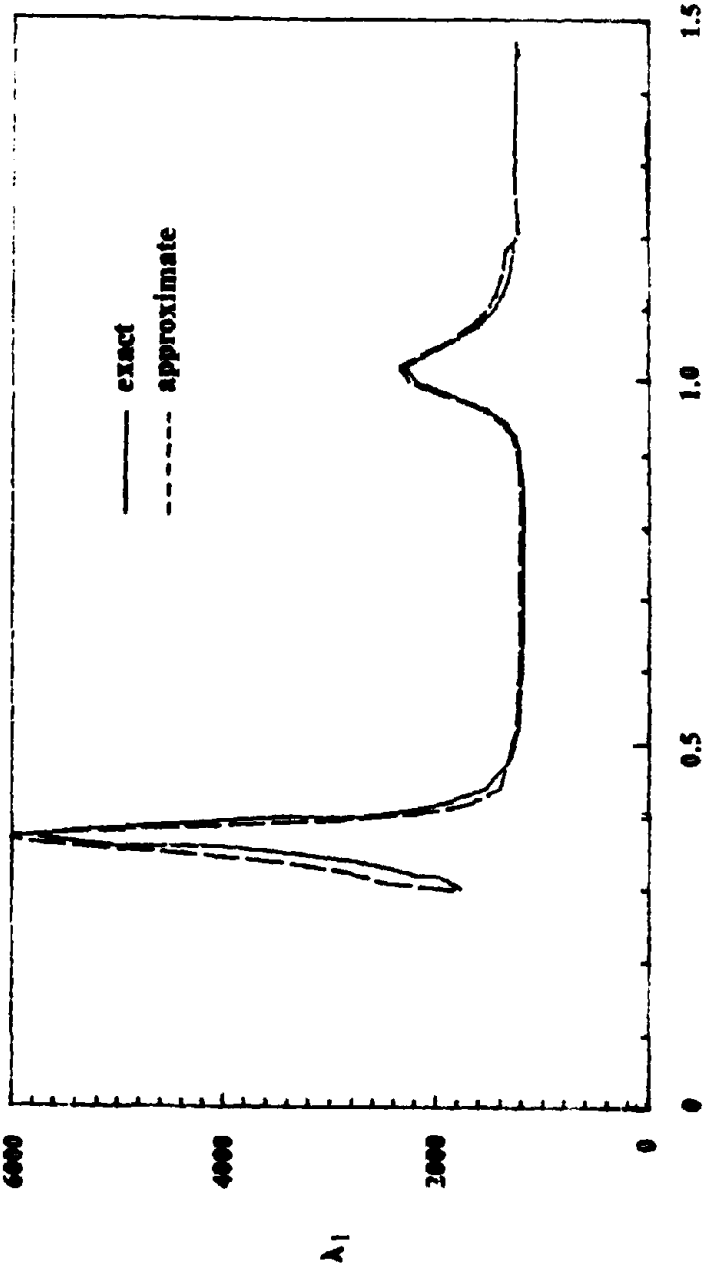

Fig6.4b. Spectral Moment λ_1, ϵ_{11}=0.01

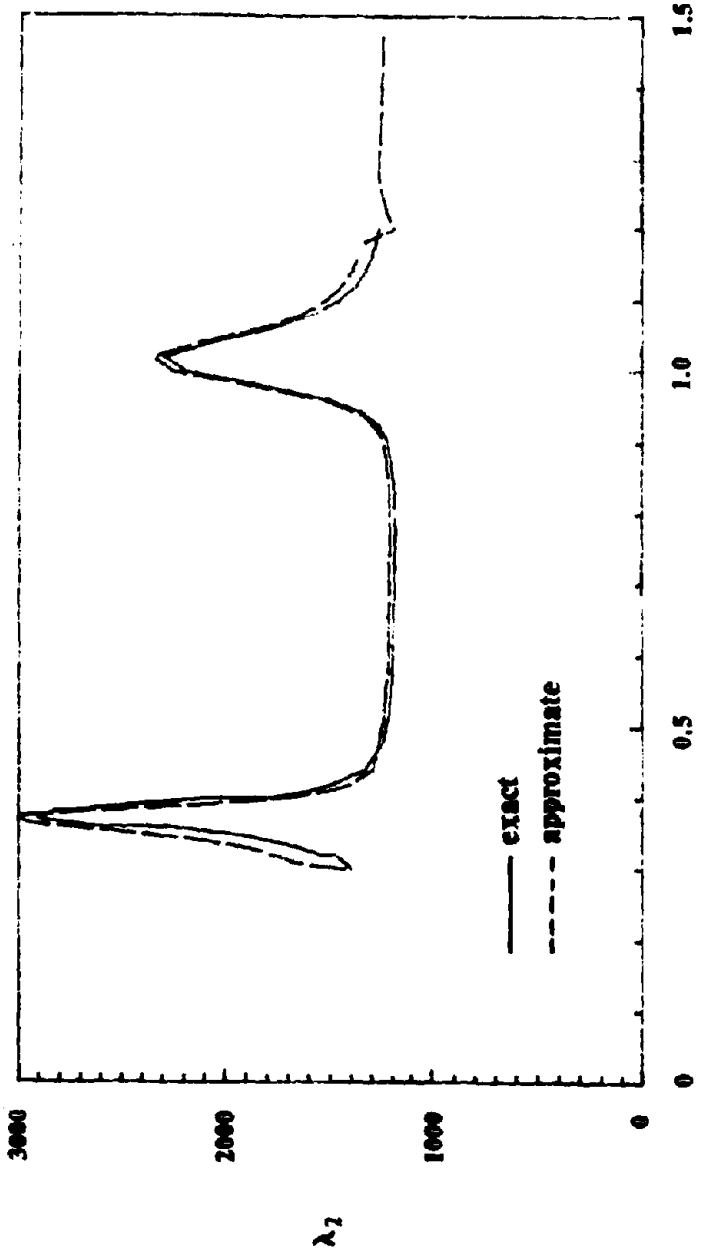

Fig6.4c. Spectral Moment λ_2, ϵ_{11}=0.01

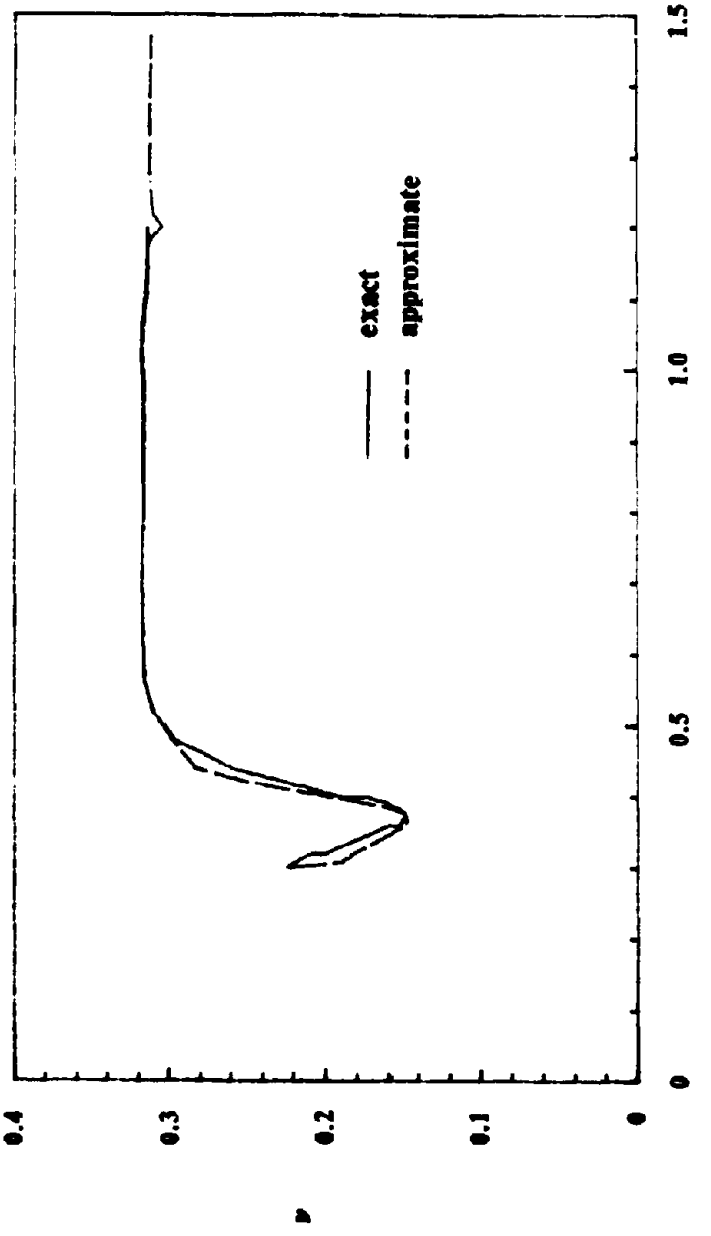

Fig6.5a. Mean Zero-Crossing Rate ν, ϵ_{11}=0.01

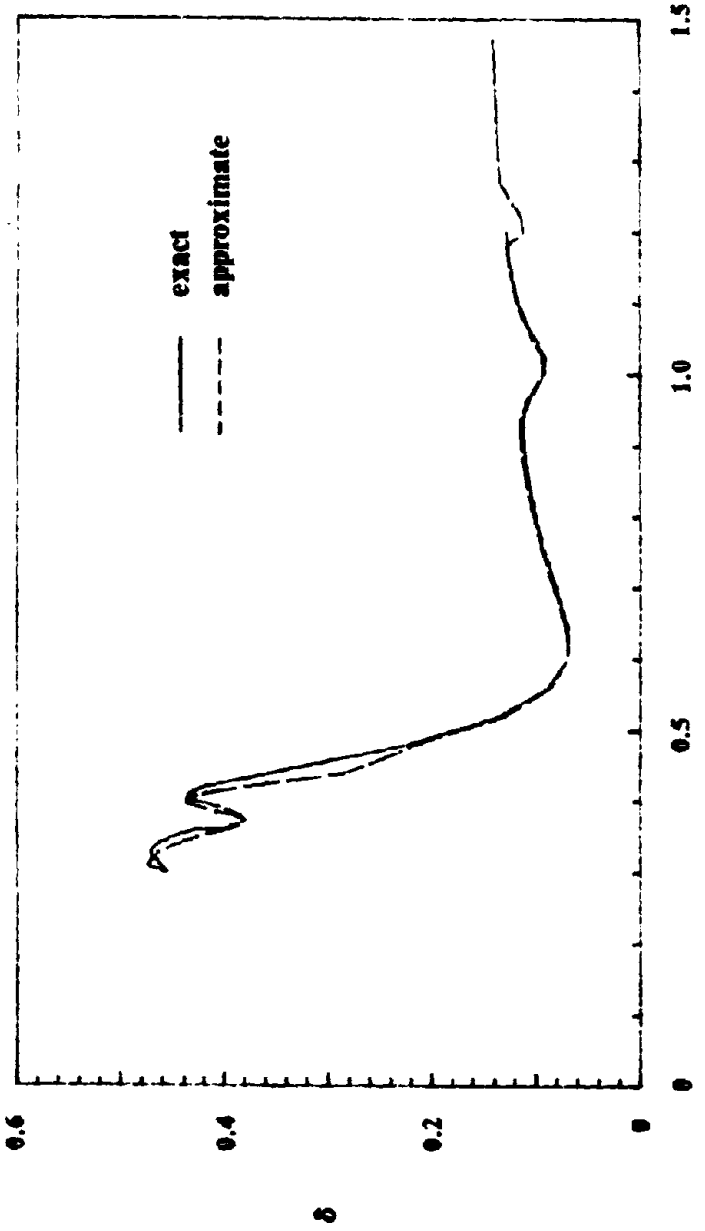

Fig6.5b. Shape Factor δ, ϵ_{11}=0.01

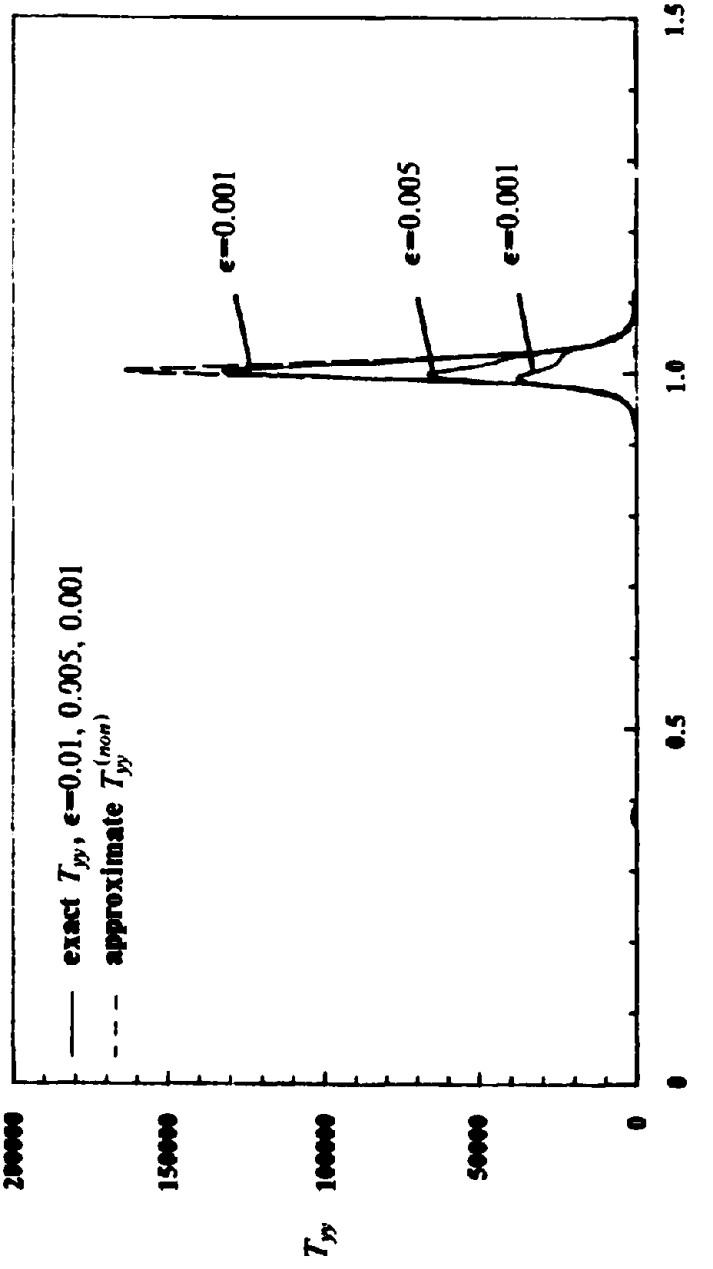

Fig6.6. Transfer Function $T_{yy}^{(non)}(\omega)$ without Interaction

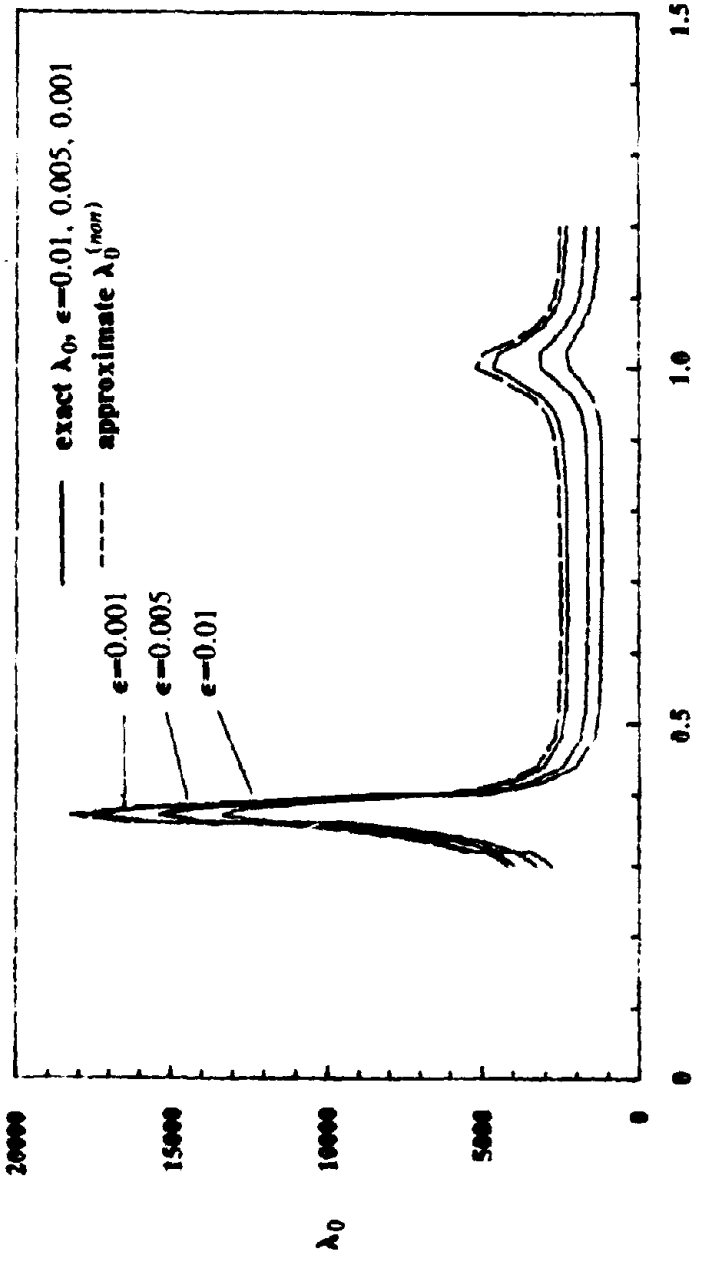

Fig6.7. Spectral Moment $\lambda_0^{(non)}$ without Interaction Calculated from $H_1^{(non)}(\omega)$

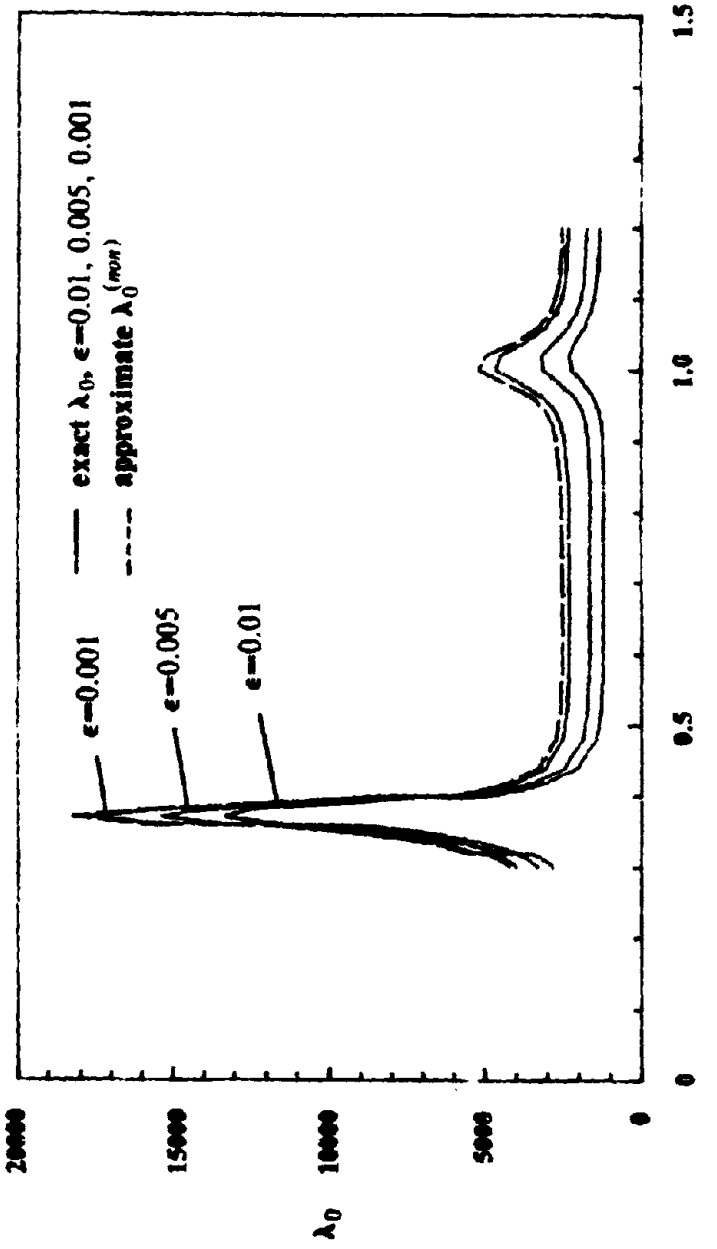

Fig6.8. Spectral Moment $\lambda_0^{(non)}$ without Interaction Calculated from Modal Combination

CHAPTER 7

SUMMARY AND CONCLUSIONS

7.1 Summary of Thesis

The general problem of finding the dynamic characteristics of arbitrary PS systems was investigated. Previous investigators have approximated or have neglected altogether one or more of the properties of such systems which include: interaction effects, correlation between subsystem modal responses and between support motions, non-classical damping, multiple-support excitations, and single or multiple tuning. In this study, all of these effects are accounted for correctly by analyzing the combined equations of motion. This large system of equations is effectively reduced to a tractable and manageable form through a systematic application of the perturbation theory. Two approaches are provided: one based on modal analysis and the other based on frequency response methods. In the modal approach, simple formulations are provided for the complex-valued mode shapes and frequencies which in all but the multiply tuned case are in closed form. These modal properties are applicable to a variety of response analysis methods; references to some of these methods have been made. For the purpose of this study, a general modal combination rule for systems with complex-valued and closely spaced mode shapes and frequencies was developed for stationary stochastic input specified by its power spectral density function as well as by its response spectrum. These methods are particularly well-suited for the analysis of PS systems.

In the frequency response approach, simple closed form solutions for the frequency response function was obtained for all but the MDOF/MDOF systems, which can be used in cases where the input motion is stationary and is described by a power spectral density function.

For further insight into the behavior of PS systems, algebraic expressions for the response were obtained for the special and important case of white noise input. Several properties of the system were revealed, such as the relation between the mass ratios and interaction, the relation

between the proximity of the subsystem frequencies and the corresponding tuning or resonance effects, and the relation between the mass ratios, the difference of subsystem damping values and the corresponding non-classical damping effects. Many other properties are explicitly included in the expressions for the response and were cited in the text.

The PS system was also analyzed without accounting for interaction effects. In the frequency response approach, the equations of motion were decoupled to two sets of equations corresponding to the coordinates of the two subsystems, as has been commonly done in the past. However, in the modal approach, the combined set of equations are retained and closed form expressions for the mode shapes and frequencies are obtained for all cases. These expressions were used in the modal decomposition method and simple closed form formulae were derived for a set of generalized participation factors which can be readily used to find the response of the system.

7.2 Conclusions and Recommendations

The main contribution of this work is the development of an accurate and computationally feasible modal analysis technique for PS system. The expressions that were obtained for the complex mode shapes and frequencies and the modal combination method are easily implemented into a digital computer. Such an implementation was used to derive the figures and tables in this study.

Different formulations can be used for various types of base input; a partial list follows:

1. For stationary stochastic input and for input specified by its response spectrum, the modal decomposition method developed in Chapter 2 is used.
2. For non-stationary, non-white input, a number of existing methods including those in Refs.14, 30, 8 can be used.
3. For deterministic input, the decoupled modal differential equations in Eq.2.25 can be integrated.

In many PS systems, the masses of the secondary subsystem are very small in comparison

to those of the primary subsystem. If the masses are small enough to satisfy the non-interaction criteria, the corresponding non-interaction formulations can be used, which are in closed form and easily calculated. These same formulations can also be used for those systems that do not satisfy the criteria, to provide a simple estimate of the response behavior. The results are conservative, which is often acceptable in preliminary design stages.

References

1. *International Mathematics and Statistics Library*, IMSL Inc., 1979.

2. American Society of Mechanical Engineers, *ASME Boiler and Pressure Vessel Code*, ANSI/ASME BPV-III-1-A Section III, Rules for Construction of Nuclear Power Plant Components, Division 1, Appendix N, July 1981.

3. A. D. Aleksandrov, *Mathematics: Its Content, Methods, and Meaning*, 1, M.I.T. Press, Cambridge, Massachusetts, 1963.

4. M. Amin, W. J. Hall, N. M. Newmark, and R. P. Kasawara, "Earthquake Response of Multiple Connected Light Secondary Systems by Spectrum Methods," in *Proceedings*, ASME First National Congress on Pressure Vessel and Piping Technology, San Francisco, California, May 1971.

5. K. J. Bathe and E. L. Wilson, "Stability and Accuracy Analysis of Direct Integration Methods," *Earthquake Engineering and Structural Dynamics*, vol. 1, pp. 283-291, 1973.

6. J. M. Biggs and J. M. Roesset, "Seismic Analysis of Equipment Mounted on a Massive Structure," in *Seismic Design of Nuclear Power Plants*, ed. R. J. Hansen, pp. 319-343, M.I.T. Press, 1970.

7. D. E. Cartwright and M. S. Longuet Higgins, "The Statistical Distribution of the Maxima of a Random Function," *Proceedings of the Royal Statistical Society*, vol. 237, pp. 212-232, 1956.

8. T. K. Caughey, "Nonstationary Random Inputs and Responses," in *Random Vibration, Volume 2*, ed. S. H. Crandall, Chapter 3, pp. 56-84, M.I.T. Press, Cambridge, Mass, 1963.

9. M. K. Chakravarti and E. H. Vanmarke, "Probabilistic Seismic Analysis of Light Equipment Within Buildings," in *Proceedings*, Fifth World Conference on Earthquake Engineering, vol. II, Rome, Italy, 1973.

10. R. W. Clough and J. Penzien, *Dynamics of Structures*, McGraw-Hill Book Co., Inc., New York, N.Y., 1975.

11. S. H. Crandall and W. D. Mark, *Random Vibration of Mechanical Systems*, Academic Press, New York, N.Y., 1963.

12. A. F. Curtis and T. R. Boykin, "Response of Two-Degree-of-Freedom Systems to White-Noise Base Excitation," *Journal of the Acoustical Society of America*, vol. 33, pp. 655-663, 1961.

13. A. G. Davenport, "Note on the Distribution of the Largest Value of a Random Function with Application to Gust Loading," in *Proceedings*, Institution of Civil Engineers, vol. 28, pp. 187-196, 1964.

14. A. Debchandhury and D. A. Gasparini, "State Space Random Vibration Theory," Case Institute of Technology, Dept. of Civil Engineering Research Report ENG 77-193o4, October 1980.

15. A. Der Kiureghian, "Structural Response to Stationary Excitation," *Journal of the Engineering Mechanics Division*, vol. 106, no. EM6, pp. 1195-1213, Dec. 1980.

16. A. Der Kiureghian, "A Response Spectrum Method for Random Vibration Analysis of MDF Systems," *Earthquake Engineering and Structural Dynamics*, vol. 9, pp. 419-435, 1981.

17. A. Der Kiureghian, A. Asfura, J. L. Sackman, and J. M. Kelly, "Seismic Response of Multiply Supported Piping Systems," in *Proceedings*, Seventh International Conference on Structural Mechanics in Reactor Technology, Chicago, Illinois, 1983.

18. A. Der Kiureghian, J. L. Sackman, and B. Nour-Omid, "Dynamic Analysis of Light Equipment in Structures: Modal Properties of the Combined System," *Journal of the Engineering Mechanics Division*, vol. 109, no. EM1, Feb., 1983.

19. A. Der Kiureghian, J. L. Sackman, and B. Nour-Omid, "Dynamic Analysis of Light Equipment in Structures: Response to Stochastic Input," *Journal of the Engineering*

Mechanics Division, vol. 109, no. EM1, Feb., 1983.

20. A. Erdelyi, *Asymptotic Expansions*, Dover, New York, New York, 1956.

21. W. C. Hurty and M. F. Rubinstein, *Dynamics of Structures*, Prentice Hall, Inc., Englewood Cliffs, N.J., 1964.

22. T. Igusa and A. Der Kiureghian, "Response Spectrum Method for Systems with Non-Classical Damping," in *Proceedings*, ASCE-EMD Specialty Conference, West Lafayette, Indiana, May 23-25, 1983.

23. T. Igusa, A. Der Kiureghian, and J. L. Sackman, "An Investigation of the Spectral Density Function and Spectral Moments for Equipment-Structure Systems," unpublished paper.

24. K. Kanai, "Semi-Empirical Formula for Seismic Characterization of the Ground," *Bulletin of Earthquake Research Institute*, vol. 35, University of Tokyo, Tokyo, Japan, June, 1967.

25. K. K. Kapur and L. C. Shao, "Generation of Seismic Floor Response Spectra for Equipment Design," in *Proceedings*, Specialty Conference on Structural Design of Nuclear Plant Facilities, ASCE, Chicago, Illinois, December, 1973.

26. M.-C. Lee and J. Penzien, "Stochastic Seismic Analysis of Nuclear Power Plants and Piping Systems subjected to Multiple Support Excitations," Report Number UCB/EERC-80/19, Earthquake Engineering Research Center, University of California, Berkeley, Calif., June 1980.

27. K. R. Leimbach and J. P. Sterkel, "Comparison of Multiple Support Excitation Solution Techniques for Piping Systems," in *Proceedings*, Fifth International Conference on SMiRT, Berlin, Germany, August 13-17, 1979.

28. Y. K. Lin, *Probabilistic Theory of Structural Dynamics*, McGraw-Hill Book Co., Inc., New York, N.Y., 1967.

29. R. H. Lyon, "On the Vibration Statistics of a Randomly Excited Hard-Spring Oscillator," *Journal of the Acoustical Society of America*, vol. 32, pp. 716-719, 1960. Part II: Vol. 33, pp. 1395-1403, 1961.

30. S. F. Masri, "Response of a Multi-Degree-of Freedom System to Nonstationary Random Excitation," *Journal of Applied Mechanics*, vol. 45, no. 3, pp. 649-656, September 1978.

31. T. Nakhata, N. M. Newmark, and W. J. Hall, "Approximate Dynamic Response of Light Secondary Systems," Structural Research Series Report No. 396, Civil Engineering Studies, University of Illinois, Urbana, Ill., 1973.

32. A. H. Nayfeh, *Perturbation Methods*, Wiley, New York, New York, 1973.

33. N. M. Newmark, "Earthquake Response Analysis of Reactor Structures," *Nuclear Engineering and Design*, vol. 20, no. 2, pp. 303-322 . 1972.

34. J. Penzien and A. K. Chopra, "Earthquake Response of Appendage on a Multi-Story Building," in *Proceedings*, Third World Conference on Earthquake Engineering, New Zealand, 1965.

35. K. A. Peters, D. Schmitz, and U. Wagner, "Determination of Floor Response Spectra on the Basis of the Response Spectrum Method," *Nuclear Engineering and Design*, vol. 44, pp. 255-262 . 1977.

36. G. C. Ruzicka and A. R. Robinson, "Dynamic Response of Tuned Secondary Systems," Report Number UILU-ENG-80-2020, Department of Civil Engineering, University of Illinois, Urbana, Ill., Nov. 1980.

37. J. L. Sackman and J. M. Kelly, "Seismic Analysis of Internal Equipment and Components in Structures," *Engineering Structures*, vol. 1, no. 4, pp. 179-190, July, 1979.

38. R. H. Scanlan and K. Sachs, "Earthquake Time Histories and Response Spectra," *Journal of the Engineering Mechanics Division*, vol. 100, no. EM4, pp. 635-655, August, 1974.

39. D. E. Shaw, "Seismic Structural Response Analysis for Multiple Support Excitation," in *Proceedings*, Third International Conference on Structural Mechanics in Reactor Technology, Paper K5/2, London, England, September 1-5, 1975.

40. A. K. Singh, "A Stochastic Model for Predicting Maximum Response of Light Secondary Systems," thesis presented to the University of Illinois at Urbana, Illinois, in 1972, in partial fulfillment of the requirements for the degree of Doctor of Philosophy.

41. M. P. Singh, "Generation of Seismic Floor Spectra," *Journal of the Engineering Mechanics Division*, vol. 101, no. EM5, pp. 594-607, Oct. 1975.

42. M. P. Singh, "Seismic Design Input for Secondary Structures," *Journal of the Structural Division*, vol. 106, no. ST2, pp. 505-517, Feb. 1980.

43. M. P. Singh, "Seismic Response by SRSS for Nonproportional Damping," *Journal of the Engineering Mechanics Division*, vol. 106, no. EM6, pp. 1405-1419, Dec. 1980.

44. E. H. Vanmarcke, "Properties of Spectral Moments with Applications to Random Vibration," *Journal of the Engineering Mechanics Division*, vol. 98, no. EM2, pp. 425-446. , Apr. 1972

45. E. H. Vanmarcke, "On the Distribution of the First-Passage Time for Normal Stationary Random Processes," *Journal of Applied Mechanics*, vol. 42, pp. 215-220 , Mar. 1975.

46. E. H. Vanmarke, "A Simplified Procedure for Predicting Amplified Response Spectra and Equipment Response," in *Proceedings*, Sixth World Conference on Earthquake Engineering, vol. III, New Delhi, India, 1977.

47. K. M. Vashi, "Seismic Spectral Analysis of Structural Systems Subjected to Nonuniform Excitation at Supports," in *Proceedings*, Second ASCE Specialty Conference, vol. 1-A, pp. 188-211, New Orleans, Louisiana, December, 1975.

48. R. Villaverde and N. M. Newmark, "Seismic Response of Light Attachments to Buildings," Structural Research Series No. 469, University of Illinois, Urbana, Illinois, February, 1980.

49. G. B. Warburton and S. R. Soni, "Errors in Response Calculations of Non-Classically Damped Structures," *Journal of Earthquake Engineering and Structural Dynamics*, vol. 5, pp. 365-376, 1977.

50. E. L. Wilson, A. Der Kiureghian, and E. P. Bayo, "A Replacement for the SRSS Method in Seismic Analysis," *Earthquake Engineering and Structural Dynamics*, vol. 9, pp. 187-194, 1981.

EARTHQUAKE ENGINEERING RESEARCH CENTER REPORTS

NOTE: Numbers in parentheses are Accession Numbers assigned by the National Technical Information Service; these are followed by a price code. Copies of the reports may be ordered from the National Technical Information Service, 5285 Port Royal Road, Springfield, Virginia, 22161. Accession Numbers should be quoted on orders for reports (PB --- ---) and remittance must accompany each order. Reports without this information were not available at time of printing. The complete list of EERC reports (from EERC 67-1) is available upon request from the Earthquake Engineering Research Center, University of California, Berkeley, 47th Street and Hoffman Boulevard, Richmond, California 94804.

UCB/EERC-77/01 "PLUSH - A Computer Program for Probabilistic Finite Element Analysis of Seismic Soil-Structure Interaction," by M.P. Romo Organista, J. Lysmer and H.B. Seed - 1977 (PB81 177 651)A05

UCB/EERC-77/02 "Soil-Structure Interaction Effects at the Humboldt Bay Power Plant in the Ferndale Earthquake of June 7, 1975," by J.E. Valera, H.B. Seed, C.F. Tsai and J. Lysmer - 1977 (PB 265 795)A04

UCB/EERC-77/03 "Influence of Sample Disturbance on Sand Response to Cyclic Loading," by K. Mori, H.B. Seed and C.K. Chan - 1977 (PB 267 352)A04

UCB/EERC-77/04 "Seismological Studies of Strong Motion Records," by J. Shoja-Taheri - 1977 (PB 269 655)A10

UCB/EERC-77/05 Unassigned

UCB/EERC-77/06 "Developing Methodologies for Evaluating the Earthquake Safety of Existing Buildings," by No. 1 - B. Bresler; No. 2 - B. Bresler, T. Okada and D. Zisling; No. 3 - T. Okada and B. Bresler; No. 4 - V.V. Bertero and B. Bresler - 1977 (PB 267 354)A08

UCB/EERC-77/07 "A Literature Survey - Transverse Strength of Masonry Walls," by Y. Omote, R.L. Mayes, S.W. Chen and R.W. Clough - 1977 (PB 277 933)A07

UCB/EERC-77/08 "DRAIN-TABS: A Computer Program for Inelastic Earthquake Response of Three Dimensional Buildings," by R. Guendelman-Israel and G.H. Powell - 1977 (PB 270 693)A07

UCB/EERC-77/09 "SUBWALL: A Special Purpose Finite Element Computer Program for Practical Elastic Analysis and Design of Structural Walls with Substructure Option," by D.Q. Le, H. Peterson and E.P. Popov - 1977 (PB 270 567)A05

UCB/EERC-77/10 "Experimental Evaluation of Seismic Design Methods for Broad Cylindrical Tanks," by D.P. Clough (PB 272 280)A13

UCB/EERC-77/11 "Earthquake Engineering Research at Berkeley - 1976," - 1977 (PB 273 507)A09

UCB/EERC-77/12 "Automated Design of Earthquake Resistant Multistory Steel Building Frames," by N.D. Walker, Jr. - 1977 (PB 276 526)A09

UCB/EERC-77/13 "Concrete Confined by Rectangular Hoops Subjected to Axial Loads," by J. Vallenas, V.V. Bertero and E.P. Popov - 1977 (PB 275 165)A06

UCB/EERC-77/14 "Seismic Strain Induced in the Ground During Earthquakes," by Y. Sugimura - 1977 (PB 284 201)A04

UCB/EERC-77/15 Unassigned

UCB/EERC-77/16 "Computer Aided Optimum Design of Ductile Reinforced Concrete Moment Resisting Frames," by S.W. Zagajeski and V.V. Bertero - 1977 (PB 280 137)A07

UCB/EERC-77/17 "Earthquake Simulation Testing of a Stepping Frame with Energy-Absorbing Devices," by J.M. Kelly and D.F. Tsztoo - 1977 (PB 273 506)A04

UCB/EERC-77/18 "Inelastic Behavior of Eccentrically Braced Steel Frames under Cyclic Loadings," by C.W. Roeder and E.P. Popov - 1977 (PB 275 526)A15

UCB/EERC-77/19 "A Simplified Procedure for Estimating Earthquake-Induced Deformations in Dams and Embankments," by F.I. Makdisi and H.B. Seed - 1977 (PB 276 820)A04

UCB/EERC-77/20 "The Performance of Earth Dams during Earthquakes," by H.B. Seed, F.I. Makdisi and P. de Alba - 1977 (PB 276 821)A04

UCB/EERC-77/21 "Dynamic Plastic Analysis Using Stress Resultant Finite Element Formulation," by P. Lukkunapvasit and J.M. Kelly - 1977 (PB 275 453)A04

UCB/EERC-77/22 "Preliminary Experimental Study of Seismic Uplift of a Steel Frame," by R.W. Clough and A.A. Huckelbridge 1977 (PB 278 769)A08

UCB/EERC-77/23 "Earthquake Simulator Tests of a Nine-Story Steel Frame with Columns Allowed to Uplift," by A.A. Huckelbridge - 1977 (PB 277 944)A09

UCB/EERC-77/24 "Nonlinear Soil-Structure Interaction of Skew Highway Bridges," by M.-C. Chen and J. Penzien - 1977 (PB 276 176)A07

UCB/EERC-77/25 "Seismic Analysis of an Offshore Structure Supported on Pile Foundations," by D.D.-N. Liou and J. Penzien 1977 (PB 283 180)A06

UCB/EERC-77/26 "Dynamic Stiffness Matrices for Homogeneous Viscoelastic Half-Planes," by G. Dasgupta and A.K. Chopra - 1977 (PB 279 654)A06

UCB EERC-77/27 "A Practical Soft Story Earthquake Isolation System," by J.M. Kelly, J.M. Eidinger and C.J. Derham - 1977 (PB 276 814)A07

UCB/EERC-77/28 "Seismic Safety of Existing Buildings and Incentives for Hazard Mitigation in San Francisco: An Exploratory Study," by A.J. Meltsner - 1977 (PB 281 970)A05

UCB EERC-77 29 "Dynamic Analysis of Electrohydraulic Shaking Tables," by D. Rea, S. Abedi-Hayati and Y. Takahashi 1977 (PB 282 569)A04

UCB EERC-77 30 "An Approach for Improving Seismic - Resistant Behavior of Reinforced Concrete Interior Joints," by B. Galunic, V.V. Bertero and E.P. Popov - 1977 (PB 290 870)A06

UCB EERC-78/01 "The Development of Energy-Absorbing Devices for Aseismic Base Isolation Systems," by J.M. Kelly and D.F. Tsztoo - 1978 (PB 284 978)A04

UCB EERC-78/02 "Effect of Tensile Prestrain on the Cyclic Response of Structural Steel Connections, by J.G. Bouwkamp and A. Mukhopadhyay - 1978

UCB EERC-78/03 "Experimental Results of an Earthquake Isolation System Using Natural Rubber Bearings," by J.M. Eidinger and J.M. Kelly - 1978 (PB 281 686)A04

UCB EERC-78/04 "Seismic Behavior of Tall Liquid Storage Tanks," by A. Niwa - 1978 (PB 284 017)A14

UCB EERC-78/05 "Hysteretic Behavior of Reinforced Concrete Columns Subjected to High Axial and Cyclic Shear Forces," by S.W. Zagajeski, V.V. Bertero and J.G. Bouwkamp - 1978 (PB 283 858)A13

UCB EERC-78/06 "Three Dimensional Inelastic Frame Elements for the ANSR-I Program," by A. Riahi, D.G. Row and G.H. Powell - 1978 (PB 295 755)A04

UCB EERC-78/07 "Studies of Structural Response to Earthquake Ground Motion," by O.A. Lopez and A.K. Chopra - 1978 (PB 282 790)A05

UCB EERC-78/08 "A Laboratory Study of the Fluid-Structure Interaction of Submerged Tanks and Caissons in Earthquakes," by R.C. Byrd - 1978 (PB 284 957)A08

UCB EERC-78/09 Unassigned

UCB EERC-79/01 "Seismic Performance of Nonstructural and Secondary Structural Elements," by I. Sakamoto - 1979 (PB81 154 593)A05

UCB EERC-79/11 "Mathematical Modelling of Hysteresis Loops for Reinforced Concrete Columns," by S. Nakata, T. Sproul and J. Penzien - 1979 (PB 298 274)A05

UCB EERC-79/12 "Damageability in Existing Buildings," by T. Blejwas and B. Bresler - 1979 (PB 80 166 978)A05

UCB EERC-79/13 "Dynamic Behavior of a Pedestal Base Multistory Building," by R.M. Stephen, E.L. Wilson, J.G. Bouwkamp and M. Button - 1979 (PB 286 650)A07

UCB EERC-79/14 "Seismic Response of Bridges - Case Studies," by R.A. Imbsen, V. Nutt and J. Penzien - 1979 (PB 286 503)A10

UCB EERC-79/15 "A Substructure Technique for Nonlinear Static and Dynamic Analysis," by D.G. Row and G.H. Powell - 1979 (PB 288 077)A10

UCB/EERC-79/16 "Seismic Risk Studies for San Francisco and for the Greater San Francisco Bay Area," by C.S. Oliveira - 1979 (PB 81 120 115)A07

UCB/EERC-79/17 "Strength of Timber Roof Connections Subjected to Cyclic Loads," by P. Gülkan, R.L. Mayes and R.W. Clough - 1979 (HUD-000 1491)A07

UCB/EERC-79/18 "Response of K-Braced Steel Frame Models to Lateral Loads," by J.G. Bouwkamp, R.M. Stephen and E.P. Popov - 1979

UCB/EERC-79/19 "Rational Design Methods for Light Equipment in Structures Subjected to Ground Motion," by J.L. Sackman and J.M. Kelly - 1979 (PB 292 357)A04

UCB/EERC-79/20 "Testing of a Wind Restraint for Aseismic Base Isolation," by J.M. Kelly and D.E. Chitty - 1979 (PB 292 833)A03

UCB/EERC-79/21 "APOLLO - A Computer Program for the Analysis of Pore Pressure Generation and Dissipation in Horizontal Sand Layers During Cyclic or Earthquake Loading," by P.P. Martin and H.B. Seed - 1979 (PB 292 835)A04

UCB/EERC-79/22 "Optimal Design of an Earthquake Isolation System," by M.A. Bhatti, K.S. Pister and E. Polak - 1979 (PB 294 735)A06

UCB/EERC-79/23 "MASH - A Computer Program for the Non-Linear Analysis of Vertically Propagating Shear Waves in Horizontally Layered Deposits," by P.P. Martin and H.B. Seed - 1979 (PB 293 101)A05

UCB/EERC-79/24 "Investigation of the Elastic Characteristics of a Three Story Steel Frame Using System Identification," by I. Kaya and H.D. McNiven - 1979 (PB 296 225)A06

UCB/EERC-79/25 "Investigation of the Nonlinear Characteristics of a Three-Story Steel Frame Using System Identification," by I. Kaya and H.D. McNiven - 1979 (PB 301 363)A05

UCB/EERC-78/26 "Studies of Strong Ground Motion in Taiwan," by Y.M. Hsiung, B.A. Bolt and J. Penzien - 1978 (PB 298 436)A06

UCB/EERC-78/27 "Cyclic Loading Tests of Masonry Single Piers: Volume 1 - Height to Width Ratio of 2," by P.A. Hidalgo, R.L. Mayes, H.D. McNiven and R.W. Clough - 1978 (PB 296 211)A07

UCB/EERC-78/28 "Cyclic Loading Tests of Masonry Single Piers: Volume 2 - Height to Width Ratio of 1," by S.-W.J. Chen, P.A. Hidalgo, R.L. Mayes, R.W. Clough and H.D. McNiven - 1978 (PB 296 212)A09

UCB/EERC-78/29 "Analytical Procedures in Soil Dynamics," by J. Lysmer - 1978 (PB 298 445)A06

UCB/EERC-79/01 "Hysteretic Behavior of Lightweight Reinforced Concrete Beam-Column Subassemblages," by B. Forzani, E.P. Popov and V.V. Bertero - April 1979(PB 298 267)A06

UCB/EERC-79/02 "The Development of a Mathematical Model to Predict the Flexural Response of Reinforced Concrete Beams to Cyclic Loads, Using System Identification," by J. Stanton & H. McNiven - Jan. 1979(PB 295 875)A10

UCB/EERC-79/03 "Linear and Nonlinear Earthquake Response of Simple Torsionally Coupled Systems," by C.L. Kan and A.K. Chopra - Feb. 1979(PB 298 262)A06

UCB/EERC-79/04 "A Mathematical Model of Masonry for Predicting its Linear Seismic Response Characteristics," by Y. Mengi and H.D. McNiven - Feb. 1979(PB 298 266)A06

UCB/EERC-79/05 "Mechanical Behavior of Lightweight Concrete Confined by Different Types of Lateral Reinforcement," by M.A. Manrique, V.V. Bertero and E.P. Popov - May 1979(PB 301 114)A06

UCB/EERC-79/06 "Static Tilt Tests of a Tall Cylindrical Liquid Storage Tank," by R.W. Clough and A. Niwa - Feb. 1979 (PB 301 167)A06

UCB/EERC-79/07 "The Design of Steel Energy Absorbing Restrainers and Their Incorporation into Nuclear Power Plants for Enhanced Safety: Volume 1 - Summary Report," by P.N. Spencer, V.F. Zackay, and E.R. Parker - Feb. 1979(UCB/EERC-79/07)A09

UCB/EERC-79/08 "The Design of Steel Energy Absorbing Restrainers and Their Incorporation into Nuclear Power Plants for Enhanced Safety: Volume 2 - The Development of Analyses for Reactor System Piping, "Simple Systems" by M.C. Lee, J. Penzien, A.K. Chopra and K. Suzuki "Complex Systems" by G.H. Powell, E.L. Wilson, R.W. Clough and D.G. Row - Feb. 1979(UCB/EERC-79/08)A10

UCB/EERC-79/09 "The Design of Steel Energy Absorbing Restrainers and Their Incorporation into Nuclear Power Plants for Enhanced Safety: Volume 3 - Evaluation of Commercial Steels " by W.S. Owen, R.M.N. Pelloux, R.O. Ritchie, M. Faral, T. Ohashi, J. Toplosky, S.J. Hartman, V.F. Zackay and E.R. Parker - Feb. 1979(UCB/EERC-79/09)A04

UCB/EERC-79/10 "The Design of Steel Energy Absorbing Restrainers and Their Incorporation into Nuclear Power Plants for Enhanced Safety: Volume 4 - A Review of Energy-Absorbing Devices," by J.M. Kelly and M.S. Skinner - Feb. 1979(UCB/EERC-79/10)A04

UCB/EERC-79/11 "Conservatism In Summation Rules for Closely Spaced Modes," by J.M. Kelly and J.L. Sackman - May 1979(PB 301 328)A03

UCB/EERC-79/12 "Cyclic Loading Tests of Masonry Single Piers; Volume 3 - Height to Width Ratio of 0.5," by P.A. Hidalgo, R.L. Mayes, H.D. McNiven and R.W. Clough - May 1979(PB 301 321)A08

UCB/EERC-79/13 "Cyclic Behavior of Dense Coarse-Grained Materials in Relation to the Seismic Stability of Dams," by N.G. Banerjee, H.B. Seed and C.K. Chan - June 1979(PB 301 373)A13

UCB/EERC-79/14 "Seismic Behavior of Reinforced Concrete Interior Beam-Column Subassemblages," by S. Viwathanatepa, E.P. Popov and V.V. Bertero - June 1979(PB 301 326)A10

UCB/EERC-79/15 "Optimal Design of Localized Nonlinear Systems with Dual Performance Criteria Under Earthquake Excitations," by M.A. Bhatti - July 1979(PB 80 167 109)A06

UCB/EERC-79/16 "OPTDYN - A General Purpose Optimization Program for Problems with or without Dynamic Constraints," by M.A. Bhatti, E. Polak and K.S. Pister - July 1979(PB 80 167 091)A05

UCB/EERC-79/17 "ANSR-II, Analysis of Nonlinear Structural Response, Users Manual," by D.P. Mondkar and G.H. Powell July 1979(PB 80 113 301)A05

UCB/EERC-79/18 "Soil Structure Interaction in Different Seismic Environments," A. Gomez-Masso, J. Lysmer, J.-C. Chen and H.B. Seed - August 1979(PB 80 101 520)A04

UCB/EERC-79/19 "ARMA Models for Earthquake Ground Motions," by M.K. Chang, J.W. Kwiatkowski, R.F. Nau, R.M. Oliver and K.S. Pister - July 1979(PB 301 166)A05

UCB/EERC-79/20 "Hysteretic Behavior of Reinforced Concrete Structural Walls," by J.M. Vallenas, V.V. Bertero and E.P. Popov - August 1979(PB 80 165 905)A12

UCB/EERC-79/21 "Studies on High-Frequency Vibrations of Buildings - 1: The Column Effect," by J. Lubliner - August 1979 (PB 80 158 553)A03

UCB/EERC-79/22 "Effects of Generalized Loadings on Bond Reinforcing Bars Embedded in Confined Concrete Blocks," by S. Viwathanatepa, E.P. Popov and V.V. Bertero - August 1979(PB 81 124 018)A14

UCB/EERC-79/23 "Shaking Table Study of Single-Story Masonry Houses, Volume 1: Test Structures 1 and 2," by P. Gülkan, R.L. Mayes and R.W. Clough - Sept. 1979 (HUD-000 1763)A12

UCB/EERC-79/24 "Shaking Table Study of Single-Story Masonry Houses, Volume 2: Test Structures 3 and 4," by P. Gülkan, R.L. Mayes and R.W. Clough - Sept. 1979 (HUD-000 1836)A12

UCB/EERC-79/25 "Shaking Table Study of Single-Story Masonry Houses, Volume 3: Summary, Conclusions and Recommendations," by R.W. Clough, R.L. Mayes and P. Gülkan - Sept. 1979 (HUD-000 1837)A06

UCB/EERC-79/26 "Recommendations for a U.S.-Japan Cooperative Research Program Utilizing Large-Scale Testing Facilities," by U.S.-Japan Planning Group - Sept. 1979(PB 301 407)A06

UCB/EERC-79/27 "Earthquake-Induced Liquefaction Near Lake Amatitlan, Guatemala," by H.B. Seed, I. Arango, C.K. Chan, A. Gomez-Masso and R. Grant de Ascoli - Sept. 1979(NUREG-CR1341)A03

UCB/EERC-79/28 "Infill Panels: Their Influence on Seismic Response of Buildings," by J.W. Axley and V.V. Bertero Sept. 1979(PB 80 163 371)A10

UCB/EERC-79/29 "3D Truss Bar Element (Type 1) for the ANSR-II Program," by D.P. Mondkar and G.H. Powell - Nov. 1979 (PB 80 169 709)A02

UCB/EERC-79/30 "2D Beam-Column Element (Type 5 - Parallel Element Theory) for the ANSR-II Program," by D.G. Row, G.H. Powell and D.P. Mondkar - Dec. 1979(PB 80 167 224)A03

UCB/EERC-79/31 "3D Beam-Column Element (Type 2 - Parallel Element Theory) for the ANSR-II Program," by A. Riahi, G.H. Powell and D.P. Mondkar - Dec. 1979(PB 80 167 216)A03

UCB/EERC-79/32 "On Response of Structures to Stationary Excitation," by A. Der Kiureghian - Dec. 1979(PB 80166 929)A03

UCB/EERC-79/33 "Undisturbed Sampling and Cyclic Load Testing of Sands," by S. Singh, H.B. Seed and C.K. Chan Dec. 1979(ADA 087 298)A07

UCB/EERC-79/34 "Interaction Effects of Simultaneous Torsional and Compressional Cyclic Loading of Sand," by P.M. Griffin and W.N. Houston - Dec. 1979(ADA 092 352)A15

UCB/EERC-80/01 "Earthquake Response of Concrete Gravity Dams Including Hydrodynamic and Foundation Interaction Effects," by A.K. Chopra, P. Chakrabarti and S. Gupta - Jan. 1980(AD-A087297)A10

UCB/EERC-80/02 "Rocking Response of Rigid Blocks to Earthquakes," by C.S. Yim, A.K. Chopra and J. Penzien - Jan. 1980 (PB80 166 002)A04

UCB/EERC-80/03 "Optimum Inelastic Design of Seismic-Resistant Reinforced Concrete Frame Structures," by S.W. Zagajeski and V.V. Bertero - Jan. 1980(PB80 164 635)A06

UCB/EERC-80/04 "Effects of Amount and Arrangement of Wall-Panel Reinforcement on Hysteretic Behavior of Reinforced Concrete Walls," by R. Iliya and V.V. Bertero - Feb. 1980(PB81 122 525)A09

UCB/EERC-80/05 "Shaking Table Research on Concrete Dam Models," by A. Niwa and R.W. Clough - Sept. 1980(PB81 122 368)A06

UCB/EERC-80/06 "The Design of Steel Energy-Absorbing Restrainers and their Incorporation into Nuclear Power Plants for Enhanced Safety (Vol 1A): Piping with Energy Absorbing Restrainers: Parameter Study on Small Systems," by G.H. Powell, C. Oughourlian and J. Simons - June 1980

UCB/EERC-80/07 "Inelastic Torsional Response of Structures Subjected to Earthquake Ground Motions," by Y. Yamazaki April 1980(PB81 122 327)A08

UCB/EERC-80/08 "Study of X-Braced Steel Frame Structures Under Earthquake Simulation," by Y. Ghanaat - April 1980 (PB81 122 335)A11

UCB/EERC-80/09 "Hybrid Modelling of Soil-Structure Interaction," by S. Gupta, T.W. Lin, J. Penzien and C.S. Yeh May 1980(PB81 122 319)A07

UCB/EERC-80/10 "General Applicability of a Nonlinear Model of a One Story Steel Frame," by B.I. Sveinsson and H.D. McNiven - May 1980(PB81 124 877)A06

UCB/EERC-80/11 "A Green-Function Method for Wave Interaction with a Submerged Body," by W. Kioka - April 1980 (PB81 122 269)A07

UCB/EERC-80/12 "Hydrodynamic Pressure and Added Mass for Axisymmetric Bodies," by F. Nilrat - May 1980(PB81 122 343)A08

UCB/EERC-80/13 "Treatment of Non-Linear Drag Forces Acting on Offshore Platforms," by B.V. Dao and J. Penzien May 1980(PB81 153 413)A07

UCB/EERC-80/14 "2D Plane/Axisymmetric Solid Element (Type 3 - Elastic or Elastic-Perfectly Plastic) for the ANSR-II Program," by D.P. Mondkar and G.H. Powell - July 1980(PB81 122 350)A03

UCB/EERC-80/15 "A Response Spectrum Method for Random Vibrations," by A. Der Kiureghian - June 1980(PB81 122 301)A03

UCB/EERC-80/16 "Cyclic Inelastic Buckling of Tubular Steel Braces," by V.A. Zayas, E.P. Popov and S.A. Mahin June 1980(PB81 124 885)A10

UCB/EERC-80/17 "Dynamic Response of Simple Arch Dams Including Hydrodynamic Interaction," by C.S. Porter and A.K. Chopra - July 1980(PB81 124 000)A13

UCB/EERC-80/18 "Experimental Testing of a Friction Damped Aseismic Base Isolation System with Fail-Safe Characteristics," by J.M. Kelly, K.E. Beucke and M.S. Skinner - July 1980(PB81 148 595)A04

UCB/EERC-80/19 "The Design of Steel Energy-Absorbing Restrainers and their Incorporation into Nuclear Power Plants for Enhanced Safety (Vol 1B): Stochastic Seismic Analyses of Nuclear Power Plant Structures and Piping Systems Subjected to Multiple Support Excitations," by M.C. Lee and J. Penzien - June 1980

UCB/EERC-80/20 "The Design of Steel Energy-Absorbing Restrainers and their Incorporation into Nuclear Power Plants for Enhanced Safety (Vol 1C): Numerical Method for Dynamic Substructure Analysis," by J.M. Dickens and E.L. Wilson - June 1980

UCB/EERC-80/21 "The Design of Steel Energy-Absorbing Restrainers and their Incorporation into Nuclear Power Plants for Enhanced Safety (Vol 2): Development and Testing of Restraints for Nuclear Piping Systems," by J.M. Kelly and M.S. Skinner - June 1980

UCB/EERC-80/22 "3D Solid Element (Type 4-Elastic or Elastic-Perfectly-Plastic) for the ANSR-II Program," by D.P. Mondkar and G.H. Powell - July 1980(PB81 123 242)A03

UCB/EERC-80/23 "Gap-Friction Element (Type 5) for the ANSR-II Program," by D.P. Mondkar and G.H. Powell - July 1980 (PB81 122 285)A03

UCB/EERC-80/24 "U-Bar Restraint Element (Type 11) for the ANSR-II Program," by C. Oughourlian and G.H. Powell July 1980(PB81 122 293)A03

UCB/EERC-80/25 "Testing of a Natural Rubber Base Isolation System by an Explosively Simulated Earthquake," by J.M. Kelly - August 1980(PB81 201 360)A04

UCB/EERC-80/26 "Input Identification from Structural Vibrational Response," by Y. Hu - August 1980(PB81 152 308)A05

UCB/EERC-80/27 "Cyclic Inelastic Behavior of Steel Offshore Structures," by V.A. Zayas, S.A. Mahin and E.P. Popov August 1980 PB81 196 180)A15

UCB/EERC-80/28 "Shaking Table Testing of a Reinforced Concrete Frame with Biaxial Response," by M.G. Oliva October 1980(PB81 154 304)A10

UCB/EERC-80/29 "Dynamic Properties of a Twelve-Story Prefabricated Panel Building," by J.G. Bouwkamp, J.P. Kollegger and R.M. Stephen - October 1980(PB82 117 128)A06

UCB/EERC-80/30 "Dynamic Properties of an Eight-Story Prefabricated Panel Building," by J.G. Bouwkamp, J.P. Kollegger and R.M. Stephen - October 1980(PB81 200 313)A05

UCB/EERC-80/31 "Predictive Dynamic Response of Panel Type Structures Under Earthquakes," by J.P. Kollegger and J.G. Bouwkamp - October 1980(PB81 152 316)A04

UCB/EERC-80/32 "The Design of Steel Energy-Absorbing Restrainers and their Incorporation into Nuclear Power Plants for Enhanced Safety (Vol 3): Testing of Commercial Steels in Low-Cycle Torsional Fatigue," by P. Spencer, E.R. Parker, E. Jongewaard and M. Drory

UCB/EERC-80/33 "The Design of Steel Energy-Absorbing Restrainers and their Incorporation into Nuclear Power Plants for Enhanced Safety (Vol 4): Shaking Table Tests of Piping Systems with Energy-Absorbing Restrainers," by S.F. Stiemer and W.G. Godden - Sept. 1980

UCB/EERC-80/34 "The Design of Steel Energy-Absorbing Restrainers and their Incorporation into Nuclear Power Plants for Enhanced Safety (Vol 5): Summary Report," by P. Spencer

UCB/EERC-80/35 "Experimental Testing of an Energy-Absorbing Base Isolation System," by J.M. Kelly, M.S. Skinner and K.E. Beucke - October 1980(PB81 154 072)A04

UCB/EERC-80/36 "Simulating and Analyzing Artificial Non-Stationary Earthquake Ground Motions," by R.F. Nau, R.M. Oliver and K.S. Pister - October 1980(PB81 153 397)A04

UCB/EERC-80/37 "Earthquake Engineering at Berkeley - 1980," - Sept. 1980(PB81 205 674)A09

UCB/EERC-80/38 "Inelastic Seismic Analysis of Large Panel Buildings," by V. Schricker and G.H. Powell - Sept. 1980 (PB81 154 338)A13

UCB/EERC-80/39 "Dynamic Response of Embankment, Concrete-Gravity and Arch Dams Including Hydrodynamic Interaction," by J.F. Hall and A.K. Chopra - October 1980(PB81 152 324)A11

UCB/EERC-80/40 "Inelastic Buckling of Steel Struts Under Cyclic Load Reversal," by R.G. Black, W.A. Wenger and E.P. Popov - October 1980(PB81 154 312)A08

UCB/EERC-80/41 "Influence of Site Characteristics on Building Damage During the October 3, 1974 Lima Earthquake," by P. Repetto, I. Arango and H.B. Seed - Sept. 1980(PB81 161 739)A05

UCB/EERC-80/42 "Evaluation of a Shaking Table Test Program on Response Behavior of a Two Story Reinforced Concrete Frame," by J.M. Blondet, R.W. Clough and S.A. Mahin

UCB/EERC-80/43 "Modelling of Soil-Structure Interaction by Finite and Infinite Elements," by F. Medina - December 1980(PB81 229 270)A04

UCB/EERC-81/01 "Control of Seismic Response of Piping Systems and Other Structures by Base Isolation," edited by J.M. Kelly - January 1981 (PB81 200 735)A05

UCB/EERC-81/02 "OPTNSR - An Interactive Software System for Optimal Design of Statically and Dynamically Loaded Structures with Nonlinear Response," by M.A. Bhatti, V. Ciampi and K.S. Pister - January 1981 (PB81 218 851)A09

UCB/EERC-81/03 "Analysis of Local Variations in Free Field Seismic Ground Motions," by J.-C. Chen, J. Lysmer and H.B. Seed - January 1981 (AD-A099508)A13

UCB/EERC-81/04 "Inelastic Structural Modeling of Braced Offshore Platforms for Seismic Loading," by V.A. Zayas, P.-S.B. Shing, S.A. Mahin and E.P. Popov - January 1981(PB82 138 777)A07

UCB/EERC-81/05 "Dynamic Response of Light Equipment in Structures," by A. Der Kiureghian, J.L. Sackman and B. Nour-Omid - April 1981 (PB81 218 497)A04

UCB/EERC-81/06 "Preliminary Experimental Investigation of a Broad Base Liquid Storage Tank," by J.G. Bouwkamp, J.P. Kollegger and R.M. Stephen - May 1981(PB82 140 385)A03

UCB/EERC-81/07 "The Seismic Resistant Design of Reinforced Concrete Coupled Structural Walls," by A.E. Aktan and V.V. Bertero - June 1981(PB82 113 358)A11

UCB/EERC-81/08 "The Undrained Shearing Resistance of Cohesive Soils at Large Deformations," by M.R. Pyles and H.B. Seed - August 1981

UCB/EERC-81/09 "Experimental Behavior of a Spatial Piping System with Steel Energy Absorbers Subjected to a Simulated Differential Seismic Input," by S.F. Stiemer, W.G. Godden and J.M. Kelly - July 1981

UCB/EERC-81/10 "Evaluation of Seismic Design Provisions for Masonry in the United States," by B.I. Sveinsson, R.L. Mayes and H.D. McNiven - August 1981 (PB82 166 075)A08

UCB/EERC-81/11 "Two-Dimensional Hybrid Modelling of Soil-Structure Interaction," by T.-J. Tzong, S. Gupta and J. Penzien - August 1981(PB82 142 118)A04

UCB/EERC-81/12 "Studies on Effects of Infills in Seismic Resistant R/C Construction," by S. Brokken and V.V. Bertero - September 1981 (PB82 166 190)A09

UCB/EERC-81/13 "Linear Models to Predict the Nonlinear Seismic Behavior of a One-Story Steel Frame," by H. Valdimarsson, A.H. Shah and H.D. McNiven - September 1981(PB82 138 793)A07

UCB/EERC-81/14 "TLUSH: A Computer Program for the Three-Dimensional Dynamic Analysis of Earth Dams," by T. Kagawa, L.H. Mejia, H.B. Seed and J. Lysmer - September 1981(PB82 139 940)A06

UCB/EERC-81/15 "Three Dimensional Dynamic Response Analysis of Earth Dams," by L.H. Mejia and H.B. Seed - September 1981 (PB82 137 274)A12

UCB/EERC-81/16 "Experimental Study of Lead and Elastomeric Dampers for Base Isolation Systems," by J.M. Kelly and S.B. Hodder - October 1981 (PB82 166 182)A05

UCB/EERC-81/17 "The Influence of Base Isolation on the Seismic Response of Light Secondary Equipment," by J.M. Kelly - April 1981 (PB82 255 266)A04

UCB/EERC-81/18 "Studies on Evaluation of Shaking Table Response Analysis Procedures," by J. Marcial Blondet - November 1981 (PB82 197 278)A10

UCB/EERC-81/19 "DELIGHT.STRUCT: A Computer-Aided Design Environment for Structural Engineering," by R.J. Balling, K.S. Pister and E. Polak - December 1981 (PB82 218 496)A07

UCB/EERC-81/20 "Optimal Design of Seismic-Resistant Planar Steel Frames," by R.J. Balling, V. Ciampi, K.S. Pister and E. Polak - December 1981 (PB82 220 179)A07

UCB/EERC-82/01 "Dynamic Behavior of Ground for Seismic Analysis of Lifeline Systems," by T. Sato and A. Der Kiureghian - January 1982 (PB82 218 926)A05

UCB/EERC-82/02 "Shaking Table Tests of a Tubular Steel Frame Model," by Y. Ghanaat and R. W. Clough - January 1982 (PB82 220 161)A07

UCB/EERC-82/03 "Behavior of a Piping System under Seismic Excitation: Experimental Investigations of a Spatial Piping System supported by Mechanical Shock Arrestors and Steel Energy Absorbing Devices under Seismic Excitation," by S. Schneider, H.-M. Lee and W. G. Godden - May 1982 (PB83 172 544)A09

UCB/EERC-82/04 "New Approaches for the Dynamic Analysis of Large Structural Systems," by E. L. Wilson - June 1982 (PB83 148 080)A05

UCB/EERC-82/05 "Model Study of Effects of Damage on the Vibration Properties of Steel Offshore Platforms," by F. Shahrivar and J. G. Bouwkamp - June 1982 (PB83 148 742)A10

UCB/EERC-82/06 "States of the Art and Practice in the Optimum Seismic Design and Analytical Response Prediction of R/C Frame-Wall Structures," by A. E. Aktan and V. V. Bertero - July 1982 (PB83 147 736)A05

UCB/EERC-82/07 "Further Study of the Earthquake Response of a Broad Cylindrical Liquid-Storage Tank Model," by G. C. Manos and R. W. Clough - July 1982 (PB83 147 744)A11

UCB/EERC-82/08 "An Evaluation of the Design and Analytical Seismic Response of a Seven Story Reinforced Concrete Frame - Wall Structure," by F. A. Charney and V. V. Bertero - July 1982(PB83 157 628)A09

UCB/EERC-82/09 "Fluid-Structure Interactions: Added Mass Computations for Incompressible Fluid," by J. S.-H. Kuo - August 1982 (PB83 156 281)A07

UCB/EERC-82/10 "Joint-Opening Nonlinear Mechanism: Interface Smeared Crack Model," by J. S.-H. Kuo - August 1982 (PB83 149 195)A05

UCB/EERC-82/11 "Dynamic Response Analysis of Techi Dam," by R. W. Clough, R. M. Stephan and J. S.-H. Kuo - August 1982 (PB83 147 496)A06

UCB/EERC-82/12 "Prediction of the Seismic Responses of R/C Frame-Coupled Wall Structures," by A. E. Aktan, V. V. Bertero and M. Piazza - August 1982 (PB83 149 203)A09

UCB/EERC-82/13 "Preliminary Report on the SMART 1 Strong Motion Array in Taiwan," by B. A. Bolt, C. H. Loh, J. Penzien, Y. B. Tsai and Y. T. Yeh - August 1982 (PB83 159 400)A10

UCB/EERC-82/14 "Shaking-Table Studies of an Eccentrically X-Braced Steel Structure," by M. S. Yang - September 1982

UCB/EERC-82/15 "The Performance of Stairways in Earthquakes," by C. Roha, J. W. Axley and V. V. Bertero - September 1982 (PB83 157 693)A07

UCB/EERC-82/16 "The Behavior of Submerged Multiple Bodies in Earthquakes," by W.-G. Liao - Sept. 1982 (PB83 158 709)A07

UCB/EERC-82/17 "Effects of Concrete Types and Loading Conditions on Local Bond-Slip Relationships," by A. D. Cowell, E. P. Popov and V. V. Bertero - September 1982 (PB83 153 577)A04

UCB/EERC-82/18 "Mechanical Behavior of Shear Wall Vertical Boundary Members: An Experimental Investigation," by M. T. Wagner and V. V. Bertero - October 1982 (PB83 159 764)A05

UCB/EERC-82/19 "Experimental Studies of Multi-support Seismic Loading on Piping Systems," by J. M. Kelly and A. D. Cowell - November 1982

UCB/EERC-82/20 "Generalized Plastic Hinge Concepts for 3D Beam-Column Elements," by P. F.-S. Chen and G. H. Powell - November 1982

UCB/EERC-82/21 "ANSR-III: General Purpose Computer Program for Nonlinear Structural Analysis," by C. V. Oughourlian and G. H. Powell - November 1982

UCB/EERC-82/22 "Solution Strategies for Statically Loaded Nonlinear Structures," by J. W. Simons and G. H. Powell - November 1982

UCB/EERC-82/23 "Analytical Model of Deformed Bar Anchorages under Generalized Excitations," by V. Ciampi, R. Eligehausen, V. V. Bertero and E. P. Popov - November 1982 (PB83 169 532)A06

UCB/EERC-82/24 "A Mathematical Model for the Response of Masonry Walls to Dynamic Excitations," by H. Sucuoğlu, Y. Mengi and H. D. McNiven - November 1982 (PB83 169 011)A07

UCB/EERC-82/25 "Earthquake Response Considerations of Broad Liquid Storage Tanks," by F. J. Cambra - November 1982

UCB/EERC-82/26 "Computational Models for Cyclic Plasticity, Rate Dependence and Creep," by B. Mosaddad and G. H. Powell - November 1982

UCB/EERC-82/27 "Inelastic Analysis of Piping and Tubular Structures," by M. Mahasuverachai and G. H. Powell - November 1982

UCB/EERC-83/01 "The Economic Feasibility of Seismic Rehabilitation of Buildings by Base Isolation," by J. M. Kelly - January 1983

UCB/EERC-83/02 "Seismic Moment Connections for Moment-Resisting Steel Frames," by E. P. Popov - January 1983

UCB/EERC-83/03 "Design of Links and Beam-to-Column Connections for Eccentrically Braced Steel Frames," by E. P. Popov and J. O. Malley - January 1983

UCB/EERC-83/04 "Numerical Techniques for the Evaluation of Soil-Structure Interaction Effects in the Time Domain," by E. Bayo and E. L. Wilson - February 1983

UCB/EERC-83/05 "A Transducer for Measuring the Internal Forces in the Columns of a Frame-Wall Reinforced Concrete Structure," by R. Sause and V. V. Bertero - May 1983

UCB/EERC-83/06 "Dynamic Interactions between Floating Ice and Offshore Structures," by P. Croteau - May 1983

UCB/EERC-83/07 "Dynamic Analysis of Multiply Tuned and Arbitrarily Supported Secondary Systems," by T. Igusa and A. Der Kiureghian - June 1983